The University Of Sheffield.

Methodological approaches to reconstructing storms, relative sea-level change, and coastal evolution in the Mid- and Late-Holocene.

Greg Thomas Rushby

A thesis submitted in partial fulfilment of the requirements for the degree of Doctor of Philosophy

The University of Sheffield
Faculty of Social Science
Department of Geography

Submitted: March 2022

Abstract

Predicting the future impacts of storms requires a robust understanding of storms and coastal evolution in the past. This research presents a novel combination of techniques reconstructing storms, relative sea-level and coastal change to better understand the patterns and relationships of storms and coastal morphology.

Storms are reconstructed from coastal dunes by identification of jumps in relative age, determined by portable luminescence, concurrent with changes in grain size characteristics. Reconstructed storms are combined with new documentary storms archives to produce 200-year storm chronologies for the Norfolk and North Welsh coasts. Of these ten, eight were outside the range of regional instrumental datasets extending the record of large storms in these regions by 50-60 years.

A new foraminifera transfer function is derived from a 3000-year-old salt-marsh producing one of the world's longest continuous sea-level records from a salt-marsh. Combined with two new sea-level index points (SLIPs) from a freshwater marsh, and SLIPs from literature the relative sea-level record for North Wales shows a rapid early Holocene rise (~5.3 m ka^{-1}) with stagnation to slow rise (~0.3 m ka^{-1}) in the mid- and late-Holocene. This record leaves no room for a mid-Holocene highstand in the region, improving understanding of UK mid-Holocene emergence and highlighting shortcomings some glacio-isostatic models for sea-level prediction.

By combining dune reconstructions, storm archives, historic maps and satellite derived shorelines, the evolution of a North Wales beach dune system over 500 years is reconstructed at varying resolutions. Results show ~650 m of change in the last 500 years punctuated by storm erosion in the 1850s-60s, 1880s-90s late 1930s. By comparing these reconstructed shorelines with the tidal characteristics of storms from tide gauges it is possible to demonstrate statistically significant correlations between local scale shoreline change and the very largest storm events to occur each year (sea levels >3.00m OD).

List of Contents

List of Tables

List of Figures

Glossary

AMS	Accelerator Mass Spectrometry
BIIS	British-Irish Ice Sheet
CAM	Central Age Model
CIC	Constant Initial Concentration (Model)
CRS	Constant Rate of Supply (Model)
CWT	Continuous Wavelet Transformation
GEE	Google Earth Engine
GIA	Glacio-Isostatic Adjustment
GIS	Geographical Information System/Science
GPR	Ground Penetrating Radar
GPS	Global Positioning System
ICP-MS	Inductively Coupled Plasma Mass Spectrometry
IM	Indicative Meaning
IRSL	Infra-red Stimulated Luminescence
LIA	Little Ice Age
LiDAR	Light Detection and Ranging
LOI	Loss-on-Ignition
LOO	Leave-one-out
MAT	Modern Analogue Test
MHW	Mean High Water
MHWN	Mean High Water Neap
MHWS	Mean High Water Spring
NAO	North Atlantic Oscillation
OD	Ordnance Datum
OSL	Optically Stimulated Luminescence
POSL	Portable Optically Stimulated Luminescence
PSA	Particle Size Analysis
RMSE	Root Mean Squared Error
RMSEP	Root Mean Squared Error of Prediction
RMSL	Relative Mean Sea Level
RSL	Relative Sea Level
RTK-GPS	Real-Time Kinematic Global Positioning System
SAR	Single Aliquot Regeneration
SL	Sea Level
SLIP	Sea Level Index Point
TL	Thermo-Luminescence
UAV	Unmanned Aerial Vehicle
XWT	Cross-wavelet transform

Declaration

I, the author, confirm that the Thesis is my own work. I am aware of the University's Guidance on the Use of Unfair Means (www.sheffield.ac.uk/ssid/unfair-means). This work has not previously been presented for an award at this, or any other, university.

Acknowledgements

Thanks must go to all those of have contributed to the journey of completing this thesis and to all those who have contributed to my life and getting me to this stage. Firstly, I wish to thank my supervisor Prof. Mark Bateman. Throughout these years Mark's support has been unwavering through the ups, downs and greatest challenges I have faced in this process. I extend the same gratitude to Prof. Roland Gehrels who has been a valued mentor since 2012.

Thanks also go to those I have collaborated with in the various academic ventures both within and outside of the project, in particular to Geoff Richards and Graeme Swindles. Thanks, must also go to Natural Environment Research Council for the funding behind this project.

I wish to thank the many friends and colleagues I have found along the way for their emotional and technical support, especially Laura Eddey, Rob Ashurst, Rhoda Ballinger, Shasta Marrero, and Rupert Perkins. A special thanks to Sandra Bryvik for her unrelenting and unyielding criticism from a very Swedish point of view.

I owe many of my achievements to the love and support of my family throughout my life. You have been guides, mentors and friends. You have kept my will to succeed alive and if I can ever be half as good a person as any of you, then my life will have been a success.

Finally, I wish to give my biggest thanks to my beloved partner Michael Hingston who has stood by me every step of the way through delivering this work. I would have never made it without you. Thank you.

Chapter 1.

Introduction

1.1. Rationale

Predictions of coastal population growth in the 21st century vary, though most suggest that the number of people living in low elevation coastal zones, and more specifically within the 100-year coastal floodplain, will increase in the range of 35-40% by 2030 and 40-85% by 2060 relative to year 2000 populations (Balk *et al.* 2009, McGranahan *et al.* 2007, Neumann *et al.* 2015). Within those same time periods, many studies suggest increases in the magnitude (Brown *et al.* 2010, Karim and Mimura 2008, Kim *et al.* 2017, Woth *et al*. 2006), the frequency (Beniston, *et al.* 2007, Mori *et al*. 2019) or both (Fortunato *et al.* 2019, Gaslikova *et al.* 2013, Lowe and Gregory 2005, Yasuda *et al*. 2014) of coastal storms. Combined, these future changes pose a substantial challenge for the management of coastal risk in affected regions. Superimposed upon changes in coastal populations and changing storminess are changes in coastal morphology (Banno and Kuriyama 2020, Gomez-Pujol *et al.* 2011, Ortega-Sanchez *et al.* 2008) which itself may be influenced by changing coastal storm characteristics (Bullard *et al.* 2019, Montruiel and Bullard 2012, Pye and Blott 2016). Coastal erosion can enhance coastal flood risk further by the loss of natural buffers and barriers of coastal flooding exposing coastal populations and altering the area of coastal floodplains (Dawson *et al.* 2009, Moller *et al*. 2014, Sutton-Grier *et al.* 2015).

In the context of these future changes, and the potential for substantial changes in coastal risk they bring, it is increasingly necessary to improve our understanding how these events may change further in the future. To make such predictions about the future requires a robust understanding of storms, relative sea level, and coastal evolution in the past (Haigh *et al.* 2009, Pye and Blott, 2016, Talke and Jay, 2013, Wahl *et al.* 2017, Woth *et al*. 2006). This thesis explores the potential of utilising and combining different methodologies to

reconstructing past storms, relative sea-level and coastal change with the goal of improving understanding of flood risk and coastal evolution in a changing climate.

1.2. Coastal storms, past, present and future

In December and January of 2013/14, the UK was subjected to a series of intense weather events which led to some of the most substantial and widespread coastal flooding since the devastating North Sea storm surge of 1953 (Baxter 2005). These events began on the 5th of December 2013 with the formation of an intense low-pressure system in the North Atlantic which progressed east across the north of Scotland, into the North Sea and onwards into northern Europe (Wadey *et al.* 2014). This storm was one of several over this winter which generated large storm surges, ephemeral rises in sea level driven by an inverse barometer effect with low atmospheric pressure. In concert with spring high tides, these surges produced extreme sea levels which resulted in the highest ever instrumentally recorded sea levels for both the Humber and Thames estuaries (MET Office 2014, Thorne 2014).

Storms throughout January and early February resulted in persistent and intense coastal flooding in Scotland, England, and Wales. With the estimated costs of these events exceeding £290 million (Bennett and Hartwell-Naguib 2014, Thorne 2014) and over 2500 properties flooded (Wadey *et al.* 2014), the 2013 floods intensified interest from the public, policy makers, environmental managers, and scientists in bettering understanding of the nature of coastal flood risk. In particular, focus has been given to their consequences and to how such events can be mitigated and prepared for in the context of a changing climate (Huntingford *et al.* 2014, Lowe and Gregory 2005, Thorne 2014).

The physics behind storm surges and resulting extreme sea levels are well understood and predictive physical models of storm surges already produce good agreement with measured observations during the events themselves (Horn, 2015). However, deaths and damages from surge driven extreme sea levels continue to remain high, as shown by major disasters such as Typhoon Haiyan in 2013 and Cyclone Xynthia in 2010. Horn (2015) propose that

this primarily arises because of shortcomings in mitigation and adaptation strategies for such disasters.

These terms tend to have varying definitions depending on discipline. Here, “mitigation” is used to describe action taken to reduce the number and severity of storm surges (such as through reduction in greenhouse gas emissions) and “adaptation” describes approaches to reduce impacts through use risk-based approaches to coastal defence and disaster management. Climate mitigation is beyond the scope of this thesis, here focus is instead drawn to adaptation. Adaptation to coastal storms can take many forms. Traditionally this has focussed on the use of engineered defences, typically in the form of sea walls, levees, and barriers. With increased awareness of the environmental and morphological consequences of such measures, focus has more recently been drawn to nature-based solutions, such as the restoration of salt-marshes, mangroves, and coastal dunes. Literature surrounding nature-based solutions to coastal defence and the response of physical, ecological or social systems to coastal storms is often framed around the concept of “coastal resilience” (Houser *et al.* 2015, Kombiadou *et al.* 2019, Masselink and Lazarus, 2019, Woodroffe 2007). Arising originally from studies of populations changes in ecology, resilience can most generically be defined by the ability of a coastal system to “bounce back” from a sudden disturbance, usually a coastal storm, though ongoing disturbances such as sea-level rise are also considered (Kirwan *et al*. 2016, Schuerch *et al.* 2018, Temmerman, *et al*. 2015). Whilst this generic definition is usually consistent, exactly what is “bouncing back” is discipline specific, be that the physical environment in geomorphological studies or social systems. This concept is discussed further, with particular focus on its morphological applications, in section 2.4.

Whilst these specific measures may have their own benefits and pitfalls, a common point between them is a reliance upon a robust understanding of coastal risk. Construction of appropriate defences requires an understanding of the potential area at risk, often implemented through use of inundation modelling. This is a geographical information system

(GIS) based approach which maps coastal flood extent based on a hypothetical extreme sea level using enhanced bathtub models (Williams and Lück-Vogel, 2020). These can then be superimposed against vulnerability of coastal communities and assets to ascertain risk (Oumeraci *et al.* 2015).

Whilst risk maps provide a spatial component of risk, the temporal component is often described through the recurrence interval of the given modelled sea level. Magnitude-frequency relationships provide a single metric to capture both the spatial and temporal components of coastal flood hazards. In the context of surges and extreme sea levels, this usually takes the form of an elevation of a given frequency. For instance, an extreme sea level of 15 m above ordnance datum (OD) may have a recurrence of 1 in 1000 years (or 0.001 $years^{-1}$ recurrence). Risk mapping can then be determined based on that hypothetical elevation and appropriate adaptation measures implemented. The principal UK example is the Thames barrier, which was initially constructed with the intent of withstanding 1 in 1000-year event until 2030; based on predictions of relative mean sea-level (RMSL) rise available at the time (Dawson *et al.* 2005).

The recurrence interval curves of extreme sea levels used in the UK are primarily derived from observations recorded by tide gauges (Batstone *et al.* 2013, McMillan *et al.* 2011); mostly from the UK National Network of Tide Gauges, often termed the “Class A” tide gauge network (McMillan *et al.* 2011, Wadey *et al.* 2014). Curves derived from such data can have several key uncertainties when being used to determine current and future flood risk. Primarily these uncertainties take the form of:

- Concerns over the accuracy of older tide gauges during extreme events, particularly float and well gauges which comprised most UK gauges in the first half the 20th century (Míguez *et al.* 2012, Woodworth *et al.* 2009).
- The common situation of gauges in relatively sheltered areas such as harbours (Míguez *et al.* 2012).

- The brevity of instrumental records of extreme sea levels from tide gauges, typically ~30 - 50 y (see Figure 1.1, Wadey *et al.* (2014)).

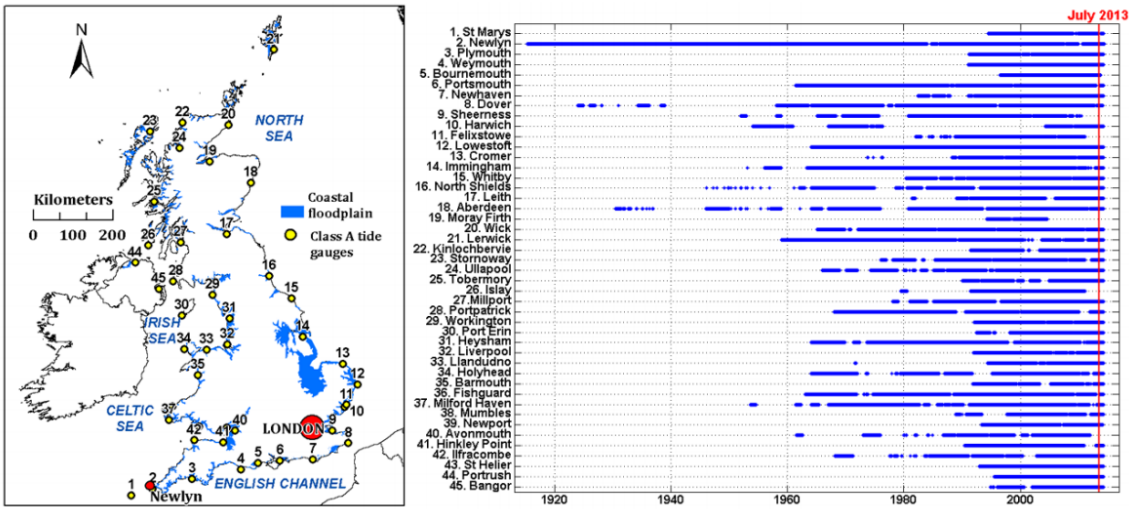

Figure 1.1. Location map of Class A UK tide gauges and the temporal coverage of their associated datasets. From: Wadey et al. (2014)

Van den Brink *et al.* (2005) highlight four areas from which uncertainties can arise; (1) the choice of probability function used; (2) the representativeness of the curve in a future with different climate parameters and coastal configuration; (3) the presence of a rare secondary population of extreme sea levels associated with a meteorological event that lies outside the temporal range of the instrumental record and; (4) the statistical validity of extrapolating the size of a 1000 year event from a 100 year dataset (as with the Thames barrier) (Cunningham *et al.* 2011, Van den Brink *et al.* 2005). The latter three of these issues all share a common source, the brevity of instrumental records of storms and sea level extremes. These issues are not unique to UK datasets and are more pronounced in places with shorter and less spatially extensive tidal records as in the UK.

Understanding how storms and extreme sea levels may change in response to future climate is a crucial for the correct interpretation and application of recurrence models for coastal defence in the future. There are two main ways in which sea level extremes may change in the future. Firstly, because of changes in the magnitude, frequency, duration, and path of storm tracks which drive storm surges. Secondly, because of relative mean sea-level

(RMSL) rise. RMSL affects recurrence models and coastal processes through the effective raising of the base level for extremes. A simplified illustration of this is shown in Figure 1.2. If RMSL rise persists it will become increasingly necessary to increase the height of coastal defences to maintain required levels of protection.

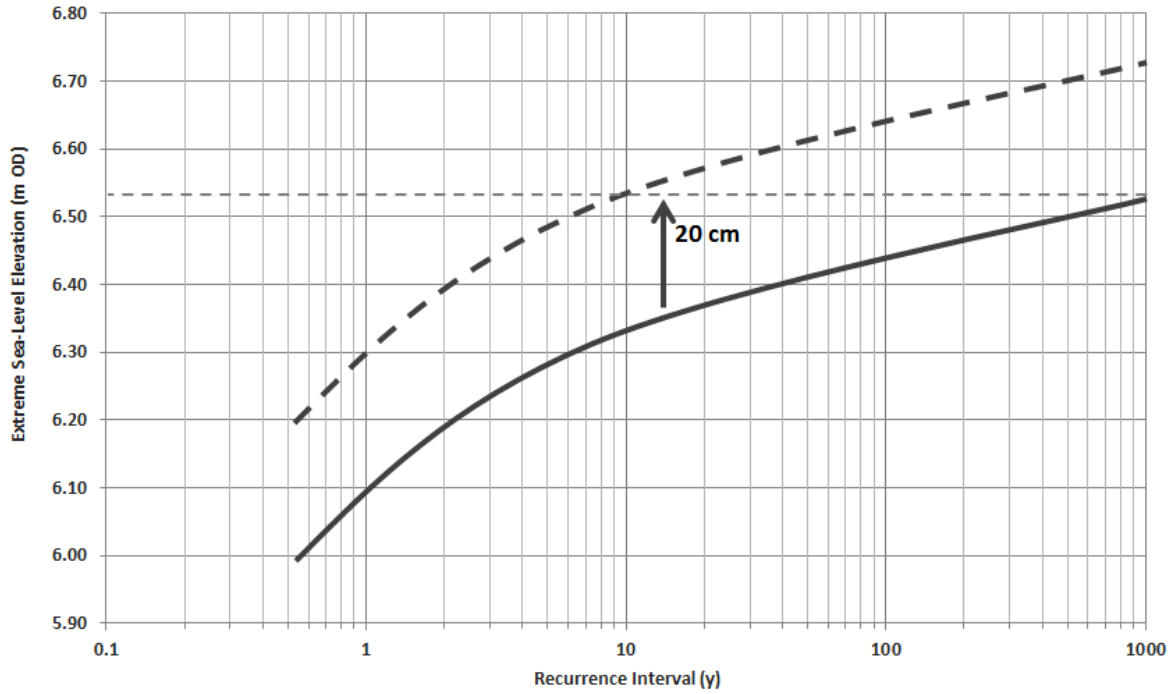

Figure 1.2. Return period curve created from Newlyn tide gauge data (Solid) and the same curve under 0.2 m of relative mean sea-level rise (Dashed). Note that under such a rise a 1 in 100-year event prior becomes a 1 in 3 year after. Adapted from Haigh (2009)

There remains considerable debate about the nature of how extreme sea levels have varied with climate and sea level in the past and of how they will change into the future. A statistical analysis of global tide gauge records conducted by Menéndez and Woodworth (2010) found that most changes in extreme sea levels observed in the last ~100 year can be attributed almost entirely to changes in RMSL rather than any increase in storminess. Similar conclusions have been drawn by several studies both before and since (Bromirski *et al.* 2003, Church *et al.* 2004, Haigh 2009, Howard *et al.* 2019, Stephens *et al.* 202, Wahl, 2017, Woodworth and Blackman 2002). A common point amongst authors in this field is that

understanding of the impact of climate change on changing storm climate and extreme sea level magnitudes is being limited the brevity of records on which their analysis is based. It is therefore imperative for the record of both past storms and regional RMSL to be extended beyond the limited temporal scope of tide gauge records and for a continuation of data archaeology in this area (Bradshaw *et al.* 2015, Haigh *et al.* 2009, Talke and Jay, 2013, Wahl *et al.* 2017, Woodworth 2022.).

1.3. Reconstructing past storms and sea levels

A common approach to overcoming the limitations of instrumental records of storms has been the use of sedimentary archives. This field has largely focussed on the use of sequential back-barrier deposits. For example, hurricane overwash of sand dune and beach sediments on the east coast of the USA (Boldt *et al.* 2010, Buynevich and Donnelly 2006, Buynevich *et al.* 2004, Carruthers *et al.* 2013, Donnelly *et al.* 2001) and more recently in New Zealand (Dougherty 2014). Such studies are expanded on further in section 2.2. Briefly, the field has been dominated by two main techniques to derive Holocene storm records; 1) the incremental dating of sandy coarse sediment overwash deposits held in finer back-barrier morphologies (Boldt *et al.* 2010, Buynevich and Donnelly 2006, Donnelly *et al.* 2001) and 2) the location of buried erosional scarps within sand and gravel barriers using utilising tools such as ground penetrating radar (GPR) to distinguish coarse-grained lag and heavy-mineral deposits associated with beachfaces following erosion (Buynevich *et al.* 2004, Dougherty 2014).

Such studies, whilst excellent methodologies for determining storm surge occurrence, provided no means by which to determine robust elevations and therefore no attribution of magnitude. Cunningham *et al.* (2011) examined a 1 km exposure left in a Netherlands foredune system by a large storm surge in 2007 which resulted in 10-15 m of lateral dune erosion. Within these dunes they found a continuous layer of shells and sediments they concluded to be of marine origin and not aeolian. Concluding this to be a storm layer,

Cunningham *et al.* (2011) postulated that the minimum elevation this layer was found represented a plausible minimum for the surge which deposited it. This work was the first to suggest that coastal dunes may be used as an archive of coastal storms that could quantify not only the date of storm occurrence, but an estimate of magnitude as well. This work is expanded on more in section 2.2.4.

Aside from direct recorded measurements and sedimentological evidence, useful records of extreme sea levels and coastal storms can be derived from historic sources. For example, Haigh *et al.* (2015) constructed a public, user-friendly database of coastal flooding based on historic sources: SurgeWatch. SurgeWatch has (as of January 2022) captured 719 storm events in the last 1000 years with impacts on the UK coasts with, where possible, surges quantified by comparison with local tide gauge data. Aside from this work however, by comparison to sedimentary archives, historic records of storms have typically seen limited application.

As illustrated by the findings of Menéndez and Woodworth (2010), storm reconstructions and predictions require consideration of additional context from of mean relative sea-level change due to its role in dictating the base level for storm elevations. Additionally, wherever significant outstanding questions about regional sea level histories remain, these should also be resolved to ensure both reconstructed and predicted extreme and mean sea levels utilising models such as glacio-isostatic adjustment (GIA) models are properly verified against empirical data (section 2.3).

1.4. UK storms and coastal change

As the most energetic storm season since 1948 (Masselink *et al.* 2016) and the stormiest recorded for the UK (Matthews *et al.* 2014) the 2013/14 storm surge season resulted in substantial coastal change around the UK coastline. On the Sefton coast 10-12 m of foredune erosion took place over the single season (Pye and Blott 2016) with similar scales of erosion taking place on beach-dune systems on England’s eastern coasts in Lincolnshire

and North Norfolk (Bullard *et al.* 2019). Substantial soft cliff erosion took place on along the east coast of England along with washover of coastal dunes and gravel barrier breaching (Spencer *et al.* 2015).

In south-west England many sandy and gravel beaches experienced substantial retreat with sediment taken offshore; in some extreme instances this completely exposed underlying shore platforms (Masselink *et al.* 2016). This prompted a flurry of studies examining the role of this single storm season in dictating coastal change (Burvingt, *et al.* 2016, 2017, Castelle *et al.* 2015, 2017**,** Masselink *et al.* 2016, Pye and Blott, 2016, Scott *et al.* 2016). However, few of these studies (Bullard *et al.* 2019, Pye and Blott 2016) place these changes in their longer-term context, against either the years before or after this season. Pye and Blott (2016) note that the changes seen at Sefton only represented a small deviation from longer term trends of coastal change there, concluding that this single event alone was unlikely to have a substantial impact on longer term erosion.

In a study of a beach dune system on the Lincolnshire coast in the years following the storms, Bullard *et al.* (2019) found that the system recovered rapidly during the first post-storm year and that over four years the dunes had advanced further seaward than expected based on longer-term historic trends (Montruiel and Bullard 2012). However, the dunes are still yet to return to their pre-storm conditions. Similarly to Pye and Blott (2016), Bullard *et al.* (2019) found that despite the high energy conditions of this season, the change on this system represented only a minor disturbance relative to longer term trends.

The relative lack of a longer term (years to decades) view of storm driven extreme events in dictating coastal change is common amongst beyond just the 13/14 season and of UK coastlines. This is primarily a data driven problem due to a lack of high-quality shoreline and coastal monitoring data of sufficient temporal scope to place the impacts of storms in their longer-term context. Even in the UK, which has a relatively strong coastal monitoring heritage, the coastlines which have sufficiently high resolution morphological and

hydrodynamic data spanning decades, or even 5-10 years, are few (with the Sefton coast (Pye and Blott, 2016) being one of these few examples). This is unfortunate given the importance of the decades to centuries timescale for coastal management. In the UK this timescale is of particular concern for Coastal Change Management Areas, a concept introduced in 2012 as a policy means to mitigate the impacts of climate change and relative sea-level rise in additional to the already implemented Shoreline Management Plans (NPPF, 2019, Kirby *et al*. 2021).

1.5. Research aim and study regions.

There are three main challenges that this thesis seeks to tackle:

1. Instrumental records of storm surges are too short term in scope. This results in high uncertainty in risk-based approaches to coastal flood risk. Approaches to tackling this using sedimentary archives have largely been constrained to back-barrier deposits, limiting the potential locations where such data can be derived.

2. Sea-level change presents an important background signal to changes in storm surges and coastal evolution. Resolution of unanswered questions in regional relative sea-level histories is required to improve understanding of the relationship of past storms with sea level and changing climate and to determine the impact of these on coastal evolution.

3. The importance of coastal storms in dictating the evolution of coasts on timescales most relevant to coastal management (decades to centuries) is poorly understood due to a lack of high-resolution monitoring data on most shorelines.

To tackle these, this research aims **to explore how utilising combined methodologies of paleoenvironmental techniques, historical archives, geophysics, remote sensing, and**

instrumental data can help resolve these challenges even in regions which may be relatively data sparse.

Achieving this requires a study region where extreme sea levels and coastal storms represent both an appreciable coastal hazard and are already known to have a meaningful (albeit poorly quantified) role in governing coastal morphology. Further, it requires a location with diverse coastal morphologies with potential to record storms and a strong record of both historical and instrumental records of coastal storms to compare reconstructed storms. The UK fulfils these requirements (1.2 and 1.4). This work focuses on two UK regions, the north facing coasts of North Norfolk and south-west facing coasts of North Wales.

The North Norfolk coastline is dominated by extensive sandy beaches, sandy flats, and back-barrier salt-marshes. Positioned at the relatively shallow southern portion of the North Sea, this coastline is well documented to have had a long-standing relationship with large storm surges, including the 2013 and 1953 storms discussed above. Its north facing aspect makes it ideal for capturing low frequency high magnitude storms from the north such as the 1953 storm surge rather than the more frequent south-westerly storms. Its large potential wave fetch, and abundance of back-barrier environments and coastal dunes makes it ideal for exploring the potential of coastal dunes as a storm archive.

The coastlines of North Wales have great variety in their geomorphology, from sheer cliffs and high-energy beaches to extensive dunes and sandy estuaries. Most of the latter are constrained to the relatively sheltered areas surrounding the Menai Strait between the Isle of Anglesey and the Welsh mainland. The south-west facing coasts on the Isle of Anglesey contain several large dune systems (primarily Newborough and Aberffraw) which may also hold potential storm archives. Their south-west facing aspect gives them potential to hold archives which would otherwise not be recorded in Norfolk.

GIA models predict Wales has experienced minimal relative sea-level rise in the last 3000 years (Shennan *et al.* 2018). If true, this would make the regional ideal for storm

reconstructions for examining the potential role of changing storminess rather than relative sea level in governing extremes. However, the region remains one the most poorly understood in terms of provision of empirical Holocene relative sea-level data. This has led to mismatch between different GIA models (Bradley 2011, Peltier, 2002) and is one of the major unresolved questions in UK Holocene relative sea-level science (section 2.3). Resolution of this question has implications for the validity of different approaches to GIA modelling in predicting RMSL and in turn the role of RMSL in governing future storms. The sandy coastlines of south Anglesey are known to be relatively data sparse regarding morphological change, particularly when compared to systems such as Sefton or the North Norfolk coasts. This makes the region ideal for examining how different methods may be combined to reconstruct the relationship between storms and coastal change.

In each of these study regions, the research aims are as follows:

1. **To determine the potential of coastal dunes to act as sedimentary archives of coastal storms.**

2. **To place storm reconstructions in the context of relative sea-level change and to resolve the outstanding question of whether a mid- to late-Holocene relative sea-level highstand exists in North Wales.**

3. **To explore the potential of combining multiple approaches to reconstructing storms and coastal change for determining how changing hydrodynamic conditions may influence coastal evolution**.

1.6. Structure of thesis

This thesis is presented as a collection of peer-reviewed papers which are published or in review in internationally recognised journals. Chapter 2 comprises a review of key literature

that further sets the context for the following papers. Chapters 3-5 presents three papers which each tackle the challenges outlined in 1.5 and addresses the three research aims.

Chapter 3 presents the reconstruction of coastal storms using coastal dunes and historic archives on the North Norfolk coast. This research seeks to tackle the first objective by exploring the potential of coastal dunes to act as archives to past storms in places where archives may be more subtle than found by Cunningham *et al.* (2011). This is undertaken by applying a novel methodology utilising a portable version of optically stimulated luminescence dating (OSL). Portable OSL (POSL) provides a rapid relative age profile through a coastal dune. Combined with sedimentological and documentary data this can allow for erosive episodes in coastal dune profile to be identified as potential storm impacts (section 2.2.5).

Chapter 4 presents a reconstruction of Holocene relative sea–level change in North Wales based on based on a reconstruction from a 3000-year-old salt-marsh. This work serves a dual purpose. Firstly, it provides important relative sea-level context for the work undertaken in Chapter 5. Secondly, it tackles a longstanding question over the validity of a mid-Holocene relative sea-level highstand in North Wales with the goal of providing improved validation for glacio-isostatic adjustment (GIA) models. This is achieved using a now well-tested methodology utilising salt-marshes as late-Holocene tide gauges (Barlow *et al.* 2013) combined with relative sea-level index points from a freshwater marsh.

Chapter 5 reconstructs changes in the coastal evolution of a beach-dune system at Traeth Penhros, Anglesey. This reconstruction combines the approach used in Chapter 3 with historic maps, GPR, remotely sensed shorelines and historic datasets to explore their combined potential for quantifying the role of storms in dictating annual to decadal scale coastal change.

The supplementary material, as included in the published or submitted works, is included in at the end of each chapter.

Chapter 6 draws from conclusions of the previous chapters. It identifies research impacts, limitations and sets out possible directions for future research. Chapter 7 closes by summarising the key outputs of this research.

Chapter 2.

Literature Review

This literature review provides additional context for the works included in this thesis. Section 2.1. appraises current understanding of storms and extreme sea levels in recent centuries, with particular emphasis on the extra-tropical storms in the North Atlantic due to their direct relevance to this study. Section 2.2 explores approaches to the reconstruction of storms to provide further context for Chapters 3 and 5. Section 2.3 discusses unresolved challenges in UK regional relative sea level as context for Chapter 4. Section 2.4 examines the current understanding of coastal morphological response to storms as context for Chapter 5.

2.1. Storminess and extreme sea levels in a changing climate

In the context of coastal studies, the term storm (sometimes also cyclone or typhoon) is broadly used to refer to oceanic and atmospheric events typically lasting from hours to multiple days that feature substantially higher energy conditions than typically seen each year (Haigh *et al.* 2015). Distinction is often drawn between tropical and extra-tropical storms. Whilst the specific meteorological characteristics and scale of these may differ, particularly in terms of their impact on coasts and shorelines, they share many common traits. Both are associated with occurrence of strong winds, and as a result large waves, and both can produce a phenomenon known as a storm surge.

Storm surges, sometimes also termed tidal surges or storm tides, are ephemeral rises in ocean water that occur during storms. They arise from a combination of strong onshore winds and an inverse barometer effect associated with low pressure. This raises the sea surface by 1cm for every 1mB reduction it atmospheric pressure (Pugh and Woodworth 2014). These combine to drive nearshore sea levels higher. For populated coastlines, storm surges represent the principal geophysical / hydrometeorological hazard. NOAA (2007) note

that storm surge driven flooding is responsible for more deaths than any other component of US hurricane hazards (e.g., strong winds, large waves) in the last century (Horn, 2015).

For the UK and other North Sea coastlines the deadliest coastal storm of the last century (31st of January 1953) was so impactful due to a large storm surge component (Baxter, 2005). Storm surges typically only represent appreciable coastal hazards when coincident with higher astronomical tides. This occurred in the case of the 1953 North Sea storm surge, where the surge component arrived alongside spring high tides concurrent with the progression of the North Sea tidal amphidromes (Baxter, 2005). Due to their interaction with astronomical tides, distinction is often drawn between the surge component itself (the increase in sea level above the astronomically predicted level) and combined effect of the surge and astronomical tide in concert (often referred to as extreme sea level). The specific terms used to describe the distinction between extreme sea level and storm surge in literature is discipline dependent. For this thesis (primarily Chapter 6) the language traditionally used in oceanographic approaches to tide gauge analysis is employed (Haigh, 2009). The term “tidal residual” or simply “residual” is used in place of storm surge. The term extreme sea level is used to describe the combined effect the residual with the astronomical tide. It should be noted the term extreme sea level does not only capture storm driven extremes, but those also driven by geophysical processes such as tsunami, though for coastlines with no contemporary appreciable tsunami hazard, this distinction is moot.

The nature of storms varies by ocean basin and the climatological and atmospheric systems that exist within that basin. For the north Atlantic Ocean, the primary major ocean body of concern to this study, there is great deal of spatial variability in storm magnitudes, frequencies, and pathways. The most noteworthy distinction in the north Atlantic is between the extra-tropical storms of the higher latitudes, which have their impacts on north-eastern USA and north-western European shorelines (Burvingt, 2018), and the tropical storms of the lower latitudes which primarily affect the Caribbean and eastern USA. For the extra-tropical

storms of the north Atlantic most storm activity is focused on the northern hemisphere winter from October to March.

North Atlantic extra-tropical storms have been shown to exhibit a link with large-scale atmospheric patterns. The most well studied of these is the North Atlantic Oscillation (NAO) (Wanner *et al.* 2001. Feser *et al.* 2015). The NAO is a large-scale atmospheric pressure differential between a relative high-pressure centre over the Azores and lower pressure over sub-polar Iceland (Hurrell 1995). The NAO is parameterised by the difference in atmospheric at sea level pressure between the Icelandic Low and the Azores High. High NAO indices (termed positive NAO) phases are associated with wetter and stormier winter weather in northwest Europe and Low NAO (negative) with below average winds and displacement of storms towards the Mediterranean (Wanner *et al.* 2001. Feser *et al.* 2015). Figure 2.1 shows the December to March (DJFM) NAO index since the early 19th century. It demonstrates substantial temporal variability and multi-decadal variations with the most noteworthy positive phases in the 1910s, 1930s and 1990s. The NAO index has been shown to explain one-third of variability in winter storm intensity in north-west Europe, with decreasing ability to explain variations prior to the 1970s (Feser *et al.* 2015).

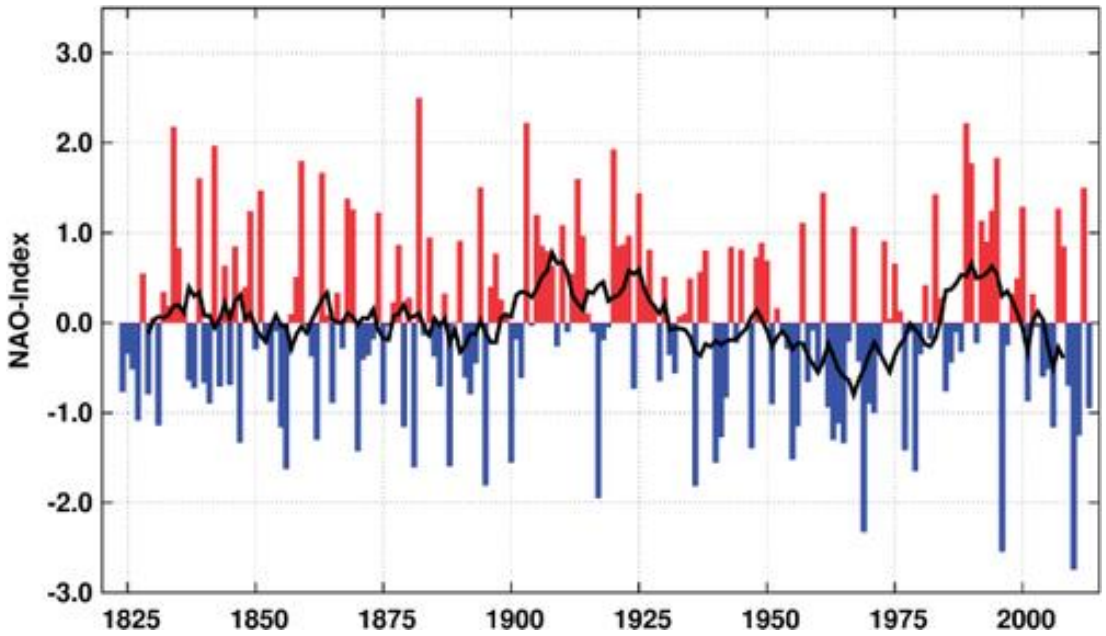

Figure 2.1. DJFM NAO index since 1823 from Feser et al. (2015) after Jones et al. (1997)

The study of past storm magnitudes, and their relationship to larger scale atmospheric phenomena or to longer-term climatic changes is contingent upon the availability of data on those storms. In a review of extra-tropical storminess in the north Atlantic, Feser *et al.* (2015) compiled the findings of 138 studies examining storminess from the perspective of the north-east Atlantic, British Isles, North Sea, Baltic Sea, and Central Europe. 75 of these were based on observations made from marine or coastal monitoring data including meteorological observation stations and tide gauges. The remaining 63 studies utilised hindcast modelling approaches to reconstruct past storm magnitudes and frequencies.

Feser *et al.* (2015) found that whilst most studies show good agreement on the existence of decadal scale fluctuations in magnitude of storm events in the last two centuries, there is substantial contradiction over the existence over any longer-term trend related to climate change. This contradiction primarily exists between observation-based and modelled datasets, with models generally suggesting an approximately linear increase in storm wind speeds and magnitude in the last 60 years. Observational data contradicts this, particularly data derived from coastal regions through tide gauges.

Studies such as Woodworth and Blackman (2002) in their examination of the Liverpool tide gauge data (one of the longest records available in northern Europe); Pugh and Maul (1999) in a similar study of UK tide gauge records; and Marcos *et al.* (2009) in a study of Mediterranean tide gauges all found that any observed increase in the magnitude of extreme sea levels could only be explained by increases in RMSL rather than any increase storm frequency or intensity. Further, pressure-based indices from meteorological observations also show no significant increase in storm magnitude in the last two centuries. Feser *et al.* (2015) suggest these differences may be a result of the difference in the timescale of these respective studies, with modelling approaches generally focussing on the period after the 1960s, a period which is dominated first by negative NAO indices until a strong positive period in the 1990s. A point of agreement between most of the observational studies included in their review is that they are limited by both the quality and quantity of data on

which they are based. Zhang *et al.* (2000) make note of limitation of the length of records on storms at the coast, with at least 40 to 50 years being required to reliably estimate underlying trends in extreme sea levels and if they are related to increasing storm magnitude or not. This conclusion on the role of these datasets in climatological studies is not dissimilar to those discussed in 1.2 regarding the application of such datasets in risk management (Van den Brink *et al.* 2005).

Debate over the respective role of storm magnitude-frequency and RMSL is not exclusive to north-western Europe and can be seen in other major ocean regions around the world (Needham *et al*. 2015). It is clear there is still a need for improved understanding of both past storm events at the coast and regional RMSL to resolve these debates. Regionally, this is crucial to better understand the future trajectory and impact of changes in the NOA.

2.2. Archives and tools for storm reconstruction

As discussed in 1.2 and 2.1 it is imperative that records of coastal storms be extended beyond the limited temporal extent of instrumental data such as tide gauges and wave buoys. This section explores some of the sources by which such data has or may be obtained.

2.2.1. Historic sources

Historic records are a viable source of information on past storms that have hitherto seen little application to improving understanding of coastal risk. Given their potentially destructive impact at the coast, storms are particularly likely to be recorded in “historical memory”. This "historical memory" can potentially be recorded in documents and records. Garnier *et al.* (2018) note that such records have potential to recreate complete time series of extreme events if such datasets are compiled and placed in the context of other numerical data. Garnier *et al.* (2018) divide such sources into five categories.

- **Municipal archives:** sources held in a town or district, most likely under the care of a local governing body. In the UK such archives are now typically held in local or regional libraries.
- **State archives:** sources usually held with central government. Older sources may be in the care of libraries, though often are held within specific government archives.
- **Private archives:** sources held by private enterprise, organisations, or businesses. These are usually records associated with work for which the organisation was contracted. Garnier *et al*. (2018) give the example of the Bedford Level Corporation in the UK who were contracted for the levelling of the Fens in the UK. These records are now held in the Cambridge Archives.
- **Scholarly books:** Whilst academic journal articles are typically easily searched through online databases and repositories, scholarly books are often not included, with these works often held in university libraries. These books may have been written by local scholars who made observations of storms and their impacts or were themselves scientists in the 19th century and early 20th century.
- **Navy / port archives:** Due to their implicit interest in the coastal zone Naval, fishing and trade ports keep records of observations of large events that may have had military or economic impact.
- **Press:** Local and national press are likely to record coastal storms that have noteworthy socio-economic impacts. Where such records are held will vary depending on the specific source; in the UK however most newspaper reports are now held in local libraries.

Despite this range of potential sources of past storms, these datasets have seen little application in peer-reviewed studies of coastal storms. Instead, such sources are generally used to provide context for the study of a specific storm rather than to provide an extensive storm record (Clemmensen *et al.* 2014, Cunningham *et al.* 2011, Pye and Blott, 2007). Notable exceptions to this are the works of Lamb (1977), Zong and Tooley (2003). In an

interdisciplinary work, Lamb (1977) explored evidence for climatic changes on timescales of the entire quaternary and through into the modern instrumental period. In chapter 18 of this seminal work, Lamb (1977) extensively explores climate since the beginning of instrumental records including examinations of storm tracks and patterns, particularly in the North Atlantic where instrumentals were relatively abundant at the time. Zong and Tooley (2003) quantified flood frequencies in three different coastal portions of Britain and their storm tracks inferred or correlated with available meteorological records. From this record Zong and Tooley (2003) identified common distinctive pathways for the most damaging storms in each region and were able to identify increasing storm driven flood frequencies in the south and south-west coasts of the UK in the last 200 years. However, they note two possible flaws with such data. Firstly, that not all storms will result in coastal flooding, potentially concealing storms from such and archives. Secondly, that such sources provide little means to accurately determine storm magnitude without concurrent instrumental data. They also note the importance of verifying storm occurrence across multiple sources, both to corroborate their existence and given context of their spatial extent.

Such sources are utilised in Chapter 3 and Chapter 5 to compile complete storm archives for Norfolk and North Wales respectively.

2.2.2. Sedimentary archives: Washover

A common avenue by which the lack of storm data has been tackled is using sedimentary archives. Sedimentary archives of past storms primarily recorded by sediments deposited inland and above the normal limit of wave-deposited sediments along a coast, or by erosional facies preserved in coastal landforms. These records of palaeostorms are largely restricted to the last 5,000–6,000 years, or since termination of the region's Holocene marine transgression (Nott, 2009).

One of the earliest studies to find evidence of coastal storms using sedimentary evidence was Emery (1969). Though this study was primarily concerned with limnology, they noted

discontinuous coastal deposits held within a freshwater kettle lake which they determined represent overwash from a nearby coastal barrier during past storms. It was several decades on from this study before investigations attempting to either quantify or date past storms from such deposits to enhance the storm record began to be published in any great number. These studies built on mainly from work by Aigner (1985), Duke (1985) and Davis *et al.* (1989) which were amongst the earliest studies to describe the sedimentary characteristics of high energy storm deposits in otherwise low energy environments such as coastal freshwater lakes, salt-marshes, lagoons, and other back-barrier environments. Davis *et al.* (1989) noted that in Florida past hurricanes had produced graded or homogenous facies of sand, gravels, or mud within the finer clastic sediments of late-Holocene coastal lagoons. Whilst important for their description of storm deposits, these earlier studies were limited by a lack of chronology for the sedimentary evidence of these past storms, primarily trying to determine the age for these events based on comparison with documentary evidence of their occurrence.

Liu and Fearn (1993) built upon this description of sedimentary records of coastal storms in a study of Lake Shelby, a near coast freshwater lake in Gulf State Park on the Alabama coast of the Gulf of Mexico. Sediment cores were taken from this lake and described. They identified five storm deposits in their cores, distinguished from surrounding gyttja and lagoonal lake sediments as relatively coarse sands. These sand layers, typically of 0.1 – 1 cm thickness, showed close mineralogical and sedimentological characteristics to the sandy coastal beaches and dunes to the lakes south. They concluded these sediments represented deposits washed over from the beach and dunes during past hurricanes.

This study was novel due to the inclusion of radiocarbon dating of stratigraphic units in these cores to provide chronological context for these storms with storm deposits dated to 3.2, 2.6, 2.2, 1.4 and 0.8 ka (^{14}C year). In 1979 hurricane Frederic (a category 3 hurricane), was observed to leave a sand layer only in the most nearshore part of Lake Shelby. The cores taken by Liu and Fearn (1993) were taken 1 km further inland than this 1979 deposit. They

suggested that the layers found in these cores were likely from events of a greater magnitude of category 4 or 5. Based on this they suggested the recurrence of a category 4 or 5 hurricane on this coastline was approximately every 600 years, and that such a hurricane was likely to strike the Alabama coast in the next 100 years.

Liu and Fearn's (1993) work sparked many papers in the decade that followed attempting to further explore the potential of extrapolating extreme hurricane occurrence from back-barrier coastal sedimentary records on the east coast of the USA. Many of these later works moved away from coastal freshwater lakes onto marsh-peat sequences in back-barrier salt-marshes (Bravo, *et al.* 1997, Kelley *et al*. 1995, Orson *et al.* 1998, Shinn *et al.* 1993, Roman *et al*. 1997). Salt-marshes offered a key advantage over freshwater lakes due to their greater hydrological and sedimentological connectivity with coastal processes. Storm surge driven flows through overwash and through inlets can result in the transport of fronting barrier sediments into salt-marshes where they can be deposited as sandy layers in the otherwise peaty and marsh sequences (Donnelly *et al.* 2001, Kelley *et al*. 1995). Provided normal salt-marsh sedimentation can continue after the event these deposits are then preserved as a record of storm occurrence.

The superior proximity and connectivity with marine processes of coastal marshes allows for events of smaller scale to be recorded in addition to more extreme events. Donnelly *et al.* (2001) demonstrated this in their study of hurricane landfalls in New England, USA. They were able to reconstruct five category 3 (based on comparison with historic records of their occurrence) or greater events dating to 1635, 1638, 1815, 1869 and 1938 (CE). Chronological context was provided by radiocarbon dating of the peaty sediments above and below the storm deposits, an approach which had now become commonplace amongst such studies due to the suitability for bulk dating of organic sediments in coastal settings.

In addition to these large events, they were also able distinguish a record of a lower magnitude event; a category 2 storm in 1954. As the surge associated with this smaller event was measured with tide gauge records (~3 m) they were able to tie this event into a

specific quantification of extreme sea level and therefore infer that the surges associated with the older events must have been of greater magnitude. This was one of the first studies to be able to tie these reconstructions directly to an extreme sea level. Novel in this study was the use of historic coastal photography in the validation of these overwash deposits, with both the 1938 and 1954 events having accompanying photography verifying the existence of overwash fans at the marsh surface. Studies of storm reconstruction from overwash deposits continued through the following decade, with focus still mostly given to hurricane landfalls in the eastern USA (Donnelly 2005, Donnelly and Webb 2004). However, some studies have extended these methods to other regions vulnerable to storms including east Asia (Monecke *et al*. 2008, Woodruff *et al*. 2009) and the Mediterranean coasts of Europe (Dezilaeu *et al.* 2011).

2.2.3. Sedimentary archives: Barriers

Back-barrier landforms capable of preserving past storms are not ubiquitous across the world's coastlines. Indeed, it is largely because of this that back-barrier reconstructions of storms have seen limited application beyond the east coast of the USA which has a relative and rich abundance of large coastal barriers and low energy back-barrier environments over which hurricane pathways directly pass. To tackle this, some studies have explored reconstructing past storms from erosional and depositional facies recorded in the barriers themselves. Buynevich *et al.* (2006) attempted an approach to reconstruct storm activity using relict beach scarps in a gravel barrier. In this approach they utilised optically stimulated luminescence (OSL) dates on preserved erosional facies in a prograded barrier sequence in the Gulf of Maine. Until this study, this area of the west Atlantic Ocean which had little data on past storms and storm climate owing to the relative lack of back-barrier settings along this coastline.

Through this work, Buynevich *et al*. (2006) reconstructed beach erosion and retreat from events in 400, 1560, 1660 and 1800 CE. They were also able to suggest that in the past 500 years extra-tropical storm intensity and frequency had increased relative to the 1000 years

prior. Crucially, this study illustrated the potential of reconstructing storms, not only from depositional facies in back-barrier deposits but from erosional facies in the barriers themselves. It was also amongst the first studies utilise chronologies derived from OSL dating methods for coastal storms as well as to utilise geophysical techniques (in this instance ground-penetrating radar [GPR]) to locate erosional storm facies in coastal barriers.

Attempts have also been made to reconstruct storm chronologies based on depositional records recorded in beach ridges. By way of trenching and radiocarbon dating, Hayne and Chappell (2001) were able to identify individual storm units amongst soil and beach deposits and determine the frequency of intense storms capable of transporting cobbles over the last 5000 years. Nott *et al.* (2009) successfully reconstructed storm impacts using OSL chronologies of coarse sand beach ridges in Queensland, Australia.

Despite this some authors have since questioned the assumed processes by which beach ridge depositional records are formed, given that the most intense events are more likely to be erosional and erase past depositional records of storms (Scheffers *et al.* 2011, Tamura, 2012). Storm chronologies have been produced from many types of coastal barrier landforms including coral rubble ridges (Hayne and Chappell, 2001, Nott *et al*. 2009), cheniers and shelly beach ridges (Mason 1993, Rhodes, *et al*. 1980), sandy beach ridge plains (Forsyth *et al.* 2010, Nott *et al*. 2009) and shell and gravel ridges (Nott 2011).

2.2.4. Sedimentary archives: Coastal dunes

A shortfall common to both overwash and barrier-based reconstructions has been the difficulty in quantifying surge and extreme sea level magnitudes for these events. Amongst the overwash studies, this has only been possible where the reconstructed event also appeared in historic monitoring datasets such as tide gauges (Donnelly *et al.* 2001). Additionally, many barrier-based approaches do not actually reconstruct single events themselves, but rather reconstruct periods of more intense storminess hundreds or thousands of years in the past. Whilst these may provide important context for coastal flood

hazards and coastal evolution, it is of little practical use for risk-based analysis or for determining the relative role of RMSL and storminess in driving current trends. To overcome this, it is necessary to pursue approaches allow for the reconstruction of individual events with a more robust indication of magnitude for events in the last few centuries.

Some authors have suggested that coastal dunes may represent future archives of such data (Cunningham *et al.* 2011). Coastal foredunes have a ridge-like morphology which is aligned parallel to the shore and may range in height from 1 m to potentially 30-35 m in extreme instances (Hesp 2002, Masselink *et al.* 2011). The individual characteristics of foredunes is a function of a wide range of factors including sand supply, vegetation type and abundance, the rate of aeolian sand accretion/erosion, the nature of local the wind/wave climate, the magnitude-frequency of extreme sea levels and hence dune scarping and overwash, the overall beach barrier state (stable, prograding or retreating), mean sea-level changes, and anthropogenic impacts (Hesp 2002). At its most basic level the morphodynamic relationship of coastal foredunes with their fronting beach can be described as the balance between constructive aeolian processes and marine processes which may be both destructive and constructive (Pye *et al.* 2007). Storm surges represent the most significant marine events which may influence dune morphodynamics and geomorphology, primarily as agents of erosion, though depositional landforms may also form because of their impact.

The way dune systems respond to storm surges and extreme sea levels largely depends on an event's magnitude. In relatively minor events waves may erode sand from the upper beach, resulting in a fall in the beach level and a strong negative beach sediment budget. In larger events however, where a storm surge reaches a sufficient elevation that waves may physically impact the dune face, sand can be removed directly by marine excavation forming a dune scarp; a steep slope formed at the dune face (Figure 2.2A.) (Morton and Sallenger 2003, Pye *et al.* 2007). Upper beachfaces associated with dune scarps are typically composed of coarse-grained lag or heavy-mineral deposits concentrated along a flattened

topographic profile which may be subsequently buried following dune recovery (Dougherty 2014). In the most extreme instances foredunes may be overtopped, flattened, selectively breached or even completely eroded (Hesp 2002, Pye *et al.* 2007). There are also several mechanisms of post-event erosion, including slumping and wind scour from exposed sand faces (Pye *et al.* 2007).

Despite being net erosive processes, not all the potential morphological consequences of storm surges for coastal dunes are erosional. Depositional features associated with marine influence on coastal dunes, and barriers moreover, are described by Morton and Sallenger (2003) and include perched fans and washover terraces (see Figure 2.2D and 2.2E)

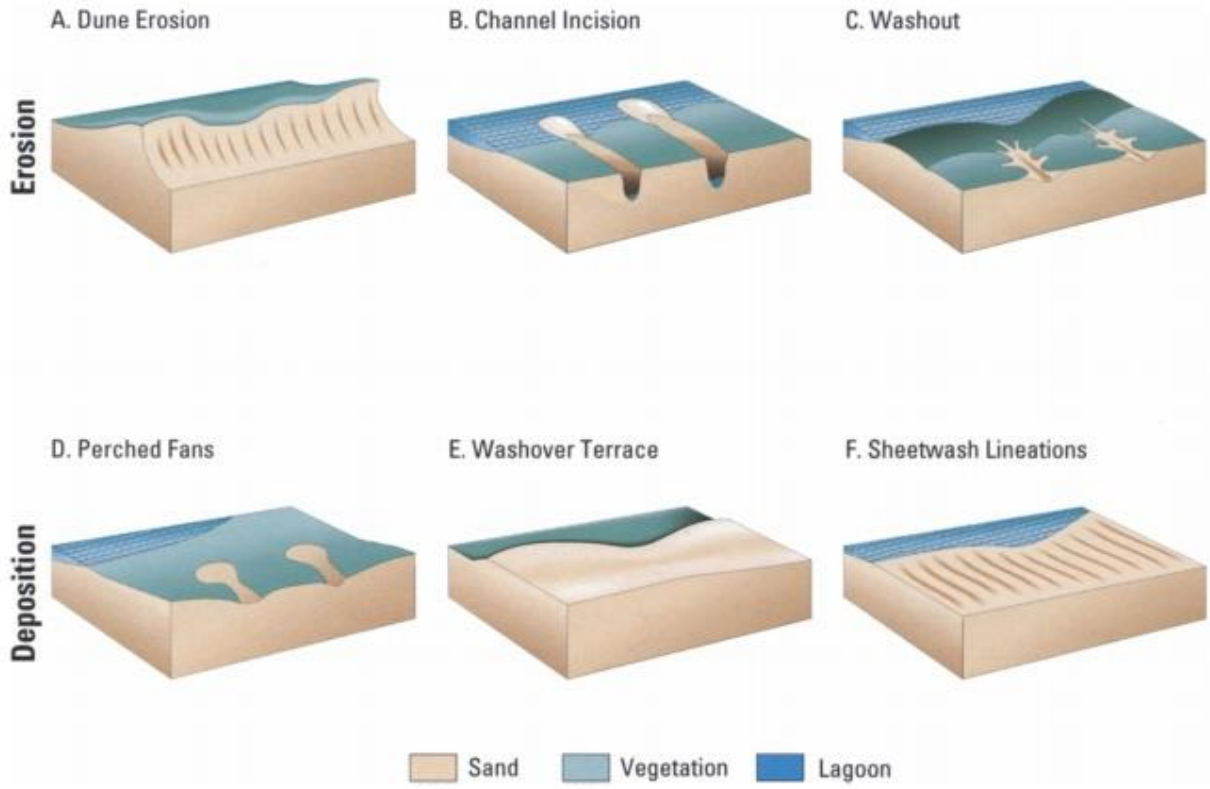

Figure 2.2. Range of erosional and depositional landforms which form because of extreme sea levels on sandy beaches and barriers. A, D & E are forms which may occur on dunes. From Morton and Sallenger (2003)

Perched fans are shore perpendicular, lobate to elongate features of marine washover. Isolated perched fans may occur on dunes where water level exceeds the lowest dune elevations but is blocked by higher elevations (Morton and Sallenger 2003). If perched fans

are spaced sufficiently close together then they may merge to form a washover terrace; a shore parallel elongate deposit which forms where land elevations are relatively uniform alongshore and lower than the maximum storm surge (Morton and Sallenger 2003).
In the event any of erosive marine incursion, provided dunes are not protected by any significant man-made structures such as sea walls, foredunes will release sand slowing the rate of beach lowering, limiting wave energy, and slowing frontal dune erosion. During subsequent fair weather, waves may gradually transport sand back on to the beach so aeolian transport may allow the dunes to rebuild (Pye *et al.* 2007), subsequently concealing and burying surge related erosive and depositional landforms.

Foredunes may follow several possible courses in their recovery. They may revegetate and reform to various degrees by dune crest deposition, scarp slumping or filling and revegetation; gradually retreat as a steep, scarped, landward rebuilding foredune or be re-established as a new foredune zone or ridge some distance behind the erosional foredune (Hesp 2002). It should be noted storm impacts are likely to be variable alongshore, usually reflecting variations in local bathymetry and dune geomorphology (mainly crest height and width) and storm wave dynamics such as wave focussing (Pye *et al.* 2007).

Cunningham *et al.* (2011) examined a 1 km exposure left in a Netherlands foredune system by a large storm surge in 2007 which resulted in 10-15 m of lateral dune erosion. Within this exposure they found a discontinuous layer of marine shells within the sand which was ~15 cm thick and in most locations exceeded +4 m above MSL peaking at + 6.6 m above MSL. Due to the presence of the shells and bivalves within the shell layer the study ruled out the possibility of aeolian transport. Furthermore, the convolute bedding structure was considered indicative of saturation by water and as the layer was held at elevations substantially above mean high water (~ 0.9 m) the sediments were concluded to have been storm surge deposits. Through the use of ground penetrating radar (GPR) Cunningham *et al.* (2011) found that this shell layer extended 1 km inland and was proposed to have been

deposited when water from the storm surge entered the inner dunes through gaps creating extensive perched fans.

The shell layer was then dated using optically stimulated luminescence (OSL) techniques. Despite the difficulties commonly associated with dating flood deposits by OSL, for instance the uncertainty over whether the quartz in flood deposits is reset during deposition potentially resulting in over estimation of age, Cunningham *et al.* (2011) did extract a reasonably robust age from the deposit of 1760-1785 CE. The study compared these dates with historic records of storm surges in the area and found documentary evidence of two surges which occurred on consecutive years in 1775 CE and 1776 CE providing some validation that the sediments were indeed deposited by a storm surge. This study was noteworthy in that it showed the potential for deposits of sediment held at elevation in dunes to act as a record of historic storm surge elevation, in this case with the maximum height at which the deposit can be observed representing a minimum storm surge height. This method however requires replication in other locations to determine if the approach is both valid and widely applicable for informing coastal flood risk. It remains unclear if such an approach may be more widely applicable to other dune fields, particularly where the sedimentary evidence of past events preserved in dunes may be more subtle than a clear shell layer.

2.2.5. Dune reconstruction tools: OSL and POSL

The studies above examining reconstruction of storms from sedimentary archives all rely on chronological context provided by geochronological techniques. Some of the most widely used techniques include radiocarbon (Barlow *et al.* 2013) uranium series (Hearty *et al.* 2007) and, for younger sediments (0-200 y) fallout radionuclides (Marshall *et al.* 2007). Radiocarbon has found substantial use in storm reconstructions from the Holocene from salt-marshes, due to their high biogenic composition. However, radiocarbon has significant issues when used in reconstructions of the period from ~1350 CE to 1850 CE, the Little Ice Age (LIA) (Maan 2002). This period was characterised by significant oscillations in global atmospheric carbon which results in a great deal of so called “wiggle” in the calibration curve

(Reimer *et al.* 2009). Furthermore, radiocarbon is constrained to sediments with well-preserved biogenic material making it difficult to apply to more minerogenic landforms such as coastal sand dunes; which have been highlighted as potential sedimentary archives of extreme sea-level magnitudes during the Little Ice Age and the late-Holocene moreover (Cunningham *et al.* 2011). With the small temporal range of fallout radionuclides and uranium series constrained largely to carbonate sediments many of the studies mentioned above instead utilised luminescence dating

Luminescence dating has been applied in coastal settings since its inception (Bateman 2015) with such settings having been used in the original development and validation of thermally stimulated (TL) and optically stimulated luminescence (OSL) techniques (Jacobs 2008). It is a radiometric technique relying on the use of accumulating signal within quartz and feldspar grains, common and durable materials in coastal sedimentary settings both offshore and onshore. Being able to directly date the occurrence of sediment deposition, its long potential temporal range (potentially in excess of 200 ka^{-1}), and its reporting of dates in calendar years are amongst its chief attractions (Jacobs 2008). However, it was noted by Jacobs (2008) that the technique has yet to obtain routine large-scale use in coastal settings; citing a lack of precision compared to radiocarbon and uranium series as a key reasons for this.

The fundamental basis for luminescence dating is that in natural settings buried mineral grains are subject to natural irradiation, either from surrounding radionuclide decay or cosmogenic radiation. This ionizing radiation causes the production and displacement of free electrons into traps within imperfections of the crystal lattices of quartz and feldspar grains (Aitken 1998). This accumulation of electrons within these traps continues over time and is proportional to both the rate of irradiation and the time of exposure.

This stored radiation dose can be evicted by exposure to either intense heat (Thermoluminescence or TL) or light (OSL) which releases the electrons from these traps; a totally evicted sample is referred to as “bleached” or “reset”. The eviction of charge initiates a

process termed radiative recombination; this releases excess energy as photons, producing a measurable luminescence signal (Lian *et al.* 2006). In each crystal, there are several forms of trap. Some can be emptied very easily when the grains are stimulated by light, though for others, light exposure has little effect. Almost all traps are emptied by sufficient heating (~500 °C). At ambient temperatures (~20 °C), some traps only hold charge for a few days or less, while others can hold electrons for millions of years or more. The latter types are termed deep traps, it is these traps that have lifetimes sufficiently long for Quaternary dating (Lian and Roberts 2006).

It is the resetting of the stored radiation dose by natural light or intense heat during erosion, transport or formation and its subsequent accumulation upon burial which allows for the derivation of time since burial or last heating (see Figure 2.3) (Aitken 1998). In sedimentary settings this means luminescence dating can be effectively used to determine the time of formation or alteration of sedimentary landforms (Lian and Roberts 2006). Full bleaching of the luminescence signal to zero between sediment transport and deposition is vital to derivation of correct burial ages, fortunately full zeroing can occur when exposed to only 30 seconds of direct sunlight (Bateman 2015).

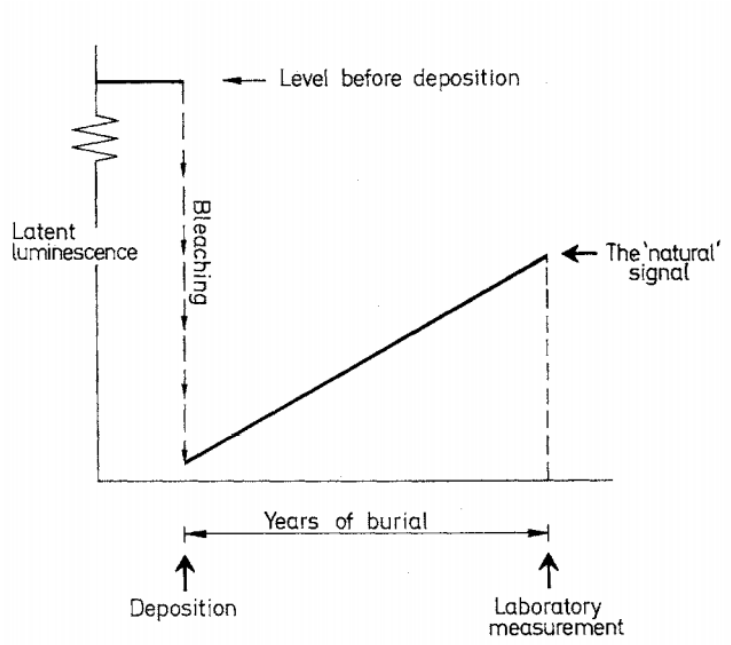

Figure 2.3. Illustration of the principle behind luminescence signal resetting and age

derivation. When grains are exposed to sunlight by erosion the latent luminescence is "bleached". Upon deposition stored luminescence increases proportionally with time and background dose rate. This "natural" signal can be measured by releasing the luminescence through stimulation by heat or light. From (Aitken (1998))

In simple terms, this phenomenon of accumulating radiation dose means that for two samples subjected to the same rate of background irradiation the sample with greater accumulated radiation dose is likely older than a sample with a smaller dose (Bateman 2015). Therefore, if it is possible to measure both the dose rate of background radiation acting on a sample and the total radiation dose accumulated within the sample since burial (termed the palaeodose) it follows that time since burial can be calculated according to Equation 1.

Equ 1. $$\text{Time since burial(a)} = \frac{\text{Accumulated Radiation/Palaeodose(Gy)}}{\text{Annual Radiation Dose Rate (Gya}^{-1}\text{)}}$$

Provided samples have been collected and transported in a way that results in no light contamination, palaeodose is determined by evoking the "natural" luminescence by stimulating or specific wavelengths of light (in OSL) or heat (in TL) and measuring the emitted luminescence using a photomultiplier. To determine the palaeodose in Grays (Gy) from the measured natural signal it is necessary to understand the way the mineral grains respond to increasing doses of radiation and how this relates to the luminescence released upon stimulation. This is achieved by subjecting the bleached grains to known radiation doses from a calibrated source (a process termed "regeneration") and subsequently stimulating produce luminescence. From this a dose-response curve (or growth curve) can be constructed (see Figure 2.4). Using this curve, and the natural signal, the palaeodose can then be estimated (Lian and Roberts 2006). Since laboratory radiation sources typically only expose the sample to specific types of radiation, often beta or gamma, whereas in the natural environment the sample is exposed to alpha, beta, gamma and cosmogenic radiation, the palaeodose estimate produced is therefore more commonly and accurately referred to as the "equivalent dose" (symbolised by D_e) (Lian and Roberts 2006).

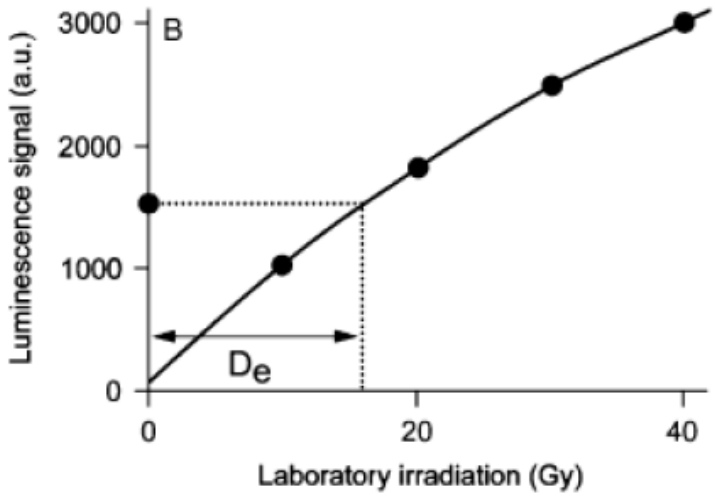

Figure 2.4. A dose-response curve (or growth curve) of laboratory radiation (Gy) against luminescence signal (arbitrary units) showing how D_e is determined from such a curve. From Wintle (2008)

There are a number of ways to determine the background dose rate for age derivation; either through use of a portable gamma spectrometer in the field, measurement of alpha, beta and gamma counts in the lab, or through direct measurement of radionuclide content, often using inductively coupled mass spectrometry (ICP-MS) (Bateman 2015). Several factors can complicate this assessment. For instance, it is necessary to estimate the average water content over the entire period of sample burial as water can absorb or attenuate radiation. It is also necessary to establish if at any time since deposition/heating, the U-series decay chain has been in a disequilibrium (Lian and Roberts 2006). Methods of dose rate determination have remained similar in recent decades (Duller 2004).

Prior to 1980 D_e was largely determined by TL, however since then the use of OSL for quartz grains and infrared stimulation (IRSL) for potassium feldspars has become increasingly prevalent (Wintle 2008). This is especially true for geoscience applications where optical methods have largely superseded TL due to the better bleaching of the traps measured by optical methods than those measured in TL (Lian and Roberts 2006). The only particular disadvantage of optical dating to thermal is that, during measurement, there is no way to separate the luminescence originating from thermally stable traps deep traps from

that originating from thermally unstable traps. The latter are filled during irradiation in the lab but do not remain filled lengths of time relevant to dating purposes. This issue is relatively simple to overcome by heating prior to measurement (Lian and Roberts 2006). The required preheat temperature is usually determined by way of a preheat plateau test, a simple test where D_e is determined for a sample under a range of different of different preheats so that any variations in D_e with preheat are evident (Murray and Wintle 2000).

The exact nature of method and mineral used for given sample varies with many factors including the nature of the environment from which it was sampled, the type of material sampled, and the likely age range of the sample. Broadly speaking however, quartz is now considered to be the preferred material, particularly for dating sediments as young as the Holocene due to a phenomenon of loss of luminescence signal in feldspars upon storage termed anomalous fading. This can result in the underestimation of age in feldspars (Wintle 2008). Though the relative suitability of different methods and mineral choice is more complex and generally situation specific, the respective merits of each mineral choice are appraised at greater length by Wintle (2008).

Traditionally the growth curve used to determine D_e in optical dating was constructed by using multiple sub-samples (small discs termed aliquots), each being given a different regeneration dose and the results then combined. This approach has largely been superseded by approaches which only require a single aliquot to determine the entire necessary range of the growth curve (Wintle 2008). Single aliquot approaches are not only more time and resource efficient but do not suffer from the issues of multiple aliquot approaches; namely the potential introduction of noise and the need for normalisation due to potential differences between aliquots resulting from differing numbers of grains or grains with differing luminescence brightness (Duller 2004). The development of single aliquot methods was particularly important for the dating of quartz where the scatter about the growth curve using multiple aliquots was substantial (Duller 2004). In particular, the optical

dating of quartz was revolutionised by the development of the single aliquot regenerative (SAR) dose protocol (Murray and Wintle 2000, Wintle *et al.* 2006).

SAR is a method for determining D_e using only a single aliquot. Prior to the development of SAR, OSL dating of quartz was significantly hindered by issues surrounding changes in luminescence sensitivity; the amount of luminescence emitted for a given radiation dose (Duller 2004). It had been noted that the sensitivity of quartz grains can change during laboratory irradiation and that the amount of change can vary greatly from one sample to another. The SAR method proposed by Murray and Wintle (2000) was developed primarily to combat this issue of changing sensitivity (Duller 2004, Murray and Wintle 2000, Wintle 2008).

In the Murray and Wintle (2000) SAR the natural OSL signal is measured first (symbolised by L_N) as a result bleaching the light sensitive luminescence signal from the aliquot. The dose response curve is then determined by an iterative process of regenerating the grains with known radiation doses and measuring luminescence from the sample with different levels of irradiation. The level of irradiation in each of these regenerations (R_x) is chosen to produce OSL signals (L_x) bracketing L_N allowing for portion of the curve surrounding L_N to be properly characterised, producing a more accurate D_e. After the measurement of each regeneration the aliquot is tested for any changes in sensitivity; this is done by giving a radiation dose which is fixed throughout the entire process and measuring the OSL produced after this dose (T_x). If sensitivity has not changed then this value should always be the same, if it has changed then it possible to effectively correct values for this by plotting luminescence signal (L_x) as a function of laboratory dose but by Lx/Tx as a function of laboratory dose (Duller 2004, Murray and Wintle 2000, Wintle 2008, Wintle and Murray 2006) .

Within SAR several internal checks can be incorporated to check the reliability of the D_e produced. For example, a check can be performed on if sensitivity corrections have been effective by repeating a regeneration at the beginning and end of the sequence and

checking the ratio (termed recycling ratio) between their respective values is close to unity, if not then sensitivity correction have been ineffective. Another common test applied is a dose recovery tests. These tests attempt to determine any changes in luminescence sensitivity that results from preheating of the samples. Simply put they bleach a sample and give it a known dose before any heating, a SAR protocol is then undertaken on the sample (Wallinga *et al.* 2001).

In the dating of young sediments (<1000 years in age) there are a number a significant potential limitations of OSL that can arise. Madsen and Murray (2009b) highlight four main problems which can arise in the optical dating of sediments <1000 years in age:

(1) Insufficient luminescence sensitivity of samples at the low doses of irradiation involved with dating young samples can result a poor ratio of signal to noise and as produce imprecise results.

(2) Thermal transfer, the phenomenon of the transfer of charge from light insensitive traps to light sensitive traps during pre-heating, is a substantial issue in young samples. This transferred signal can represent a significant addition to a natural OSL signal as the natural signals from young samples are already likely to be small, this results in over estimation of D_e. It has been noted that using lower pre-heats can limit the effects of this transfer (Bailey *et al.* 2001). It is now common practice to for young OSL studies to undertake and report preheat plateau tests to select the optimum preheat to minimize thermal transfer (Madsen and Murray 2009b);

(3) Incomplete bleaching is a significant issue for young sediments as, similarly to 2, the residual dose may represent a large proportion of the natural OSL signal potentially resulting in substantial overestimations of D_e.;

(4) Alterations in the sedimentary environment may result in changes in the dose rate over time, this is particularly problematic in situations where sedimentation rates are high as, for example, the influence of cosmogenic radiation on the dose rate may have changed significantly over time as the sediment is successively buried. In this instance this could

potentially lead to inconsistent dose rates over time and potential over or underestimation of age. As a result, particularly in near surface samples, it is necessary to model the temporal variability of sample depth to determine accurate dose rates. As noted by Madsen and Murray (2009b) this need not be an especially complex model.

Coastal sand dunes, as well as their inland counterparts are generally considered to be the most suitable environment for the application of luminescence dating (Bateman 2015), being composed almost entirely of mineral material suitable for luminescence dating. Furthermore aeolian sediments have a high probability of being fully reset during transport and the reasonably rapid accumulation of sediment on dunes limits potential for re-exposure (Bateman 2015). As a result luminescence has found significant application in studies of coastal sand dunes (Choi *et al.* 2014, Cunningham *et al.* 2011, Giannini *et al.* 2007, Tamura *et al.* 2011) . These studies range in timescale from in excess of 700 ka (Murray-Wallace 2002), in work which as able to show that over the last 11 interglacials sea level maxima in south-eastern Australia did not exceed +6m of present day levels; to use in dunes of late-Holocene age to derive the ages of the occurrence of extreme sea levels (Buynevich *et al.* 2006, Cunningham *et al*. 2011).

Despite the suitability of coastal dunes for luminescence dating they are not without significant potential issues. For instance, consideration needs to be given to the potential for the resetting of sediments ages during dune reworking, though of course this may in some cases be a virtue when looking for evidence of instances of dune erosion and rebuilding, e.g. when looking for evidence of storm impacts (Buynevich *et al.* 2004, Dougherty 2014). Another crucial consideration, whilst not necessarily an issue exclusive to coastal dunes, but certainly.an especially pertinent issue for them, is post-depositional disturbance of sediments (Bateman *et al.* 2003, Bateman *et al.* 2007). Such disturbance can mix sediments of different ages and potentially reset sediments by allowing entry of sunlight in instances of burrowing by animals. Post-depositional disturbance can be overcome simply targeting sampling away from clearly disturbed units (Roberts *et al.* 2008) or, in cases where disturbance is less clear,

by adopting the dating of single grains to omit recently zeroed or much older grains from the analysis (Bateman *et al.* 2008).

Since the development of SAR protocols there have been many successful attempts at dating of young coastal dunes by OSL. One of the first of such studies using SAR was by Bailey *et al.* (2001). This study examined sand deposition at the Aberffraw dunes, Anglesey, North Wales. Using sand-sized quartz as their dosimeter they produced a chronology for these dunes of the last 700 years with their youngest age at 20+/- 10 years. The study was noteworthy in that it was one of the first to demonstrate that samples from coastal sand dunes have the potential to be sufficiently reset for the purposes of dating young sediments (Madsen and Murray 2009b). Subsequent studies of young coastal sand dunes also further demonstrated their suitability for OSL by producing robust and in some cases independently verified ages (Ballarini *et al.* 2003, Nielsen *et al.* 2006, Madsen and Murray 2009b, Cunningham *et al.* 2011) with studies such as Ballarini *et al.* (2003) even producing robust ages on decadal timescales.

The approaches outlined above can provide an important chronological constraint for reconstructions. However, as with most absolute geochronological techniques, OSL is burdened by the time (2-6 months for OSL, Stone *et al.* 2015) and financial costs of the laboratory protocols to obtain them (Bateman *et al*. 2015). These constraints impose an upper limit on the number of ages that can be practicably or financially obtained for Quaternary studies and reconstructions. This is important given the widespread application of age-depth models that interpolate ages based on dated points, the fewer the number of such dated points, the greater the potential error in the model (Blaauw, 2010, Blaauw and Christen, 2011). Since their development in 2005 (Sanderson and Murphy, 2010), portable OSL (POSL) readers have seen increasing application to resolve the challenge of prohibitive time and financial costs to produce complete chronologies via lab based OSL approaches.

POSL provides a quick (minutes per sample) measurement of photon counts by blue (OSL) and infra-red (IRSL) stimulation (Stone *et al*. 2015). These readers offer the advantage of

fast, simple, and cost-effective measurements of stored luminescence signals. The goal of POSL measurements is not to provide full absolute ages for individual samples, but rather to provide rapid first-order estimates of relative age within a sediment sequence though the production of instantly derived chronologies. Such POSL derived profiles have seen application in assisting with targeting of sampling for full OSL dating (Sanderson and Murphy, 2010) and delineating stratigraphic breaks in relative age as indication of changing landscape dynamics (Bateman, *et al.* 2015, Munyikwa, *et al.* 2012, Stone *et al.* 2015, 2019). Most applications of POSL have focussed on its use in determining changing climatological conditions in governing desert dune evolution (Munyikwa, *et al.* 2012, Stone *et al.* 2015, 2019), though the technique has seen some application to coastal dunes.

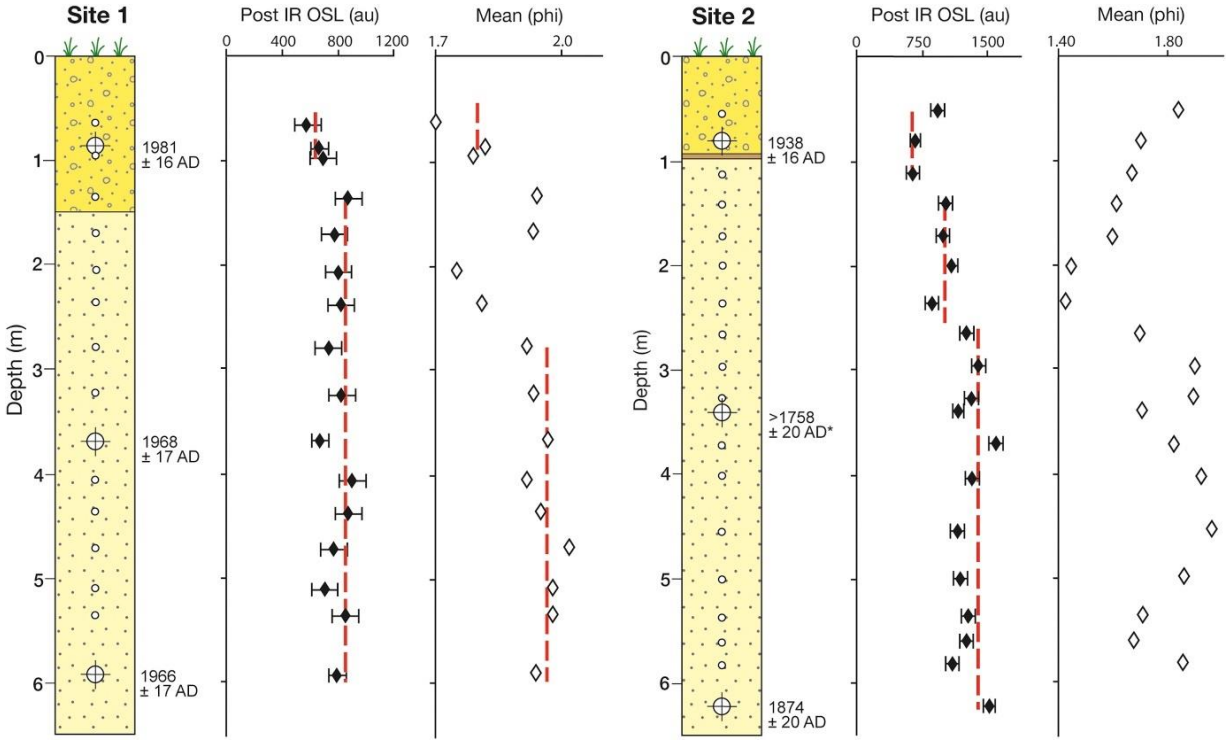

Figure 2.5. Stratigraphy of two dune samples compared with down-core post-IR OSL portable measurements and mean particle size. Note dashed lines indicate observed groups of data only. (From Bateman et al. 2015).

Bateman *et al.* (2015) explored the application of POSL to coastal dunes on the North Norfolk coast. In this study, dunes were sampled from crest to dune base at 25 cm intervals and collected in light tight containers for later POSL measurement in a light-controlled

setting. Such uses of POSL are contingent on the measured signal being dominated by a signal related to burial age rather than other variables such as particle size, mineral types, and moisture content. To overcome this, Bateman *et al*. (2015) undertook particle size analysis of POSL samples to determine if grain size changes impact POSL chronologies. Bateman *et al.* (2015) found that POSL values increased with depth in their dune sites in conformation with the law of superposition and that POSL values were also consistent with relative dune ages with older dunes (confirmed by full SAR OSL ages, site 2 in Figure 2.5.) producing a higher POSL signal. This study demonstrated the potential of POSL to generate accurate high-resolution chronologies in coastal dunes. They noted the potential for POSL to identify phases in dune development and that such phases could be used to identify changes in morphology driven by climatological or hydrodynamic processes governing dune development such as coastal storms.

Chapter 3 builds on this work by the potential for utilising coastal dunes as archives of past storms and extreme sea level through use of OSL and POSL chronologies. Chapter 3 particularly builds on the work of Bateman *et al.* 2015 by exploring the potential of phases in dune development identified by POSL chronologies to act as indication of storm impacts on coastal dunes. These tools are further explored in Chapter 5.

2.2.6. Dune reconstruction tools: GPR

In addition to chronological context from OSL, many of the studies discussed in 2.2.2, 2.2.3 and 2.2.4 combine OSL chronologies with morphological context from geophysical techniques. Particularly popular since the late 1980s and early 1990s is the use of ground-penetrating radar (GPR). GPR is a non-invasive technique that provides context on subsurface morphologies. GPR systems detect differences in electrical properties of subsurface structures by the transmission of high frequency electromagnetic (EM) energy from 10-1000 MHz in range. (Robinson *et al.* 2013). As a pulse of energy transmits downwards, the velocity of that pulse is changed as it encounters materials with different electrical properties (usually expressed by that material’s dielectric constant). These

changes result in redirection and reflection of some of the energy back to the GPR system where it is measured by an EM receiver. It is the detection of these reflections by the EM receiver that allows subsurface properties to be inferred (Neal 2004, Robinson *et al.* 2013). As a GPR system is moved linearly across the ground, multiple samples allow for 2D reflection profiles to be produced, usually termed a radargram (Figure 2.6)

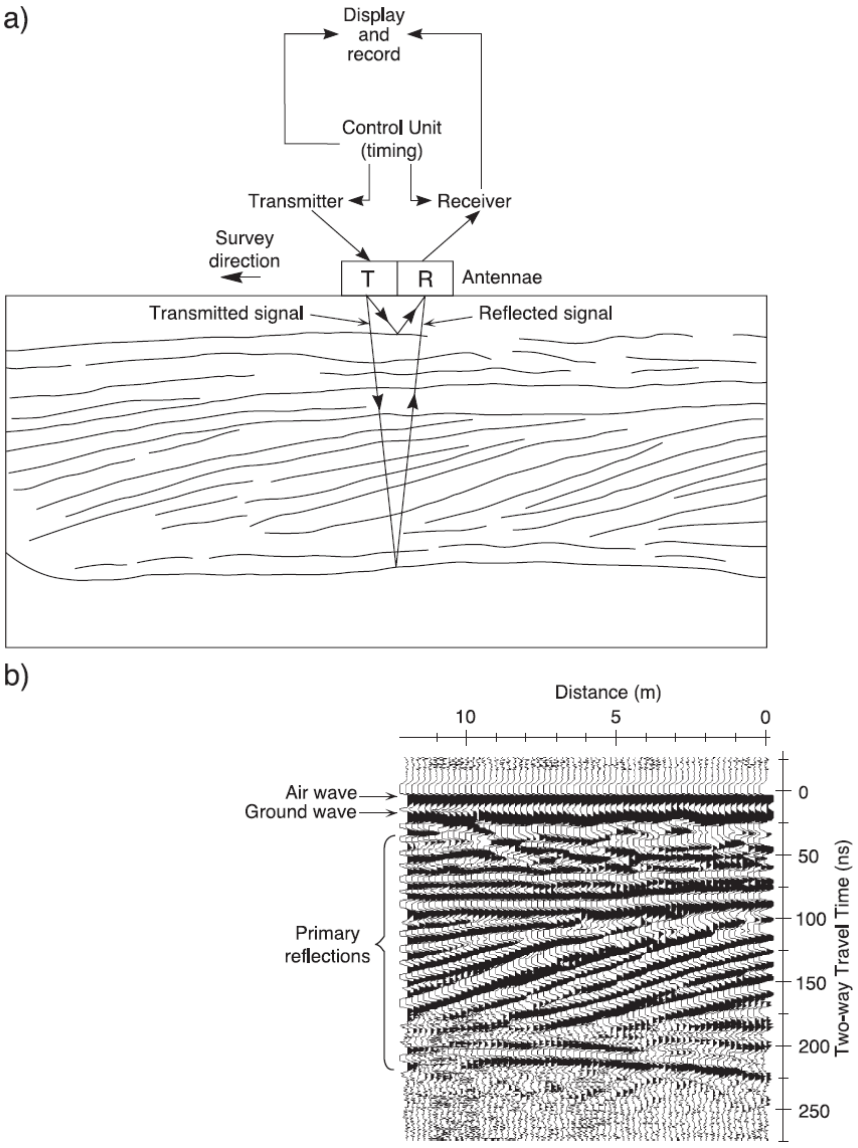

Figure 2.6. GPR data acquisition and the resulting radar reflection profile (radargram). (a) Illustration of data acquisition at a single survey point, showing GPR system components and subsurface reflectors. (b) Radargram resulting from plotting of traces from adjacent survey points. From Neal 2004.

Initially the vertical axis of a radargram is represented as the two-way travel time from the EM emitter back to the receiver. This travel time can be converted into depth by an assumption of EM pulse velocity through the target material. These velocities have generally been well quantified for most materials through common midpoint gather surveys, though where highly variable underlying materials are expected such surveys should be conducted on site (Bristow *et al*. 2001, Sensors and Software 2021). Dry aeolian sands typically produce velocities of ~0.15 m ns^{-1}. Selection of appropriate equipment for GPR studies requires an understanding of the potential depth of penetration in the study site. There is a trade-off between the maximum resolution of GPR data and the depth of penetration. Aeolian sands generally allow for good penetration depth in GPR studies (>10 m for a 100 MHz antenna), however superior resolution (allowing for more subtle structures to be observed) can be obtained by using higher frequency antenna at the cost of penetration depth.

GPR has seen widespread application in morphological studies across many environments, however GPR has various shortcomings which are largely environment dependent. Focus here is given to the application of GPR in coastal dunes. GPR has seen extensive application in the study of both contemporary dune fields and palaeo-dunes and has been used to reconstruct depositional histories (Clemmensen *et al*. 2009) and coastal dune evolution in response to changes in hydrodynamic and climatological forcing (Nobes, *et al.* 2016. Rodriguez-Santalla *et al.* 2021**,** Tamura *et al.* 2020). Many of the contemporary applications of GPR to coastal dunes have emerged from earlier work exploring the application of GPR to linear desert dunes. Bristow *et al*. (2000) describe the main ways in which GPR can be used to identify internal dune structures in such settings. In this study GPR profiles were collected across the leading edge of a sinuous linear dune in the Namib Sand Sea. Their results produced high-resolution radargrams of sedimentary structures in the dune. Due to the strong contrast in dielectric properties, the clearest distinction was between the dune sands and the underlying carbonate gravel. However, internal dune

structures could be clearly identified in places of cross-stratification. Using the changing orientation of cross-bedded structures Bristow *et al*. (2000) were able to identify changing patterns in dune development corresponding with changing wind direction. Further, they were able relate internal structures to a five-stage model of linear dune evolution.

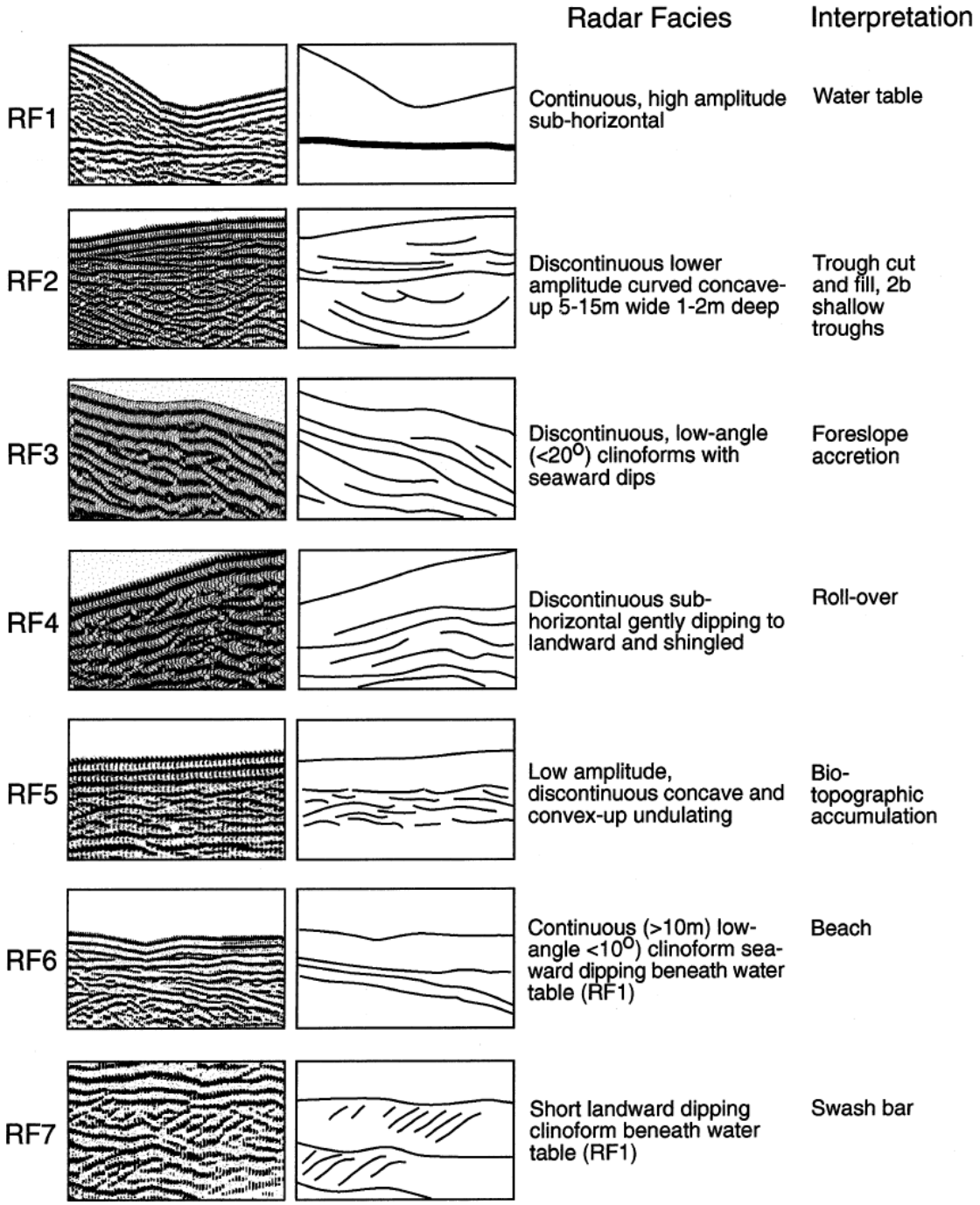

Figure 2.7. Radar facies of GPR profiles from the North Norfolk Coast from Bristow et al. (2001)

Bristow *et al.* (2001) extended the use of GPR from desert dunes to coastal foredunes in a study of dunes at Holkham in North Norfolk. In this study they defined seven key facies in the dune profiles (Figure 2.7). Identification of the water table is common to many lowland GPR studies and often represent the maximum limit of GPR data, though some recent studies have experimented with looking beyond the water table in coastal settings using high frequency antennae (Rodriguez-Santalla *et al.* 2021). The most frequently observed facies at Holkham were low-angle offshore dips within the dunes, interpreted as the result of phases of dune accumulation. They also identified erosion surfaces extending from the beach into the dunes, which were attributed to the creation of dune cliffs subsequently covered by later dune foreslope activity. These erosion events were linked to documented storms, although their age was unknown. This was the first study to identify erosional and subsequent depositional facies in coastal dunes and associate them with storm activity.

Studies have since further explored the potential of GPR in identifying the relationship between storms and the internal structures of coastal dunes. Bristow and Pucillo (2006) were able to quantify rates of coastal progradation by combining GPR with OSL ages in Guichen Bay south-east Australia. This was achieved by identification of a succession of stabilized foredunes within relict beach ridges alongside which truncation surfaces due to coastal storms were identified. Switzer *et al.* (2006) utilised GPR to identify a sand lens associated with a large-scale washover event in the last 800 years in dunes on the south-east Australian coast. Similarly, Cunningham *et al.* (2013) later utilised this method to determine the scale of the 1953 storm surge deposit in coastal dunes in the Netherlands. In a study of beach ridge coastal dunes in south-east Australia Tamura *et al.* 2019 were able combine GPR with OSL dating to identify an extreme dune treat over a period of 550 years related to ancient storms. Using this they proved that a more recent storm of similar scale in the 1970s, whilst unprecedented in instrumental records is recurrent in longer term geologically derived data.

GPR is utilised in Chapter 5 to provide context for morphological context for POSL based storm reconstruction techniques used in at a study site in North Wales. The work of Bristow *et al.* (2001) (Figure 2.7) informs the interpretation of GPR profiles presented in Chapter 5.

2.3. Unresolved questions in UK Holocene RMSL

As discussed in 1.3 and 2.1 understanding of changes in coastal storms, and in particular extreme sea levels, cannot be separated from a discussion of relative mean sea level (RMSL). Mean sea-level change is a complex phenomenon which varies in both space and time owing to the wide variety of potential processes which influence it (Gehrels and Long 2008). Mean sea level is usually determined as the average height of the sea over a period, commonly a year, though for a more accurate value a period of 19 years is more suitable to account for the 18.6-year cycle in the moon's declination. As RMSL represents a point in space relative to both sea and land the processes controlling it can be logically separated into those related to changes in the vertical level of land (isostatic changes) and in the ocean itself. In the past, literature has referred to changes in ocean levels have as "eustatic" changes. This term has inconsistently been used to mean any of geocentric sea-level change (change relative to a terrestrial reference frame due to changes in ocean volume or sea floor) or mean sea-level change (change due to volumetric changes only), or as a synonym for barystatic changes (changes due to the addition or subtraction of water mass to or from the ocean) (Gregory *et al*. 2019). To avoid this confusion this thesis eschews the now deprecated term eustatic in favour the definitions given by Gregory *et al*. (2019).

Sea level has fluctuated significantly throughout the Earth's history. Global mean sea level change (change in the area-weighted mean of the entire global ocean surface (Gregory *et al*. 2019)) is controlled on long-term geological timescales (10^7-10^8 years) by changes in ocean basin volume resulting from tectonics via seafloor spread and, to a lesser extent, ocean floor sedimentation (Miller *et al.* 2005, 2011). The action of such processes is evident in sea-level curves derived from oxygen isotope analysis of deep-sea cores (Kominz *et al.* 2008, Miller *et al.* 2005) which have demonstrated that over the past ~120 million years sea-level has

varied with an amplitude of ~200 m (Miller *et al.* 2011). However, processes on such timescales bear little relevance to sea-level changes on timescales relevant to the study of coastal storms and their relationship with coastal change, instead controlling the emergence and submergence of continental coastlines.

Over the Quaternary, global mean sea level has varied with an amplitude of ~120 m (Church *et al.* 2008) and has fluctuated along with the growth and retreat of land-based ice. On this timescale, barystatic sea-level changes are mostly due to the exchange between ocean water with land-based ice. Whilst this exchange dominates the mean sea-level change signal over the Quaternary, how this manifest in sea-level change regionally exhibits substantial spatial variability. Relative to the Earth's centre, the sea surface varies in altitude by over 100 m due to variations in ocean floor rock density (the geoid) and regional variations in the Earth's gravitational field. These effects are mostly consistent over the course of centuries but the gravitational effect of changes in the mass of ice-sheets can influence surface topography on shorter time-scales (Gehrels and Long 2008, Mitrovica *et al*. 2001). The influence of steric changes in water density driven by changing temperature (thermosteric) or salinity (halosteric) are also more apparent at these timescales than over longer periods. In areas of ocean warming the ocean surface expands, raising sea level. Conversely, under ocean cooling sea level falls. In the next century thermosteric rise are projected to be most pronounced in the north-west Atlantic (Fox-Kemper *et al*. 2021). However, these processes vary further on even shorter timescales due to natural climatic cycles such as El Niño and the NAO.

Isostatic change on this timescale is primarily controlled by the loading and unloading of glacial ice mass resulting in regionally variable patterns of glacio-isostatic adjustment (GIA). This scale of change primarily controls regional coastline position and the submergence or emergence of landscapes, such as Doggerland; a southern North Sea landscape exposed during lower regional RMSL at the last glacial maximum and subsequently submerged during the Holocene by progressively rising sea levels (Walker *et al.* 2020). It is on

Quaternary and shorter timescales that RMSL change becomes more pertinent for the study of coastal storms and change. This is particularly true for the study of Holocene RMSL, a timescale over which many of the processes driving RMSL are still ongoing. All the studies discussed in 2.2 reconstruct storms that took place during the Holocene, particularly in the late-Holocene when the rate of sea-level change is slow (typically <~1mm/yr) allowing for sequential storm deposits in coastal landforms to arise.

During the Holocene relative sea-level change varied significantly across the globe. These differences broadly fit under the five categorised regions proposed by (Clark *et al.* 1978), see Figure 2.8.

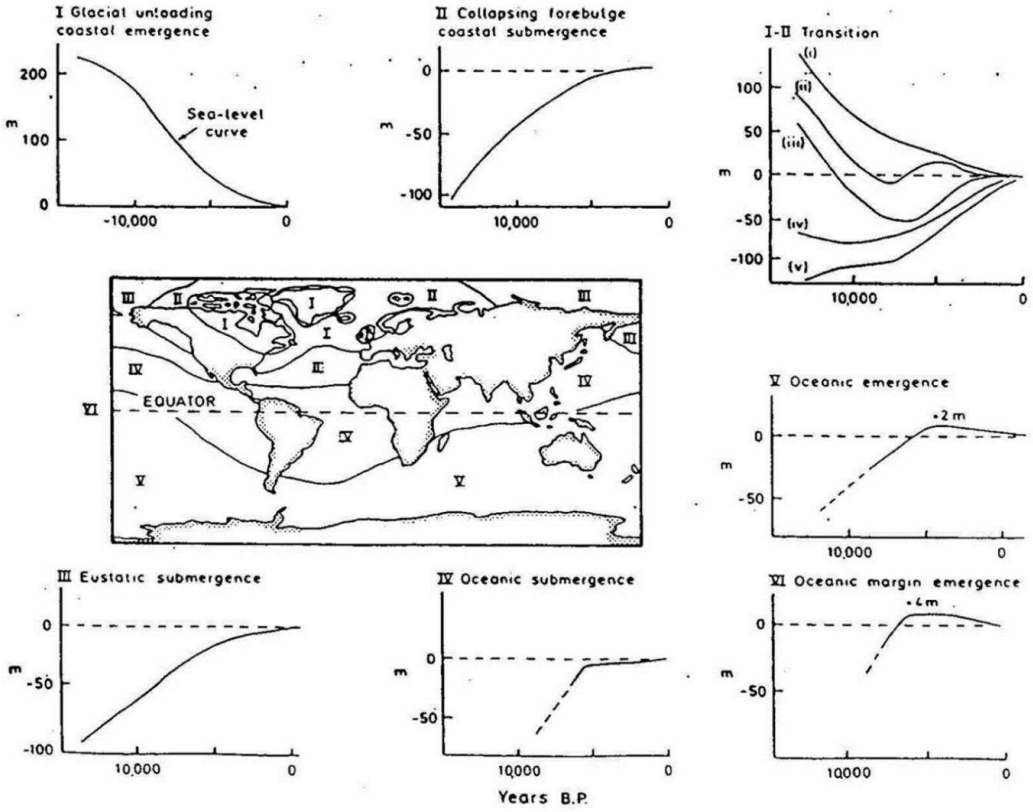

Figure 2.8. Regions of sea-level change across the globe from Clark et al. (1978)

These differences in Holocene relative sea level arise from spatial differences in the relative importance of different processes. For example, Figure 2.8.I shows the Holocene relative sea-level history for regions previously, or still currently, covered with large continental ice sheets. In such regions as glacial ice was removed following the decline from the last glacial maximum regional RMSL fell due to the GIA driven land uplift outpacing any increase in

ocean level due to transfer of water from ice to the ocean. Contrastingly, Figure 2.8.II highlights regions which exist within a collapsing forebugle; areas peripheral to glaciated areas where land level was raised above its equilibrium position during glacial maximum. Following the removal of ice, the land level here lowers back towards its equilibrium position. Here this isostatic fall is superimposed on barystatic and steric sea-level rise, resulting in curves with a rapid RMSL rise in the early and mid-Holocene.

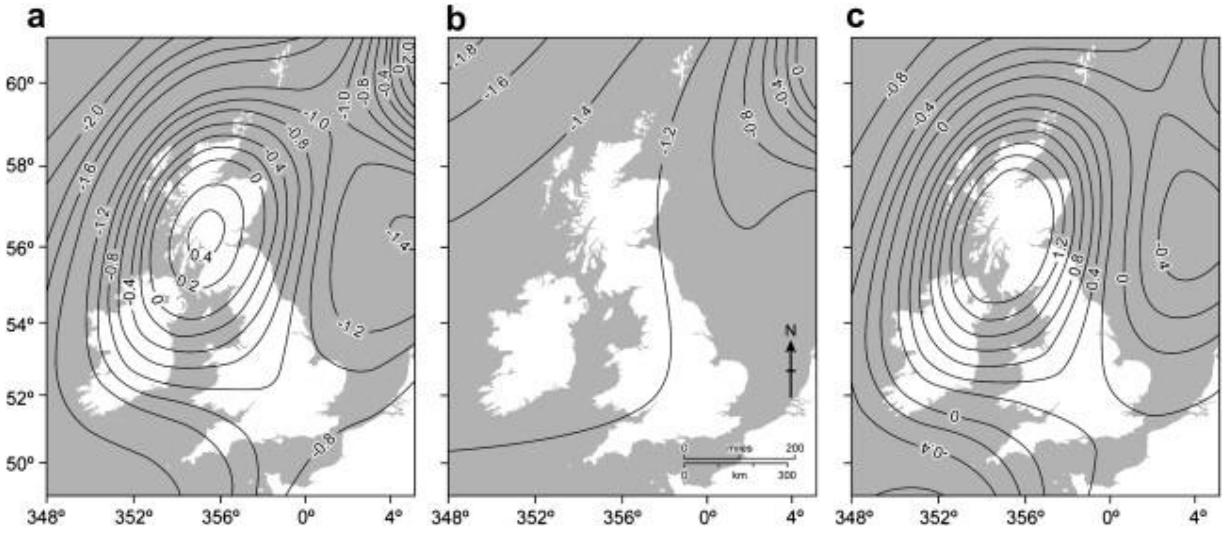

Figure. 2.9. Gehrels (2010) after Bradley et al. (2009). GIA model simulations of (a) Predicted rates of present-day UK vertical land motion in mmyr^{-1}. (b) Vertical land motion due to non-regional effects (i.e., primarily the influence of the deglaciation of Fennoscandian Ice Sheet). (c) Vertical land motion due to regional effects (demise of the British–Irish Ice Sheet).

Whilst Figure 2.8 does show the existence of large-scale regions of different Holocene relative sea-level curves, in reality substantial differences can exist even on much finer spatial scales. This is particularly true of regions subjected to the isostatic effects of multiple ice sheets. In the UK, Holocene relative sea-level histories are largely governed by the complex interplay between the isostatic effects of two former ice sheets, the British-Irish Ice Sheet and the Fennoscandian Ice Sheet. Such complexities are often explored through use of GIA models (Figure 2.9). These numerical models simulate solid Earth responses to loading and unloading of ice masses. In combination with predictions of barystatic and steric

sea-level rise produced from climate models, modelled GIA allows for the production regional scale relative sea-level predictions and reconstructions (Lowe *et al.* 2009)

The complexity of these isostatic interactions in the UK results in a gradient in sea-level histories from north to south. This complexity has been explored through reconstruction of sea level index points (SLIPs) as markers of past relative sea level derived from geological and palaeoenvironmental indicators (Shennan *et al.* 2018). SLIPs are usually defined by four attributes, their location, age, altitude and sea-level tendency. SLIP age is usually determined by geochronological techniques, most in the UK have been determined using ^{14}C based techniques (Shennan *et al*. 2006). The altitude of a SLIP can be determined by surveying relative to a benchmark, in the UK this is usually Ordnance Datum Newlyn. The altitude of sea level at the time the SLIP was formed requires determining the water depth at which it was located at formation, this is termed the indicative meaning (IM). For most SLIPs IM describes the vertical difference between a common tide level (e.g., Mean High Water) and mean sea level. For some indicators determining IM requires more bespoke approaches such as quantitative reference water level based on proxy evidence. SLIPs are also often categorised as basal, intercalated, or limiting. Basal SLIPs are found at the bottom of a sedimentary sequence and considered unaffected by issues such as sediment compaction which can resulting in misleading past sea level altitudes. Intercalated SLIPs are found within a sedimentary sequence and are vulnerable to the sediment compaction. Limiting SLIPs provide lower or upper limits for past sea levels (Hijma *et al*. 2015).

For the UK, SLIPs have been compiled into a single database and presented alongside the outputs of GIA models for those regions by Shennan *et al.* (2018), these are presented alongside sea level predictions of different GIA models in Figure 2.10. Both models and SLIPs suggest that for the western coasts of the northern UK mainland, relative sea-level rose to a maximum in the mid-Holocene, before falling as the rate of isostatic uplift in these regions overtook the rate of barystatic sea-level rise (29, 30, 31 in Figure 2.10). This in line with the ongoing rate of uplift continuing in south-east Scotland (Figure 2.9a). This existence

of a highstand becomes less pronounced moving further south, being replaced entirely with a constant, albeit slowing, rise over the Holocene to present day levels as isostatic rise is either minimal or replaced by land level fall.

Whilst the UK does have one of the strongest records of regional differences of relative sea-level change in the world, there remain unresolved questions in its records. Primarily, this takes the form of misfits between GIA modelled predictions and data from suggested by SLIPs (Bradley *et al.* 2011). These are particularly noteworthy in Wales where some GIA models predict (Peltier *et al.* 2002) a mid-Holocene highstand in North Wales, which cannot be validated by geological data due to an absence of late-Holocene data for this region; with the entirety of relative sea-level for North Wales constrained to the north coast of the Anglesey between 11,000 years BP and 4500 years BP (Bedlington, 1994, Heyworth and Kidson, 1982, Roberts *et al.* 2011).

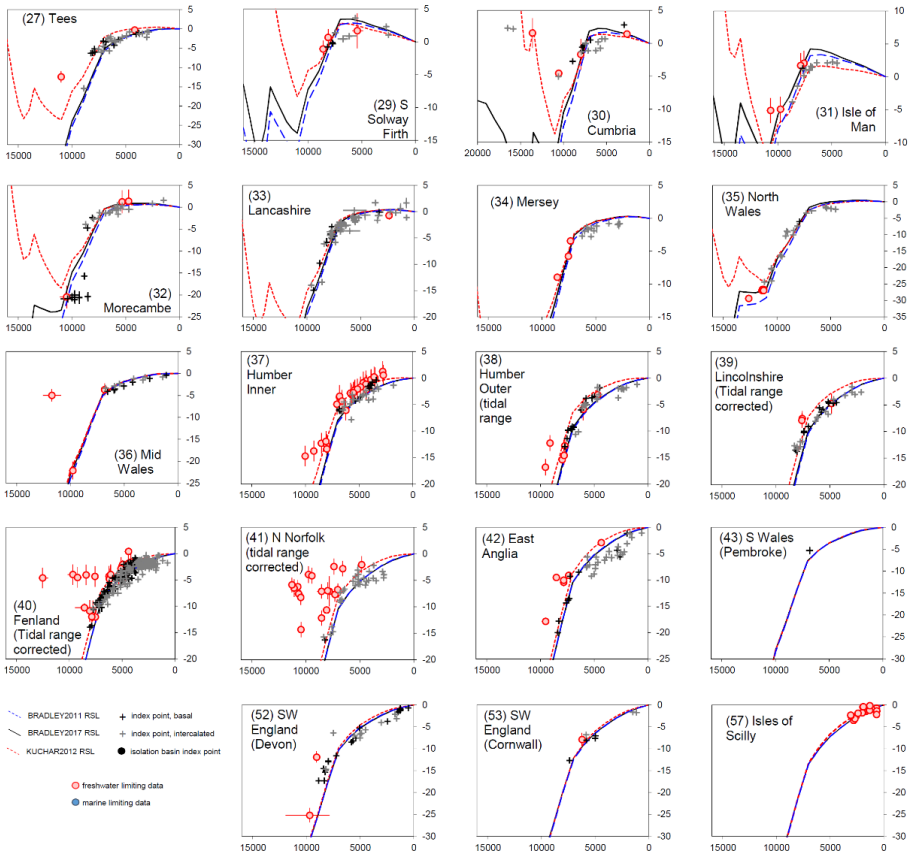

Figure 2.10: Selection of sea level plot from based on GIA modelling and SLIPS from Shennan et al. (2018).

The misfit between geological data and models in North Wales have implications beyond just regional interest. Given the importance of a robust understanding of GIA for future sea level predictions (Lowe *et al*. 2009), resolution of such mismatches is vital to ensure the future accuracy of GIA based predictions, particularly for regions where geological sea-level records may be less plentiful.

Given that GIA models from Bradley *et al.* (2011) and Kuchar (2012) suggest that this region may have maintained a steady sea level for the late-Holocene it is also important to improve understanding here for the reconstruction of past extremes. If relative sea-level in the region has remained steady for the late-Holocene, this gives it excellent potential for the reconstruction of past extremes from coastal deposits. Regions with rapid rates of either relative sea-level rise or fall are potentially more problematic for reconstructions of storms. In situations of Holocene relative sea-level fall, whilst records are relatively easily accessible as they will be some distance in land, they are unlikely to yield information on changing storminess given the primary driver of differences in intensity implied by storm records would be primarily driven by the rate of sea-level change itself. In situations of rapidly rising relative sea level, storm archives are more likely to be submerged and eroded by subsequent coastal processes. In situations of slow RMSL rise, slow fall, or stagnation differences between storm deposits are more likely to be a function of changing weather conditions rather than sea level. Therefore, further validation of the pattern of Holocene relative sea-level change in North Wales is needed to explore its potential as a region for storm reconstructions, as well as to provide ground truthed validation for RMSL correction of any reconstructed past extreme sea levels. Chapter 4 explores these challenges through the reconstruction of late-Holocene relative sea level in North Wales, both to provide a resolution to the mismatch between GIA models and empirical data, as well as providing important sea level context for Chapter 5.

2.4. Coastal change and storms

2.4.1. Concepts: morphodynamics, resilience and equilibria

Coastal changes are often described using the framework of the coastal morphodynamic system. (Figure 2.11). At the core of this model is a feedback loop between coastal processes which drive sediment transport and result in changes in morphology, these morphologies then have feedback on coastal processes due to their interaction with nearshore hydrodynamics. External to this central model are other factors which drive changes in processes Masselink *et al.* (2013). Primarily these sources are the wind/wave climate, the tidal regime/prism, and the magnitude-frequency of high energy stochastic events (coastal storms) (Banno and Kuriyama 2020, Gomez-Pujol *et al.* 2011, Ortega-Sanchez *et al.* 2008). It is through alteration of these energy sources that consequences of climate change with be reflected in changing coastal morphology and shorelines (French and Burningham, 2013). This will occur either by increasing frequency or intensity of atmospheric drivers of these energy sources, or by RMSL raising the effective base level for the magnitude of these processes (Allenbach *et al.* 2015, Ritphring *et al.* 2018, Somphong *et al.* 2020, Vitousek *et al.* 2017). Of these, coastal storms are particularly noteworthy. They can rapidly reshape coastlines and coastal geomorphology, particularly on sandy shorelines where sediments are typically large enough to not be easily transported in large volumes and large distances by low energy coastal conditions but can during extreme events.

Coastal resilience has been an increasingly popular concept for conceptualising how sudden perturbing events, such as coastal storms, can affect change (Houser *et al.* 2015, Kombiadou *et al.* 2019, Masselink and Lazarus 2019, Woodroffe 2007). This concept is often closely linked with another term, vulnerability, the degree to which a coast is likely to be affected by or withstand a disturbance (Woodroffe, 2007). The concept of resilience is multi-faceted and has been applied in many different contexts including law, ecology, psychology, and sustainability science (Kombiadou *et al.* 2019). This has led to some ambiguity over its application to coastal systems where it has seen substantially increasing application in

literature in the last decade (Kombiadou *et al*. 2019.) Recent reviews of the term for coastal studies have attempted to address some of these diverging conceptions of the term (Kombiadou *et al.* 2019, Masselink and Lazarus 2019). A common point between all applications is that it describes the ability of a system to “bounce back” from a disturbance. This disturbance may be a single temporal pulse (such a storm) or an ongoing press/ramp disturbance such as sea-level rise.

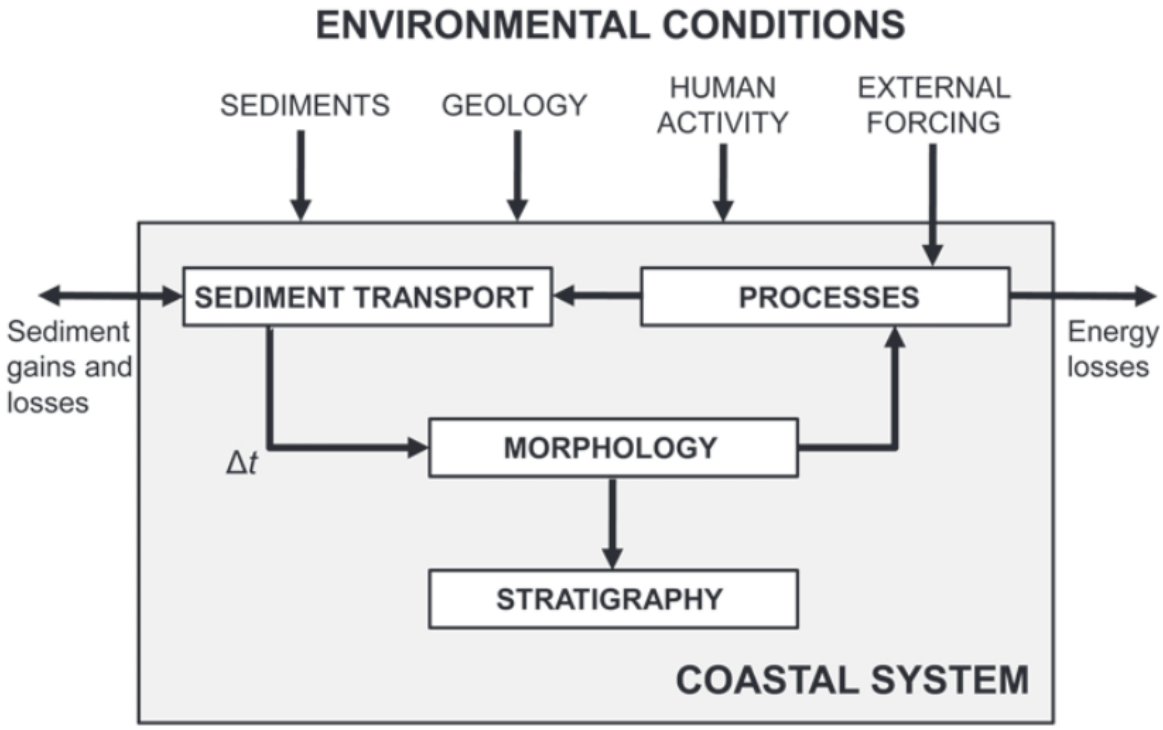

Figure 2.11. The Coastal morphodynamic system illustrating the fundamental feedback between process and morphology in coastal systems and the role of external forcing factors (Masselink et al. 2013).

In the study of morphological systems, resilience is related to, and often used in tandem with, the concepts of morphological equilibrium and feedbacks. Equilibrium (or a “regime” in engineering literature) describes a condition where the forces that may drive change are effectively cancelled out by the change they illicit over some timescale (Wright and Thom, 1977). It is a condition brought about by the dominance of self-organising negative feedbacks over change-amplifying positive feedbacks. A common simple example is the sand eroded from dunes during a storm being redeposited as an offshore sand bar,

effectively protecting the system from future storm waves (Haslett 2009, Masselink *et al*. 2013). Over time this allows dunes to regain sediment whilst the bar is gradually eroded, returning the system to its original condition. In practice equilibria can be recognised by the persistence of a landform or morphological feature over a given timeframe. A beach in equilibrium may fluctuate in its morphology due to short term perturbations such as storms but ultimately to return to its average state after a given time. Such conditions are typically referred to as a static or steady-state equilibrium (Figure 2.12). “Dynamic equilibrium” describes situations where short-term changes may still be resisted by negative feedbacks, but a longer-term underlying trend driven by either a positive feedback or a change in environmental conditions (Figure 2.11) effectively changing the “base” condition to which the system returns after shorter-timescale perturbations. In Figure 2.12 this example dynamic equilibrium is being driven by accumulation river borne sediment in the coastal zone. In “Metastable” or “meta-state” equilibrium the environment may switch between multiple state of equilibrium after stimulation by some kind of trigger, such as storms, tsunami or human intervention in the system. It is worth noting that the specific equilibrium type a system may be considered to occupy will depend on the spatial and temporal scale examined. Over the timescale of a single summer a beach profile may appear to be in steady-state as minor fluctuations occur with wave events. Over an entire year, this may appear to manifest more as a meta-state, as the beach occupies a winter profile following erosion of the berm by a large storm. On the timescale of years, decades or centuries, a dynamic equilibrium may become more evident as the annual fluctuations appear small in scale compared to ongoing trend dictated by environmental conditions such as sediment deliver or sea-level rise.

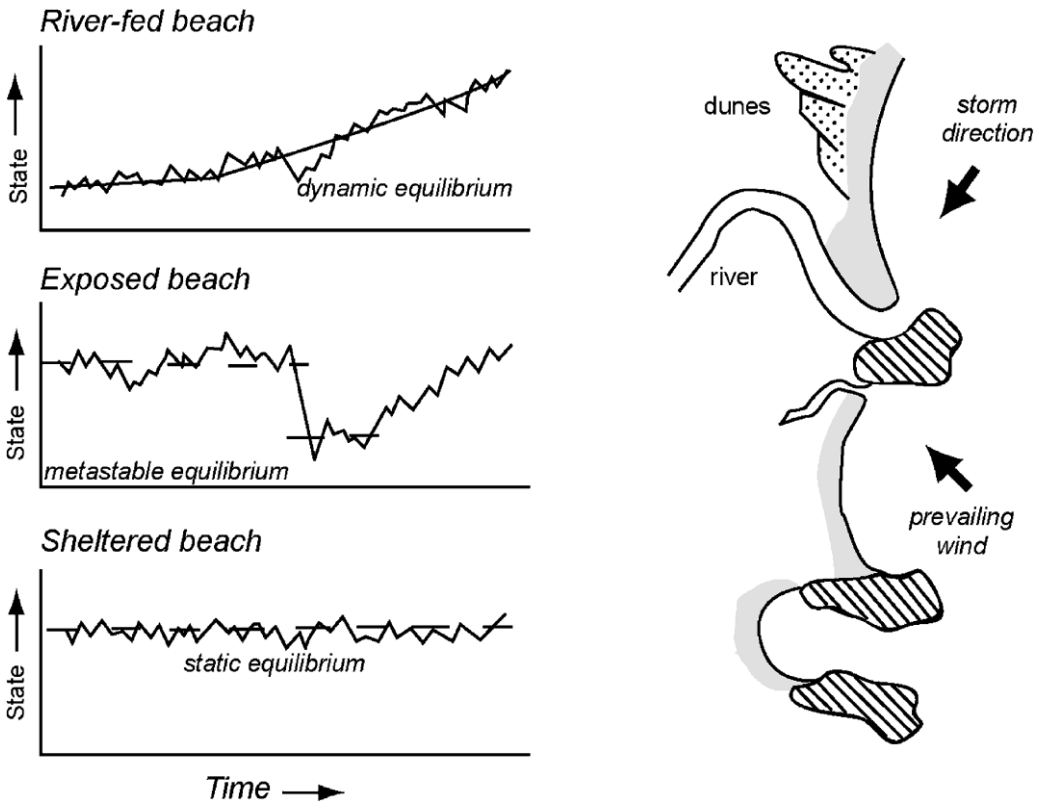

Figure 2.12. Examples of different types of equilibrium from Woodroffe (2007)

It is out of concepts of equilibrium that the term resilience began to gain popularity, though initially primarily in ecological system contexts, being codified by Gunderson and Pritchard (2002) who initially proposed “engineering” and “ecological” definitions of the term. In their definitions, engineering resilience is effectively the time it takes to return to the equilibrium, with high resilience being a shorter return time. Ecological resilience by contrast refers to the ability of the system to absorb change, or the magnitude of disturbance that can potentially be absorbed before the system redefines its structure. Attempting to reconcile these differing definitions, Masselink and Lazarus (2019) proposed the revised definition of “the capacity of the socioeconomic and natural systems in the coastal environment to cope with disturbances, induced by factors such as sea level rise, extreme events and human impacts, by adapting whilst maintaining their essential functions”. In their review, Masselink and Lazarus (2019) note that even with adoption of the new consistent working definition, resilience will ultimately require means of quantification to be more useful in management

contexts and to compare across study sites. Though progress has been made in this area, attempts to quantify resilience have tended to be site-specific (Best *et al.* 2018)

2.4.2. Studying coastal storm response

Storms can result in substantial geomorphological change, including shoreface sediment entrainment and nearshore profile change; erosion of beaches, dunes, and cliffs; barrier breaching and overwash; and modification of tidal inlets (Forbes *et al.* 2004). To aid in management of these changes, there has been substantial research aiming to provide a sound scientific basis for managing coastal response to these events and environmental forcing.

Records of coastal change in response to extreme events exist in documentary historical accounts of multiple centuries in age. Garnier *et al*. (2018) note this in their compilation of historical records of storms in northern-western Europe where they found written accounts of large-scale coastal erosion and dune destruction on in Portugal in the 17th century. Similar records of coastal change are also mentioned in UK storm datasets, like the SurgeWatch database, which also summarises coastal consequences as recorded in sources such as newspaper archives from the time of those storms (Haigh *et al.* 2015).

Whilst such historic reports of coastal change resulting from storms are useful for determining regional flood impacts of individual events and for tackling issues of incomplete storm records from instrumental records, they are of little practical use in detailed study of coastal change from storms. This is a result of a lack of quantitative data. It wasn't until the 1960s that quantitative data on coastal morphology and change began to be obtained in sufficient temporal or spatial resolution and scale for changes following storms to be meaningfully quantified. Largely this occurred due to the rapid techniques proposed by Emery (1961) which allowed for beach profiles and shoreline positions to be recorded through simple surveying techniques. These techniques could be applied to a shoreline shortly following a storm to allow for impacts to be directly quantified.

As technology has developed, these approaches have been augmented with the advent of coastal imaging, RTK-GPS (Real-time kinematic global positioning systems), post storm LiDAR (Light Detection and Ranging) surveys, and UAVs (unmanned aerial vehicles) that have allowed for the morphological consequences of single events to be quantified rapidly over entire beaches, as opposed to over single transects from beach profiles. These tools, in various combinations, have seen substantial application in the study of coastal response to single events and single storm seasons (Brooks *et al*., 2016, Burvingt *et al* 2016., Burvingt *et al*., 2017, Castelle *et al*., 2015, Dissanyake *et al*., 2015, Dodet *et al*., 2019, Le Mauff *et al*., 2018, Masselink *et al*., 2016, Pye and Blott 2016, Scott *et al*. 2016, Splinter *et al*., 2014).

As with the reconstruction of storms themselves, many of the early studies of coastal response to storms were devised following observations of erosion driven by hurricane landfall on the north-eastern US coast (Brown, 1939, Ziegler *et al.* 1959, Hayes 1967, Wright *et al.* 1970, McLean and Thom, 1975, Morton, 1976). It wasn't until the late 1990s and early 2000s that many quantitative studies began to explore responses to storms of a smaller scale than hurricanes beyond the US east coast. This is largely a result of the increasing application of coastal monitoring techniques to more beaches globally, effectively increasing the opportunity for storm impacts to be observed.

In a review of these and other studies, Morton (2002) compiled a collection of factors that contribute to the unique response of different beaches to storms. These factors have since guided studies of beach responses to storms. They summarise these factors as:

- **Storm characteristics and tidal interaction.** This primarily captures the storm intensity / magnitude. Storms with larger extreme sea levels and higher wave heights or wind speed typically result in a larger scale coastal response. This is also in part depends on the storm timing, with even extreme low-pressure events with large surges resulting in minimal impact if occurring alongside low tide. Tidal interaction is however less important in microtidal settings than in macrotidal.

- **The location relative to the storm path.** This dictates if water and waves during storms are directed onshore, offshore, or alongshore. This is crucial to dictating beach response with onshore energy more likely to illicit onshore accumulation in the form of either deposition on the beachface itself, or in overwash deposits, with offshore washout of sediment occurring in the opposite conditions. The role of the storm paths, and the importance of coastal configuration relative to that path is now well understood and typically explored through hindcast modelling relative to on the ground observations (Booth, *et al.* 2016, Liu *et al.* 2016)
- **Clustering of the storm events.** Successive storms over single winters are common, but their cumulative impacts in that season are variable by shoreline. Instances of subsequent storms causing increased erosion have been recorded (Karunarathna *et al*. 2014, Morton and Paine, 1985), as well as cumulative storms having no significant effect (Burvingt, 2018, Chute, 1946, Dissanayake *et al.* 2015, Masselink *et al.* 2015). The importance of storm clustering in a single season remains poorly constrained. The 2013/14 storm in north-western Europe has been well studied for the impact of storm clustering in governing morphological change. In studies of LiDAR profiles before and after this season a common observation has been that the first storm amongst a cluster of storms that elicits the most change, regardless of if subsequent storms are of greater or smaller magnitude. (Angnuureng *et al.* 2017, Burvingt, 2018, Dissanayake *et al.* 2015, Masselink *et al.* 2015).
- **Duration of backbeach flooding and the nature of the backbeach environment.** Duration of flooding is largely controlled by the duration of the storm itself. If the exposure time of a beach to a storm is long (>12 hours) then it is possible for wave action and erosive processes to occur over multiple high tides, maximising potential sediment transport. This factor has since been shown to be particularly important in governing dune erosion with the persistent wetting of the dune toe allowing for undercutting, dune collapse and scarping (Bales *et al.* 2000, Pye and Blott, 2007).

The backbeach environment has also been found to be important in governing beach response, with systems possessing coastal foredunes typically showing more muted changes in the beach position and profile than those without. This is due to an exchange of sediment between the foredune and the beach that can occur in the event of dune erosion effectively returning sediment to the beach itself (Pye and Blott, 2007)

- **Type and density of coastal development.** The presence and nature of artificial coastal structures complicates coastal response. High-velocity currents present during storms can be deflected or focussed by closely spaced artificial structures and can result in localised focussing of scour and erosion, whereas widely spaced structures with smaller footprints tend to have minimal interactions (Morton 2002.)

The studies cited above are primarily concerned with instantaneous beach response to coastal storms. Such studies are numerous, particularly in North America and north-west Europe, however studies taking a longer-term view of coastal change and its relationship with storms are comparatively few. This due to a higher data requirement for such studies, with years to decades of monitoring data required to understand longer-term responses to large storms, and the relationship of coastal change with changing storm magnitude and frequency.

2.4.3. A longer term view

In one of the earliest studies to take a longer-term view, Clarke and Eliot (1988) noted the existence of characteristic patterns of shore-parallel and shore-normal movements of sediment on a New South Wales (Australia) beach from 1975-1985. This was derived from profiles surveyed from eighteen stations along a 2 km long beach at monthly frequency for those 10 years. These sediment movements occurred as low-frequency variations on the volume of sediment stored above mean low water. Though they were unable to quantitatively verify it, due to a lack of quantitative data on storm magnitudes available regionally, they were amongst the earliest studies to suggest a possible relationship of

onshore-offshore beachface sediment fluxes with storm occurrence, or lack thereof, in the winters across that decade.

Larson and Kraus (1994) utilised 11 years of high-resolution beach profiles made on a North Carolina beach to explore spatial and temporal characteristics of beach profile change. They noted several changes in beach state within a given year, primarily driven by seasonal differences in storminess, with spring and autumn profiles being nearly identical as a transitional state between summer and winter profiles; with winter profiles being distinctly steeper and more reflective than more dissipative conditions in summer. One of the key findings from their study was that large storms transported sand into the nearshore from the seaward portion of the profile. This was against conventional understanding at the time that storms were primarily drivers of offshore sediment flux than onshore; this conclusion suggested that beach response to storms may be unique to individual beach conditions both in space and time rather described by a standard morphological response.

In a study more specifically targeted at examining the impact of very large storms, Morton *et al.* (1994) studied the recovery of south-eastern Texas beaches following a category 3 hurricane. They found that whilst the pattern of beach response to these events was consistent (forebeach accretion, followed by backbeach accumulation, dune formation and dune expansion) the scale and rate of these recoveries was highly variable between beaches, with only two profiles ever returning to pre-storm conditions in that decade and most experiencing four to five years of partial recovery before entering an erosional phase reflecting longer term behaviour. They found only 67% of the sediment eroded by the hurricane did return over than 10-year period, with the remainder speculated to have been transported alongshore to contribute to nearby spit accretion.

In a study of extra-tropical storms in the Gulf of St. Lawrence, Forbes *et al.* (2004) created a storm record from recorded wind, wave, and water level data in combination with hindcast wave time series and models. They compare this storm record with records of coastal response including visual observations, photo/video, and historical charts, and maps. From

this they explored changes in coastal configuration from the 1700s to the present day. From their historic map data, they found substantial changes in shoreline configuration and back/shore and dune morphology along the Prince Edward Island coast. In comparison with their storm record, they hypothesised that this the trimming and removal of dunes on this coastline may have occurred in one major storm season having been rendered vulnerable by grazing pressure following agricultural development in the early 19th century. This study was one of the first to utilise historic data from maps in concert with historic data on storms to determine the scale of storm impacts beyond contemporary monitoring approaches. They also explored the relationship between coastal recession rates from aerial photogrammetry and the storm record. Forbes *et al.* (2004) found that there was a poor correlation with storm magnitudes and frequencies over their observational period, though they attributed this largely to deficiencies in the climatological and water level data available for storms for their study region.

In the UK, Pye and Blott (2008) explored decadal scale variations in dune erosion on the Sefton coast. Their goal was the test the hypothesis that changing magnitude and frequency of high tides had a significant influence on front dune change. They were able to achieve this owing to consistent levelling surveys on this coast which had been conducted since 1979. Using these beach and dune profiles they calculated changing beach and dune volumes and explored the correlation of these with changing extreme tidal magnitude and frequency data available from tide gauges in Liverpool. Whilst they were unable to find a relationship with changing tidal magnitude-frequency, they did find a modest relationship between dune/erosion and accretion with the NAO index. Esteves *et al.* (2008, 2011) later expanded on this study of the Sefton coast to explore the role of changing storminess on a further 16 km of the same coastline. They examined rates of change in shoreline position from 1984 to 2005 based on historic map data and compared this with hindcast model data of changing storminess characteristics. As with previous studies they were unable to establish any statistically significant relationship between long-term shoreline position and modelled storm

parameters, however there were periods of more pronounced change associated with positive NAO winter indices.

2.4.4. Overcoming data challenges

The studies examining the decadal and longer response of coastal systems to changes in storminess and extreme sea levels discussed above raise one key challenge. These studies all note the quantity and quality of data both the morphological change elicited by storms and of the storm characteristics themselves as limitations. The challenges of gathering storm data are dealt with in 2.2, here focus is given to the lack of available morphological data. Except for Forbes *et al.* (2004) these studies all take place on beaches with a relative wealth of coastal monitoring data. Cross-shore datasets spanning decades are relatively rare, with few beaches worldwide holding such data, with many of those that do having experienced inconsistent approaches in the collection of that data as the agencies tasked with collecting that data themselves change (Baptista *et al.* 2014).

Forbes *et al.* (2004) overcame the lack of long-term shoreline data through use of historic maps, with shorelines determined from the highwater mark shown on these maps. They also utilised photo and video documentation taken during events gathered from regional libraries and newspaper archives. This approach is applicable to many coastlines, particularly to those with strong naval heritage. However, as with monitored data, it is still not ubiquitous in its temporal or spatial resolution.

An avenue by which the lack of long-term shoreline may be overcome is through the application of satellite data. Publicly available data from Earth observation satellites has been identified as a low coast means by which such data may be obtained. This has been aided by proliferation of this data in recent years by tools such as Google Earth Engine (GEE) (Gorelick *et al.* 2017). Satellite data has already seen extensive application to morphological studies, particularly in fluvial settings in application to meandering rivers (Monegaglia *et al.,* 2018). The Landsat and Sentinel satellite missions have seen application

in measurement of shoreline change usually through the application of parameters such as MNDWI (Modified Normalized Difference Water Index) which uses green and short-wave infra-red bands to distinguish between open water features and land. The limitation the 30 m pixel resolution on Landsat imagery can be overcome with the application of subpixel shoreline detection using pixel detection algorithms (Liu *et al.* 2017). These utilise the distinction between sand-coloured pixels, and water-coloured pixels and the arrangement of those colours around each other to distinguish sub-pixel shoreline position based on a machine learning training set.

Vos *et al*. (2019a) refined this methodology and presented a single toolkit (CoastSat) for reconstruction of shoreline change using Landsat imagery from 1984. CoastSat is a global shoreline mapping toolbox utilizing publicly available satellite imagery via GEE (Vos *et al*. 2019). CoastSat allows for the rapid acquisition of top-of-atmosphere imagery from GEE from the Landsat 5, 7, 8 and Sentinel-2 missions. CoastSat can apply a subpixel shoreline detection algorithm optimized for sandy beach coastlines to automatically detect shoreline positions. Greater detail on the nature of the algorithm and the CoastSat toolkit can be found in Vos *et al*. (2019). For their sites they produced horizontal errors of 7.3 m to 12.7 m against monitored shoreline positions. These errors were larger for macro-tidal dissipative beaches due to the large horizontal differences between the position of the sea-sand interface moving a greater distance depending on the stage of the tide than on reflective or microtidal beaches.

Tools such as these can present a vital data source for overcoming the data availability challenge for understanding the relationship of storms with longer-term coastal change.

Chapter 5 combines these tools with the methodology first explored in Chapter 3 and tide gauge records of storm surges (2.2.1).

Chapter 3.

Can sand dunes be used to study historic storm events?

Publication and copyright

The contents of this chapter are published in;

Bateman, MD., Rushby, G., Stein, S., Ashurst, RA., Stevenson, D., Jones, JM., Gehrels, WR. 2018. Can sand dunes be used to study historic storm events? *Earth Surface Processes and Landforms*. 43(4), 779-790. https://doi.org/10.1002/esp.4255

Nature and extent of contributions

The research presented in this chapter was originally devised by Bateman who undertook initial fieldwork and contributed to analysis and paper writing. Rushby was involved in measurement of results, site visits, results analysis and paper writing. Stein, Ashurst and Stevenson contributed to sampling and sample preparation. Jones and Gehrels contributed with field site visits and paper comments.

Abstract

Knowing the long-term frequency of high magnitude storm events that cause coastal inundation is critical for present coastal management, especially in the context of rising sea levels and potentially increasing frequency and severity of storm events. Coastal sand dunes may provide a sedimentary archive of past storm events from which long-term frequencies of large storms can be reconstructed. This study uses novel portable optically stimulated luminescence (POSL) profiles from coastal dunes to reconstruct the sedimentary archive of storm and surge activity for Norfolk, UK. Application of POSL profiling with supporting luminescence ages and particle size analysis to coastal dunes provides not only information of dunefield evolution but also on past coastal storms. In this study, seven storm events, two major, were identified from the dune archive spanning the last 140 years. These appear to correspond to historical reports of major storm surges. Dunes appear to be only recording (at least at the sampling resolution used here) the highest storm levels that were associated with significant flooding. As such, the approach seems to hold promise to obtain a better understanding of the frequency of large storms by extending the dune archive records further back to times when documentation of storm surges was sparse.

3.1. Introduction

On the 5 December 2013, a deep depression north of Scotland, UK, in conjunction with spring tides, produced an extreme storm surge down the east coast of Britain (Sibley *et al.*, 2015). During this water reached 6.05 m OD (Ordnance Datum, which approximates mean sea level) at Kings Lynn (Spencer *et al.*, 2015) and 6.31 m OD at Wells-Next-The-Sea in Norfolk causing extensive damage to coastal infrastructure, housing and farmland (Figure 3.1). This was the worst event since the disastrous flooding of southern North Sea coasts in 1953 (Baxter, 2005; Gerritsen, 2005) when several thousand deaths occurred across NW Europe (>300 on the east coast of the UK), as well as extensive breaching of coastal flood defences (Spencer *et al.*, 2015). Knowing the long-term frequency of such high magnitude events as well as more frequent severe storms is critical for present coastal management (Lewis *et al.*, 2013) particularly for low-lying coastlines where small changes in sea levels can translate into flooding a long way inland. It is also of increasing importance given rising sea levels (Church *et al.*, 2013) and the potential for future increased storminess over central Europe (Zappa *et al.*, 2013). North Sea storm surge levels are thought to be going to be substantially higher and more frequent by the end of this century (Vousdoukas *et al.*, 2016). The return period for extreme water levels to that of the 1953 storm surge was forecast to be around 50 years but given rising mean sea levels, will be less for an equivalent surge in the near future (Wolf and Flather, 2005). While hydrological modelling allows better prediction of peak storm-tide height along coastlines, further refinement requires better understanding of beach parameters and other coastal zone factors (Lewis *et al.*, 2013). To achieve this also requires an understanding of the response of specific segments of the coastline over longer timescales (Andrews *et al.*, 2000). Coastal sand dunes may provide a sedimentary archive of past storm events.

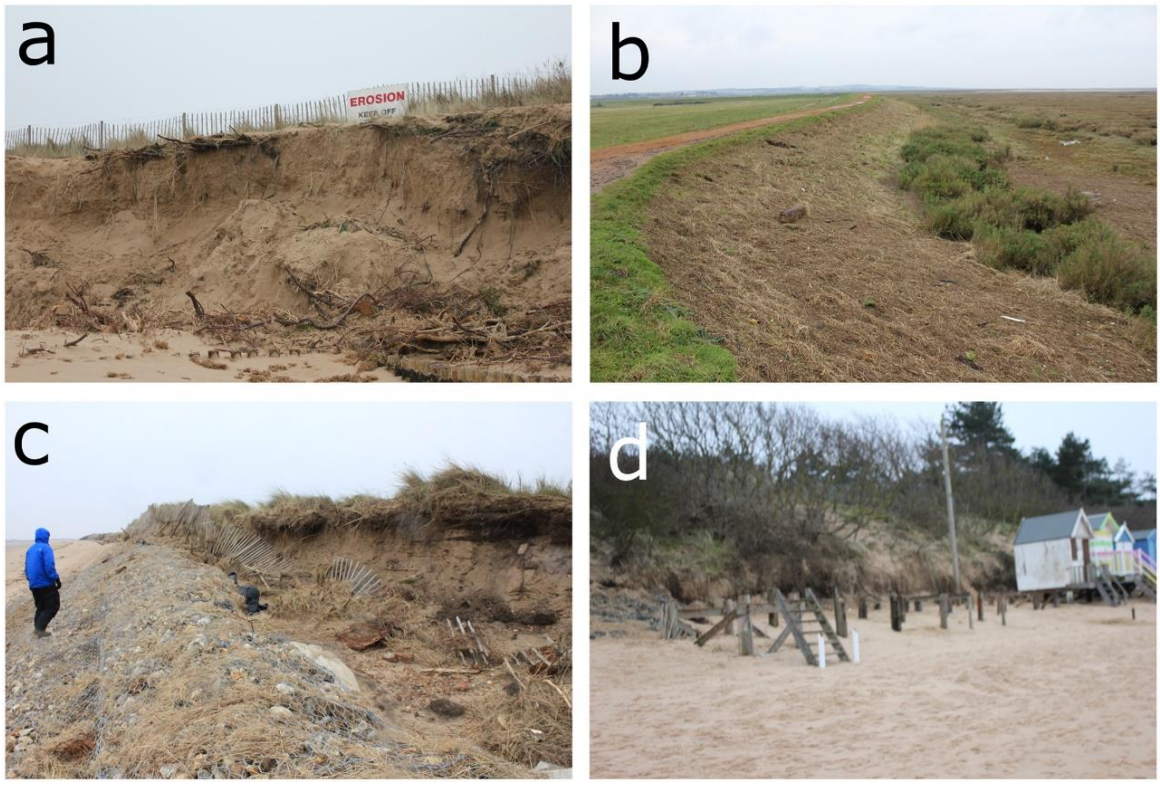

Figure 3.1. North Norfolk coastal damage resulting from the December 2013 storm surge in the North Sea. (a) Dune scarping at Brancaster, note metal pilings used to limit erosion on beach. (b) Flotsam left on an artificial sea-wall. The tidal surge reached the top but did not breach the wall on this occasion. (c) Erosion behind gabions placed to protect dunes at Brancaster. (d) Piles of former beach huts on Wells-Next-The-Sea destroyed in the storm surge.

Coastal dunes serve as an important buffer zone protecting low-lying coastal areas, and their growth is a function of accommodation space, sediment supply, wind and preservation. In particular wide beaches, providing a plentiful sediment supply, and a sequence of years without high-intensity storms promote dune development (Puijenbroek *et al.*, 2017). During storm events they can be modified (Spencer *et al.*, 2015). The nature of this modification is partly a function of how well dunes have coalesced to form a perpendicular barrier to the sea, the height above OD of the dune crest and any low points within the dunes. If waves come into direct contact with dunes, then erosion may take the form of breaching and overwash aprons (Figure 3.2(a); Steers *et al.*, 1979). This is more likely to occur where dunes are poorly developed (i.e., non continuous along the back beach or low in elevation)

and/or the magnitude of the storm exceeds the height of the dunes. Alternatively, scarping may occur in which the leading slope of a dune is eroded away leaving a vertical face in the dune on the seaward side (Figure 3.2(b)). This vertical face in sand is unstable so after a storm event it collapses until a slope at the angle of repose is re-established (Figure 3.2(c)). Recovery can be quick (<5 years, Brooks *et al.*, 2016). This is more likely to occur for well-established dunes with high crestlines and/or during lower magnitude storm events in which waves are sufficiently high to reach dune fronts but not to over top them. Storms can also modify dunes through deflation and/or the deposition of coarser aeolian sediments moved on high winds during the storm (Figure 3.2(d)). It is these erosion layers and storm deposited sediments which raises the potential for actively accreting dunes to have recorded longer-term coastal storm records.

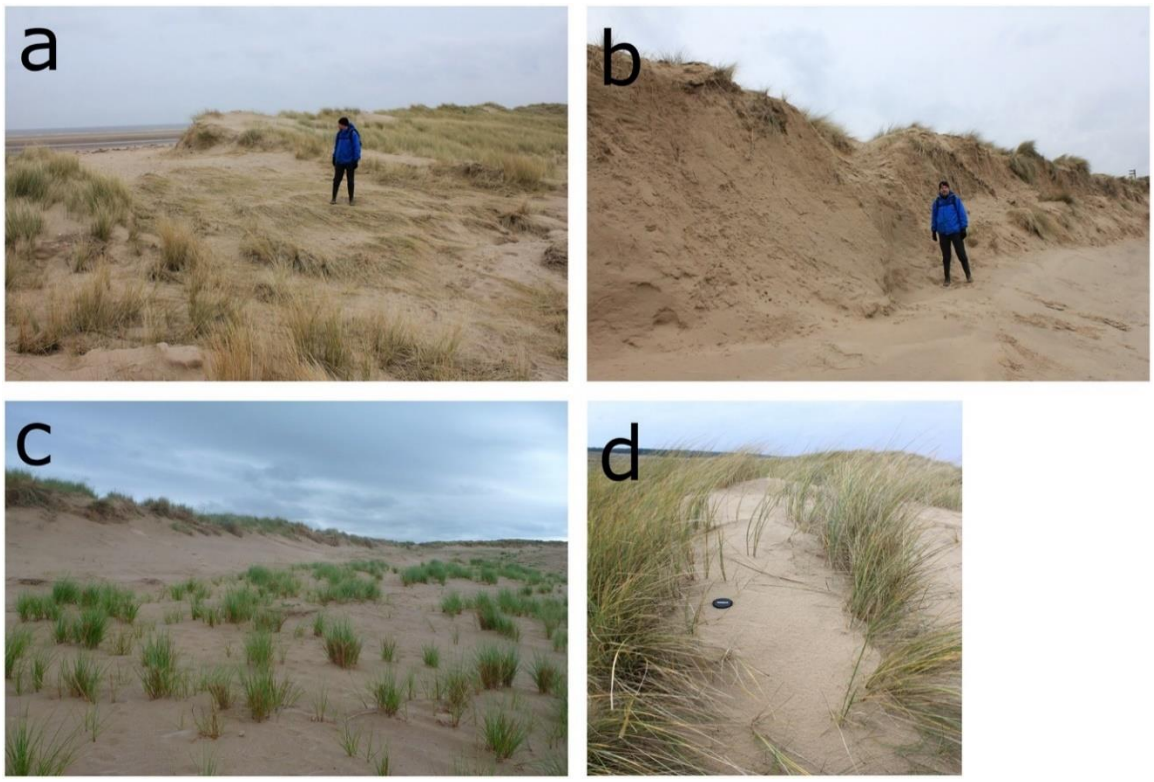

Figure 3.2. Impacts on coastal dunes of Storm surges. (a) Breaching of dune by waves forming sediment fan in newly formed interdune low. (b) Dune erosion forming 'scarped' vertical sand cliffs. (c) The same dunes as shown in (b) but 12 months on with collapsed and newly deflated sediment piled up against dunes. (d) Thin sheet of coarse-grained sand deposited by 2013 storm event on dune crest.

Given the above, for dunes to record a record of previous low frequency high magnitude storms within their stratigraphy they need to meet the following requirements:

- form a continuous back beach barrier (or inland barrier).
- have crest lines consistently higher than all but the most extreme storm events preventing overtopping and erosion away of the sediment archive.
- be in an area in which sediment supply is allowing active dune accretion thereby allowing dunes affected by storm scarping to be restored and dune crests to build up.

Proof of concept work has been carried out using innovative new portable optically stimulated luminescence (POSL) to establish high resolution relative coastal sand dune chronologies (Bateman *et al.*, 2015). Actual age determinations are not possible with this method, but total POSL counts can be viewed as a proxy for age, with older samples having a higher luminescence signal than younger samples. Unless the background dose creating the luminescence signal changes through time the POSL response with age should be linear. Down core dune profiles showed a pattern of very similar POSL signals suddenly stepping up in signal (Bateman *et al.*, 2015). These were interpreted as similar aged sediment deposition through dune accretion with the steps indicating hiatuses in dune construction caused by storms or tidal surges. This study seeks to examine coastal dune stratigraphy using POSL profiles from coastal dunes to determine if dunes act as sedimentary archives of storm and surge activity.

3.1.1. Region of study

This study focuses on the Norfolk coastline near Holkham, ~20 km west of Hunstanton and 3 km east of Wells-Next-The-Sea. This is within the UK Environment Agency's 'Superfrontage 2' stretch of coastline for shoreline management purposes (East Anglian Coastal Group, 2010). This study area was chosen as the north-facing coastline has a long fetch and a long history of being impacted by storms and storm surges. It is fronted by broad

sandy beaches and/or subtidal sand flats providing sediment to the ~6.5 km of well-developed coastal dunes (Figure 3.3).

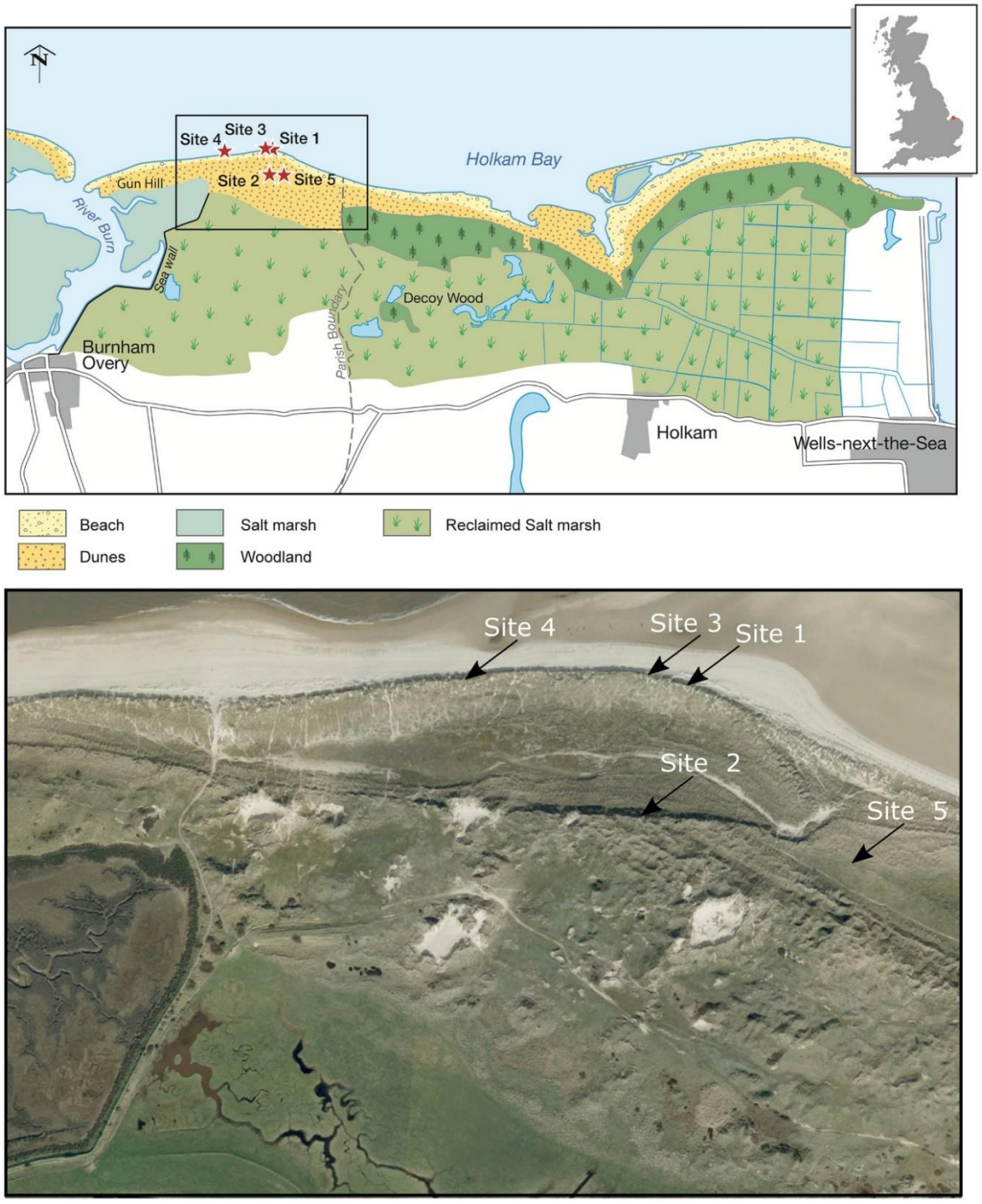

Figure 3.3. The coastal area between Burnham Overy and Wells-Next-The-Sea including the sampled dunes sites of this study. Sites 1, 3 and 4 were on the foredunes found at the back of the present-day beach. Sites 2 and 5 in inland dunes. Lower image modified from 2007 Digital Globe/Get Mapping image on Google Earth.

Oronsaye (1990) showed dune accumulation was dominantly by wind with a northerly component. This makes the site idea for capturing the results of low frequency high magnitude storms from the north such as the 1953 storm surge rather than prevailing UK storms which are from the south-west. Despite a backdrop of sea levels rising over the past 7500 years on average by $0.6 \pm 0.2\ mma^{-1}$ (corrected for changes in tidal range; Shennan and Horton, 2002), Brooks *et al.* (2016) showed that the coastline around Holkham Bay is prograding, increasing the likelihood of dune sediment preservation. A map from 1781 by Biedermann shows dunes in existence at Holkham at this time (Hiskey, 2003) and based on historic maps and aerial imagery, dune formation has continued to the present.

The work of Bristow *et al.* (2001) at Holkham, using GPR, reported two items critical to the current study. First, it showed that the dunes have never been free dunes moving inland with time but always, once established, have been pinned by vegetation responding only to erosion and accretion without much lateral movement. The stacking of dune sediment, rather than overturning during movement, greatly enhances the potential for dunes to retain records of storm events and for successful application of luminescence dating. Second, Bristow *et al.* (2001) were able to identify erosion surfaces extending from the beach into the dunes which they attributed to creation of dune cliffs subsequently covered by latter dune foreslope activity. These erosion events were linked to documented storms, although their age was unknown.

Three sets of dunes were selected for this study (Figure 3.3). The first set of sites (Sites 1, 3 and 4) were located at three positions along the dunes found at the back of the present beach. The second set of dunes (Site 2) was from a line of dunes parallel to the coast, approximately 300 m inland, and interpreted as an older formation than the back-beach dunes (Figure 3.3). The final set (Site 5) was on a less distinct set of dunes between sets 1 and 2 (Figure 3.3).

3.2. Methods

At all sample sites dune crest locations were selected and a Dormer engineering sand drill used to core down to dune base. The latter was established based on abney level surveys of the dune height above beach and from a change in sediment size from well-sorted medium sand to much coarser less sorted beach sand. At approximately 25 cm intervals, samples for POSL measurements and particle size analysis were collected in light-tight small plastic containers. Full optically stimulated luminescence (OSL) dating samples were also collected from near the dune surface, mid-core and base of core at most sites. This resulted in the collection of a total of 75 POSL and sediment samples and 12 samples for OSL dating.

For each POSL sample, any potentially light contaminated was removed and the sample material gently dried. All POSL measurements were undertaken with a SUERC portable OSL reader (Sanderson and Murphy, 2010) with measurements as per Bateman *et al.* (2015). Samples for full OSL dating were prepared as per Bateman and Catt, 1996), measured at the single aliquot level using a Risø luminescence reader and the single aliquot regeneration protocol (Murray and Wintle, 2003). Dose rates were determined from in situ field gamma-spectrometer measurements or elemental analysis. Results are shown in Table 3.1 (see 3.9. for full details on the PSOL and OSL methods employed)

Table 3.1. OSL related data for sampled sites within the Holkham dunes

Sample site	Sample code	Depth from surface (m)	Water content (%)	K (%)	U (ppm)	Th (ppm)	Cosmic dose rate (μGy ka^{-1})	Total dose rate (μGy ka^{-1})	D_e (Gy)	n	Age (years CE)
Site 1	Shfd13041	0.87	3.3	0.5	0.4	1.1	187 ± 9	835 ± 34	0.027 ± 0.014	24	1981 ± 16
	Shfd13042	3.68	3.6	0.5	0.34	1.0	129 ± 6	755 ± 35	0.034 ± 0.013	24	1968 ± 17
	Shfd13043	5.93	4.3	0.5	0.46	1.1	99 ± 5	753 ± 35	0.035 ± 0.013	24	1966 ± 17
Site 2	Shfd13044	0.80	3.4	0.5	0.4	1.1	189 ± 9	836 36±	0.071 ± 0.013	24	1938 ± 16
	Shfd13045	3.40	2.1	0.5	0.43	1.1	134 ± 7	798 ± 36	0.203 ± 0.013	24	<1758 ± 20
	Shfd13046	6.22	5.1	0.5	0.43	1.2	95 ± 5	743 ± 34	0.103 ± 0.014	24	1874 ± 20
Site 3	Shfd14097	1.00	3.2	0.5	0.38	1.0	185 ± 9	818 ± 46	0.038 ± 0.014	24	1968 ± 17
	Shfd14098	6.36	2.2	0.5	0.40	1.1	94 ± 5	747 ± 46	0.054 ± 0.013	25	1943 ± 18
Site 4	Shfd14099	1.00	2.9	0.4	0.37	1.0	185 ± 9	725 ± 38	0.013 ± 0.019	13	1995 ± 30
	Shfd14100	6.05	4.3	0.5	0.40	0.9	98 ± 5	734 ± 45	0.107 ± 0.018	17	1868 ± 26
Site 5	Shfd14101	0.84	3.9	0.5	0.31	0.9	188 ± 9	796 ± 46	0.036 ± 0.015	21	1965 ± 20
	Shfd14102	2.90	3.5	0.4	0.39	1.0	144 ± 7	687 ± 38	0.046 ± 0.014	22	1945 ± 20

All samples also underwent particle size analysis using a Horiba LA-950 laser diffraction particle size distribution analyser to detect changes in depositional environment. For this, sub-samples were riffled down and treated with 0.1% sodium hexametaphosphate, before dispersal in de-ionised water within the instrument using ultrasound and pumping. Resultant data were used to calculate the mean and median grain size of each sample (Φ), as well as sorting, skewness, and probability distribution (Table 3.2). Particle size showed nearly all samples to be well to moderately well sorted, unimodal with mean values in line with those found for dunes elsewhere (Lancaster, 2013). Within this were thin layers of slightly coarser and less well sorted sand which are interpreted as being aeolian storm deposits. As shown in Figure 3.4 particle size distributions from what are thought to be a storm deposit are slightly coarser, with a coarser tail and the 5th and 95th percentile further apart indicating poorer sorting

Table 3.2. Particle size measurement results. Entries shaded yellow indicate samples >5% coarser and/or where sorting is >5% worse than the average for that dune. Lines indicate where OSL shows a temporal hiatus in the dune record. Entries in red are those identified as potential storm deposits

Dune Phase	Depth (m)	Mean (M_z)	Sorting (σ_I)	Skew (SK_I)	Kurtosis (K_G)	Dune Phase		Depth (m)	Mean (M_z)	Sorting (σ_I)	Skew (SK_I)	Kurtosis (K_G)
Site 1 (Back-beach dune)							**Site 3 (Back-beach dune)**					
1	0.64	1.70	-0.45	0.03	1.06			0.78	1.80	-0.47	0.04	1.08
	0.87	1.82	-0.44	0.04	1.07			1.15	1.81	-0.46	0.05	1.08
	0.96	1.79	-0.46	0.05	1.04			1.50	1.99	-0.43	0.07	1.10
2	1.35	1.94	-0.45	0.10	1.08			**1.82**	**1.77**	**-0.45**	**0.05**	**1.05**
	1.70	1.93	-0.44	0.07	1.06			2.16	1.86	-0.46	0.06	1.07
	2.05	**1.75**	**-0.44**	**0.04**	**1.04**			2.56	1.91	-0.45	0.08	1.07
	2.37	**1.81**	**-0.47**	**0.07**	**1.04**			2.84	2.00	-0.44	0.06	1.11
	2.79	1.92	-0.45	0.07	1.06			3.16	1.96	-0.42	0.05	1.09
	3.23	1.93	-0.44	0.06	1.05			3.35	1.88	-0.43	0.05	1.07
	3.68	1.97	-0.44	0.07	1.07			3.70	1.84	-0.45	0.06	1.08
	4.07	1.92	-0.40	0.06	1.07			4.04	1.85	-0.44	0.06	1.07
	4.37	1.95	-0.42	0.07	1.06			4.44	1.90	-0.47	0.11	1.08
	4.72	2.02	-0.42	0.07	1.11			4.65	1.98	-0.44	0.07	1.08
	5.10	1.98	-0.45	0.07	1.06			**4.94**	**1.80**	**-0.46**	**0.04**	**1.07**
	5.36	1.98	-0.42	0.04	1.09			5.26	2.01	-0.43	0.07	1.10
	5.93	1.94	-0.44	0.08	1.05			**5.86**	**1.80**	**-0.48**	**0.07**	**1.05**

Dune Phase	Depth (m)	Mean (M_z)	Sorting (σ_I)	Skew (SK_I)	Kurtosis (K_G)	Dune Phase		Depth (m)	Mean (M_z)	Sorting (σ_I)	Skew (SK_I)	Kurtosis (K_G)
Site 4 (Back-beach dune)							**Site 2 (Inland Dune)**					
1	0.57	1.71	-0.47	0.04	1.05	1		0.51	1.83	-0.46	0.05	1.05
	1.18	1.74	-0.46	0.04	1.05			0.80	1.70	-0.47	0.04	1.05
	1.35	1.92	-0.44	0.07	1.07			1.11	1.67	-0.46	0.01	1.06
	1.65	**1.75**	**-0.49**	**0.07**	**1.05**	2		1.41	1.62	-0.46	0.02	1.08
	1.93	1.87	-0.45	0.07	1.08			1.72	1.60	-0.45	0.02	1.07
	2.21	1.92	-0.44	0.07	1.08			**2.00**	**1.45**	**-0.48**	**0.04**	**1.08**
	2.54	1.84	-0.45	0.04	1.10	3		**2.36**	**1.43**	**-0.50**	**0.01**	**1.04**
	2.83	1.81	-0.48	0.06	1.07			2.66	1.70	-0.48	0.04	1.05
	3.09	1.83	-0.46	0.07	1.09			2.97	1.90	-0.44	0.05	1.07
	3.38	1.80	-0.48	0.06	1.05			3.27	1.90	-0.46	0.05	1.06
	3.91	1.80	-0.48	0.06	1.05			**3.40**	**1.71**	**-0.51**	**0.05**	**1.03**
	4.21	1.84	-0.47	0.07	1.08			3.72	1.82	-0.47	0.04	1.05
	4.50	1.75	-0.48	0.06	1.04			4.04	1.92	-0.47	0.06	1.05
	4.77	**1.71**	**-0.46**	**0.07**	**1.04**			4.55	1.96	-0.44	0.05	1.05
	5.07	1.93	-0.45	0.07	1.07			5.00	1.86	-0.49	0.06	1.03
	5.31	1.88	-0.44	0.07	1.07			5.37	1.71	-0.47	0.02	1.04
	5.54	1.81	-0.32	0.06	1.06			**5.61**	**1.68**	**-0.45**	**0.01**	**1.07**
	5.85	1.67	-0.54	0.07	1.04			5.83	1.85	-0.46	0.04	1.07
								6.22	1.82	-0.44	0.03	1.06
Site 5 (Inland dune)												
1	0.68	1.83	-0.48	0.07	1.06							
	0.94	1.80	-0.47	0.06	1.06							
	1.23	1.71	-0.47	0.04	1.04							
	1.53	1.78	-0.49	0.06	1.04							
	1.78	1.90	-0.45	0.08	1.05							
	2.04	1.84	-0.48	0.06	1.07							
	2.30	1.92	-0.44	0.06	1.06							
	2.55	**1.59**	**-0.47**	**0.01**	**1.07**							

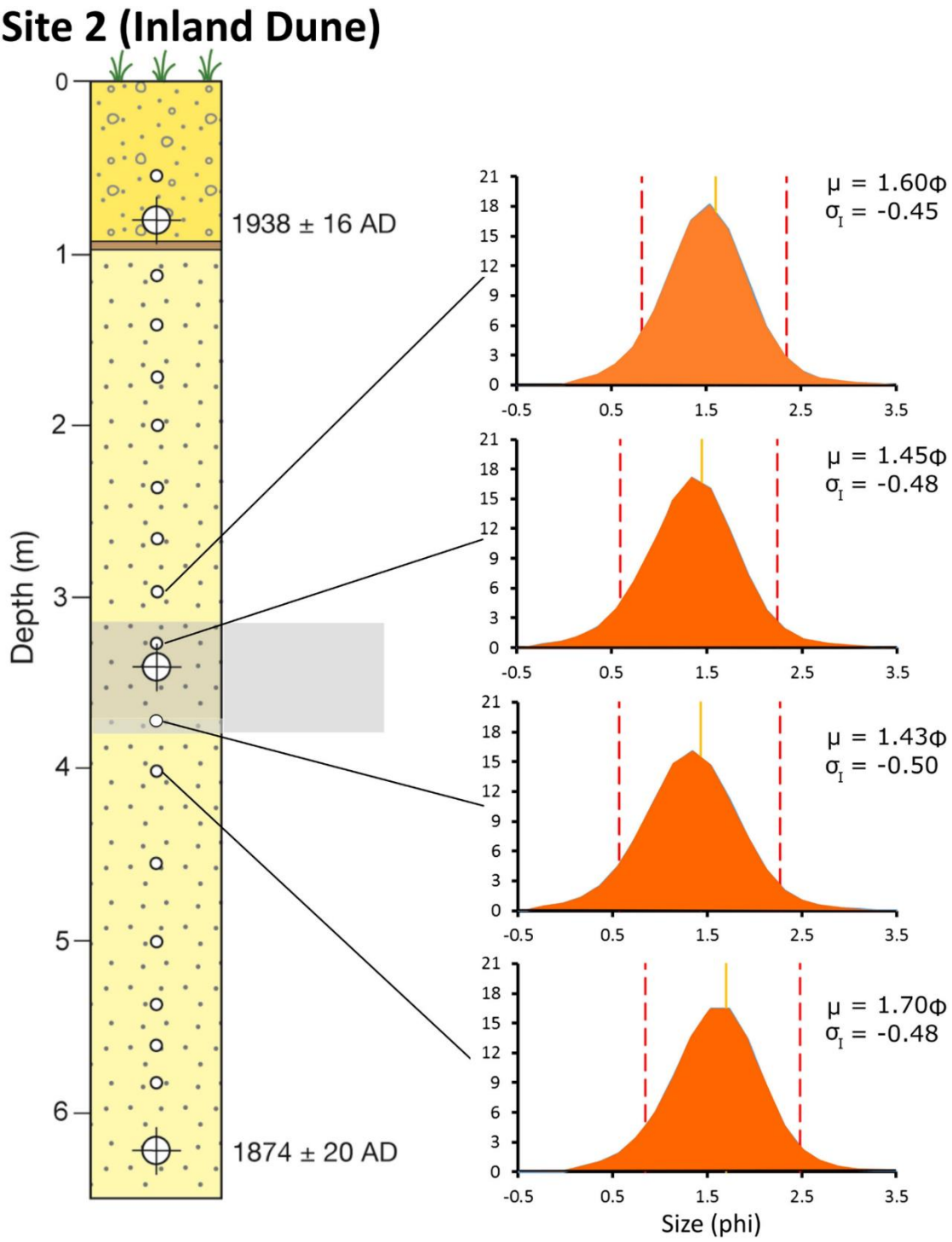

Figure 3.4. Down core stratigraphy and sample points of site 2 with particle size distributions from above, within and below what is interpreted as coarser aeolian unit deposited during a storm. Dashed red lines are the 5th and 95th percentiles and the orange solid line the 50th percentile. Note the shift to coarser sediment for the middle two samples, the extended coarse (left) tail and the greater width between the 5th and 95th percentile indicating poorer sorting.

To provide a long-term context for the Holkham dunes two approaches were used. First, changes in coastline were reconstructed from historical maps (1st series Ordnance Survey), aerial imagery (Crown copyright Royal Air Force aerial photographs 1946, Norfolk County Council aerial survey 1988) and Get Mapping imagery 2007 (via Google Earth). This resulted in 11 time slices spanning 175 years back to 1840.

The second approach was to reconstruct a coastal storm flooding record from reported observations and secondary documentary sources (Table 3.3). Brooks *et al.* (2016) reported 21 observed north Norfolk coastal storms from 1883 to 2013. This record was extended back to 350 BCE and up to 283 storms by the addition of the works of Galloway (2013), Kington (2010), Zong and Tooley (2003), Harland and Harland (1980), Lamb (1977) and others (see Table 3.3) based on a variety of archival documentary sources including floodstones (see http://floodstones.co.uk/), Parish records and the Times Newspaper. Only storms where coastal flooding around the North Sea had been reported were included. This storm record was refined by filtering out pre 1200 CE events where the record was limited (n = 12), storms reporting only minor flooding not in Eastern England (n = 61) and summer storms (n = 16). The latter was on the basis that these were not near the Spring or Autumn equinox tides and more likely caused by rainfall related flooding rather than sea inundation. Finally, the dataset was split into two: (1) storms where there was an explicit reference to them causing coastal flooding in eastern England (n = 189); and (2) storms where there was major/catastrophic coastal flooding in NW Europe in which, while the sources do not explicitly state flooding in England, such flooding may have occurred (n = 21). As with all such compilations of data, recording of storms is highly dependent on them being deemed at the time sufficiently out of the ordinary to merit recording and/or have caused significant damage/death. With increased coastal protection, coastal flooding is likely to have diminished with time. Data compilations are also highly dependent on survival of the original documents and, given their very diverse nature, finding them for inclusion in the database. With the advent of the instrumental record, increased shipping and coastal activity and better record keeping so events are more likely

to have been observed and recorded. Thus, the compiled database can be expected to have an unquantified bias towards more storms being recorded more recently. A final caution stems from the judgement call of those compiling storm events (including the present authors) as to whether coastal flooding was entirely localised and thereby only of significance to the present study if Norfolk was mentioned or more regional but only recorded at specific places. We can be reasonably sure that Norfolk was affected by the storm of 27 October 1882 as it caused flooding to the south in London and to the north in Whitby (Zong and Tooley, 2003). However, the storm of 21 December 1881 is only recorded as causing flooding in London (Zong and Tooley, 2003) and it is unclear whether Norfolk was also affected but not recorded in the London Times.

Table 3.1. Main documentary sources used to compile coastal storm flooding record. Also shown is the number of storms corroborated by other sources in the database.

Documentary source	Period covered (years CE)	Number of storms	Corroborated storms
Brooks *et al.*, 2016	1883–2013	20	8
Clemmensen *et al.*, 2014	1872	1	
Galloway, 2013	1287–1404	8	4
Cunningham *et al.*, 2011	1775–1176	2	
Kington, 2010	1099–2006	16	6
Pye and Blott 2007	1851–1856	2	
Zong and Tooley, 2003	1788–1993	132	14
Harland and Harland, 1980	1287–1978	16	10
Lamb, 1977	245–1973	117	17

3.3. Results

In this section the POSL, OSL dating, and particle size analysis are initially looked at to establish the storm record as archived in the dunes. Major storm events are interpreted where both a phase change (step) occurs in the POSL profiles and there is evidence for coarser sediments within a dune. Minor storms are interpreted where there is evidence only for coarser sediments within a dune. The storm record interpreted from the dunes is then compared with the archived mapping of the area and documented storm record.

3.3.1. Dune archive

In the back-beach dunes (Sites 1, 3 and 4) POSL results show that most have similar POSL signals all the way down the cores (Figure 3.5). These are interpreted as showing that the majority of dune construction was essentially in a single phase (Figure 3.5). The only exceptions to this are the uppermost 1 m of sediments at Site 1 and Site 4 which have a lower POSL signal. These are interpreted as indicating more recent small-scale dune modification. The basal increase of POSL signal at Site 4 is believed to relate to the underlying beach rather than the dune itself. Full OSL ages support the POSL results. The dune at Site 4 dates to 1995 ± 30 years CE and the uppermost dune sediments at Site 1 dates to 1981 ± 16 years CE (dark brown shading in Figure 3.5). The lowermost dune sediments at Site 1 and the majority of dune sediments at Site 3 are attributed to around 1966 ± 17 years CE (mid-brown on Figure 3.5). The basal sediments at Site 3 show a phase change in the POSL and appear slightly older dating to 1943 ± 18 years CE (light brown shading in Figure 3.5).

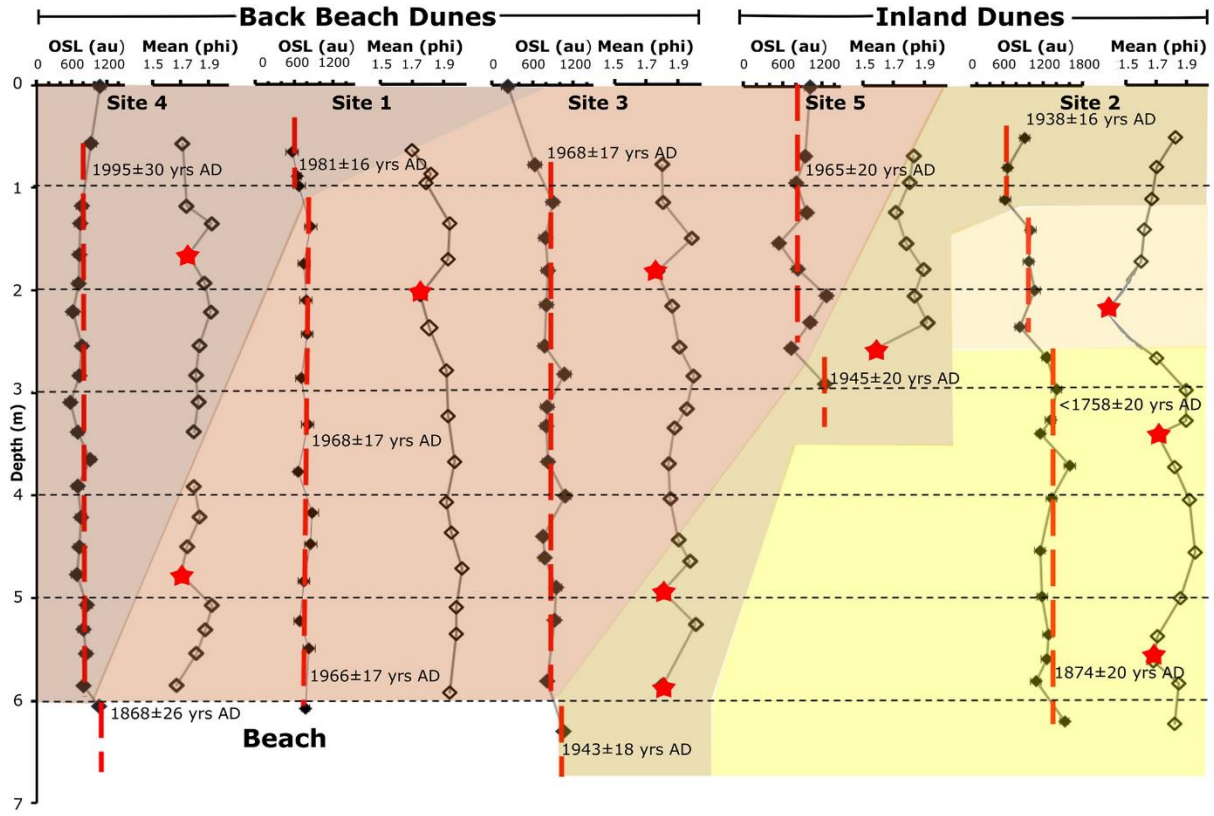

Figure 3.5. Downcore portable OSL and mean grain size for sampled dune sites. Phases of dune accumulation based on phases within dunes identified by portable luminescence (red dashed lines) and between dunes based on OSL ages. Coarser sediments inferred to relate to storms indicated with red stars. Note sites have been re-ordered based on their age and localities with sites 1, 3 and 4 from the dune found at the back of the beach dunes and sites 2 and 5 from inland dunes. The background colour changes indicate sediments of a similar age based on the full OSL ages.

Particle size results for the back-beach sites showed coarser layers at 2.0 m at Site 1, at 1.8 m, 5.0 m and 5.8 m at Site 3 and at 1.65 m and 4.8 m at Site 4 (see red stars in Figure 3.5). One of these coarser layers, that at 5.8 m at site 3, corresponds with a step up in POSL signal. This is interpreted as indicating a major storm event that modified the dunes through either erosion or dune movement and deposited a coarse layer before dune accretion resumed after the storm. This major storm event is dated at Site 3 to 1943 ± 18 years CE. The six other identified coarse layers (with no step up in POSL) are interpreted as resulting from three lower magnitude storms which caused dune accretion to briefly be interrupted

with coarser sediment deposition before normal dune accretion resumed (like that shown in Figure 3.2(d)). The storm associated with the upper coarser layer at Site 4 dates to ~1981 ± 16 years CE. The coarser layer at 2.0 m in site 1 probably corresponds with the 4.8 m layer in site 4 and the 1.65 m layer in Site 3 and this storm event dates to ~1966 ± 17 years CE. The coarser layer at 5.0 m at site 3 is a third storm event which dates to after 1943 ± 18 years CE.

The inland dunes show a slightly more complex history. Site 5, based on the two phases separated by a step in the POSL data (Figure 3.5), appears to show an upper sand unit 2.5 m thick, which deposited in a single phase overlying a slightly older sand unit. This is confirmed by the full OSL ages which suggest the upper sediment accumulated around 1965 ± 20 years CE and the lower sediment at 1945 ± 20 years CE. Site 2 has three phases of accumulation recorded in the POSL data separated by two steps at around 1.4 m and 2.5 m. (Figure 3.5). An upper unit which full OSL ages date to 1938 ± 16 years CE and therefore is of similar age to the basal sediments at Site 5 (light brown shading in Figure 3.5), a middle unit that unfortunately was not sampled for OSL dating and a lower unit dated to 1874 ± 20 years CE (yellow shading in Figure 3.5). The inland dunes appear to have ceased accumulating after around 1945 ± 20 years CE with dune formation switching to the present-day back beach dunes by 1966 ± 17 years CE (Figure 3.6). Such a change in dunefield can likely be attributed to a significant storm event sometime between 1945 and 1966. During this event sediment was likely eroded and moved offshore before being fed back onshore supplying sediment to the present back beach dunes.

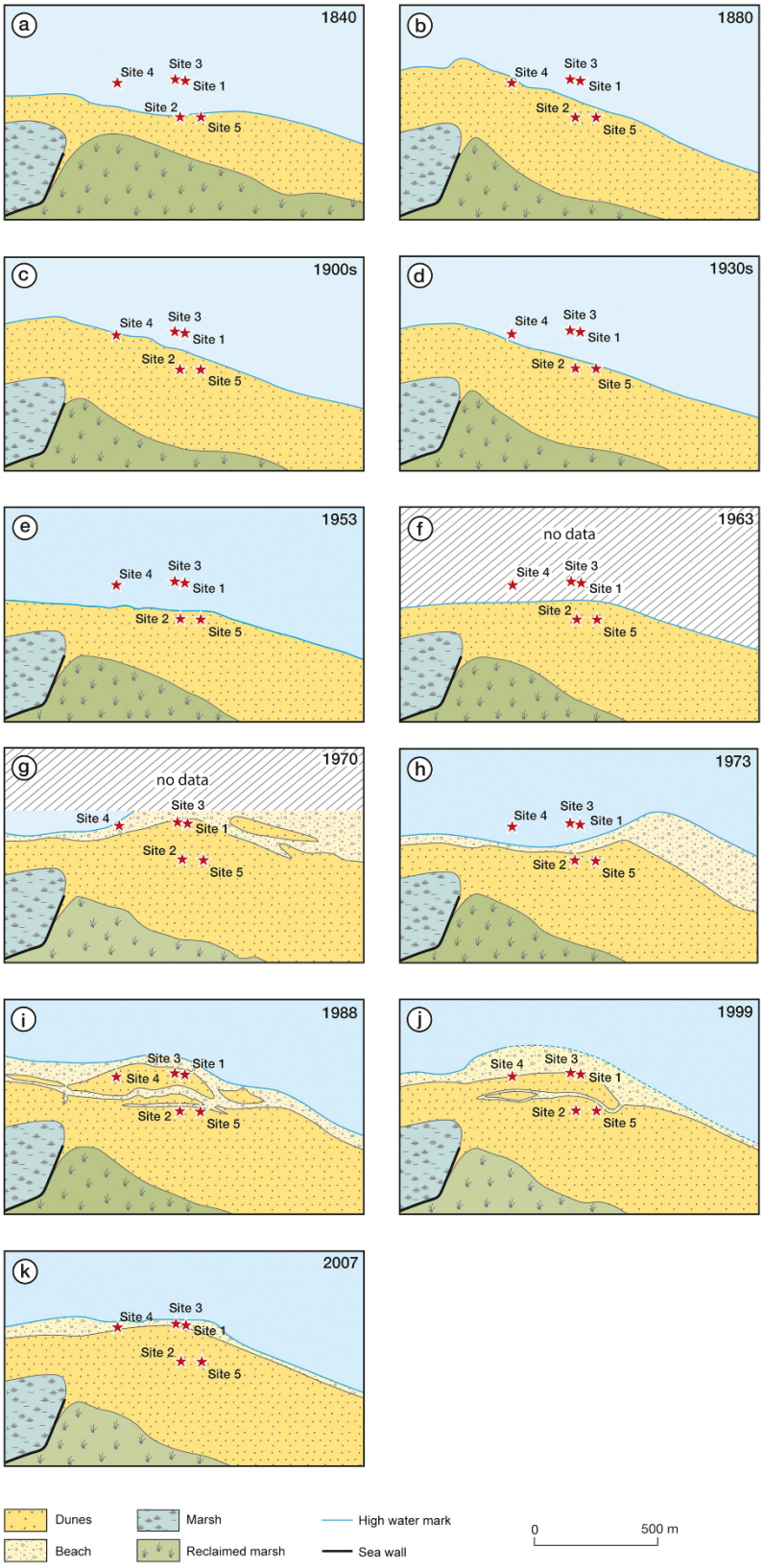

Figure 3.6. Historical map and imagery evidence for Holkham progradation of shoreline in relation to the sampled dune sites. Note the seawall acts as a point of reference for all time slices shown.

Particle size data from the inland dune sites shows a coarser basal sediment at Site 5 and a coarser layer around 2.15 m down the core at Site 2 (Table 3.3). Both these coarser layers correspond to changes in POSL and are interpreted as indicating major coastal storm events which modified the dunes. The coarser layer at Site 5 probably corresponds to that found at Site 3 and dates the storm to around 1945 ± 20 years. The site 2 coarser layer was not dated but falls within the periods 1874–1945 years CE. A further two coarser layers are observed at 3.4 m and 5.6 m depth at Site 2, which as the POSL does not change significantly, are attributed to lower magnitude storms which did not modify the dune, and which occurred sometime after 1874 ± 20 years CE.

In summary, the dunes sampled provide a ~ 140-year record (Table 3.4). Within this, at least two major storm events modified the dunes and/or caused evulsion of the system and new dune-lines to be formed. One took place in the late 19th to early 20th century and a second in the 1950s. Five smaller storms are interpreted from the record to have occurred in the 1980s, 1960s, 1930s and two late in the 19th century.

Table 3.2. Summary of the storms extracted from the dune archive at Holkham

Storm date	Sites	Dunes affected	Evidence	Storm magnitude	Attributed storm
~1995	Site 4	Back-beach	Coarse sand layer, no POSL change	Minor	1978
~1966	Sites 1,3,4	Back-beach	Coarse sand layer, no POSL change	Minor	1961
~1945	Sites 3,5	Inland and Back-beach	Coarse sand layer, jump in POSL and dune system avulsed to back-beach dunes	Major	1953
~1938	Site 2	Inland	Dune system avulsed to dunes associated with site 5	Minor	1938

Between ~1874–1945	Site 2	Inland	Coarse sand layer, jump in POSL	Major	1897
Between ~1874–1945	Site 2	Inland	Coarse sand layer, no POSL change	Minor	1883
Between ~1874–1945	Site 2	Inland	Coarse sand layer, no POSL change	Minor	1875
Pre 1874	Site 2	Inland	Inland dune initiation and presumed dune avulsion from previous dunes	Major	1850's?

3.3.2. Archive mapping and storm record

Historical maps and imagery show that the inland dune sites (sites 2 and 5) could not have existed prior to 1840 as where they were found was part of the beach before this time (Figure 3.6). Coastal progradation after this date would have provided accommodation space for the formation of the dunes associated with Site 2. Maps show that site 1, 3 and 4 (presently at the back of the beach) only appear above the high-tide line after 1970 and first appears on an aerial photograph from 1988. Within the limits of the time slices available this confirms that over the last 160 years the coastline associated with the Holkham dunes has been prograding northwards. The mapping shows some erosion of dunes on the western side of the study area during the 1930s and 1950s as indicated by Site 4 being further offshore at these points. A significant re-organisation appears to have taken place between 1973 and 1988 whereby a formerly inter-tidal and beach area rapidly became dunes. The map/aerial imagery supports both the full SAR OSL ages and the POSL data.

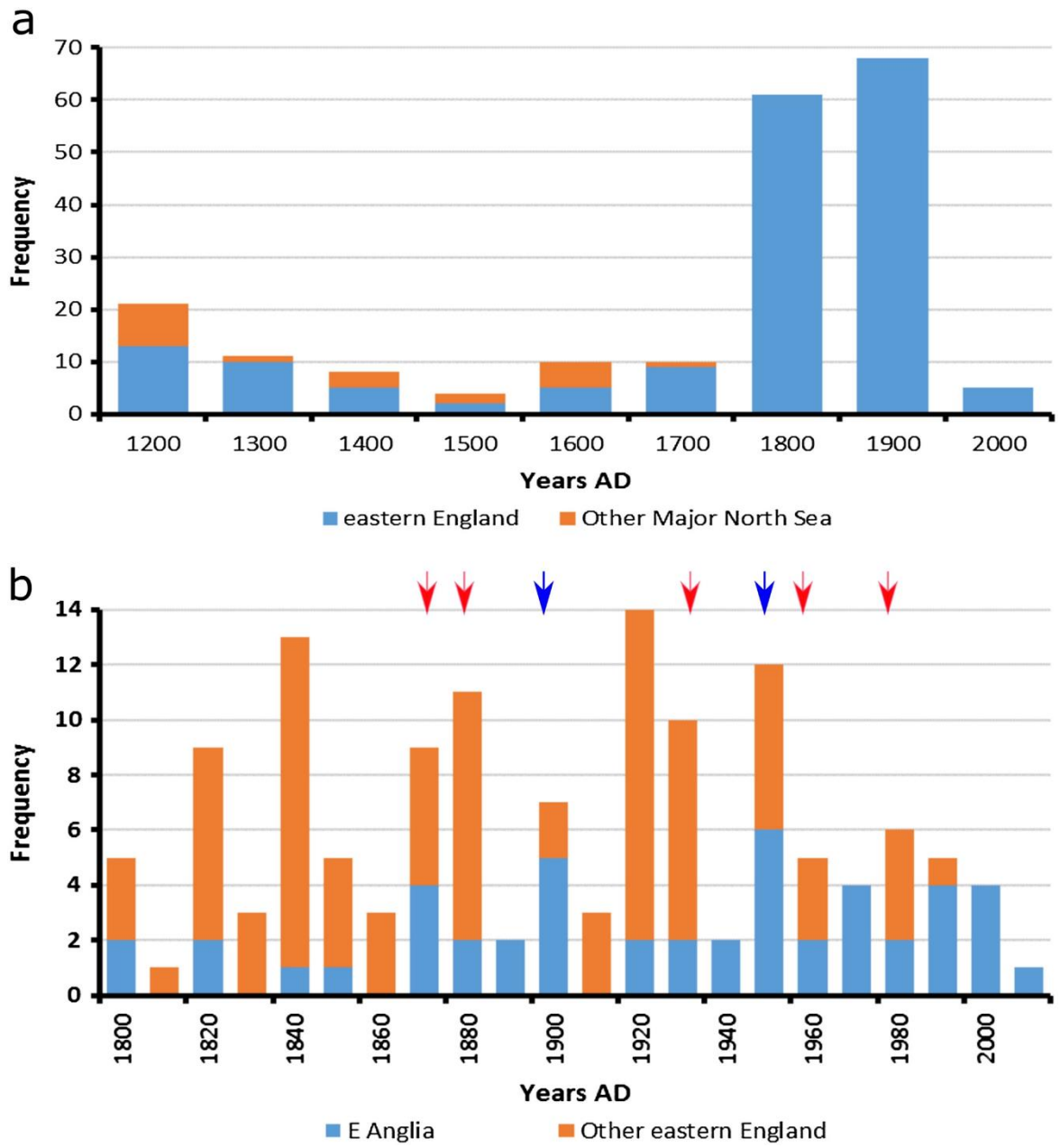

Figure 3.7. Storm record compiled from published records (see text for details). (a) Storm record since 1200 CE (number of storms per century) including those reported for eastern England and major storm events elsewhere in southern North Sea known to have cause significant flooding/loss of life. (b) Storm record back to 1800 CE (number of storms per decade) for East Anglia and elsewhere in eastern England. Blue arrows denote the approximate age when the Holkham dune archive indicates that a new line of dunes formed.

Over the last c. 800 years, the record reconstructed from observations and documentary sources indicates that storms causing coastal flooding in eastern England occurred approximately once every nine years (Figure 3.7(a)). Relatively low storm frequency is apparent within the period 1400–1600 CE and a very large apparent increase in storminess has occurred since 1800. As previously discussed, this can at least partly be attributed to better and more frequent records. Focusing on the period since 1800 and the East Anglia region (Figure 3.7(b)), once again storms causing coastal flooding to appear to have increased with time, averaging over the whole period to two per decade. Of note are the decades of 1870s, 1900s, 1950s, 1970s, 1990s and 2000s, decades that all seem to have had four or more storms in East Anglia. There is no correlation between frequency of flooding in East Anglia and that of eastern England (correlation coefficient = −0.074).

In a reanalysis of synoptic pressure patterns using the Jenkinson daily weather type for the Lincolnshire coast, Montreuil and Bullard (2012) also reconstructed on-shore storms for the period 1870–2012. They found that windstorms were higher than average in terms of frequency between 1871 and the 1920s, relatively infrequent up to until 1955 and peaked 1955–1970, 1975–1988 and from the mid-1990s to 2000. This closely follows the documentary-based storm record.

3.4. Discussion

Documentary evidence and luminescence dating have rarely been combined in an integrated analysis (Benito *et al.*, 2011). This study is the first to attempt it on coastal systems. Based on the luminescence and particle size data the Holkham dune sedimentary archive has recorded two major storm events (one late 19th–early 20th century, one in the 1950s) of sufficient magnitude to modify dunes and/or cause evulsion of the system and a further five other storms (two late 19th century, 1930s, 1960s 1980s). Clearly the dune archive is not preserving a record of all the documented storms within this period (Figure 3.7(b)). Based on documentary evidence for the last 140 years, an average of three storms a decade affect East Anglia compared with the 0.5 storms per decade extracted from the Holkham dune archive. That the dunes at Holkham are not recording all documented storms in the region probably in part reflects that not all the documented storms impacted directly on Holkham. On average only 2.2 storms per decade are recorded if storms are restricted to only those documented as directly impacting on Norfolk. While reducing the mismatch, this still probably over-represents the number of storms directly experienced at Holkham.

The key to preserving a storm trace in the dune archive is the magnitude of the storm and any accompanying storm surge. Some storms simply will not be of sufficient magnitude to cause dune erosion and/or deposition of a coarse sand layer on the crest. Given the age ranges of the dated levels in the dune archive, an exact attribution to known high magnitude storm surges cannot be given. However, in the recent record, the last significant flooding event prior to 2013 was on 11 January 1978 (Figure 3.8; Table 3.4). During this storm surge extensive flooding occurred across north Norfolk (Harland and Harland, 1980; Brooks *et al.*, 2016). This may have laid down the uppermost coarse sand layers identified in the back-beach dunes. The storm identified as having deposited a coarser layer in the back beach dunes during the 1960s is less certain. Harland and Harland (1980) describe the 20 March 1961 storm as causing ‘heavy seas, strong winds and damage and destruction’ but no sea elevation data is known. More certain is the 1953 storm surge which attained a sea elevation

of 5.15 m OD at Wells-Next-The-Sea (Brooks *et al.*, 2016; Figure 3.7) and caused major flooding in the area (Figure 3.8). It would seem likely that the coarser layers with associated erosion found in Sites 3 and 5 along with the change in dune position from the inland dunes (before 1950s) to the present-day back beach dunes (post 1960; Figure 3.5) relates to this major event (Table 3.4). In a study of the UK's Lincolnshire coastline, Montreuil and Bullard (2012) noted the symbiotic relationship of storms initially causing coastal erosion but then transporting back onshore large quantities of sediment to reform dunes. 15 February 1938 saw a storm surge which flooded the Brancaster marshes and the contours of beach and sandhills (dunes) completely changed (Harland and Harland, 1980). Sea elevations during the storm surge are not known. This may be recorded in the sand dune archive as the upper most sediment unit at Site 2 after which mapping shows the dunes avulsed to those associated with site 5 (Figure 3.6). The major storm event associated with the middle sand unit at Site 2 could relate to the flood associated with the storm of 28 November 1897 (Figure 3.8) in which flooding reached 4.49 m OD (Brooks *et al.*, 2016; Table 3.4). The minor storms identified in the lower Site 2 dune sediments could be from 11 March 1883 storm which flooded to 5.49 m OD at Wells-Next-The-Sea (ibid) and the storm of 14 October 1875 which flooded coasts from London to Whitby (Zong and Tooley, 2003; Table 3.4). While undated, if dune-line initiation occurs post a major coastal storm event (as per the 1953 flooding) then the establishment of the inland dunes around site 2 must have been before ~1878. The line of inland dunes could therefore relate to dune avulsion after the series of powerful storms in the 1850s which are recorded as having breached Spurn Head near Hull and caused coastal flooding from Hull, the Fenlands down to London (Zong and Tooley, 2003).

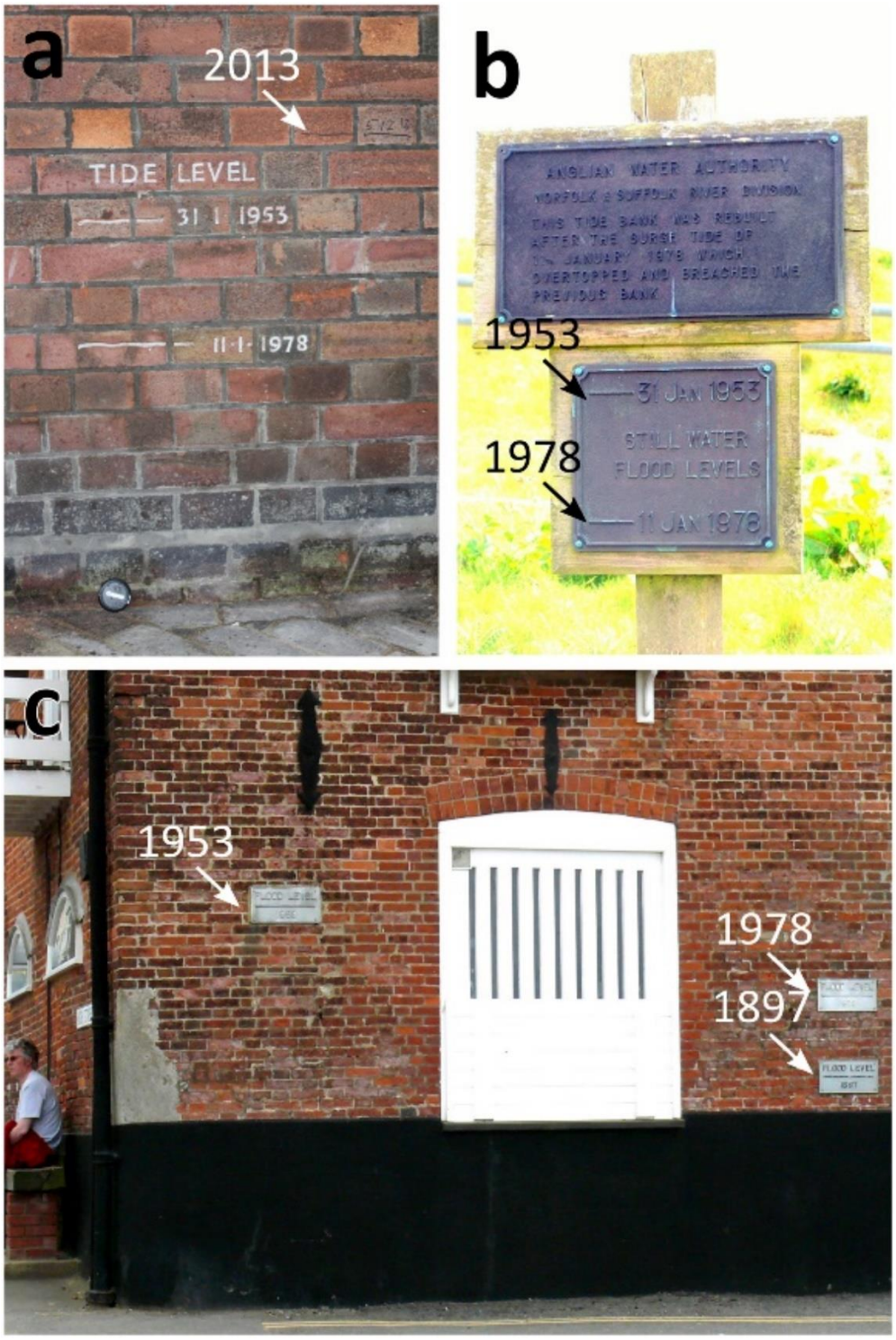

Figure 3.8. Preserved flood markers around North Norfolk. (a) Flood markers for 2013 at 6.31 m OD, 1978 at 5.94 m OD and 1953 at 6.15 m storms found on the Granary building, Wells-Next-The-Sea. (b) Flood markers for 1978 at 5.93 m OD and 1953 at 6.13 m OD storms found on Beach Road Wells-Next-The-Sea. (c) Flood markers for 1953 at 6.55, OD, 1978 at 5.98 m OD and 1897 at 5.54 m OD storms recorded on the Quay building in Blakeney.

3.5. Future Directions

Overall, from the above it would appear that, with the appropriate interrogation, coastal dunes can act as sedimentary archives of storm surge activity. If such research ultimately aims to give coastal managers a better understanding of return intervals of coastal storm surges and spatial extent of flooding, then moving beyond the instrumental record is required. They also show that while dune erosion/breaching during major storms may be dramatic, providing they are followed by several years without such storms, dunes appear to recover by either rebuilding or re-establishing a new dune line. At Holkham, extending the record to older inland dunes should uncover sedimentary archives for documented storms in March 1820, November 1794, February 1736, January 1734 and even potentially November 1404 (Kington, 2010, Harland and Harland, 1980, Galloway, 2013). All these are reported to have had major storm surges associated with them (ibid).

Research on the dune sedimentary archive will only really add value to coastal managers when it is able to, with confidence, identify previously unrecorded storm surges at localities and/or extend the record back to where documentary evidence is patchy. Before this is achieved further evaluative steps should be undertaken:

A better understanding is required as to whether subsequent events could, through erosion, ‘overwrite’ earlier storm archives and closely spaced events might be combined in the dune archive. This may account for the decades where four or more storm events have been documented (e.g., 1900s and 1950s, Figure 3.7(b)), but only one or less events are recorded in the dunes. Use of ground penetrating radar, as employed by Cunningham *et al.* (2011), and continuous or more high-resolution sampling for POSL might help in this regard.

That the dunes at Holkham are not recording all documented storms in the region also probably reflects that not all these storms impacted directly on Holkham. Sixteen coastal dune fields exist for Norfolk and Suffolk (Pye *et al.*, 2007). Future research extending the examination of the dune archive to this extensive regional dune record would remove the

current mismatch between comparing a regional documentary storm record with a site-specific dune archive record. This would also allow a more rigorous evaluation of the efficacy of the dune archive in recording storm events.

An alternative explanation for the difference between documented storms and the Holkham dunes is that only high magnitude events erode and/or deposit sand on dunes and so it is only high magnitude events that are recorded in the dune archive. Further research would be needed to establish a better idea of a threshold above which storm events sufficiently impact on dunes for them to be recorded in the sedimentary record. Such an approach has been successfully undertaken in the context of the relationship between beach storm ridges and tropical cyclone activity in Australia (Forsyth *et al.*, 2010).

3.6. Conclusions

Application of POSL profiling with supporting luminescence ages and detailed particle size analysis to coastal dunes, as well as providing information of dunefield evolution can also provide information of past coastal storms. In this study, seven storm events, two major, were identified from the dune archive. These spanned the last 140 years and seemed to fit well with documentary evidence of major storm surges which have affected north Norfolk. Targeting of dunefields, which stack sediment rather than overturning, greatly enhances the potential for dunes to retain records of storm events and for successful application POSL profiling. Dunes do not appear to be recording (at least at the sampling resolution used here) all recorded storm events only ones in which sea elevations were particularly elevated and significant flooding occurred. As such the approach seems to hold promise to extend the dune archive records further back in time when less is known about storm surges to get a better understanding of their frequency, and older dunes and extending the record to a regional level would allow this. The work also has coastal management implications in that, providing high intensity storm events are followed by a number of years without such storms, dunes recover by either rebuilding or re-establishing a new dune line.

3.7. Acknowledgements

Sarah Henderson and the Holkham Estate are thanked for their assistance in working at Holkham. Gill Tyson is thanked for her cartographic assistance with the figures. This research was funded through a White Rose Consortium Grant held by Dr Katherine Selby at the University of York. It was also funded through a NERC grant to GR (Ne/L002450/1).3.8. Supplementary Information

3.8. Supplementary Information

3.8.1. Portable OSL methodology

More controlled POSL measurements were conducted at the Sheffield University luminescence laboratory. For each sample, the sediment from the top and bottom of the plastic container, which was potentially light contaminated during sampling, was removed, dried. The remaining POSL sample material was dried at 30oC for 24 hours before measurement. All POSL measurements were undertaken with a SUERC portable OSL reader (Sanderson and Murphy, 2010). POSL measurement followed that outlined in Bateman *et al*. (2015) with each sample spread as a monolayer across the bottom of a 5 cm petri dish and placed in the portable reader with measurement for 60 s. POSL results (Figure 3.5) showed that the POSL signals whilst being young do not suffer from variable residuals and the transfer effects encountered for dunes by Muñoz-Salinas *et al*., 2017).

3.8.2. OSL dating Methodology

Samples for full OSL dating were prepared as per Bateman and Catt (1996). OSL measurements were conducted in a Risø luminescence reader fitted with blue/green LEDs for stimulation and signal detected was through Hoya U340 filters. Samples were mounted as a monolayer on 9.6 mm diameter aliquots with multiple replicates of palaeodoses (De) for each sample measured using the single aliquot regeneration (SAR) protocol (Murray & Wintle, 2003). The preheat of 220oC for 10s used in the latter was derived experimentally using a dose-recovery preheat plateau test (Murray & Wintle, 2003). Overall, the samples

showed rapid OSL decay curves, good recycling and low thermal transfer. Dose rates were determined from in situ field gamma-spectrometer measurements or, where this was not possible, based on concentrations of potassium, uranium and thorium as determined by ICP-MS and ICP-OES. All dose rates were appropriately attenuated for moisture (based on present-day values) and sediment size and incorporated a cosmic dose rate following the published algorithm of Prescott & Hutton (1994). In data analysis, no appreciable difference was found whether early or late background subtraction was applied so the latter was adopted to retain a better signal to noise ratio. De distributions show most samples to be normally distributed and overdispersion were low once outliers were excluded (Figure 3.9). The final derived De values were therefore based on the Central Age Model (Galbraith and Green, 1990; Table 1). The exception to this was sample Shfd13045 which had a high OD, and the De distribution was skewed (Figure 3.9). The final De value for age calculation purposes was therefore derived using the lowest component as determined by the Finite Mixture Model (Roberts et. al., 2000; Table 1) but even then, produced an apparent over-estimation of age.

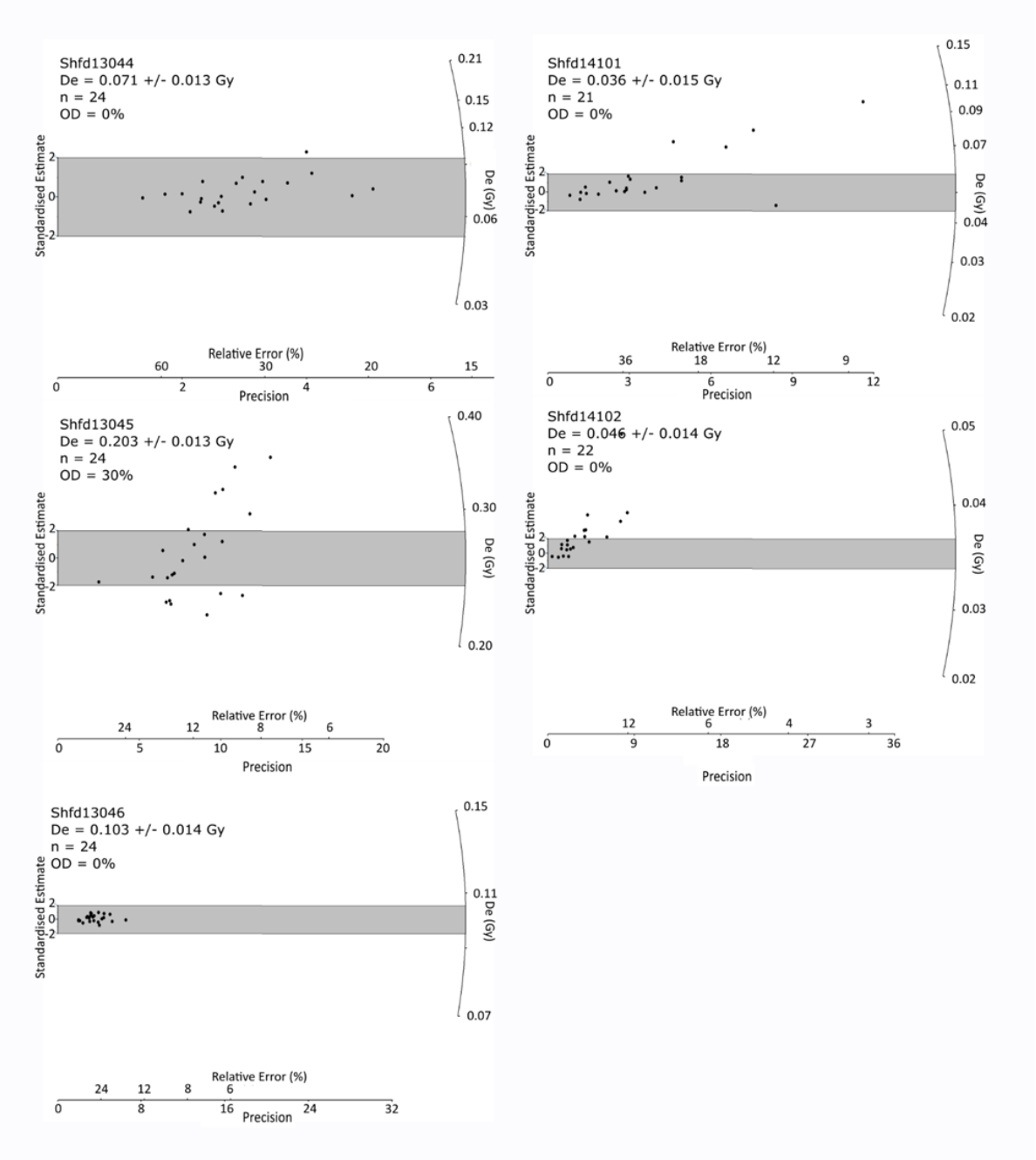

Figure 3.9. Example radial plots of OSL palaeodoses (De) for the three samples from site 2 (left column) and the two samples from site 5 (right column)

Chapter 4.

Testing the mid-Holocene relative sea-level highstand hypothesis in North Wales, UK.

Publication and copyright

Rushby, GT., Richards, GT., Gehrels, WR., Anderson, WP., Bateman, MD., Blake, WH. 2018. Testing the mid-Holocene relative sea-level highstand hypothesis in North Wales, UK. *The Holocene*. 29(9). https://doi.org/10.1177/0959683619854513

Nature and extent of contributions

This work reconstructs RMSL in North Wales and attempts to constrain a long-standing question over the existence of a mid-Holocene sea level highstand in the region. This work combines a RMSL record from a late-Holocene salt-marsh in North Wales with SLIPs derived from a freshwater marsh. The write up presented here is principally the work of the thesis author, however sections pertaining to the freshwater marsh were undertaken by Richards. Other contributors provided comments on manuscript structure and style in their role as dissertation supervisors. Blake consulted on ^{210}Pb and ^{137}Cs data and is included as a collaborator as part of contracted work in measuring these data.

Abstract

Accurate Holocene relative sea-level curves are vital for modelling future sea-level changes, particularly in regions where relative sea-level changes are dominated by isostatically induced vertical land movements. In North Wales, various glacial isostatic adjustment (GIA) models predict a mid-Holocene relative sea-level highstand between 4 and 6 ka, which is unsubstantiated by any geological sea-level data but affects the ability of geophysical models to model accurately past and future sea levels. Here, we use a newly developed foraminifera-based sea-level transfer function to produce a 3300-year-long late-Holocene relative sea-level reconstruction from a salt marsh in the Malltraeth estuary on the south Anglesey coast in North Wales. This is the longest continuous late-Holocene relative sea-level reconstruction in Northwest Europe. We combine this record with two new late-Holocene sea-level index points (SLIPs) obtained from a freshwater marsh at Rhoscolyn, Anglesey, and with previously published regional SLIPs, to produce a relative sea-level record for North Wales that spans from ca. 13,000 BP to the present. This record leaves no room for a mid-Holocene relative sea-level highstand in the region. We conclude that GIA models that include a mid-Holocene sea-level highstand for North Wales need revision before they are used in the modelling of past and future relative sea-level changes around the British Isles.

4.1. Introduction

Because of the spatial variability in the processes that drive relative sea-level (RSL) change at the coast, high-quality regional Holocene RSL data are required to enable a thorough understanding of the processes driving past and future coastal change. This is especially true for the British Isles where the unique interactions between the British and Irish Ice Sheet (BIIS) and the Fennoscandian Ice Sheet result in diverse isostatically driven Holocene sea-level histories (Shennan *et al.*, 2018). This, along with the abundance of sedimentary archives of sea-level data around the UK coast, has led to the construction of a consolidated UK and Ireland sea-level index-point (SLIP) database (Shennan *et al.*, 2006, 2018) that has been central to the development and validation of a series of quantitative glacial isostatic adjustment (GIA) models of the United Kingdom and NW Europe (Bradley *et al.*, 2011; Milne *et al.*, 2006; Shennan *et al.*, 2006). These GIA models are vital tools for simulating the response of the solid Earth to mass transfer between the oceans and the cryosphere; constraining ice-sheet thickness, extent, and dynamics; and quantifying global meltwater flux and the viscosity structure of the Earth's mantle (Bradley *et al.*, 2011; Milne *et al.*, 2006; Uehara *et al.*, 2006). Because of their ability to predict vertical land movements along the coast, GIA models are also key to predicting future RSL changes around the British Isles (Gehrels, 2010; Shennan *et al.*, 2012).

In areas where the temporal coverage of empirical RSL data is sparse, GIA models remain poorly validated and there may be a resultant mismatch between GIA sea-level predictions and empirical (geological) RSL data. North Wales has been identified as poor agreement between some GIA models and empirical SLIPs (Brooks *et al.*, 2008; Roberts *et al.*, 2011; Shennan *et al.*, 2006). This mismatch has led to a debate on the southern-most limit of ~1 to 2 m mid-Holocene sea-level highstand (Peltier, 2002; Shennan *et al.*, 2006), the existence of which is supported by SLIPs further north on the coast of Northwest England (Lloyd *et al.*, 2013). Some models, notably that of Lambeck (1996), suggest that mid-Holocene RSL was not higher than present in North Wales, while others predict a mid-Holocene highstand, in

particular the ICE-4G and ICE-5G iterations by Peltier (1994, 2004), which both predict RSL maxima of 1.33 m at 4 ka and 0.93 m at 4 ka, respectively. More recent models such as BRADLEY2011 (Bradley *et al.*, 2011) and its more recent iteration BRADLEY2017 (Shennan *et al.*, 2018) also predict a mid-Holocene highstand in North Wales, albeit of smaller magnitude. Constraining the southern-most limit of mid-Holocene emergence is of importance for the validation and future refinement of GIA models for investigating RSL, ice-loading histories and earth rheology (Bradley *et al.*, 2016).

The Holocene RSL history of North Wales is one of the least well understood in the United Kingdom with no continuous record and most SLIPs for the region only being of early- to mid-Holocene in age, and little data constraining RSL in the late Holocene (Shennan *et al.*, 2018). Until the study by Roberts *et al.* (2011), the empirical RSL data for North Wales comprised of only 12 SLIPs and one limiting point (Bedlington, 1994; Heyworth and Kidson, 1982; Prince, 1988; Shennan *et al.*, 2006). Roberts *et al.* (2011) expanded upon this greatly with the addition of 10 new SLIPs and 9 limiting dates derived from estuarine sequences in the NE Menai Strait. Despite this step forward in understanding of RSL in North Wales, any high-resolution appraisal of late-Holocene RSL changes remains limited, as the most recent SLIP in the Roberts *et al.* (2011) dataset is dated to 4.25–4.83 ka BP.

The goal of this study is to better constrain the southern-most limit of mid-Holocene emergence by expanding upon the North Wales sea-level dataset with data from the late Holocene (4 ka BP–present) to test the mid-Holocene highstand hypothesis in North Wales. The objectives of this study are to (1) produce the first high-resolution late-Holocene RSL reconstruction for North Wales from a 3300-year-long salt-marsh sedimentary sequence believed to be the longest continuous salt-marsh sequence in the United Kingdom; (2) combine this reconstruction with additional basal SLIPs derived from a nearby tidally influenced back-barrier freshwater marsh, using a novel groundwater modelling approach; (3) combine these data with regional SLIPs derived from previous studies (Roberts *et al.*, 2011; Shennan *et al.*, 2006, 2018) and produce complete Holocene RSL history for North

Wales; and (4) compare the RSL history of North Wales with various GIA model predictions to assess their ability to accurately simulate North Wales Holocene RSL changes.

4.2. Study area

4.2.1. North Wales

The coastlines of North Wales and the Isle of Anglesey have great variety in their geomorphology, from sheer cliffs and high-energy beaches to extensive dunes and sandy estuaries. Most of the latter are constrained to the relatively sheltered areas surrounding the Menai Strait. The southern coast of Anglesey is predominantly subject to onshore south-westerly winds and waves. Tides are semi-diurnal with a mean tidal range of 3.72 m recorded at Holyhead tide gauge.

Contemporary vertical land motion along the North Wales coastline based on interpolated Continuous Global Positioning Satellite (CGPS) data carries large uncertainties and is estimated to be between –0.4 and 0.4 mma^{-1} (Bradley *et al.*, 2009). The vertical land motion rate becomes increasingly negative moving south because of the combined effects of the response to the BIIS and Fennoscandian ice sheets (Bradley *et al.*, 2009; Simon *et al.*, 2018).

4.2.2. Malltraeth salt marsh

Malltraeth salt-marsh (53°10′21″N, 4°23′0″W) is situated on the eastern side of the Malltraeth estuary on the south Anglesey coast (Figure 4.1). The estuary overlies beds of Namurian (Middle Carboniferous) grits and sandstones and is flanked at its mouth by igneous rocks of the Gwna group (Horak and Evans, 2011). The estuary is one of the few low-energy depositional coastal environments in North Wales that harbour substantial salt-marshes, owing to the shelter provided by the western Newborough dunes extending across the estuary's mouth. The marsh forms part of the Newborough Warren National Nature Reserve maintained by Natural Resources Wales. This reserve is mostly comprised of open sand dunes extending along the Abermenai Point spit in the east and afforested dunes to the

west. Trees were planted atop the dunes between 1947 and 1965 originally as an effort to stabilize the dunes and protect the village of Newborough from wind-blown sand (Rhind *et al.*, 2001).

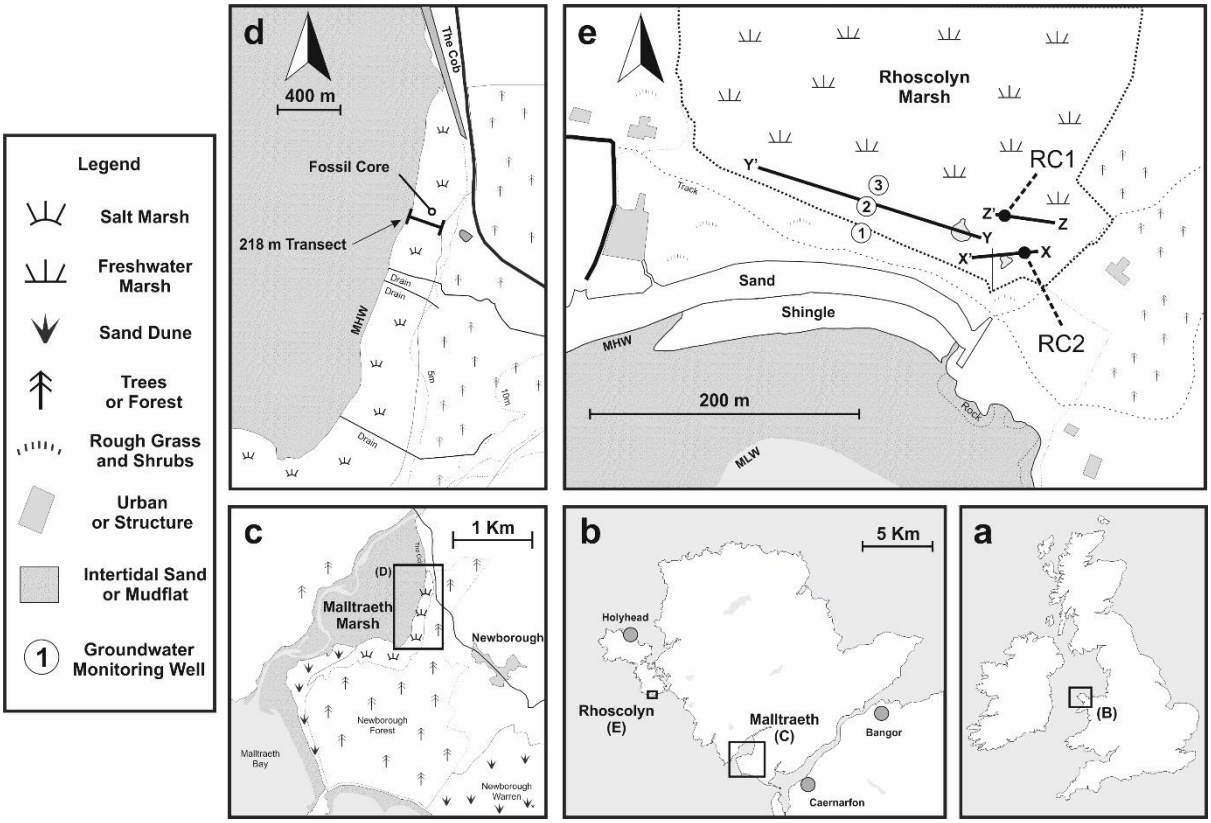

Figure 4.1. Location map of study sites and sampling strategies: (a) United Kingdom, (b) Isle of Anglesey, (c) Malltraeth estuary and surrounding area, (d) North portion of Malltraeth salt-marsh and sampling locations and (e) Rhoscolyn freshwater marsh and sampling locations.

The contemporary salt-marsh is 0.9 km^2 in area. The northernmost extent of the marsh is bound by a sea wall known as the 'Cob', by woodland to the east and the afforested dunes to the south. The marsh was once part of a much larger (1600 ha) marsh system extending north into a much larger estuary (Clout, 2007). This estuary and area of marsh was reclaimed in the early 1800s with the construction of the Cob (Packham and Liddle, 1970). Packham and Liddle (1970) suggest that following straightening of the Cefni channel in 1945 CE, sedimentation in estuary was altered and resulted in the rapid lateral expansion of the

southern part of the Malltraeth marsh. The southern area of the marsh has also contained a number of artificial drainage ditches in the past and, since the 1940s, a decoy pond. Given the potential complexities of rapid sedimentation and human influences, the southern portion of the marsh was avoided. Instead, the area of the marsh shown in Figure 4.1 was chosen to collect cores and to construct sea-level transfer functions from surface foraminiferal samples. Human influence was notably minimal in this area of the marsh and there is little evidence in the stratigraphy of former tidal creeks. The gradient from upper salt-marsh vegetation to the unvegetated tidal flat occurs over ~220 m, and ~1.5 m change in elevation.

4.2.3. Rhoscolyn freshwater marsh

The second site used in this study, Rhoscolyn marsh (53°14′44″N, 4°35′18″W) on Holy Island in western Anglesey, is a back-barrier freshwater marsh fronted by Borth Wen beach. The site extends approximately 0.55 km inland and covers an area of around 300 km2. The vegetation is dominated by Phragmites australis and drainage is via a single culvert, which exits below the sand barrier through a tidal sluice. A small pond is present in the south-east of the marsh. The fronting beach is predominantly sandy, leading to a rocky shoreline to the south. The Rhoscolyn back-barrier system overlies late Precambrian rocks comprising the South Stack and New Harbour Groups. These consist of the interbedded psammites and pelites of the South Stack Group and the pelites of the New Harbour Group (Collins and Buchan, 2004; Hassani *et al.*, 2004; Lisle, 1988). The freshwater peat is mostly underlain by glacial till.

4.3. Methodology

4.3.1. Salt-marsh sea-level reconstruction

Owing to the varying frequency of tidal inundation from high to low marsh, salt-marshes typically exhibit strong zonation in their flora and fauna. Many studies have shown that in salt-marshes, tidal inundation represents the primary control on the distribution of microfauna, such as foraminifera and diatoms, that can therefore serve as proxies for sea-

level change (Edwards *et al.*, 2004; Patterson *et al.*, 2004; Roe *et al.*, 2009; Scott and Medioli, 1978) and act as 'Late-Holocene tide gauges' (Barlow *et al.*, 2013, 2014; Edwards and Horton, 2000; Gehrels, 1994, 2000). Past sea levels can be reconstructed from salt-marsh sediments by determining their 'indicative meaning', that is, the tidal elevation at which the sediments were originally deposited. This is achieved by relating fossil microfauna in cores to the elevation of the marsh surface where the living counterparts of the microfossils are found. The principle underpinning this methodology and the use of quantitative techniques to determine indicative meaning are appraised at length by Barlow *et al.* (2013). This study first constructs and then applies a local foraminifera-based transfer function to determine indicative meanings for salt-marsh sediments in a core from Malltraeth marsh.

In total, 48 surface training set samples were taken from the surface of the salt-marsh along a 218-m transect spanning from 53°17′72.86″N, 4°38′01.92″W to 53°17′77.49″N, 4°38′30.23″W to construct the transfer function used to reconstruct former RSL changes; 20 initial reconnaissance cores were collected at 10 m intervals along the same transect with a 20-mm diameter gouge and sediments logged in the field according to Troels-Smith (1955). From this reconnaissance, the primary fossil core for further analysis (foraminifera, radiocarbon, particle size analysis (PSA) and loss-on-ignition (LOI)) was taken in the high marsh (at 53°10′39.648″N, 4°22′52.7016″W). The selection of this 'master' core was based on obtaining the thickest salt-marsh sequence possible while also minimizing compaction issues by avoiding the marsh overlaying the mudflat substrate further seaward (Brain *et al.*, 2012). The fossil core was collected with a 60-mm diameter Eijkelkamp gouge corer to a depth of 80 cm. The upper 65 cm of this core was the salt-marsh sequence and the lower 15 cm the underlying sand layer. A replicate core was taken for ^{210}Pb and ^{137}Cs dating. These cores were removed from the core barrel, wrapped in non-PVC cling film, and encased in plastic tubing for transportation. All samples were refrigerated at 4°C until subsampled for foraminifera and other analyses. Elevations of all field samples were surveyed with a dumpy

level to an Ordnance Datum (OD) flush bracket benchmark (S7594) on the south corner of a former church in Malltraeth (53°11′33.468″N, 4°23′7.4796″W).

From the fossil core, 2 mL of sediment was subsampled at 1 cm intervals for foraminifera. At 2.5 cm intervals, 3.375 cm^3 subsamples were taken to determine downcore trends LOI and PSA. LOI was performed using a modified Gale and Hoare (1991) method using 5.0 ± 0.10 g, with heating over 24 h at 430°C. For PSA, subsamples were riffled down and treated with 0.1% sodium hexametaphosphate, before dispersal in deionized water within the instrument using ultrasound and pumping. Resultant data were used to calculate the mean and median grain size of each sample, as well as sorting, skewness, and probability distribution. PSA samples were then analysed in a Horiba LA-950 laser diffraction particle size distribution analyser.

Both surface and fossil foraminifera were sampled and analysed using the standard techniques of Scott and Medioli (1980). Foraminifera subsamples were wet sieved between 500 and 63 µm and treated and stored in a rose Bengal 30% ethanol solution to stain living foraminifera and preserve the samples. Foraminifera were identified and wet-picked from a Bergeroff tray under an Olympus SZ61 microscope. Foraminifera taxonomy is based on De Rijk (1995).

Seven 1 cm slice subsamples were taken for bulk radiocarbon at 5, 20, 25, 35, 50, 55 and 65 cm depth (GR-A-R1 to GR-A-R9). Plant macrofossils would have been preferred but were not found in the decomposed organic sediment. Two further samples were taken at 60 cm depth, one for radiocarbon dating of the humin fraction and another of plant fragments found at this depth (though this was later determined to likely have been rootlet material). With debris, rootlets and other potentially non-contemporaneous detritus removed, one humin fraction (GR-A-R8), one plant macrofossil (GR-A-R9) and seven bulk (GR-A-R1 to R7) radiocarbon ages were determined by accelerator mass spectrometry (AMS). AMS ^{14}C analysis was conducted at the 14CHRONO Centre of Queens University Belfast. Calibration was undertaken using CALIB 7.1 Radiocarbon Calibration software (Stuiver *et al.*, 2018).

The ^{210}Pb sample core (0–30 cm) was chopped into 30 continuous 1 cm slices, freeze dried, weighed, and sieved to <2 mm. The <2 mm sediment was homogenized in a Teemer mill. After settling in Petri dishes for 21 days to allow for equilibrium to establish between ^{214}Pb, ^{226}Ra and its daughter isotopes, radionuclide activity concentrations were measured using the EG&G Ortec planar (GEM-FX8530-S N-type) HPGe Gamma spectrometer in the Plymouth University Consolidated Radioisotope Facility (CoRIF). Total ^{210}Pb was measured by its gamma emissions at 46.5 keV and the supported component calculated by the subtraction of ^{226}Ra activity, which was measured by the gamma emission of ^{214}Pb at 295 and 352 keV with correction for ^{214}Bi emissions. The instrument was calibrated using traceable radioactive standard spiked soils provided by AEA Technology Plc. Calibration relationships were obtained using EG&G GammaVision software and verified by comparison tests between laboratories with International Atomic Energy Agency (IAEA) supplied materials.

4.3.2. Freshwater marsh sea-level reconstruction

Many back-barrier systems in North Wales are closed from the sea and contain deposits of freshwater peat. Gehrels and Anderson (2014) show that these systems can be suitable environments for sea-level reconstructions, provided that the groundwater table was coupled to sea level during the period covered by the sea-level reconstruction. By combining empirical observations with groundwater modelling, it is possible to reconstruct Holocene sea-level changes. The procedure for calculating past sea level from freshwater back-barrier peat is described in detail by Gehrels and Anderson (2014) and we follow the same method here.

Groundwater monitoring wells were installed on a transect perpendicular to the barrier, positioned centrally on the marsh. The wells were located at 20, 60 and 90 m. Monitoring was carried out with Aqua TROLL 200 data loggers, which measure fluctuations in temperature, pressure, and salinity every 15 s. Monitoring was carried out for 32 consecutive months in well 1, and 17 consecutive months for wells 2 and 3.

An Eijkelkamp gouge corer was used to undertake a stratigraphic survey of 36 cores along three shore parallel transects behind the barrier (Figure 4.1), providing a picture of the morphology of the valley floor and the stratigraphy of the Holocene infill. A 'Russian' chamber corer was used to collect samples for analysis in the laboratory and to obtain samples for radiocarbon dating. For palaeo sea-level determinations, the interface between the Holocene base and freshwater peat was sampled in two cores (RC1 and RC2; Figure 4.1).

Plant macrofossils were sampled from the basal peat samples for ^{14}C dating. AMS ^{14}C analyses were performed by the Natural Environment Research Council (NERC) Radiocarbon Laboratory. Calibration was carried out using CALIB 7.1 (Stuiver *et al.*, 2018) to calibrated years before the present (cal. year BP).

A Trimble R6-3 Differential Global Positioning Satellite (GPS) was used to survey elevations relative to UK OD. A further survey was undertaken to measure the topographic gradient at the edge of the marsh to estimate the gradient in the groundwater in the area where basal peat is formed, following the methods described in Gehrels and Anderson (2014).

4.4. Results

4.4.1. Salt-marsh surface foraminifera

The foraminifera across the Malltraeth marsh surface comprise four agglutinated species (Figure 4.2): *Jadammina macrescens, Trochammina inflata, Miliammina fusca* and *Haplophragmoides wilberti*. The calcareous species were grouped into three genera: *Elphidium*, including *williamsoni* and *excavatum*; *Ammonia* consisting of *beccarii* variants; and *Quinqueloculina*. The upper limit of foraminifera on the marsh is at 2.08 m OD.

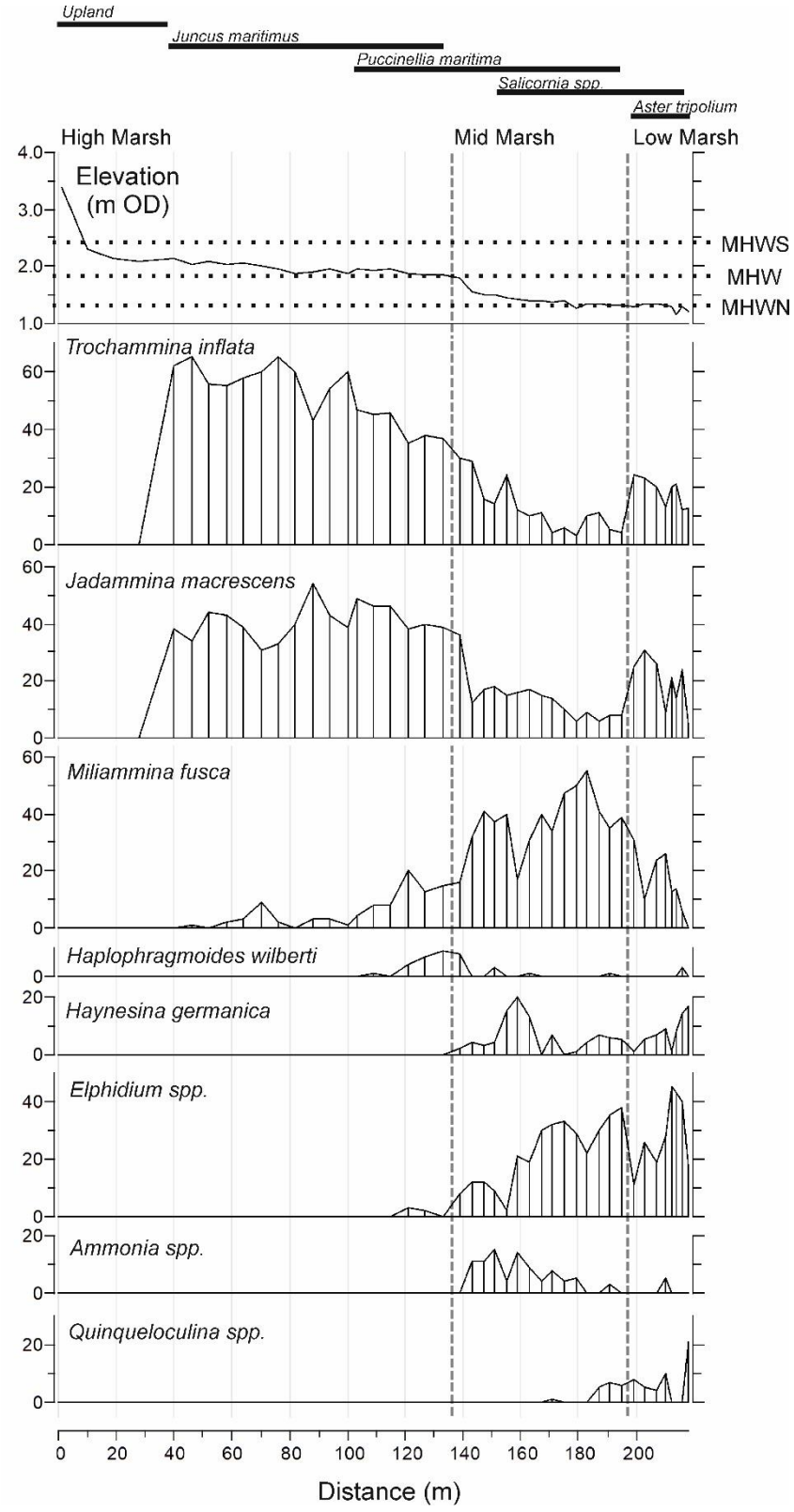

Figure 4.2. Distribution of surface salt-marsh dead foraminifera from original 44 samples, elevation profile, tidal elevations, and vegetation zonation. Elevations of mean high water (MHW) of spring (MHWS) and neap (MHWN) tides are shown on elevation profile.

The marsh exhibits strong zonation in foraminifera along the elevation gradient. The high marsh is dominated entirely by agglutinated species, primarily by *J. macrescens* and *T. inflata*. In the mid-marsh, *M. fusca* becomes the dominant species with calcareous foraminifera increasing in abundance moving further seaward. Among the agglutinated species, the relative abundance of *J. macrescens, T. inflata* and *M. fusca* represents the strongest indicator of elevation, with *H. wilberti* primarily occupying a small niche at the boundary of the mid- and high-marsh zones.

The marsh stratigraphy is mostly composed of an organic silt overlying a sand deposit, believed to be of aeolian origin associated with sand from the Newborough dunes, which ranges from 7.5 cm thick at its most seaward to at least 20 cm at its most landward (Figure 4.3). Moving seaward, this sand is replaced by a sandy clay.

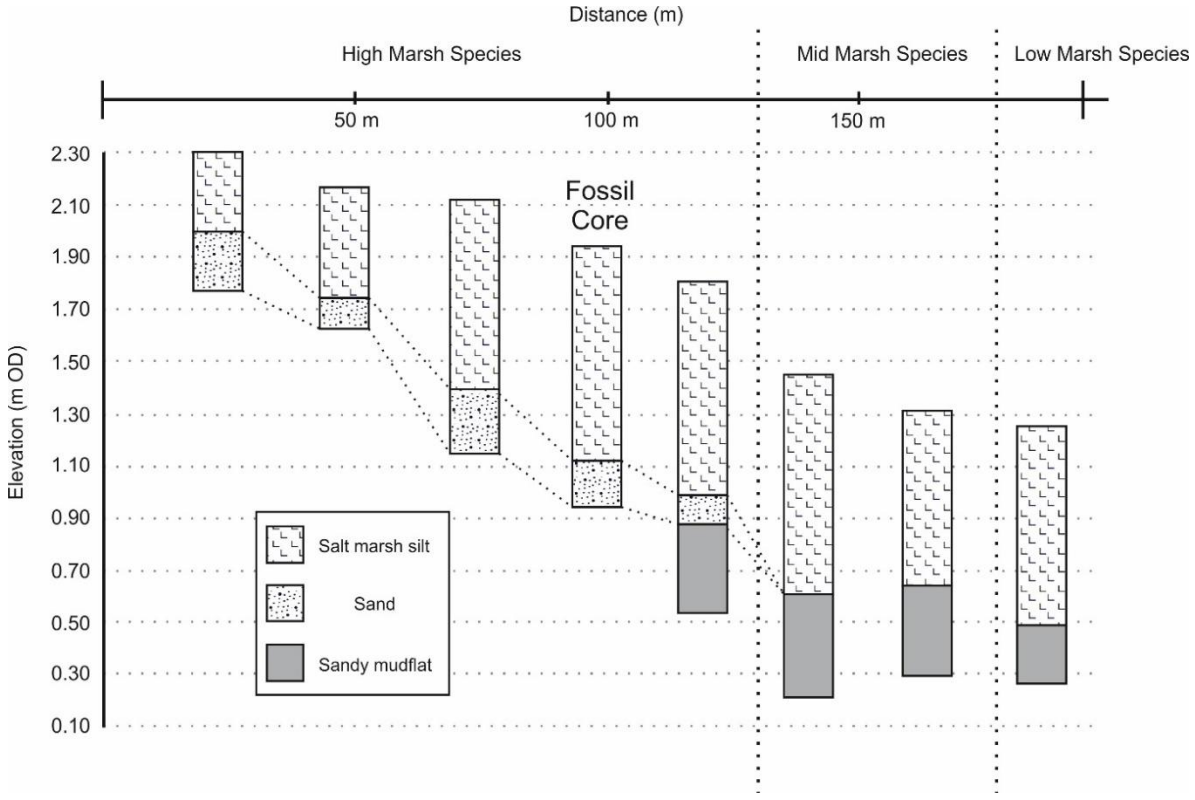

Figure 4.3. Stratigraphy of Malltraeth salt-marsh along study transect, landward to seaward.

The median particle size in the core (Figure 4.4) is dominated by the silt fraction. The sandy substrate is reflected in a sharp increase in median particle size and reduced silt content.

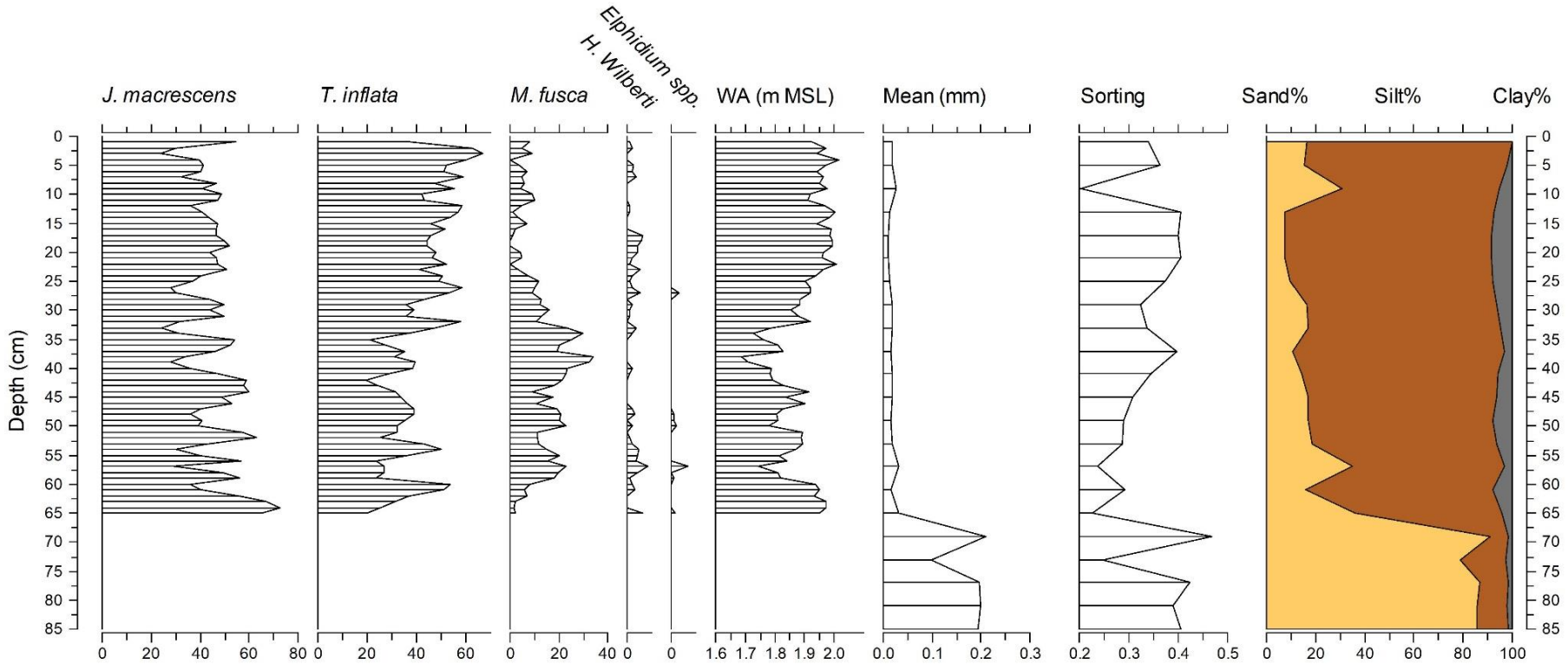

Figure 4.4. Fossil core dead foraminifera distributions, WA reconstruction and particle size data

The fossil foraminiferal assemblage consists only of species, also found in the modern training dataset, and is dominated almost entirely by agglutinated foraminifera, with some incidences of damaged *Elphidium spp*. and *Ammonia spp*. The species distribution in the upper core is representative of its position at the surface slightly above the boundary of the mid- and high marsh. The main changes downcore occur in the abundance of *M. fusca*, which tends to be more abundant at greater depth. *H. wilberti* is found intermittently throughout the fossil assemblage though always comprises <10% of the assemblage at any given depth. Foraminifera were not found in the underlying sand.

4.4.2. Salt-marsh chronostratigraphy

Of the nine salt-marsh radiocarbon samples, three (GR-A-R1, R2, R6) returned modern radiocarbon ages (>1950) (Table 4.1). These results were therefore separately analysed by bomb-spike calibration using CALIBomb (Reimer *et al.*, 2004). GR-A-R6 produced ages younger than the overlying GR-A-R2. GR-A-R6 also produced young ages compared with the GR-A-R3 only 5 cm lower in the core. These apparent age reversals may be a result of modern carbon contamination from active root networks, reworking of recent material or simply an artefact of slow marsh growth in this period. GR-A-R9 yielded a modern age at a depth of 60 cm; it is likely this sample was rootlet material rather than a significant plant macrofossil. The humin fraction sample GR-A-R8 produced an age consistent with the two surrounding bulk samples. Based on these considerations, radiocarbon samples GR-A-R3 and R9 were discarded, leaving seven samples that were used in the calculation of the age–depth model (Figure 4.5e).

Table 4.1. Radiocarbon content reported as $F^{14}C$ as per Reimer et al. (2004).

Sample Code	Depth (cm)	Material Type	$F^{14}C \pm 1\sigma$	2σ age range (ka BP)	2σ age range (CE)	CPAV
GR-A-R1	**5 cm**	**Bulk**	**1.0454 ± 0.0034**	**0.0085 – 0.0091 0.0613 – 0.0615**	**2009 – 2008 1956 – 1956**	**0.655 0.345**
GR-A-R2	**20 cm**	**Bulk**	**1.0181 ± 0.0040**	**0.0613 – 0.0628**	**1956 – 1955**	**1.000**
GR-A-R6	**30 cm**	**Bulk**	**1.1946 ± 0.0051**	**0.0298 - 0.0334 0.0588- 0.0597**	**1988 – 1984 1959 - 1958**	**0.915 0.085**
GR-A-R3	**35 cm**	**Bulk**	**0.9153 ± 0.0036**	**0.766 - 0.71 0.657 - 0.632**	**1252 - 1308 1361 - 1386**	**0.881 0.119**
GR-A-R7	**50 cm**	**Bulk**	**0.7675 ± 0.0034**	**2.369 - 2.319 2.244 - 2.243 2.228 – 2.066**	**351 – 301 BCE 226 – 225 BCE 210 – 48 BCE**	**0.113 0.001 0.886**
GR-A-R4	**55 cm**	**Bulk**	**0.7139 ± 0.0031**	**2.933 – 2.824**	**915 – 806 BCE**	**1.000**
GR-A-R8	**60 cm**	**Humin Fraction**	**0.6943 ± 0.0031**	**3.248- 3.031**	**1230 – 1013 BCE**	**1.000**
GR-A-R9	**60 cm**	**Plant Macrofossil**	**1.1114 ± 0.0032**	**0.0228 - 0.0188**	**1995 - 1999**	**0.944**
GR-A-R5	**65 cm**	**Bulk**	**0.6836 ± 0.0037**	**3.443 – 3.225 3.155 – 3.153**	**1425 – 1207 BCE 1137 – 1135 BCE**	**0.998 0.002**

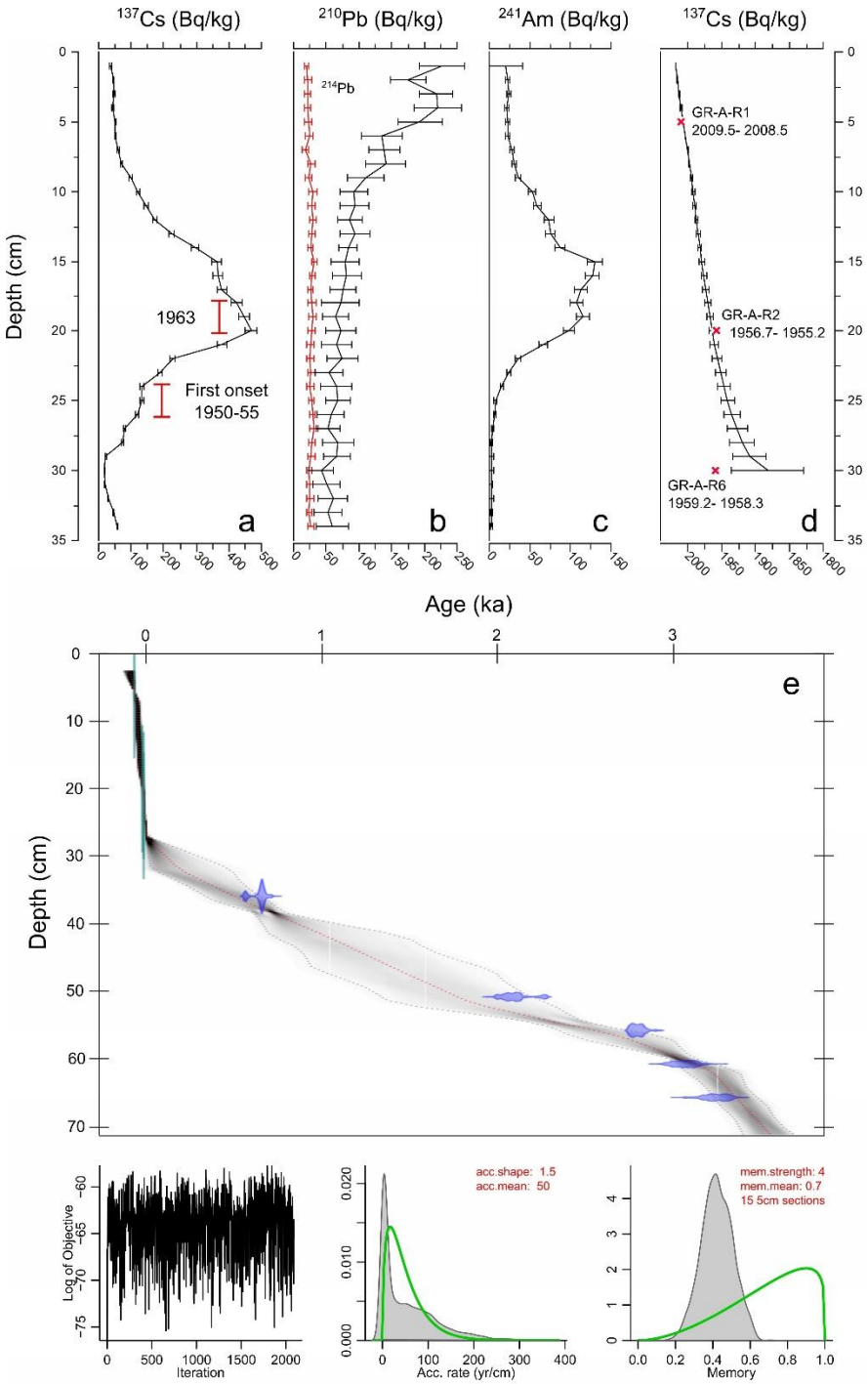

Figure 4.5. (a–d) Gamma spectrometry results for salt-marsh core: (a) ^{137}Cs depth profile with suggested age marker and radiocarbon results for comparison, (b) ^{210}Pb and ^{214}Pb depth profile, (c) ^{241}Am depth profile, (d) ^{210}Pb age–depth model derived using CRS model (Appleby, 2001) radiocarbon sample results included for comparison and (e) age–depth model derived using Bacon (Blaauw and Christen, 2011).

The ^{137}Cs depth profile (Figure 4.5a) shows increase with depth until 14 cm, reaching a peak at 19 cm. ^{137}Cs values at 17, 18 and 19 cm all exist within error of one another presenting some difficulty in determining an exact depth to confidently attribute to the 1963 ^{137}Cs deposition peak. This wide peak may be a result of mobility of ^{137}Cs within the profile (Foster *et al.*, 2006). ^{137}Cs reaches a minimum (17.16 Bq/kg) at 29 cm. Below 30 cm ^{137}Cs once again increases with depth although to levels consistent with the upper 5 cm of the core.

Three ^{137}Cs age markers can be used to date sediments: the fallout from the 1986 Chernobyl reactor incident, the 1963 weapons peak and the first significant environmental presence of this radionuclide around 1950 to 1955. The 1963 weapons peak may be reasonably interpreted at any depth between 17 and 19 cm. This is particularly likely when considered alongside the Am-241 activity, which has notable peaks at 14 and 18 cm and is associated with the maximum fallout signal of early 1960s but not of the initial fallout of the 1950s or 1986 (Marshall *et al.*, 2007). Caution should be taken when interpreting 241Am in this way as Plutonium isotopes which were associated with the 1950s and 1986 can also be a primary source of 241Am in modern sediment archives due to the decay of 241Pu with a half-life of 14.4 years (Marshall *et al.*, 2007). The onset of significant environmental radionuclides is also difficult to determine given potential vertical movement of ^{137}Cs although a range of 22 to 24 cm is suggested here. There is no clear indication of the 1986 Chernobyl fallout within the profile.

The total ^{210}Pb activity profile broadly demonstrates a typical exponential decay but contains several small peaks (most notably in the upper 7 cm). This uneven decay prevents the use of the Constant Initial Concentration (CIC) model for ^{210}Pb age derivation, and the Constant Rate of Supply (CRS) model was used instead (Appleby, 2001).

The depth for A(0) (the total inventory of $^{210}Pb_{xs}$ of the entire core) is usually defined as the point where $^{210}Pb_{xs}$ is at or approximating zero. In this study, $^{210}Pb_{xs}$ at no point reaches zero; therefore, the minimum value of $^{210}Pb_{xs}$ was used, which occurs at 29 cm. This A(0) is justified in the context of the ^{137}Cs data as this value placed the year 1963 at 18 cm depth.

Bomb-spike calibrated radiocarbon samples GR-A-R1 and R2 are consistent with the age–depth model produced from the ^{210}Pb. GR-A-R6, however, is 60 years younger than the age suggested by the ^{210}Pb and plots outside the ^{210}Pb error margin. This further reinforces the likelihood that GR-A-R6 is anomalous and should be discarded.

The age–depth model of the core (Figure 4.5e) was derived using Bacon in the statistical computing environment R (Blaauw and Christen, 2011). The methodology is based on controlling core accumulation rates using a gamma autoregressive semi-parametric model with an arbitrary number of subdivisions along the sediment. Greater detail on the statistical model used is available in Blaauw and Christen (2011). The model was run with a section thickness of 5 cm (res = 5) and a memory strength of 4 (mem. strength = 4). This age–depth model was produced using radiocarbon samples GR-A-R1, R2, R3, R4, R5, R7, R8 and the inferred 1963 and 1950–1955 ^{137}Cs age markers. The ^{210}Pb model was excluded from the final age–depth model as this results in artificially inflating the precision of the final model at these depths, as per Kemp *et al.* (2013). Because of the lack of ages between 35 and 50 cm depth, uncertainty is high between 40 and 45 cm; therefore, caution should be taken with interpretation of sea-level reconstruction results between 0.5 and 2 ka BP.

4.4.3. Transfer function and sea-level derivation

Surface-foraminifera distributions (Figure 4.2), plus four additional samples taken to target elevations not covered by the original transect (SURF –45 to –48 at 1.66, 1.71, 1.79 and 1.83 m OD), were used as the training set informing the transfer function. Calcareous foraminifera were eliminated from the training set because of their usual dissolution upon burial in salt-marsh sediment (Gehrels, 2000). The eight most seaward samples (SURF –1 to –9) were excluded from the transfer function as they comprised almost entirely of calcareous species and produced residuals >0.2 m when included. The four most landward samples (SURF –40 to 44) were also excluded as they contained few intact foraminifera (<10), likely due to their proximity to the upper vertical limit of salt-marsh foraminifera. In total, 36 samples inform the transfer function.

The transfer function was produced using a weighted averaging partial least squares (WA-PLS) technique using the C2 program (Juggins, 2003). WA-PLS is the most widely used approach for unimodal species–environment responses (Barlow *et al.*, 2013). C2 model performance is assessed by a coefficient of determination (R2), an apparent root mean square error (RMSE) and a root mean square error of prediction (RMSEP), a value which represents maximum bias (Gehrels, 2000). The RMSEP was produced using a leave-one-out jack-knifing approach and is considered the strongest indicator of the predictive strength of the transfer function. The transfer function performance is presented in Figure 4.6, and a statistical summary is presented in Table 4.2. The relationship between observed and foraminifera-predicted elevation (Figure 4.6) is very strong, indicating the excellent performance of the transfer function (R2 = 0.92 for component 1). These results suggest that the transfer function is suitable for application to reconstructing past sea levels.

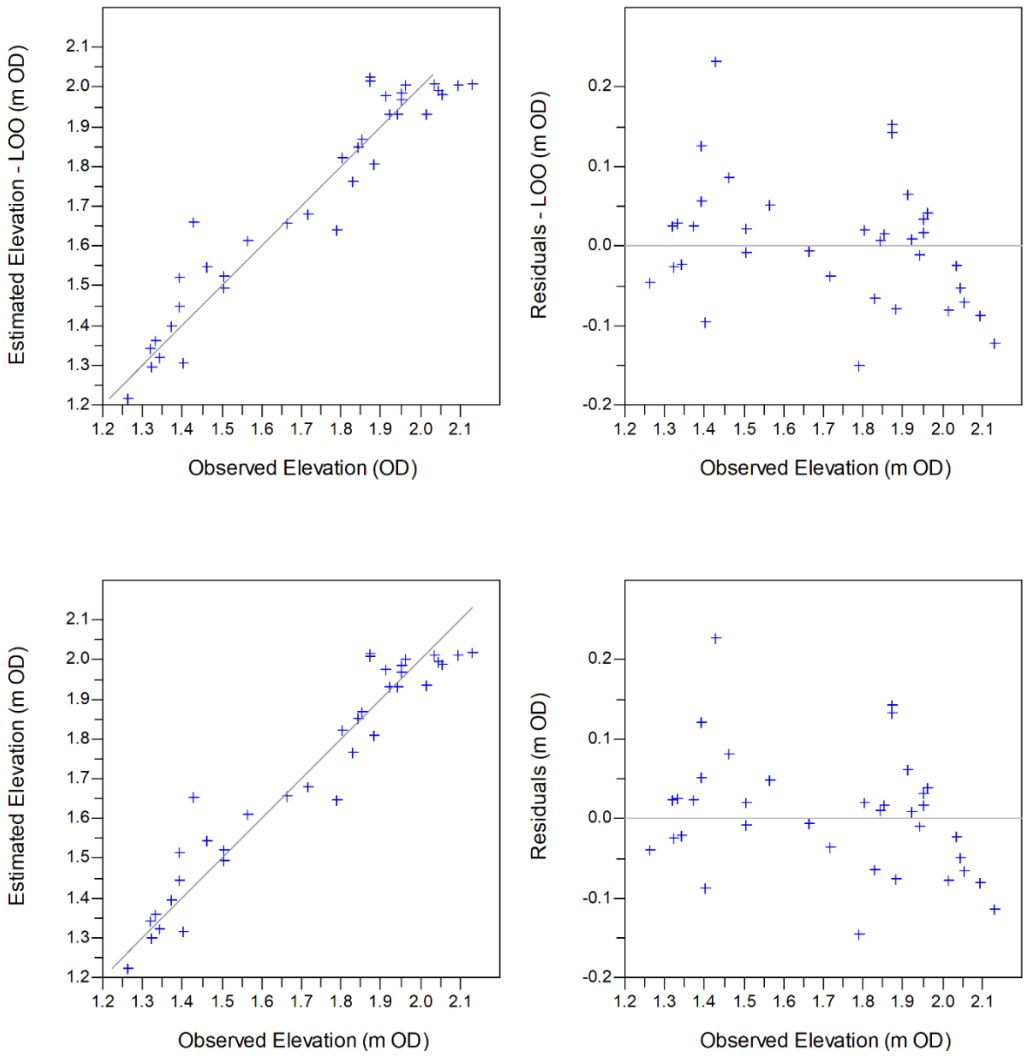

Figure 4.6. Relationship between predicted and observed elevations for chosen first component of transfer function created using WA with leave-one-out (LOO) cross-validation

Table 4.2. Model performance for transfer function components.

Component	R^2	RMSE	RMSEP	%Change
Component 1	0.93	0.08	0.08	...
Component 2	0.93	0.07	0.08	-2.2
Component 3	0.93	0.07	0.08	0.04

The transfer function's first component was chosen for sea-level analysis as subsequent components did not produce RMSEP values 5% greater, as per Barlow *et al.* (2013).

The sea-level parameters derived from the age–depth model (Figure 4.5e) and indicative meaning predictions of the transfer function can be found in the Supplementary Information (4.8, Table 4.5). Also shown are the results of a modern analogue technique (MAT) which was used to quantify the similarity of each fossil sample to its nearest modern analogue. All fossil samples were found to have a 'close' modern analogue (20th percentile of similarity according to Watcham *et al.*, 2013). None reached the 'good' threshold of the 5th percentile, but 54 of 65 fossil samples were within the 10th percentile.

Sea level (SL) is calculated by subtracting the indicative meaning predictions of the transfer function (I) from the elevation of each core sample (E). The results of the full late-Holocene sea-level reconstruction are also presented in Figure 4.8a. Typically, it is necessary to determine a compaction error component for such a reconstruction (Brain *et al.*, 2012). However, as the salt-marsh data in Figure 4.8a show a good fit with the basal SLIP RC1, we suggest that the compaction component is likely negligible and opt to use the transfer function's RMSEP for 2σ as our standard error margin of ±0.16 m.

4.4.4. Rhoscolyn SLIPs

At Rhoscolyn, the stratigraphy of the back-barrier marsh consisted of Phragmites peat overlying woody peat deposits, which vary from 2 cm to 2 m in thickness (Figure 4.7). The site is a closed back-barrier freshwater transgressive system (Kraft and Chrzastowski, 1985). In a closed system, the rollover of the barrier results in onshore migration: a Phragmites swamp replaces the carr as groundwater rises in response to changing hydraulic gradients, driven by RSL rise. As such, it is reasonable to expect that the carr or fen peat was deposited at the leading edge of the Holocene transgression and can be expected to represent an archive of past sea-level rise (Gehrels and Anderson, 2014). The stratigraphy contained a large sand deposit in transect Y–Y1, which was interpreted as an overwash deposit based on its geometry.

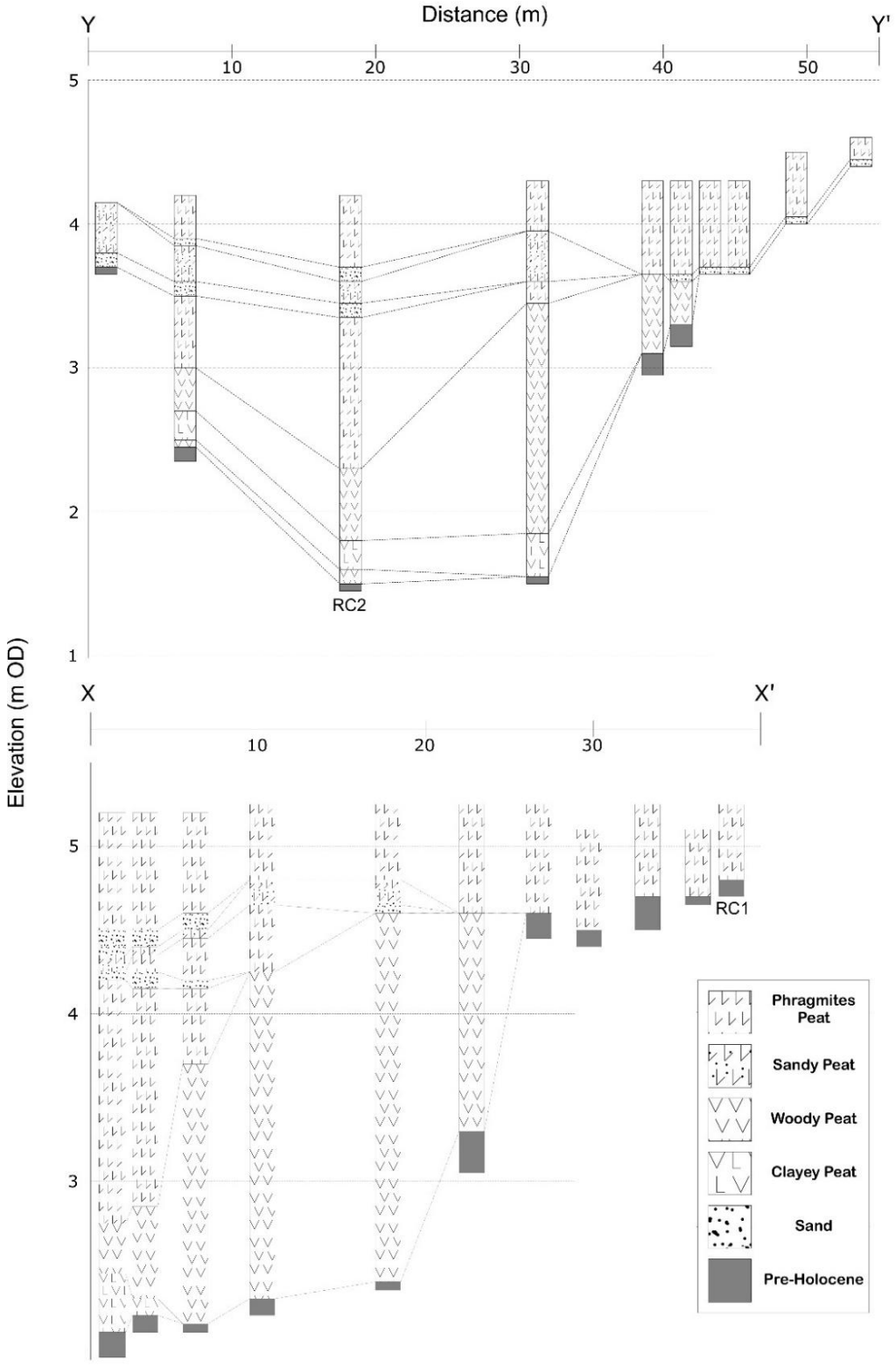

Figure 4.7. Stratigraphy of Rhoscolyn freshwater back-barrier marsh. Transects run west to east.

For coastal freshwater back-barrier wetlands to be suitable archives of sea-level data, it is necessary to demonstrate a link between tidal and groundwater oscillations. Wavelet coherence analysis was applied to the tide-gauge and groundwater well data, using a MATLAB script made available by Grinsted *et al.* (2004). This enabled the simultaneous analyses of two time series to examine the relationships between the signals in time-frequency space. A three-step approach was taken to analyse the data. First, a continuous wavelet transform (CWT) was applied to both datasets before applying a cross-wavelet transform (XWT) to test for significant power correlations in the signal. Finally, the coherence of the wavelets in time-frequency space was tested for significance. All significance tests were against red noise, using Monte Carlo methods.

Wavelet analyses, using the technique presented by Grinsted *et al.* (2004), provide a robust insight into the tidally induced groundwater oscillations. Cross-wavelet power highlights periods that share a high-power signal for a particular time period. This is clearly identifiable in the wavelet analyses for the semi-diurnal tide and shows that the tidal and groundwater signals are slightly out of phase with each other, which is to be expected as the tidal signal takes time to propagate through the barrier. The power of wavelet analyses enables a clear identification of a tidal signal in the groundwater, at greater distances than is possible using Fast Fourier Transform–based spectral analyses. Groundwater monitoring shows a significant relationship, using Monte Carlo methods, between groundwater oscillations and the tidal movements of the sea. The groundwater is sensitive enough to oscillate in correlation to the semi-diurnal tide. The signal remains consistent through the sandy barrier at Rhoscolyn and shows that that the groundwater height in the back-barrier, and thus peat formation, is controlled by sea level (Gehrels and Anderson, 2014).

The procedure for calculating past sea level from freshwater back-barrier peat is described by Gehrels and Anderson (2014), and the same method is followed here. The reconstruction of past mean sea level, from basal peat, follows the relationship SL = E – I, where E is the elevation of the sample, and I is the indicative meaning. The determination of I is

complicated by the existence of a gradient in the groundwater. As our sample formed a distance behind the barrier, we must correct for the influence of the gradient. As such, we calculate an original past mean sea level from SL = E – I – GW, where GW is the correction for the groundwater gradient.

The groundwater gradient was estimated by measuring the topography along the edge of the marsh, where it formed against the valley edge, as it is the modern-day analogue to where the basal peats formed. The gradient of 0.47 ± 0.04 m per 100 m and the fact that sea level was lower in the past necessitate a calculation of the distance between the present-day location of the samples and the original position of the palaeobarrier further seaward at the time the basal peat formed.

Landward barrier migration is a result of RSL rise and can be calculated as a function of offshore gradient from R = 1/tanθ S (Bruun, 1962). The original indicative meaning was taken as the average height of peat formation directly behind the barrier. From this, the estimated past sea level was used to calculate the offshore distance of the palaeobarrier. This process was repeated iteratively, until there was no variation in indicative meaning for three iterations (Table 4.3). Vertical error was calculated by running these iterations for two standard deviations in the groundwater gradient estimates. Using radiocarbon results and SLIP parameters shown in Table 4.4, RC1 and RC2 are plotted in Figure 4.8a and c. The RC1 late-Holocene basal sample provides a SLIP younger than any in the current North Wales database (Shennan *et al.*, 2018) at 1.9 ka BP and –0.33 m lower than present day. The RC2 Holocene basal SLIP is in good agreement with the existing SLIPs of Bedlington (1994), Heyworth and Kidson (1982) and Roberts *et al.* (2011), indicating a sea level –5.49 m at ca. 7.4 ka BP (Figure 4.8c).

Table 4.3. Groundwater model iterations.

Iteration		RC1	RC2
	Height (m OD) Depth (m) Sample Height (m OD) Initial Indicative Meaning (m OD)	5.19 0.49 4.70 4.90	4.19 2.65 1.54 4.90
1	Shore Distance (m) IM Correction Sea level	67.00 0.31 -0.51	23.00 0.11 -3.47
2	Shore Distance (m) IM Correction Sea Level	42.55 0.20 -0.40	286.61 1.35 -4.71
3	Shore Distance (m) IM Correction Sea Level	33.06 0.16 -0.36	388.99 1.83 -5.19
4	Shore Distance (m) IM Correction Sea Level	29.37 0.14 -0.34	428.76 2.02 -5.38
5	Shore Distance (m) IM Correction Sea Level	27.93 0.13 -0.33	444.21 2.09 -5.45
6	Shore Distance (m) IM Correction Sea Level	27.38 0.13 -0.33	450.21 2.12 -5.48
7	Shore Distance (m) IM Correction Sea Level	27.16 0.13 -0.33	452.54 2.13 -5.49
8	Shore Distance (m) IM Correction Sea Level		453.44 2.13 -5.49
9	Shore Distance (m) IM Correction Sea Level		453.79 2.13 -5.49

Table 4.4. SLIP parameters for Rhoscolyn freshwater samples.

Index Point	Age (Ka BP)	Error +	Error -	RSL	RSL +error	RSL - error
RC1	**1.87**	**2.32**	**1.87**	**-0.33**	**0.04**	**0.05**
RC2	**7.38**	**7.45**	**7.37**	**-5.49**	**0.81**	**0.48**

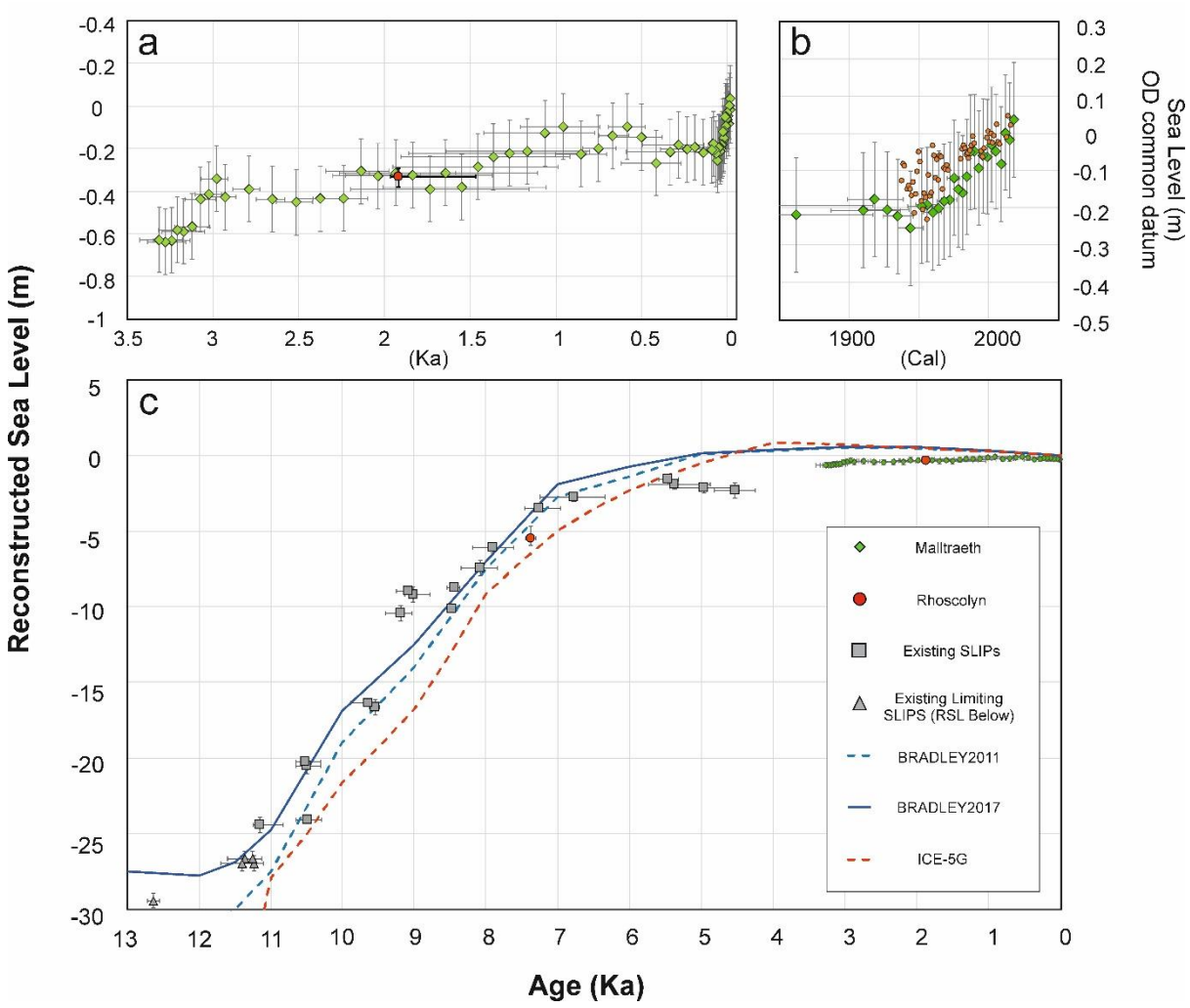

Figure 4.8. (a) Late-Holocene sea-level history for North Wales derived from Malltraeth marsh. Red dot indicates freshwater sample RC1. (b) Post-industrial sea-level acceleration in Malltraeth. Orange data indicates Holyhead tide gauge. (c) Holocene relative sea-level changes in North Wales, compared with GIA models (Bradley et al., 2011; Peltier, 2004; Shennan et al., 2018).

4.5. Discussion

The RSL record derived from 24 SLIPs and the late-Holocene salt-marsh for North Wales (Figure 4.8c) show that RSL rose ~0.65 m in the last 3300 years and has now reached its highest level in the Holocene. Post-industrial acceleration of sea-level rise is evident in the Malltraeth data (Figure 4.8a) and begins in the early- to mid-20th century. The salt-marsh reconstruction matches with the lower limit of the tide-gauge data.

In North Wales, RSL rose ~30 m over the course of the Holocene. The data suggest that sea-level rise was fairly linear between 12 and 7 ka BP at a rate of ~5.3 m ka^{-1}. There is nothing in the data to suggest that sea level was at any point >0 m after 7 ka BP. Although there is some suggestion for RSL stability between 6 and 4 ka BP, or even potentially a small sea-level fall, the vertical uncertainty of the individual SLIPs prevents attaching any great significance to this. It is clear, however, that our new late-Holocene RSL data leave no room for a mid-Holocene RSL highstand in North Wales.

The Holocene RSL reconstruction is compared with data produced by two GIA models presented in Shennan *et al.* (2018) (BRADLEY2011 and BRADLEY2017) and with predictions from the ICE-5G model (Peltier, 2004). The BRADLEY2011 and BRADLEY2017 models predict sea level well between 12 and 7 ka BP. The prediction from BRADLEY2017 is slightly closer to the empirical data and produces sea levels greater than the limiting SLIPs between 13 and 11 ka BP, whereas BRADLEY2011 underestimates sea level in this period. This improvement likely stems from the higher grid resolution of ~35 km in BRADLEY2017 compared with ~70 km in BRADLEY2011 (Shennan *et al.*, 2018). Both BRADLEY models presented in Shennan *et al.* (2018) overestimate sea level in the mid- and late Holocene, reaching a highstand at 5 ka BP and predicting late-Holocene sea levels >0 m. ICE-5G has a poor fit to the entire empirical dataset, underpredicting sea level prior to 7 ka BP and overestimating after 5 ka BP. It also predicts a larger highstand than either BRADLEY model.

The differences between these models may be a result of the different way the ICE-5G (and its subsequent iterations) and the BRADLEY models handle the rate of global ice melt in the mid-Holocene. ICE-5G and 6G (Argus *et al.*, 2014) infer a slowdown in global melt rate ~8 ka BP, ~4 m (ICE-5G) and ~2 m (ICE-6G) equivalent sea level (ESL: the spatially uniform sea-level change from mass exchange between the ice sheets and the oceans; Farrell and Clark, 1976) rise between 7 and 4 ka BP and no melt after 4 ka BP (Bradley *et al.*, 2016). The BRADLEY models assume that the slowdown of ESL started later (~7 ka BP) and that

melt also ended later (Bradley *et al.*, 2016). This can have the effect of 'drowning' mid-Holocene highstands with greater late-Holocene contributions. For the regional BRADLEY models, it may also be a result of incorrect estimation of isostatic change for the Holocene or, perhaps most likely, a composite of these effects. Attributing a cause to this mismatch is complicated by a general GIA modelling problem, that many possible variables in the Earth model can provide similar predictions with equally good fit to the empirical data (Stockamp *et al.*, 2016). Despite the closer fit of the BRADLEY models to the geological data, it is clear there is still need for further refinement of model parameters to successfully match this region's RSL data with GIA model predictions, particularly for the mid- to late Holocene.

The false predictions of a mid-Holocene highstand and overestimation of late-Holocene sea level have implications for GIA model, and sea-level predictions for the United Kingdom. This is particularly true if these differences stem from errors in determination of regional scale isostatic adjustment, as accurate models of future isostatic adjustment are vital in predicting future RSL changes, particularly in regions where isostatic contributions are a dominant factor, such as Southwest England (Gehrels *et al.*, 2011). Further work from the Britice-Chrono project may help to better resolve the British–Irish Ice Sheet and its isostatic contributions and enable the reduction in misfits during the late Holocene, particularly if it is able to better resolve the Irish Sea Ice Stream (Clark *et al.*, 2018; Small *et al.*, 2017).

4.6. Conclusion

1. A continuous record of RSL changes during the past 3300 years was successfully reconstructed from Malltraeth marsh, providing the first high-resolution data for the late Holocene in North Wales.
2. The methodology put forward by Gehrels and Anderson (2014) was applied to back-barrier freshwater peat at Rhoscolyn to obtain two additional mid- to late-Holocene SLIPs for North Wales.

3. By combining the late-Holocene salt-marsh data and freshwater sea-level data with previously published SLIPs, a more complete Holocene RSL reconstruction for North Wales is presented.
4. There is no evidence in the sea-level reconstruction to suggest the existence of a mid-Holocene highstand in North Wales.
5. There is a need for further refinement of GIA model parameters for the mid- to late Holocene to obtain a better fit between GIA model predictions and Holocene RSL reconstructions for North Wales.
6. Such improvements will increase the capability of GIA models to predict more reliably future relative land and sea levels around the British Isles.

4.7. Funding

Rushby and Richards were supported in their PhD studies by the NERC Doctoral Training Partnership ACCE (Adapting to the Challenges of a Changing Environment) (NE/L002450/1). This study was supported by the NERC Radiocarbon Facility (allocation 2035.1016) for Rhoscolyn ^{14}C samples. ^{14}C samples for Malltraeth were paid for by the Sheffield Luminescence Laboratory.

4.8. Supplementary Information

Table 4.5. Raw WA salt-marsh sea level values.

Code	Elevation (m OD) E	Age (Ka BP)	Age Min (Ka BP)	Age Max (Ka BP)	Age (Cal. Y)	WA (m MSL) I	Sea Level (m) E-I	MAT DC. (MAT)
Core-1	1.96	-0.068	-0.07	-0.067	2018	1.93	0.04	1.923
Core-2	1.95	-0.065	-0.066	-0.064	2015	1.97	-0.02	2.013
Core-3	1.94	-0.062	-0.063	-0.061	2012	1.94	0.00	2.013
Core-4	1.93	-0.059	-0.059	-0.058	2009	2.02	-0.08	1.873
Core-5	1.92	-0.055	-0.056	-0.055	2005	1.97	-0.05	1.953
Core-6	1.91	-0.052	-0.053	-0.051	2002	1.94	-0.03	1.923
Core-7	1.90	-0.049	-0.05	-0.048	1999	1.97	-0.06	2.053
Core-8	1.89	-0.046	-0.047	-0.045	1996	1.95	-0.06	1.943
Core-9	1.88	-0.043	-0.045	-0.041	1993	1.98	-0.09	1.953
Core-10	1.87	-0.04	-0.042	-0.038	1990	1.92	-0.05	1.943
Core-11	1.86	-0.037	-0.04	-0.034	1987	1.91	-0.05	1.943
Core-12	1.85	-0.034	-0.036	-0.031	1984	1.97	-0.12	2.053
Core-13	1.84	-0.031	-0.034	-0.028	1981	2.00	-0.16	1.873
Core-14	1.83	-0.028	-0.031	-0.025	1978	1.98	-0.15	1.953
Core-15	1.82	-0.025	-0.03	-0.021	1975	1.94	-0.12	1.943
Core-16	1.81	-0.022	-0.028	-0.017	1972	1.99	-0.18	2.043
Core-17	1.80	-0.018	-0.023	-0.014	1968	1.99	-0.18	2.043
Core-18	1.79	-0.014	-0.019	-0.01	1964	1.99	-0.20	2.093
Core-19	1.78	-0.01	-0.017	-0.004	1960	2.00	-0.21	2.093
Core-20	1.77	-0.006	-0.014	0.001	1956	1.96	-0.19	1.923
Core-21	1.76	-0.002	-0.012	0.008	1952	1.96	-0.19	1.923
Core-22	1.75	0.006	-0.003	0.015	1944	2.01	-0.25	2.093
Core-23	1.74	0.015	0.004	0.026	1935	1.97	-0.22	1.913
Core-24	1.73	0.023	0.009	0.039	1927	1.94	-0.20	1.923
Core-25	1.72	0.032	0.013	0.053	1918	1.90	-0.18	1.923
Core-26	1.71	0.04	0.017	0.067	1910	1.92	-0.21	2.013
Core-27	1.70	0.088	0.044	0.143	1862	1.92	-0.22	1.853
Core-28	1.69	0.137	0.06	0.241	1813	1.89	-0.19	1.943
Core-29	1.68	0.185	0.073	0.34	1765	1.89	-0.20	1.923
Core-30	1.67	0.233	0.086	0.441	1717	1.86	-0.18	1.883
Core-31	1.66	0.281	0.099	0.542	1669	1.88	-0.22	1.923
Core-32	1.65	0.366	0.22	0.571	1584	1.92	-0.27	2.013
Core-33	1.64	0.45	0.33	0.607	1500	1.79	-0.15	1.883
Core-34	1.63	0.534	0.431	0.644	1416	1.73	-0.10	1.883
Core-35	1.62	0.619	0.527	0.699	1331	1.76	-0.14	1.83
Core-36	1.61	0.703	0.598	0.791	1247	1.81	-0.20	1.83

Core-37	1.60	0.806	0.654	0.952	1144	1.83	-0.22	1.883
Core-38	1.59	0.909	0.692	1.156	1041	1.69	-0.10	1.791
Core-39	1.58	1.013	0.723	1.373	937	1.71	-0.13	1.717
Core-40	1.57	1.116	0.751	1.587	834	1.79	-0.21	1.883
Core-41	1.56	1.219	0.771	1.805	731	1.78	-0.22	1.83
Core-42	1.55	1.312	0.869	1.855	638	1.79	-0.24	1.83
Core-43	1.54	1.405	0.937	1.902	545	1.83	-0.28	1.83
Core-44	1.53	1.499	1.006	1.957	451	1.91	-0.38	1.943
Core-45	1.52	1.592	1.059	2.037	358	1.84	-0.31	1.883
Core-46	1.51	1.685	1.109	2.148	265	1.90	-0.39	1.943
Core-47	1.50	1.786	1.32	2.177	164	1.83	-0.32	1.883
Core-48	1.49	1.886	1.536	2.212	64	1.81	-0.31	1.883
Core-49	1.48	1.986	1.742	2.251	-36	1.81	-0.33	1.883
Core-50	1.47	2.086	1.923	2.29	-136	1.78	-0.31	1.83
Core-51	1.46	2.187	2.048	2.364	-237	1.90	-0.43	1.943
Core-52	1.45	2.325	2.212	2.469	-375	1.89	-0.44	1.923
Core-53	1.44	2.463	2.37	2.581	-513	1.89	-0.45	1.923
Core-54	1.43	2.602	2.528	2.697	-652	1.87	-0.44	1.853
Core-55	1.42	2.74	2.678	2.832	-790	1.81	-0.39	1.883
Core-56	1.41	2.879	2.816	2.986	-929	1.84	-0.43	1.83
Core-57	1.40	2.927	2.864	3.019	-977	1.74	-0.34	1.803
Core-58	1.39	2.975	2.901	3.056	-1025	1.81	-0.42	1.83
Core-59	1.38	3.023	2.934	3.111	-1073	1.82	-0.44	1.83
Core-60	1.37	3.071	2.968	3.176	-1121	1.94	-0.57	1.923
Core-61	1.36	3.12	2.996	3.248	-1170	1.95	-0.59	1.923
Core-62	1.35	3.156	3.046	3.267	-1206	1.93	-0.58	1.943
Core-63	1.34	3.192	3.082	3.297	-1242	1.97	-0.63	1.913
Core-64	1.33	3.229	3.11	3.331	-1279	1.97	-0.64	1.913
Core-65	1.32	3.265	3.129	3.374	-1315	1.95	-0.63	1.913

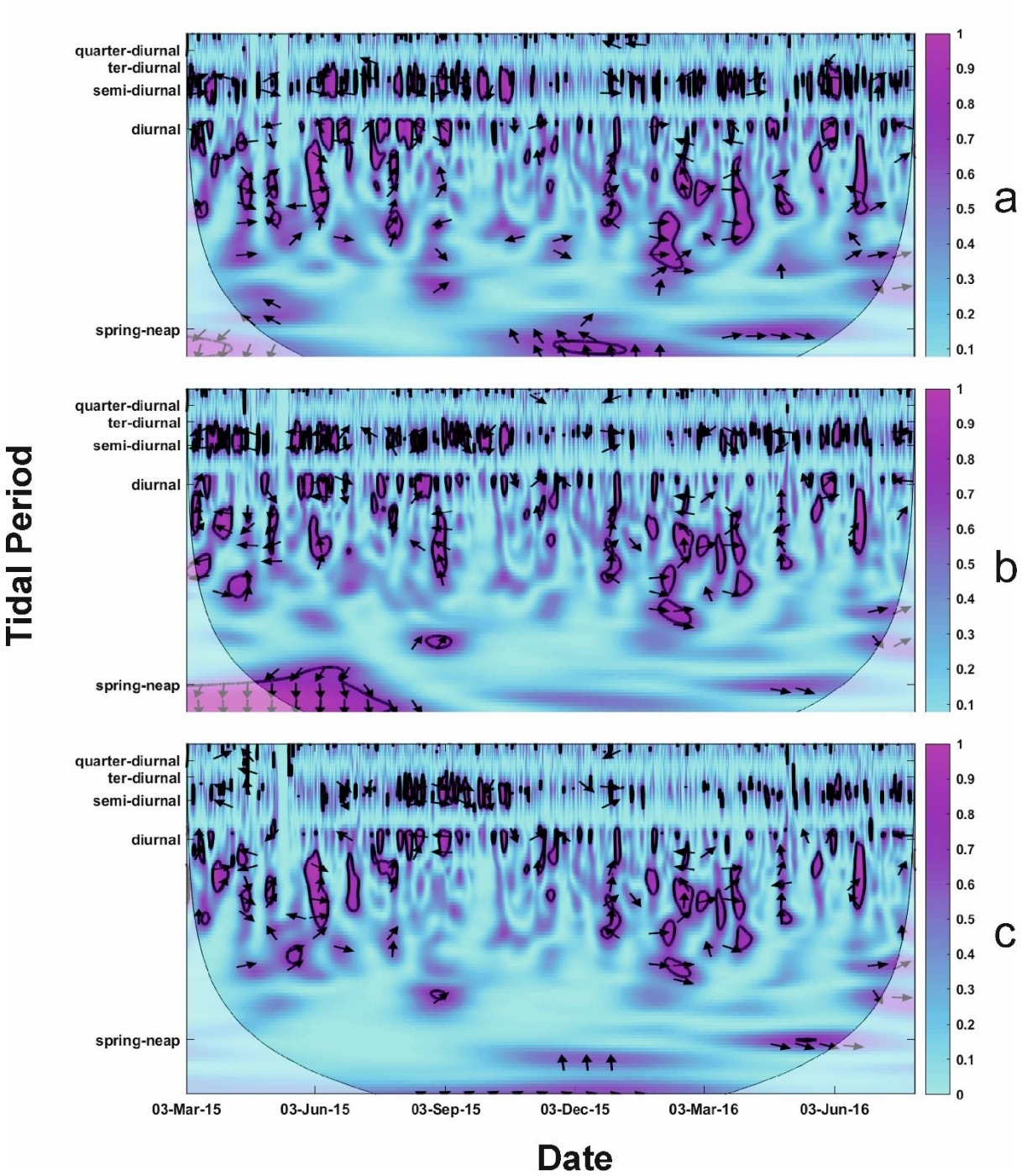

Figure 4.9. Wavelet analysis results for Rhoscolyn marsh.

Chapter 5.

Reconstructing coastal evolution and storms: A 500-year example from a North Welsh beach-dune system.

Publication and copyright

The contents of this chapter were submitted for publication in the journal Geomorphology on the 23rd of December 2021 under the following:

Rushby, GT., Bateman, MD., Gehrels, WR. Submitted 23/12/21. Reconstructing coastal evolution and storms: A 500-year example from a North Welsh beach-dune system. *Geomorphology.*

Nature and extent of contributions

This work was conceived of and written by Rushby. Bateman provided contributions to OSL analysis and paper comments. Gehrels provided comments on tidal analysis and paper comments.

Abstract

Understanding the role of storms and external forcing of beach-dune morphology across decadal to centennial timescales has been limited by the lack of long-term monitoring. Understanding change on this timescale is critical in managing coastlines under a changing climate. We present a combination of historic maps, satellite derived shorelines, chronological and sedimentological data for reconstructing the last 500 years of coastal change of a North Welsh beach-dune system. These are compared with documented storms and tide gauge data to help understanding morphological impacts of storms on this shoreline. Maps and satellite derived shorelines show that the system, has expanded ~650 m northwest in the last 500 years. This hypothesised to have been accelerated associated with construction of a sea wall in the adjacent estuary in the 1890s. Sedimentological data from coastal dunes shows dune expansion was punctuated by storm erosion associated with storms in the 1850s-60s, the 1880s-90s and particularly 1938. Statistical analysis of annual average shoreline position against thresholds in tide gauge data showed that only the largest storm events (sea level > 3.00 m OD) exhibited a significant control on shoreline position across multiple years. For coastlines where monitoring data is sparse, these combined techniques may represent a powerful toolkit in reconstructing past changes and providing morphological context for both for the purposes of coastal science and coastal management.

5.1. Introduction

Climate change and anthropogenic forcing manifest in coastal morphological change by altering the magnitude and frequency of marine, terrestrial, and atmospheric energy sources (French and Burningham, 2013). For sandy beach-dune systems, forcing is mostly expressed through changes in the wind-wave regime, the tidal regime and through changes in the magnitude-frequency and tracks of storms (Banno and Kuriyama 2020, Gómez-Pujol *et al.* 2011, Ortega-Sanchez *et al.* 2008). Over decadal and longer timescales, regional relative sea-level change can also play an important role in governing the magnitude-

frequency of marine energy sources through raising or lowering the base level for marine processes (Allenbach *et al.* 2015, Ritphring *et al.* 2018, Somphong *et al.* 2020, Vitousek *et al.* 2017).

The role of storms and storm surges in governing beach-dune morphology has been well studied on the timescale of single storms, storm clusters, or across a handful of storm seasons (Brooks *et al.*, 2016, Burvingt *et al.* 2016, Burvingt *et al.*, 2017, Castelle *et al.*, 2015, Dissanyake *et al.*, 2015, Dodet *et al.*, 2019, Le Mauff *et al.*, 2018, Masselink *et al.*, 2016, Pye and Blott 2016, Scott *et al.* 2016., Splinter *et al.*, 2014). Less studied is the role of changes in storms and other external forcing factors in governing changes across decadal to centennial timescales (e.g., Bochev-van der Burgh *et al.*, 2011, Esteves *et al.*, 2009, Esteves *et al.*, 2011, Forbes *et al.*, 2004, Pye and Blott 2008, Pye and Blott 2016). Few beaches have such longitudinal data from on the ground monitoring, but these are the timescales at which the effects of a changing climate on sandy shorelines are likely to be most clearly observed. Recently, with the proliferation of publicly available satellite data (e.g., Google Earth Engine; GEE), interannual to multidecadal datasets of coastal change can now be accessed for beaches without bespoke monitoring (Castelle *et al.* 2021, Flor-Blanco *et al.* 2021, Vos *et al.* 2019a, b). Vos *et al.* (2019b) demonstrated the potential of the python toolkit CoastSat for reconstructing sub-annual to multi-decadal shoreline positions on beaches of a range of morphologies and hydrodynamic conditions.

A parallel challenge has been the limited temporal range of most tide gauge records (< 50 years) informing the magnitude-frequency of storms (Batstone *et al.* 2013, Haigh *et al.* 2015, McMillan *et al.* 2011, Menéndez and Woodworth 2010). Despite this, tide gauge data often forms the basis for risk-based and inundation modelling approaches to coastal flood management (Dawson *et al.* 2005, Haigh *et al.* 2015, Míguez *et al.* 2012, Woodworth *et al.* 2009). To improve appraisal of coastal flood risk requires expansion of the temporal scope of storm surge recurrence and impact data beyond typically short (< 50 years) instrumental records. The record of coastal storms preserved in sedimentary archives can provide data

beyond the instrumental record (Bregy *et al.* 2018, Moskalewicz *et al.* 2020). Bateman *et al.* (2018) used portable optically stimulated luminescence (POSL) profiling, optically stimulated luminescence (OSL) ages and particle size analysis (PSA) to provide information on past coastal storms from coastal dunes. They found a total of seven storm events, two of which were large enough to directly erode the dunes over the last 140 years. More recently Bateman *et al.* (2020) combined OSL ages with coastal changes derived from historical maps and imagery to reconstruct a 200-year history of a coastal spit system in East Yorkshire, UK. In other studies, ground penetrating radar (GPR) has been demonstrated as a valuable tool for identifying in low frequency, high magnitude storms in coastal dunes (Cunningham *et al.* 2011).

This study examines the evolution of a North Wales beach-dune system over the last 500 years at various timescales (centennial, decadal, interannual) and the mechanisms that may be forcing these changes. We aim to demonstrate approaches that could be applied to any such system where observational data on morphological change is sparse. To achieve this, we first reconstruct the site's planform evolution using historic maps, images, and satellite data with OSL dune ages used to corroborate the chronology as per Bateman *et al.* (2020). We then reconstruct foredune changes as per Bateman *et al.* (2018) but combined with GPR to give enhanced morphological context. A regional storm record derived from documentary sources and proximal tide gauges is used to explore the causes of shoreline and dune changes. Finally, tide gauge data is combined with remotely sensed shoreline positions to explore the relative role of different conditions in governing morphology across multiple years.

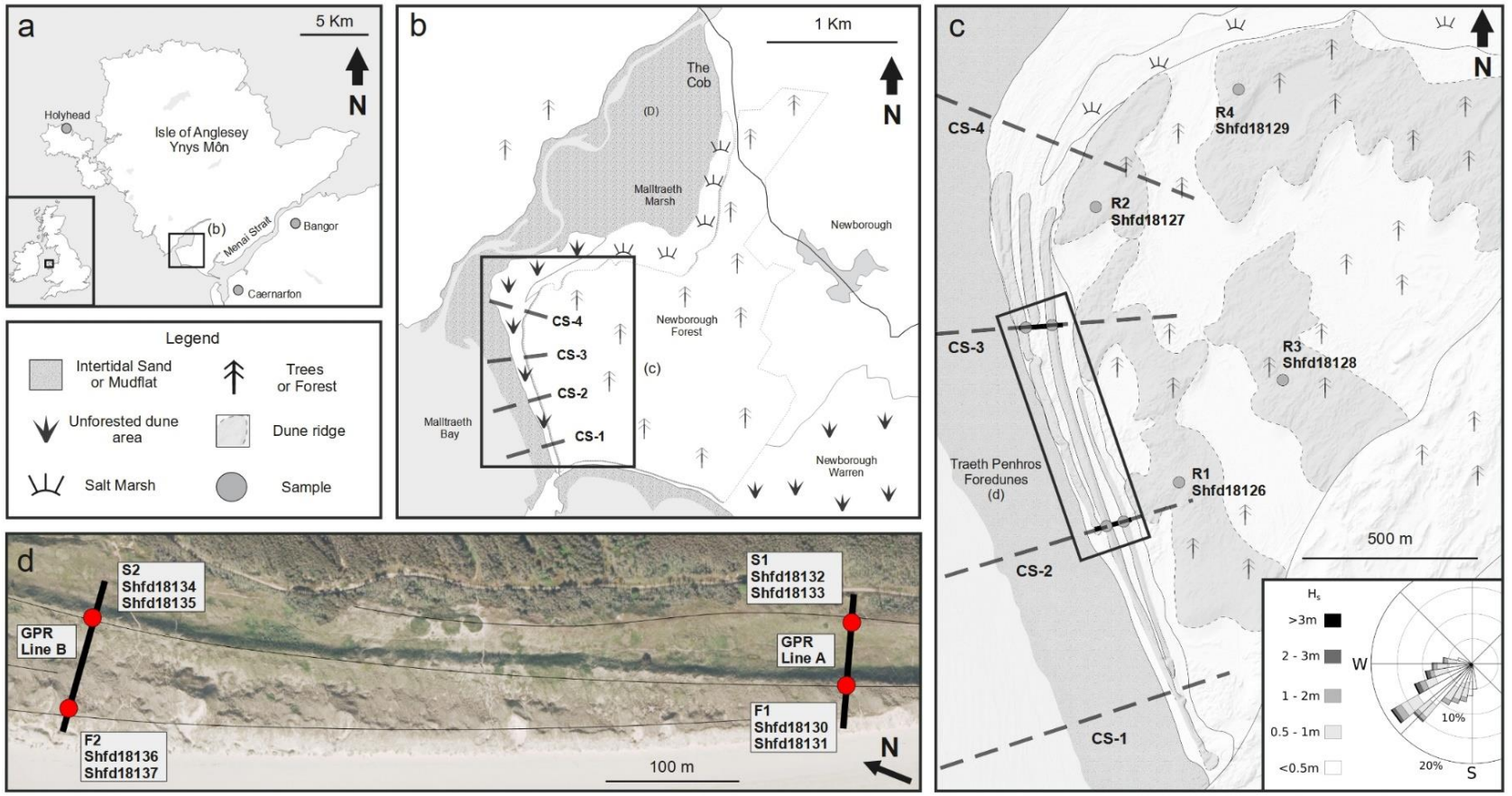

Figure 5.1. Location map of study site. a) shows the Isle of Anglesey and nearby towns. b) shows and overview of the wider estuary. c) shows the entirety of the beach-dune system to the NW of the rock ridge. Now stabilized dune areas are shown, along with foredune ridges. Also shown are CoastSat transect positions (CS-1 to CS-4), dune designations (e.g., F1), OSL sample codes (e.g., Shfd18130), and a local wave rose based on the NOAA WaveWatch III model. d) shows the foredune area and with GPR sampling lines, study dune designations and OSL sample codes.

5.2. Study area

This study is focused on the beach-dune system Traeth Penrhos on the Isle of Anglesey in North Wales at the mouth of the Malltreath estuary (west of Llanddwyn island, Figure 5.1.). This forms part of the wider beach-dune system of Newborough Warren and was chosen owing to a relative lack of inter-annual to decadal monitoring data when compared to many more well studied beach-dune systems in the UK (Bochev-van der Burgh *et al.*, 2011, Esteves *et al.*, 2009, Esteves *et al.*, 2011, Forbes *et al.*, 2004, Pye and Blott 2008, Pye and Blott 2016). This makes it ideal for exploring how the techniques used in this study may aid in understanding of systems with a relative lack of monitoring heritage.

The southern coast of the Anglesey varies in its morphology including sheer cliffs, sandy estuaries, and sandy beach dune systems. The lattermost is primarily constrained to Caernarfon Bay at the south-eastern part of the island near the Menai straight and the Malltraeth estuary. In the early Holocene the region experienced rapid sea-level rise with a slower rise since 3 ka (Rushby *et al.* 2019: Chapter 4). For the last 1000 years sea levels have remained stable until the onset of modern rise which began ~1940 (Rushby *et al.* 2019: Chapter 4). The coastline experiences semi-diurnal tides, with a mean range of 5.40 m. NOAA WaveWatch III (NWW3) model predictions since 2007 show the predominant wave direction is from the WSW and SW (Figure 5.1c.).

The Malltraeth estuary overlies Middle Carboniferous sandstones (Horak and Evans, 2011). Calcareous parabolic hind-shore dunes exist from the Malltraeth estuary to the shingle spit of Abermenai and make up the largest area of coastal dunes in Wales at ~1300 Ha (Bristow, 2003). The age of the Newborough sands remains poorly constrained; a major influx of sand is described in historic sources associated with a storm in 1331 (Bristow, 2003, Greenly, 1919, Ranwell, 1960,). Further sand influxes are known to have occurred in the 1500s, 1600s and 1700s (Bristow 2003, Pye *et al.* 2014). A large portion of these dunes are now stabilized because of forestry in the early 1950s (Ranwell, 1958). The dune-beach system at

Newborough system is separated from that of this study at Traeth Penrhos by the presence of a rock ridge which extends out to Llanddwyn Island.

Traeth Penrhos extends NW into the estuary over ~2.2 km. The beach is dissipative, with a shallow gradient and macro-tidal range. This results in large difference (> 300 m) in tidal shoreline positions on a spring tide. There are two large foredune ridges (typically > 8 m in height from beach level) on this site and one small ridge formed around sand fences as part of forestry work to protect the initial planting of Corsican Pine (Bristow, 2003, Holmes, 1957, Ranwell, 1958, 1960). Landward are four main areas of compound parabolic dunes (Figure 5.1c) with a more complex morphology in the western and north-western parts featuring echo, climbing dunes, and hummocky dunes (Pye *et al.* 2014).

5.3. Data and methods

5.3.1. Planform changes of dune and shoreline positions

Planform changes in both dune and shoreline position were determined from historical maps including 1st series Ordnance Survey; pre-OS admiralty, parish, and tithe maps (National Library of Wales, 2020) and aerial imagery. In total seven maps and images were obtained covering the range 1577 to 2020. As the time between map surveying and map publication is not always given for older maps for consistency maps are referred to by their publication date. Maps were converted and uploaded into ArcMap software, allowing manual tracing of both shoreline (mean high water: MHW) and dune positions.

Pre-1846 maps do not differentiate between dunes and the HWM merely the difference between land and sea, for the purposes of this paper these have been expressed as MHW. Georeferencing for pre-OS maps used a 1st order polynomial (affine) transformation with long-standing human structures (e.g., St. Dwynwen's Church on Llanddwyn island) and the rock promontories of Llanddwyn were used as control points.

CoastSat was used to obtain high temporal resolution shoreline data (Table 5.1) with 4471 obtained images from 03/04/1984 to 08/04/2020 using the Landsat 5, 7, 8 and Sentinel-2 missions. Images were rejected where cloud cover obscured the sand sea interface, they had poor georeferencing, experienced partial data loss, or were more than 2 hours before or after the nearest high tide. Images were also excluded if they occurred during periods of high incident wave energy and run-up due to the misleading shorelines these may produce as noted by Castelle *et al.* (2021). A digital reference shoreline was used to help identify outliers and false detections with a max distance of 100 m used. This ultimately resulted in 36 images in the final output for shoreline analysis with a data gap due to dropped scans from February 2004 to July 2009. To allow for direct comparison with historic maps, CoastSat detected shorelines were output as GEOJSON files.

Table 5.1. Parameters used in CoastSat shoreline detection.

CoastSat Parameter	Value	Explanation / Justification
cloud_thresh	0.5	Threshold on maximum cloud cover. Experimentation with values found 0.5 maintained a good balance of image quality with temporal resolution for this study.
min_beach_area	3000	Minimum area in m^2 to be labelled as a beach. This value was sufficient to avoid sections of exposed dune sand being misidentified as beach whilst still allowing for the beach to be accurately captured.
buffer_size	300	Radius in m of the buffer around sandy pixels considered in the shoreline detection.
min_length_sl	200	Minimum length in m of shoreline perimeter to be valid.
sand_colour	Bright	Determines pixel detection color for sand. Experimentation with values found Bright typically produced best results on this beach.
max_dist_ref	100	Maximum distance in m allowed from the reference shoreline.

CoastSat also allows for production of a time-series of detected shorelines against pre-defined shore-normal transects. Four transects were defined in this study spread across along the length of the beach (CS-1 to CS-4 in Figure 5.1c). Vos *et al.* (2019b) showed that on macrotidal dissipative beaches satellite derived shorelines can experience large discrepancies from manually surveyed data without tidal correction to a reference tidal datum using a single linear slope (Vos *et al.* 2019b). A tidal correction was therefore applied using 15-minute interval tidal elevations derived from the FES2014 Global tide model (Lyard *et al.* 2021). Estimates of beach gradient were measured in the field with a dumpy level. Tide-corrected time series were normalized to the shoreline position on 17/02/2002 and shoreline positions estimated from historic maps pre-dating CoastSat's range added to the transect timeseries by intersecting them with the HWM marks traced in ArcGIS (Figure 5.2)

5.3.2. Luminescence measurements (POSL and OSL)

Four forest stabilized dunes (R1-R4), two contemporary foredunes (F1-F2) and two secondary dunes (S1 and S2) were sampled for OSL. Dune crest sites were sampled using a Dormer engineering sand drill as per Bateman *et al.* (2018). Samples for POSL and PSA were collected only for foredune and secondary sites in light-tight plastic containers at 20 cm intervals for F1 and F2 and 30 cm intervals for S1 and S2. Full OSL dating samples were collected from near the dune surface and base for all sites.

For POSL samples, sediment was removed from the top and bottom of the containers to eliminate potentially bleached sediment with the remainder then dried at 30^{o}C for 24 hours. POSL measurements were undertaken with a SUERC portable OSL reader (Sanderson and Murphy, 2010). As per Bateman *et al.* (2015) samples were spread as a monolayer across a 5 cm petri dish and placed in the reader and underwent continuous wave stimulation with 60s of infrared (IR) followed by 60s of blue light (OSL) stimulation. The signal from the initial IR measurement should have been dominated by feldspars, whilst the OSL measurement will have been a quartz dominated signal. Final POSL dune profiles presented therefore normalised the OSL signal with the IR signal to account for fluctuations in feldspars down profile.

Full OSL sample dose rates were determined using a in situ field gamma-spectrometer measurements and ICP-MS analysis. Moisture attenuation was based on present day measured values and cosmic dose rate was calculated using the algorithm of Prescott and Hutton (1994). Samples were prepared as per Bateman and Catt (1996) and measured on single aliquots using a Risø luminescence reader. Samples were measured using the single aliquot regeneration (SAR) protocol (Murray and Wintle, 2003) with a monolayer mounted on 9.6mm diameter aliquots with 48 replicates for each sample. A preheat of 240^{o}C for 10s was use based on a dose-recovery preheat plateau test (Murray and Wintle, 2003). Samples showed rapid OSL decay curves with low thermal transfer and good recycling.

Replicate palaeodose (De) values for samples analyzed with the Central Age Model (CAM) of Galbriath and Green (1990) showed that four of the samples produced high overdispersion (OD; > 25%). Final derived De values for these samples were therefore calculated using an unlogged Minimum Age Model (Galbraith and Laslett, 1993). The De values for the remaining samples with low OD were based on CAM. Results are shown in Table 5.2 and De albanico distribution plots included in the supplement (5.7.1).

All samples which were analyzed for POSL also underwent particle size analysis (PSA). PSA was undertaken using a Horiba LA-950 laser diffraction particle size distribution analyzer. For this, sub-samples were riffled down and treated with 0.1% sodium hexametaphosphate then dispersed in de-ionized using ultrasound and pumping. The resultant mean grain size of each sample (Φ), as well as sorting, skewness, and probability distribution are shown in the supplement (5.7.1, Table 5.6). Samples were also analyzed in using a portable XRF (Olympus Innov-x Systems Delta 50 Premium) to provide additional geochemical context for any changes in particle size

Table 5.2. OSL related data for Malltraeth dune sample sites. De values in bold are used for age calculations

OSL Lab Code	Site Code	Depth (m)	Moisture (%)	K (%)	U (ppm)	Th (ppm)	Cosmic dose rate (uGy/ka)	Total dose rate (uGy/ka)	Overdispersion (OD %)	D_e CAM (Gy)	D_e MAM (Gy)	Dose (uGy/ka)	Age (years before 2018)	Age (Years CE)
Shfd18126	R1	3.00	3.8	0.7	0.64	2.4	140 ± 7	1371 ± 60	15.0	0.13 ± 0.03	**0.13 ± 0.03**	1371 ± 60	94 ± 22	1924 ± 22
Shfd18127	R2	4.00	3.3	0.7	0.54	2.1	124 ± 6	1392 ± 61	0.0	**0.15 ± 0.01**	0.13 ± 0.03	1392 ± 61	108 ± 9	1910 ± 9
Shfd18128	R3	4.00	2.7	0.6	0.71	2.3	124 ± 6	1359 ± 56	27.8	0.17 ± 0.03	**0.17 ± 0.03**	1359 ± 56	125 ± 23	1893 ± 23
Shfd18129	R4	5.00	3.4	0.7	0.51	1.7	109 ± 5	1330 ± 59	0.0	**0.11 ± 0.01**	0.10 ± 0.01	1330 ± 59	82 ± 7	1936 ± 8
Shfd18130	F1-T	0.50	2.4	0.7	0.74	3.0	197 ± 10	1420 ± 61	75.0	0.14 ± 0.05	**0.14 ± 0.05**	1420 ± 61	99 ± 36	1919 ± 35
Shfd18131	F1-B	6.10	4.6	0.6	0.63	2.0	96 ± 5	964 ± 49	85.7	0.17 ± 0.03	**0.17 ± 0.03**	964 ± 49	197 ± 53	1821 ± 53
Shfd18132	S1-T	0.50	0.2	0.6	0.53	1.9	197 ± 10	1242 ± 55	0.0	**0.06 ± 0.01**	0.04 ± 0.03	1242 ± 55	48 ± 8	1970 ± 8
Shfd18133	S1-B	3.00	1.0	0.7	0.63	2.3	140 ± 7	1457 ± 63	0	**0.06 ± 0.01**	0.04 ± 0.04	1457 ± 63	41 ± 7	1977 ± 7
Shfd18134	S2-T	0.50	3.8	0.7	1.19	3.9	197 ± 10	1434 ± 65	0.0	**0.13 ± 0.01**	0.11 ± 0.04	1434 ± 65	91 ± 8	1927 ± 8
Shfd18135	S2-B	5.10	3.3	0.7	0.80	3.2	108 ± 5	1212 ± 60	1.3	**0.13 ± 0.01**	0.11 ± 0.03	1212 ± 60	107 ± 10	1911 ± 10
Shfd18136	F2-T	0.50	2.7	0.8	0.80	2.7	197 ± 10	1603 ± 69	0.0	**0.11 ± 0.01**	0.09 ± 0.04	1603 ± 69	62 ± 7	1956 ± 7
Shfd18137	F2-B	5.30	3.4	0.8	0.59	2.2	106 ± 5	1185 ± 63	0.0	**0.10 ± 0.01**	0.09 ± 0.03	1185 ± 63	84 ± 10	1934 ± 10

5.3.3. Ground penetrating radar

GPR profiles A and B cross over the dune sites F1 and S1 (A) and F2 and S2 (B). Measurements were taken using a Sensors and Software Pulse Ekko Pro with a 250 MHz antennae and transmitter. 250 MHz was chosen over the more typical 100 or 200 MHz for dunes of this size (Bristow 2019, Bristow *et al.* 2001, Nobes *et al.* 2016, Tamura *et al.* 2020) to provide superior resolution for locating storm related reflectors that may have been too subtle to detect with a 100 MHz antenna. Equipment was deployed from a plastic sledge with antennae were oriented parallel to each other and 0.5 m apart. Data were collected at 0.1 m intervals with a stack of 256 measurements at each point. Topography was recorded using dumpy level and levelling staff. Data were recorded on a Sensors and Software Digital Video Logger (DVL-500P). A penetration velocity of 0.13 m/ns is assumed based on penetration velocities for unsaturated dune sands in other studies (Oliver *et al.* 2018, Tamura *et al.* 2011 a, b). Data were processed in RGPR with minimal processing routines including de-wow, time-zero correction, and topographic correction.

5.3.4. Storm archive and tide gauge data

As in Bateman *et al.* (2018), we constructed a coastal storm record from documentary sources to provide context for storms that may have impacted the dunes. When compared to North Sea coasts, documentary evidence of storms for the Irish sea is lacking, largely owing to a lower number of high population towns and cities around the Irish Sea where historical accounts are more likely to be preserved. Despite this, a record of 140 events since 1283 CE was produced. Here, an “event” refers to any historical incidence of flooding or coastal damage which is not a result of high output from rivers and is directly of action by waves or tides. Note was made of when a storm is corroborated by another historic source as this lends credence to the event’s occurrence. Only six storm events were recorded prior to 1800. Between 1800-1900 fifty-two events are recorded and between 1900-2020 eighty-one events are recorded (Table 5.3). Most of these events are recorded in archives relating to Blackpool, Merseyside, and south-west Scotland, primarily from the works of Hickey (1997),

Eden (2008), and Zong and Tooley (2003). Of the post-1800 records, thirty-four make specific reference to flooding coastal flooding in North Wales. This is likely a result of preservation bias in the source of these archives rather than an actual representation of lower flood occurrence in North Wales.

Table 5.3. Documentary sources of historical storm occurrence in Irish Sea

Source	Period covered (years)	Number of events	Corroborated	Tide Data
The Floods of 1720 (no date)	1720	1	1	0
Britton (1937)	1283	1	0	0
Ranwell (1958)	1331	1	1	0
Hickey (1997)	1720-1991	43	15	2
Beck (1953)	1720	1	1	0
Jensen (1953)	1897	1	1	0
Holford (1976)	1897	1	1	0
Met Office (1986)	1986	1	0	0
Lamb (1991)	1897-1927	3	1	0
Zong and Tooley (2003)	1859-1991	68	22	8
Eden (2008)	1938-1974	12	4	4
HR Wallingford (2008)	1990	1	1	1
Ruocco *et al.* (2011)	1999	1	1	1
BBC (2009)	2009	1	1	0
BBC (2010)	1990	1	1	1
Met Office (2010)	2010	1	1	1
Marusek (2011)	1899	1	0	0
BBC (2014)	2014	1	1	1
Met Office (2014)	2013-2014	6	6	6
Wadey *et al.* (2015)	2013	6	6	6
Met Office (2016)	2016	1	0	1
Met Office (2017)	2017	1	0	1
Met Office (2018)	2018	1	0	1
OPW (2021)	1905-2002	14	3	8

Tide gauge data obtained from the UK National Tide Gauge network via the British Oceanographic Data Centre (BODC, 2021) was used to provide context for the scale of events associated with documentary sources. We used data from the Holyhead tide gauge 20 km NW of the study site (1964-present; missing 1972-1977 and 1991-1995) and the Barmouth gauge which is 57 km to the southeast (used only to cover the 1991-1995 data gap). Extracted tidal levels were converted from local chart datum to Ordnance Datum (OD). For each historically documented event, the tidal level and tidal residual within 1 day 18 hours either side of event was examined, as per the "storm window" approach of Haigh *et al.* (2015). Within that window we extracted the tidal levels and residuals for both the highest tidal level and the highest residuals or occur.

Tide gauge data was also used to explore possible relationships between the annual frequency of extreme sea levels at different thresholds with annual average shoreline positions. To provide the tidal dataset for this, 3-day storm windows were extracted whenever a minimum tidal level of 2.7 m OD was concurrent with a residual of 0.3 m. A tide of > 2.7 m alone is not uncommon in these gauges, with a 1000 times per year recurrence in the Holyhead data (Environment Agency, 2019). This is reduced to < 10 per year when concurrent with a 0.3 m residual. A residual of 0.3 m is the smallest residual that corresponds with a historically documented event in our documentary data. The minimum sea level produced by this (3 m OD) is equal to the dune toe position. This data is winter-centred to ensure an entire winter (where most storms occur) is contained within a single year e.g., 1984 includes tide data from 01/07/1983 to 31/06/1984. In the combined data from Holyhead and Barmouth 388 events were identified. These were filtered at various thresholds and the number of events per year at those thresholds counted, e.g., 1995 featured 20 events with a sea level of > 2.7 m but only 11 events > 3.30 m. The approach used to compare this dataset with satellite derived shorelines is discussed further in sections 5.4.4 and 5.4.5

5.4. Results and Discussion

5.4.1. Historic and satellite derived shorelines

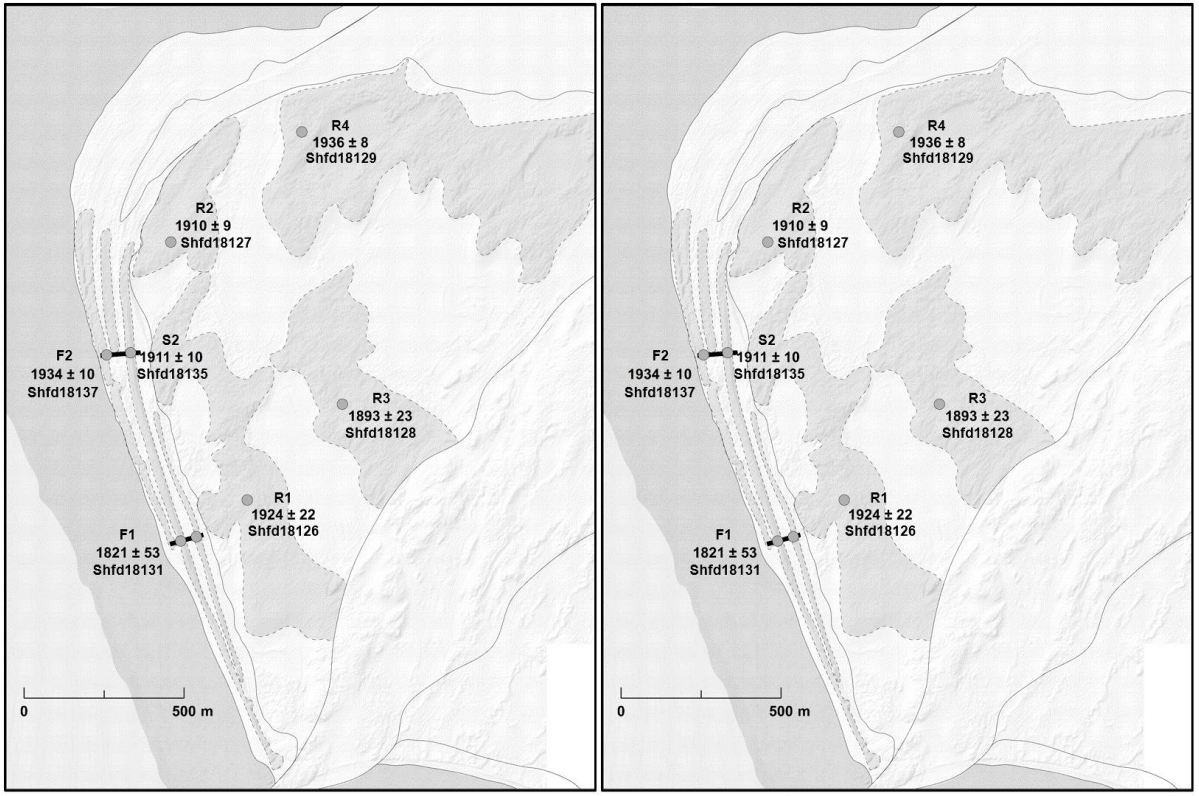

Figure 5.2. Areas defined as dune (left) and above MHW (right) in historic maps. Note dunes areas not specifically distinguished in our maps until 1891. Ages shown in year CE

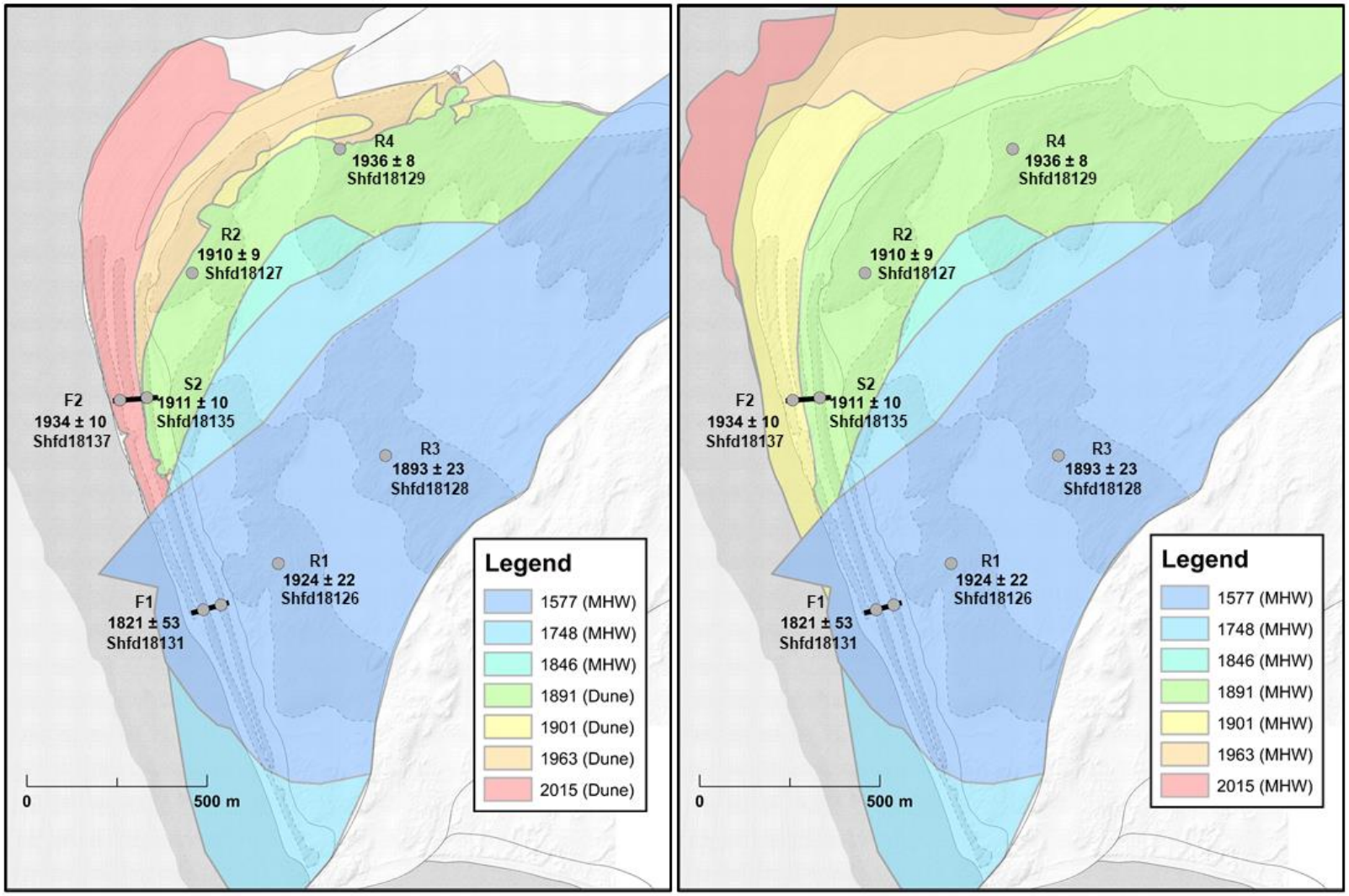

Figure 5.2. ALT Areas defined as dune (left) and above MHW (right) in historic maps. Note dunes areas not specifically distinguished in our maps until 1891. Ages shown in years CE

Historic maps show substantial change in beach dune system since 1577 (Figure 5.2). Change in shorelines from 1557 to 1748 shows expansion of the shoreline on CS-1, CS-3, and CS-4 with stability at CS-2. From 1748 to 1963 historic maps show a retreat at CS-1 of ~100 m. CS-2 shows 78 m of retreat between 1748 and 1846 with a return to its 1748 position by 1901. As discussed in Bateman *et al.* (2020), for the North Sea coast, these changes may be a result of differences between cartographers and accuracy in mapped shorelines in these earlier maps rather than meaningful changes. The historic map data for CS-1 and CS-2 more likely represents stability on this part of the shoreline in the last three centuries. Given their large scale, the broad trend of growth in CS-3 and CS-4 are likely meaningful, though their exact values are unlikely to be accurate.

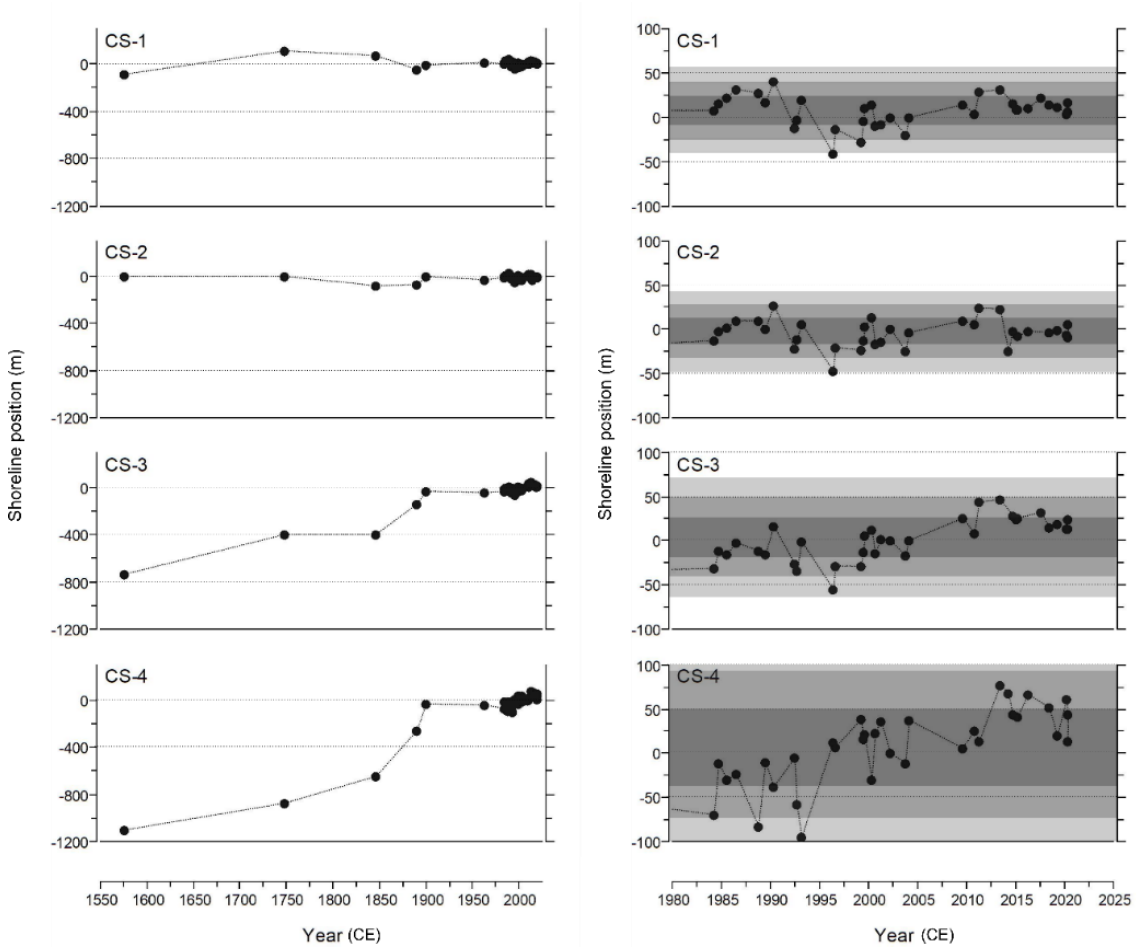

Figure 5.3. Shoreline positions from intersection of shore normal transects with historic maps (left) and satellite images (right). For satellite derived shorelines first second and third sigma confidence intervals around the 38-year mean are shaded. Shoreline positions were tidally corrected using FES2014 model outputs. FES2014 was produced by Noveltis, Legos and CLS and distributed by Aviso+, with support from Cnes (https://www.aviso.altimetry.fr/).

Satellite derived shorelines (Figure 5.3) show that since 1984, shoreline position has varied to the order of ~25 m landward and seaward of its mean position in CS-1, CS-2, and CS-3. For CS-4 this variation is larger at ~80 m landward and seaward of mean. For CS-1 and CS-2 the most advanced and retreated shorelines occur in February 1990 and March 1996 (-49 m) respectively. From 1984-1990 and 1994-1999 CS-1 and CS-2 shoreline positions are consistently seaward of the 38-year average. From 2000-2004 and 2014-2019 CS-1 and CS-2 fluctuate around the mean apart from a retreated shoreline position in 2003. 2011 and

2013 show an advanced shoreline position and there is a substantial change from 2013 to the shoreline position in 2014 in CS-2. CS-3 shows a similar scale of fluctuation in the shoreline between years but differs in the presence an underlying trend of shoreline advance. CS-4 exhibits similar differences between single and clusters of years though larger fluctuations and notable “steps” in its average shoreline position, with an average position of -10.4 m in between 1984 and 1993, 13.9 m between 1996 and 2004 and 41 m from 2009 to 2020. We suggest this reflects the continued underlying trend of the progression of the system to the northwest. The larger fluctuations may a function of increased complexity owing to tidal and fluvial controls on this part of the beach associated with estuarine processes and its proximity to the main estuary channel.

On the 500-year timescale the northwest growth of the system by ~650 m on C4 is the most noteworthy change. We suggest this is a result of the switching of the main estuary channel (Packham and Liddle, 1970) to the northwest associated with the construction of the Cob. This facilitated accumulation of sediment and the growth of dunes in this area. Further investigation of the mechanisms of this growth may be best tackled through numerical modelling of estuarine change following the construction of the Cob and the consequences of this estuarine reclamation for morphodynamics (Bennett *et al.* 2019, Jiang *et al.* 2013). Over the last 40 years the broader trend of coastal progradation to the northwest was evidenced to still be ongoing in transects CS-3 and CS-4 with relative stability seen in CS-1 and CS-2. This beach is a challenging environment for pixel detected shorelines, given its wide intertidal beach, shallow gradient, and large tidal range. Despite this we were able to reconstruct changes across single and clusters of years.

5.4.2. Dune reconstructions: OSL, GPR, POSL and PSA

OSL ages R1 to R4 (Table 5.2 and Figure 5.2) are young enough to be consistent with the changing beach-dune area in the since 1748, though many of the dune ages are younger than the mapped areas. R1 and R3 give younger ages than may be expected based on the mapped shorelines. This is likely a result of dune mobility with these ages more closely

capturing stabilization at their current positions. Using softwood poles Ranwell (1958) measured rates of inland advance on these dunes of 1.5 - 6.7 m year^{-1} prior to the growth of the present pine forest, demonstrating that these dunes were highly mobile prior to stabilization. The OSL signal of these samples may better reflect resetting caused by pedoturbation of burrowing animals (Bateman *et al.* 2003) with rabbits having caught in great numbers (Jones *et al.* 2010, Ranwell 1960,) on both these dunes and the dunes southeast of the rock ridge prior to the outbreak of myxomatosis in the region in the early 1950s (Ranwell 1960). The ages for R2, R4 and S2 are consistent with the growth of the system to the northwest.

The oldest dune age reported is for the base of dune F1 (Shfd18131) which is plausible from the historic maps but only if the area above MHW is considered as it not mapped specifically as dune until 1963. Given it is well above the beach, it is suggested dune F1 was likely already present prior to the dune fences, albeit at a smaller or incipient stage. This is supported by Welsh government aerial photographs from 1945 which shows a concentration of vegetation at the sites for both F1 and F2, suggesting the possibility that small dunes already existed at these locations before forestry interventions (Holmes, 1957).

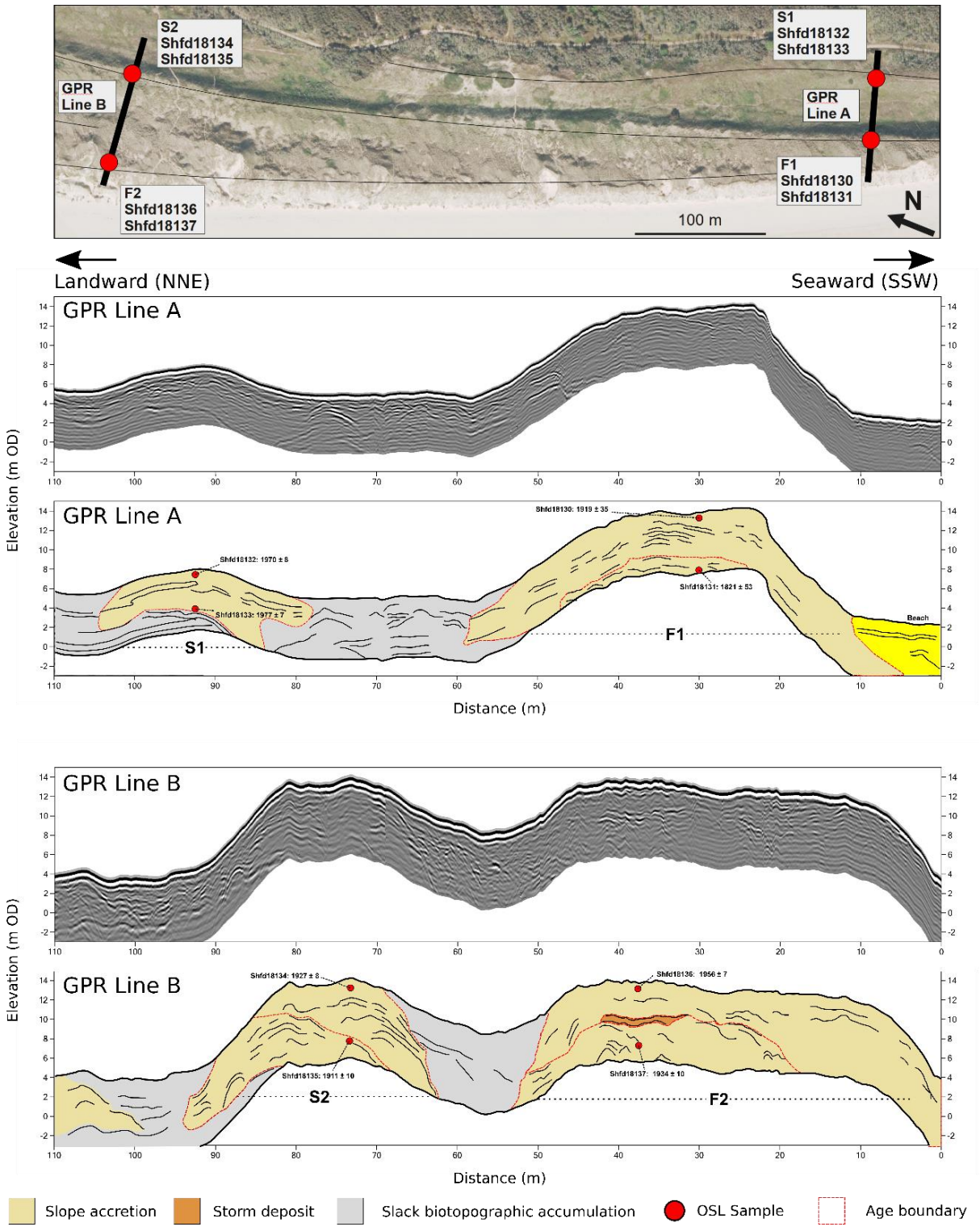

Figure 5.4. Line A (a) and Line B (b) GPR profiles with reflection interpretations and interpreted age boundaries. Distance is from the beach.

In Figure 5.4a GPR reflections for Line A are shown along with interpretations. GPR Line A starts from behind a small 2.5 m dune ridge created as part of forestry works at and moves over this small dune to an elevation of 8.0 m. After descending, the profile proceeds south-southwest passing over 35 m of interdune slack at 5 m OD before ascending the contemporary foredune (F1) which peaks at 14 m OD. The profile shape of F1 is slightly asymmetrical owing to a slow recovery from scarping of the stoss slope in the 2013/14 storm season. The reflectors in both the lee and stoss slope of dune F1 (10 m to 55 m) are typically low angle dipping landward (lee) and seaward (stoss). At the dune crest these reflectors are more often typically sub-horizontal to seaward dipping. We interpret these as foreslope accretion as observed in foredunes in other studies (Bristow and Pucillo 2006, Hesp 1988, Rodríguez-Santalla *et al.* 2021). A higher amplitude seaward dipping reflector is observed from 27 m to 32 m which was interpreted to represent coarsening of sediment. Between 60 m and 80 m reflections are typically discontinuous, low amplitude convex and concave reflectors with some high amplitude convex up reflectors, broadly we interpret this as an area of biotopographic accumulation here associated with dune slack processes. For this dune POSL data shows a gradual increase in dune age with depth from 0.30 m depth to 3.30 m indicating gradual sand accumulation (Figure 5.5). Beneath this, relative age remains constant with depth indicating a short-lived phase of rapid accumulation at-at 1821 ± 53 CE. Below this the POSL signal jumps from ~1250 to ~2250 indicating a possible third and older dune building phase. Particle size at 2.50 m and 3.70 m shows two small spikes in mean particle size (> 5% above mean) which are concurrent with spikes in sorting and iron content. These are interpreted as minor storm deposits too small in both scale and duration to appear in GPR and POSL data respectively. If the F1 top and bottom ages (Shfd18130 and 18131) are used to linearly interpolate the age of these possible hiatuses, 2.50 m corresponds to 1883 and 3.70 m to 1864.

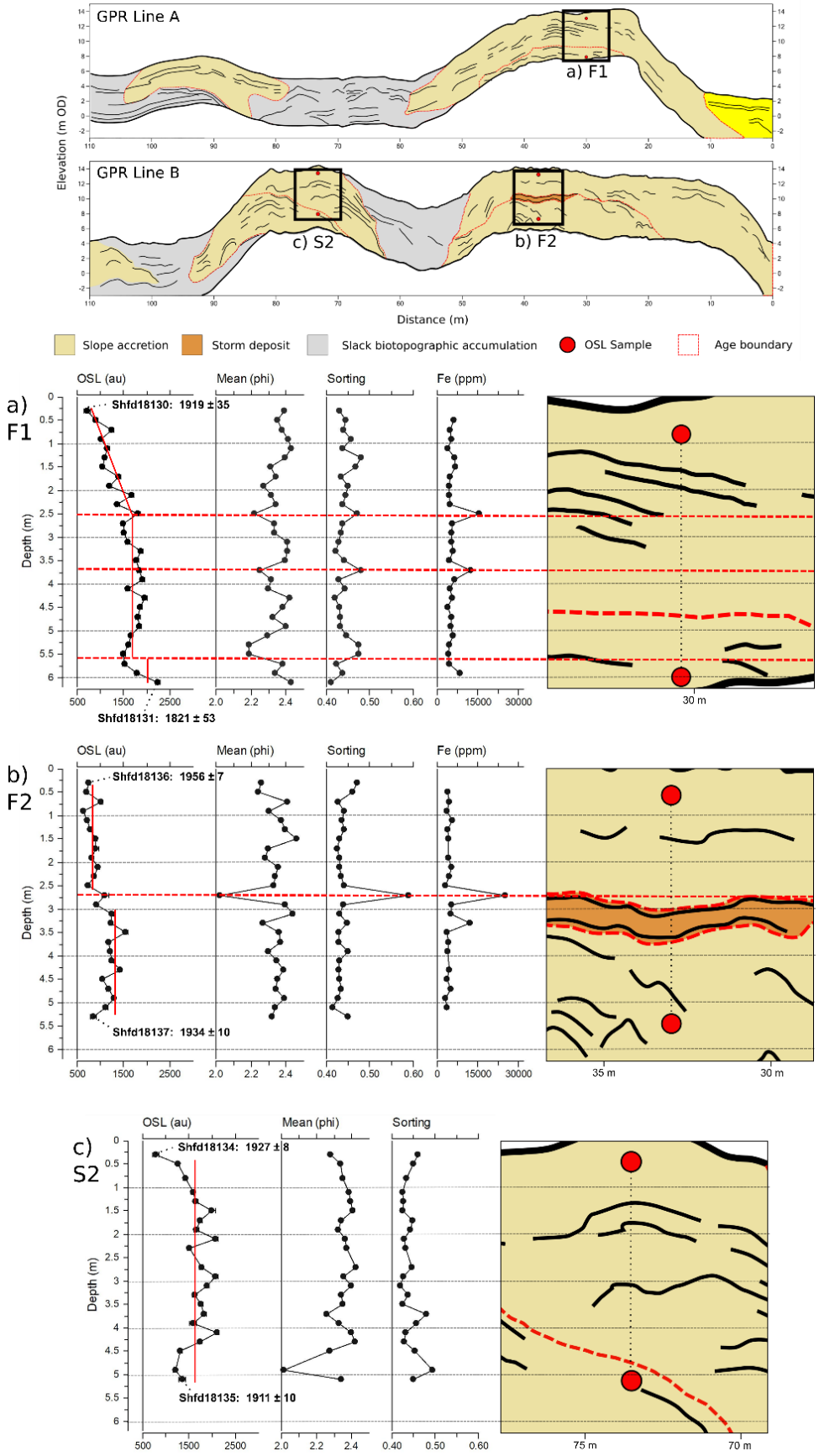

Figure 5.5. Depth profiles of OSL with GPR.

Line B begins on the slope of the F2 dune and then ascends to its crest at 14 m OD. The F2 dune has a wide crest gently dipping seaward before descending the contemporary lee slope. The stoss slope of dune F2 is shallower compared to dune F1 and at its base meets accumulating incipient foredunes. These are absent on the F1 dune which directly meets the beach. Following the dune crest is a 4m depression between dune S2 and F2. This depression does not reach down to the dunes base level. This then ascends to the crest of S2 at 14 m OD. The F2 dune also has reflectors dipping landward and seaward on the lee and stoss slopes that we interpret as foreslope accumulation. From 10 m to 30 m, a contrast of steeper reflections at depth and shallower reflections above is observed. We interpret this as a possible interface between different phases of dune building. From 32 m to 42 m a high amplitude horizontal and undulating reflector at 9.5 - 10 m OD is observed and was interpreted as a potential particle size change associated with storm activity. Beneath this reflector are several low amplitude parabolic reflections. These are interpreted to likely be associated with now buried posts associated with the dune fences around which F2 accumulated (Holmes, 1957, Bristow 2003). In the lee slope of F2, a contrast between steep and shallow angle reflectors is again noted and interpreted indicative of different phases of dune building.

Dune S2 reflectors are largely interpreted as representing foredune slope accretion. Between 63 m and 70 m reflectors dip steeply at 60º. In the 10 m seaward of this reflectors dip at more shallow angles. We interpret this as an interface between the previous stoss slope of S2 and subsequent accumulation following the formation and accumulation of F2.

POSL data and OSL ages from Shfd18135 places initial dune building between 1901 and 1921 and stabilization of the whole dune the mid-1930s. The POSL profile for dune F2 shows two phases of dune formation with a transition between phases 2.50 m to 3.10 m deep. This change accompanies the high amplitude reflection seen in the GPR data and a spike in particle size from an average of 2.32 phi to 2.02 at 2.70 m depth. This sediment is more poorly sorted and contains a spike in iron content. We suggest this coarse deposit of

storm sediment deposited at the dune crest following erosion like that described in Bateman *et al.* (2018).

Based on POSL and OSL ages we suggest accumulation of dune F2 initially grew between 1924-1944 with a later phase between 1949-1963. These phases were separated by the occurrence of a storm in the late 1930s or 1940s. The later phase of dune building may be contemporaneous with the construction of sand fences in the 1950s as Holmes (1957) reported accumulation of ~3 m of dune from 1951-1956 (0.6 my^{-1}).

5.4.3. Storm archive

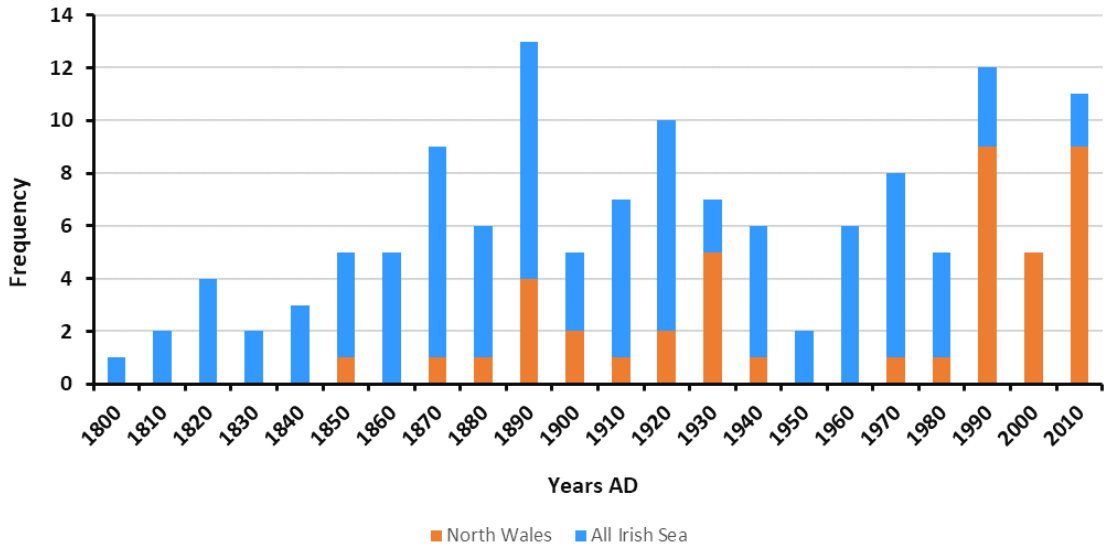

Figure 5.6. Storm archive since 1800

With the storm archive containing only seven events prior to 1800 these events are not included in Figure 5.6. These events occur in 1283, 1331, 1606, 1627, 1720, 1721 and 1789 with all but the 1606 event making specific reference to flooding in Wales. Between 1800 and 2020 storm decadal storm frequency varies with a maximum in the 1890s of 13 events (4 with reference to North Wales) and a minimum in the 1950s with only two references to Irish Sea storms mentioning damage on the east coast of Ireland. From 1850 to 2020 there has been an average of 6.8 storms per decade in the Irish Sea (4.5 in North Wales). This makes the 1870s, 1890s, 1920s, 1930s, 1970s, 1990s, and 2010s of note for their highest

storm frequency. For those events with tide gauge data available, the largest sea level was produced by a historic storm was of 3.81 m OD on the 1st of February 2002. This event had a residual of 0.876 m and a maximum residual of 1.046 m during a mid-stage of the tide. This sea level is of a 1 in 50 y recurrence in the Holyhead tide data (Environment Agency 2019). The smallest was at 2.36 m OD in 1965, though this event does not record any impacts in Wales. The smallest sea level associated with consequences in North Wales was of 3.01 m OD with a residual of 0.3 m on the 19th of March 1991. If a threshold of 3.01 m OD with a 0.3 m residual is used to filter the tide data, there are 147 storm windows between 1964 and 2020, 116 of which do not appear in historic data. This suggests either many events are missed in the historic data or that such a threshold in Holyhead's tide gauge data is a poor predictor of potential storm impacts for North Wales. Whilst both are plausibly factors, we propose the latter is more likely.

The potential range for the possible storm deposit in dune F2 (late 1930s to 1940s) lies in a period of relatively high frequency in the 1920s and 1930s followed by lower frequency conditions in the 1950s and 1960s. Attribution to a specific storm is challenging but the 1930s has many storms with consequences in North Wales (5) whereas in the 1940s only one is recorded. Five of these six events report only very minor and localized damage or coastal flooding. However, the 15th of January 1938 recorded substantial flooding and storm damage in mid and North Wales. This storm was characterized by strong south-westly winds estimated at ~40 ms^{-1} and substantial wave and storm damage to Aberystwyth with waves cascading into sea front buildings at a first-floor level and damage caused by boulders hurled by waves (BBC 2009, Zong and Tooley 2003). We suggest this storm is the most likely to be related to the storm deposit in F2. The smaller potential hiatuses in F1 are more difficult to attribute to a specific event but the mostly likely events responsible with North Welsh impacts occur in 1889 and 1859. In 1889 a storm breached the Abermenai spit at on Newborough Warren (Pye *et al.* 2014) and in 1859 a storm resulted in flooding in Bagillt, Flintshire (Zong and Tooley, 2003).

5.4.4. Tide gauge levels

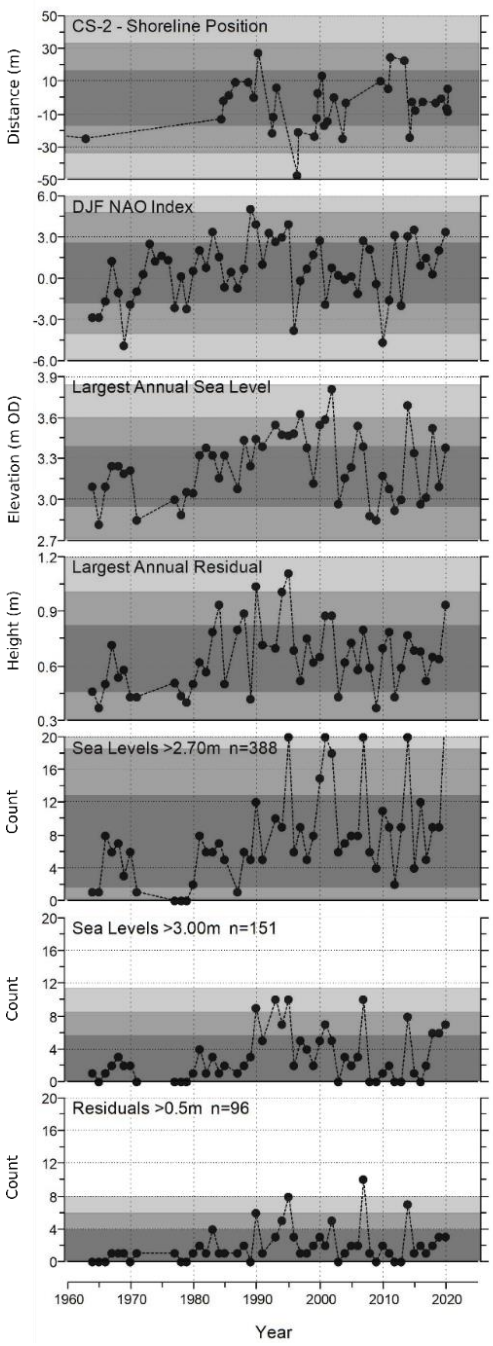

Figure 5.7. Summary of tide gauge dataset filtered at various thresholds with CS-2 shoreline data and winter NAO index for comparison. Sea level thresholds all occur with at least a 0.3 m residual and at least 2.70 m OD sea level. Each data point represents the events that took place in a winter-centred year. For example, 1984 represents 1/07/1983 to 31/06/1984. First, second and third sigma confidence intervals are shaded.

Figure 5.7 presents the tide gauge data derived from the Holyhead and Barmouth tide gauges. Both the largest annual sea level and the largest annual residual typically show smaller values in the data prior to 1971 than in later decades. The number of events per year in the 1960s is also slightly lower than in later decades. There is a data gap from 1972-1976 due to inconsistent collection and equipment changes on the Holyhead gauge. Throughout the 1960s the tide gauge data at Holyhead also often has gaps of up to months in length. Similar month-long gaps also existing in the data from 1970 to 1979. We therefore suggest interpretation of storminess in the 1960s and 1980s is likely to be misleading with this data and instead draw focus onto the data post 1980.

For the 1980s the number of events > 2.70 m remains close to average for the entirety of the decade except for 1986 in which only one event met this threshold. This is also reflected in the number of events > 3.00 m. This is consistent with the documentary reconstruction of storms in Figure 5.6 with the 1980s showing a lower incidence of impacts in North Wales than in later decades. The largest sea level of each year for the 1980s is slightly above average for the whole dataset but in only one year reaches beyond the first sigma confidence interval in 1988.

The 1990s has six years of events with greater than average frequency of > 2.70 m events with 1995 having 20 events at this threshold. The difference between the 1980s and 1990s is more pronounced in the events > 3.00 m, particularly in 1990, 1992 and 1994. 1990s also shows a greater frequency of larger residuals (> 0.5 m) and contains the three largest residuals to occur in the whole dataset. This is again consistent with the documentary data which shows the 1990s as the second most recorded impacts from storms in our dataset in the Irish Sea and joint largest (with the 2010s) for impacts in North Wales.

In the 2000s, the earlier parts of the decade (2000-2002) show higher frequency of > 2.70 m events than most of the middle and latter parts of the decade. The exception to this is 2007 when the frequency of most thresholds to was similar to 1995. The largest sea level of the entire dataset occurs in 2002 on the 1st of February. For the 2000s the years with a high

frequency of >2.70 m events are not as consistently reflected in the frequency of > 3.00m events as was the case for the 1990s. The frequency of large residuals is also not typically far from average (except for 2007) and the largest annual residual also close to average for the decade.

The 2010s shows a greater variability in the frequency of sea levels > 2.70 m between single years than in previous decades. The incidence of sea levels > 3.00 m is low for from 2010 to 2017, except for 2014. The period from December 2013 to March 2014 featured many high sea-level events in many UK tide gauge records (Brooks 2017, Masselink *et al.* 2016, Wadey *et al.* 2015). The last three years of the decade show an increase in the incidence of sea levels > 3.00 m. The frequency of large residuals is slightly above average for this decade but most notably so in 2014.

5.4.5. Comparison of tide data with satellite derived shorelines

For comparison with the tide data the satellite derived shoreline data for the shoreline transect CS-2 are also shown in Figure 5.7. This transect is assumed to be the most representative of interannual to decadal changes in the shoreline position due to of its relative stability over the entire satellite and historic map dataset compared to the other three transects. For the 1980s only the latter half of the decade is covered by the shoreline data, during which shoreline position at CS-2 is consistently close to the mean. For the 1990s the shoreline retreats from an advanced position in 1990 to its most retreated by 1996 before recovering to close to its average position by the end of the decade. This corresponds well to the period of increased frequency and large extreme sea levels in the early 1990s. For the early 2000s the shoreline fluctuates around a slightly below average position before a data gap in the late 2000s. Crucially, this misses any potential impacts from the year 2007. By the early 2010s the shoreline occupies an advanced position until the 2013/14 storm season. This results in a substantial retreat of the shoreline, which recovers to average conditions in the following year, though it does not return to the advanced position it held prior.

From a visual perspective CS-2 shoreline positions do show some correspondence to the tide data, with years with retreated shorelines corresponding to single or multiple years of higher frequency of the larger extreme sea levels. Exploring this to develop more meaningful conclusions is challenging given the temporal mismatches between the time series of the tide data (annual) and the shoreline position (point) in addition to gaps of up to years in the shoreline data. This prohibits many time-series statistical techniques. To attempt to quantitatively compare these datasets we determine the average shoreline position for each year by averaging all shoreline positions in that year. For years without any images, we linearly interpolate. We then explored correlations of these annual shoreline positions with the frequency of events at various tidal and residual thresholds, as well as with the NAO winter index. We also explored correlations in the data with 3- and 5-year moving averages applied to the shoreline data. A selection of these data is shown in Table 5.4. All statistically significant correlations ($p = < 0.05$) are included

Table 5.4. Pearson's correlation coefficients and significance values for unsmoothed and smoothed shoreline positions against tidal parameters. Values in red are statistically significant (p = < 0.05)

	Transect		Largest Residual	Largest Sea Level	Residual >0.3	Residual >0.6	Sea Level >2.7	Sea Level >3.0	Sea Level >3.3	NAO Winter
No smooth	CS-1	Pearson	0.01	-0.29	-0.21	-0.04	-0.18	-0.08	-0.01	0.19
		p	0.95	0.09	0.21	0.81	0.28	0.65	0.93	0.27
	CS-2	Pearson	-0.04	**-0.37**	-0.16	-0.10	-0.13	-0.12	-0.07	0.02
		p	0.82	**0.03**	0.34	0.56	0.46	0.49	0.71	0.89
	CS-3	Pearson	-0.19	**-0.39**	0.08	-0.05	0.13	-0.07	-0.17	0.18
		p	0.27	**0.02**	0.65	0.78	0.46	0.71	0.33	0.30
	CS-4	Pearson	-0.30	-0.17	0.21	-0.18	0.26	-0.17	**-0.43**	0.05
		p	0.08	0.34	0.21	0.30	0.13	0.33	**0.01**	0.76
3y MA	CS-1	Pearson	-0.09	**-0.40**	-0.31	-0.15	-0.28	-0.25	-0.24	0.16
		p	0.60	**0.02**	0.06	0.39	0.09	0.13	0.16	0.34
	CS-2	Pearson	-0.19	**-0.49**	-0.24	-0.18	-0.22	-0.27	-0.29	0.00
		p	0.29	**0.00**	0.16	0.29	0.20	0.11	0.08	0.98
	CS-3	Pearson	-0.28	**-0.41**	0.05	-0.11	0.09	-0.18	-0.32	0.15
		p	0.11	**0.02**	0.78	0.52	0.60	0.31	0.06	0.40
	CS-4	Pearson	-0.30	-0.16	0.26	-0.10	0.30	-0.12	-0.32	0.11
		p	0.09	0.36	0.12	0.55	0.08	0.49	0.06	0.54
5y MA	CS-1	Pearson	-0.10	**-0.38**	-0.32	-0.18	-0.30	-0.31	-0.30	0.10
		p	0.58	**0.02**	0.05	0.29	0.07	0.06	0.08	0.55
	CS-2	Pearson	-0.20	**-0.45**	-0.26	-0.21	-0.23	**-0.33**	**-0.35**	-0.06
		p	0.25	**0.01**	0.13	0.22	0.17	**0.05**	**0.03**	0.73
	CS-3	Pearson	-0.31	-0.41	0.04	-0.13	0.08	-0.22	**-0.37**	0.10
		p	0.08	0.09	0.82	0.44	0.64	0.20	**0.02**	0.58
	CS-4	Pearson	**-0.30**	-0.19	0.28	-0.09	0.31	-0.11	-0.31	0.14
		p	**0.02**	0.27	0.10	0.60	0.07	0.52	0.06	0.43

Few parameters produce statistically significant correlations with shoreline position in our data. The only shoreline transects to consistently produce significant correlations with tidal parameters is CS-2. Significant correlations only exist with parameters that indicate the presence of very large events. The most consistent parameter to be correlated with shoreline position is the largest annual storm with the higher the elevation of the largest storm of the year then the more retreated the shoreline position. This correlation is in all instances only moderate at ~ -0.4. The only tidal threshold to produce statistically significant correlations is the number of storms > 3.3 m in the unsmoothed data and the number of storms > 3.0 m in the 5-year moving average. No tidal thresholds or shoreline positions produced significant correlations with the winter NAO.

These correlations are not themselves necessarily indicative of a causal relationship. However, they may suggest that the very largest storms dictate a stronger control on annual shoreline position than an abundance of smaller storms on this specific beach. (Burvingt *et al.* 2016, Burvingt *et al.*, 2017.). This would imply that an increase in frequency of events of < 3.00m elevation would not exert much physical change on the shoreline position but that an increase in frequency, or indeed magnitude, of very large events > 3.00 m OD would elicit enhanced shoreline retreat here. This simple approach shows that statistically significant correlations between tidal thresholds and shoreline change can be determined with sufficient data. There are limitations in the approach presented here including the interpolation of years where satellite data is missing; the distance between this beach and the tide gauge (40 km) resulting in difference in the tidal prism; and the absence of wave data not allowing for co-dependency of shoreline position with both wave and tidal thresholds.

Understanding how shorelines change on the timescales of multiple years of decades in relation to hydrodynamic forcing will be key to managing shorelines under a future changing climate. Whilst these findings are far from conclusive, even for this beach alone, it does suggest that statistical analysis of tide gauge data alongside satellite derived shorelines may in future yield more valuable results in other settings. This would be particularly true of a

location with a greater abundance of available images to overcome data gaps and improve temporal resolution (Castelle *et al.* 2021). Statistical analysis of satellite derived shorelines in a location with a proximal tide gauge and a wave buoy would likely be particularly fruitful. Development of this work would also make a compelling case for the expansion of both tide gauge and wave buoy networks in the UK and beyond.

5.5. Conclusion

Coastal change at the Traeth Penrhos beach-dune system is reconstructed over; the last 500 years at low resolution using historic maps, the last 100 years at higher resolution with OSL and GPR, and the last 40 years at high resolution using satellite derived shorelines. On the 500-year timescale the system grew north-west. We suggest this is a result of the switching of the main estuary channel and estuarine dynamic changes after the building of the Cob. OSL dating verified observations of the timing of dune construction and stabilization illustrating its potential in verifying morphological observations in historic maps for sandy shorelines. In doing this, this study illustrates the potential of historic map data for reconstruction coastal changes on the scale of hundreds of meters to kilometres on decadal and longer timescales. Typically, such sources have tended to go under-utilized as a means of providing longer term morphological context in coastal studies. Satellite derived shorelines allowed for the reconstruction of changes across single and clusters of years. Over the last 40 years the broader trend of coastal progradation to the northwest was evidenced but with relative stability seen in on the southern part of the system.

Whilst the foredune ridges at Penrhos are predominantly the result of sand fences installed in 1951, our OSL and GPR data suggest that at least some existed prior to this. By combining GPR with PSA, OSL ages and POSL possible storm events impacting at Penhros were identified. This included a single large storm event which could also be identified the historic storm archive as likely to have occurred on the 15th of January 1938. This study's combination of GPR with POSL and PSA is unique amongst coastal studies and has allowed advancement upon the findings of Bateman *et al.* (2018) by further tying storm surge

impacts to the morphological development of coastal dunes. These palaeo-environmental techniques provide superior spatial and temporal resolution on the coastal evolution to historic maps, though at a finer spatial scale and with a requirement for more in field and lab analysis. Ideally, if applied to other dunes, the methods here would utilize a range of GPR antenna to provide data at varying spatial resolutions and penetration depths, such approaches are used in other studies (Tamura *et al.* 2011a; 2011b).

Through a combination of historic and documentary sources with regional tide gauge data we were able to provide climatic and hydrodynamic context for our other data sources. Analysis of tide gauge data, in combination with shoreline data allowed for a simple statistical exploration of shoreline change against storm frequency at various scale thresholds. We found statistically significant correlations between shoreline position and the largest extreme sea level to occur each year as well as with the number of events above a threshold of 3.00 m OD. We conclude that satellite derived shorelines may prove a valuable tool in investigating this in regions with an abundance of hydrodynamic data, ideally of both waves and tides. This would be especially fruitful if a combination of satellite derived shorelines, hydrodynamic data and statistical approaches were applied over multiple beaches of different morphological characteristics.

Overall, this unique combination of historic maps, satellite data and palaeo-environmental techniques and historic and documentary sources has allowed for the examination of coastal evolution on timescales of hundreds of years to single years. For coastlines where monitoring data is sparse, these techniques may represent a powerful toolkit in reconstructing past changes and providing morphological context for both for the purposes of coastal science and coastal management. On coastlines where monitoring data is lacking, but hydrodynamic data is more abundant, these datasets may be combined with statistical analysis to advance understanding of hydrodynamic thresholds in governing annual to multi-decadal coastal change.

5.6. Acknowledgements

Rushby was supported in their PhD studies by the NERC Doctoral Training Partnership ACCE (Adapting to the Challenges of a Changing Environment) (NE/L002450/1).

5.7. Supplementary Material

Table 5.5. Historic map sources and shoreline positions.

Year	Source	CS-1	CS-2	CS-3	CS-4
1577	Saxton North Wales County Map National Library of Wales. http://hdl.handle.net/10107/1445612	-85	5	-735	-1103
1748	Lewis Morris, National Library of Wales. Plans of harbours, bars, bays and roads in St. George's Channel lately survey'd under the direction of the Lords of the Admiralty, and now publish'd by their permission, with an appendix concerning the improvements that might be made in the several harbours, &c. for the better securing the navigation in those parts together with a short account of the trade and manufactures on that coast http://hdl.handle.net/10107/1445668	110	-2	-399	-870
1846	John Ralph Haslam. National Library of Wales. Apportionment of the rent-charge in lieu of tithes in the parish of Newborough in the County of Anglesey. http://hdl.handle.net/10107/4622457	77	-80	-398	-641
1891	Angl-sh36/46 OS 1:10000 obtained via Edina Digimap	-48	-67	-141	-252
1901	Angl-sh36/46 OS 1:10000 obtained via Edina Digimap	-1	-2	-31	-30
1963	Angl-sh36/46 OS 1:10000 obtained via Edina Digimap	11	-25	-38	-35
2015	Angl-sh36/46 OS 1:10000 obtained via Edina Digimap	9	-7	26	42

5.7.1. OSL Abanico Plots and OSL and PSA data

Shfd18126
R1

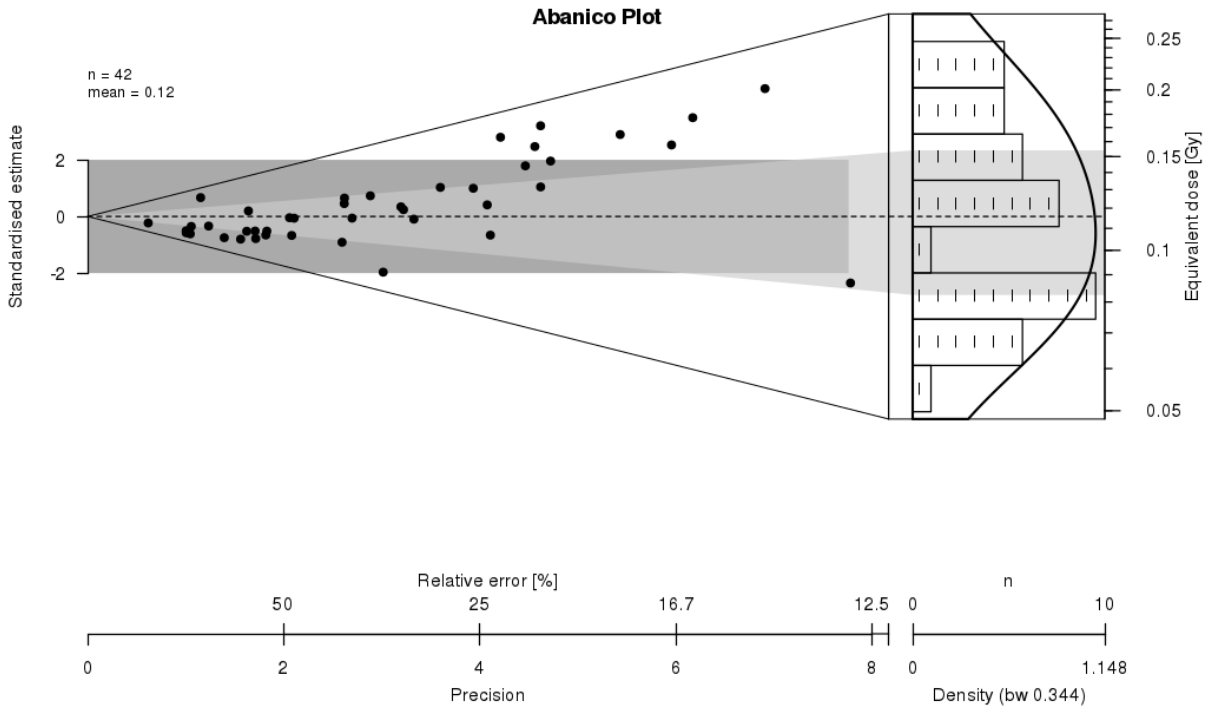

Shfd18127
R2

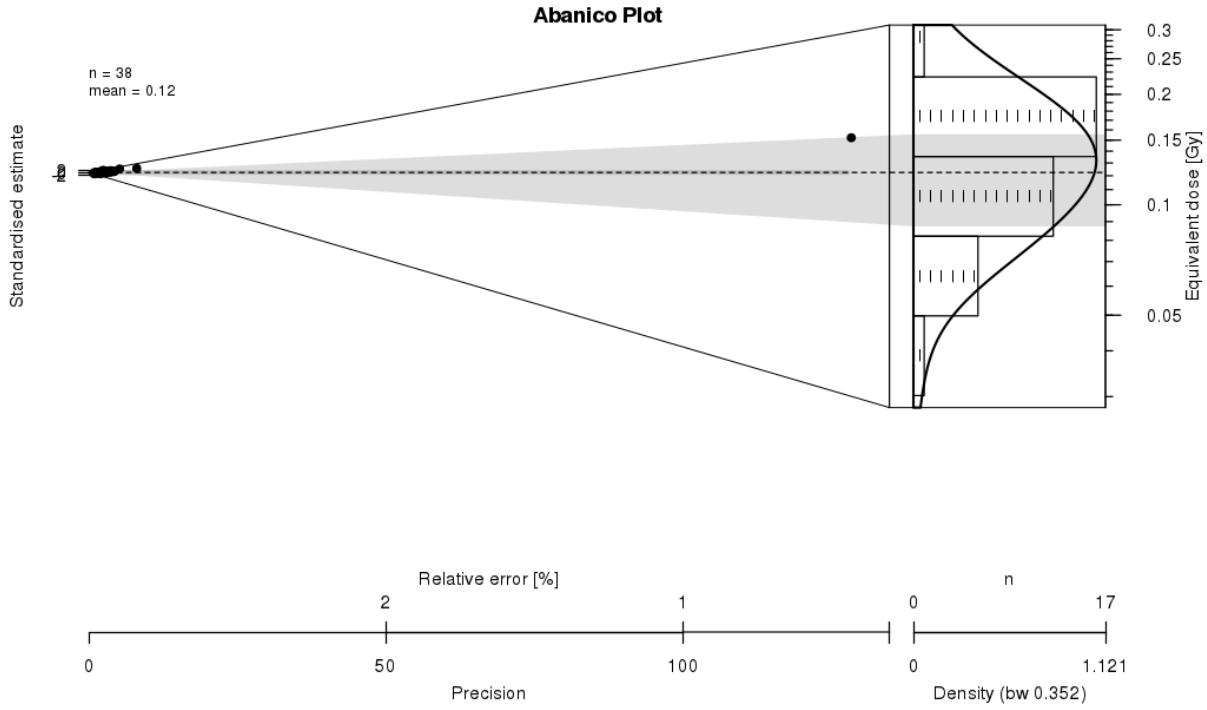

Shfd18128
R3

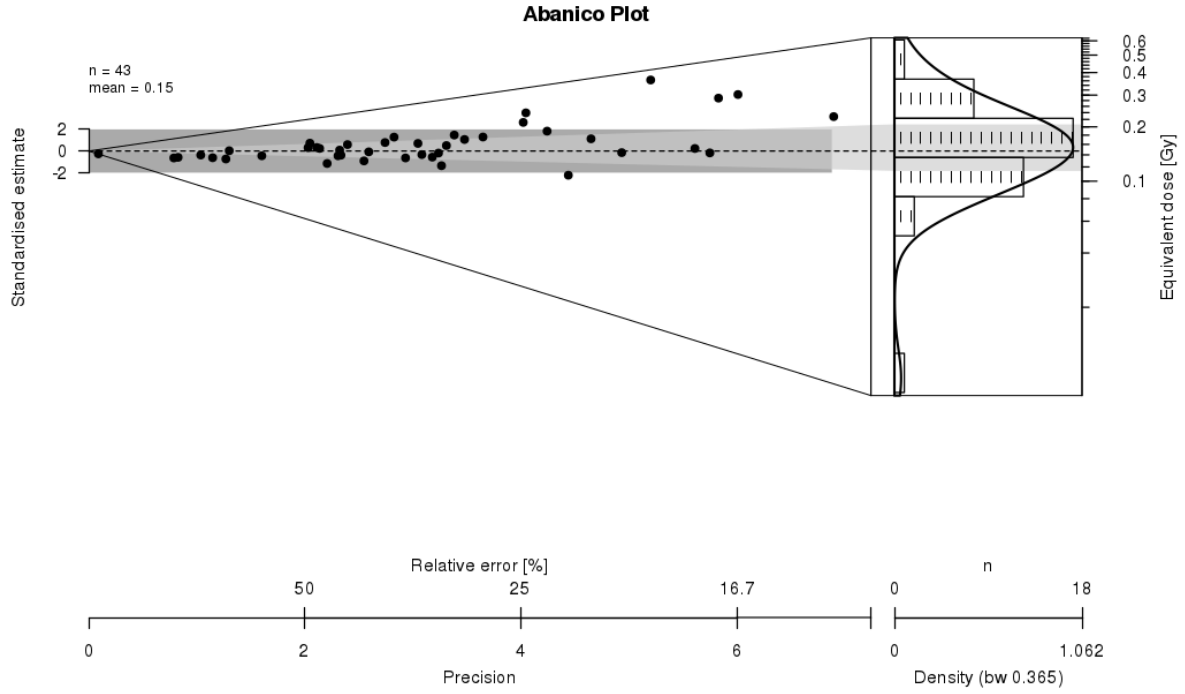

Shfd18129
R4

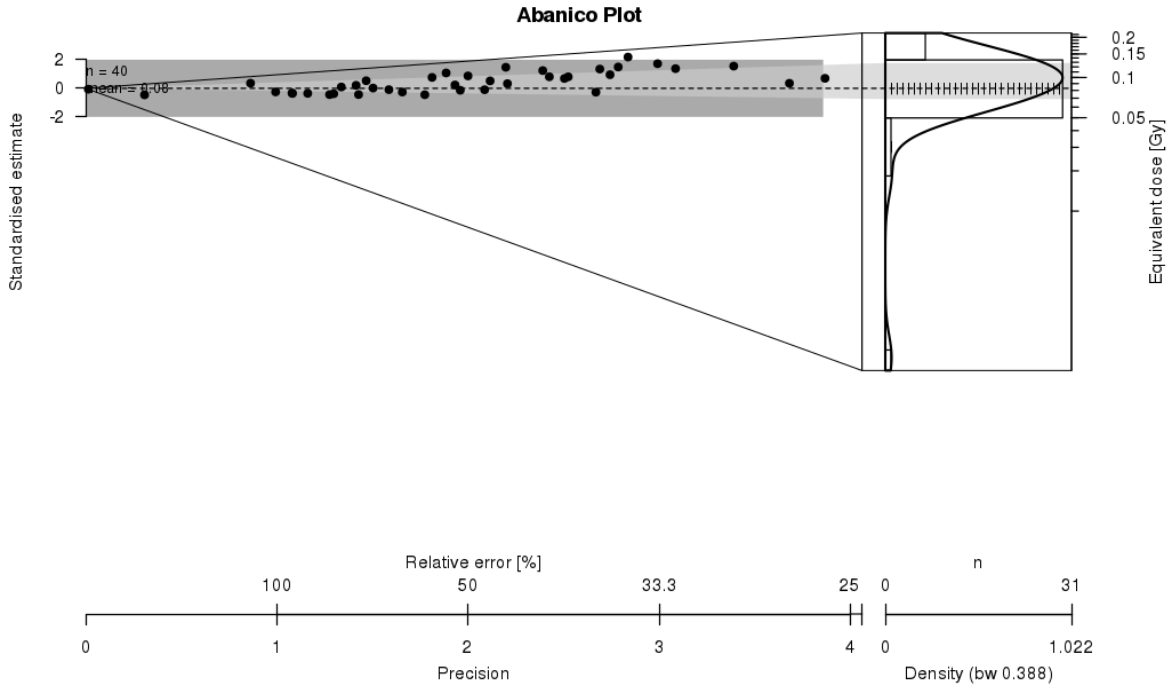

Shfd18130
F1-T

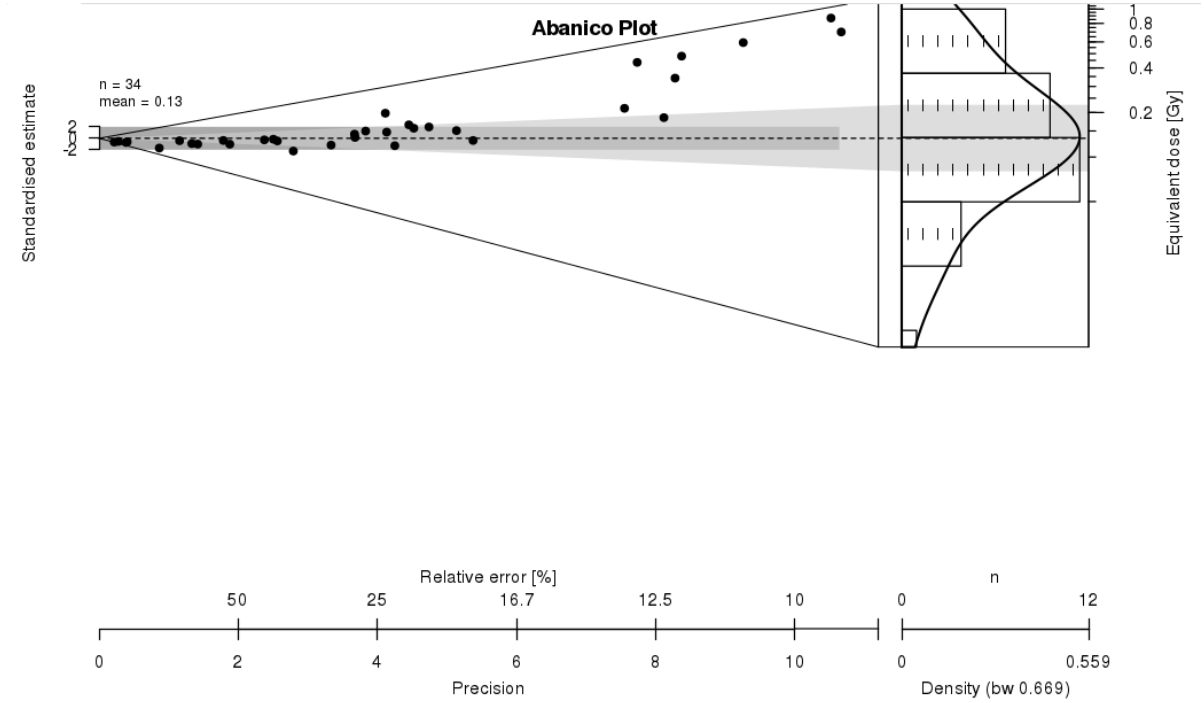

Shfd18131
F1-B

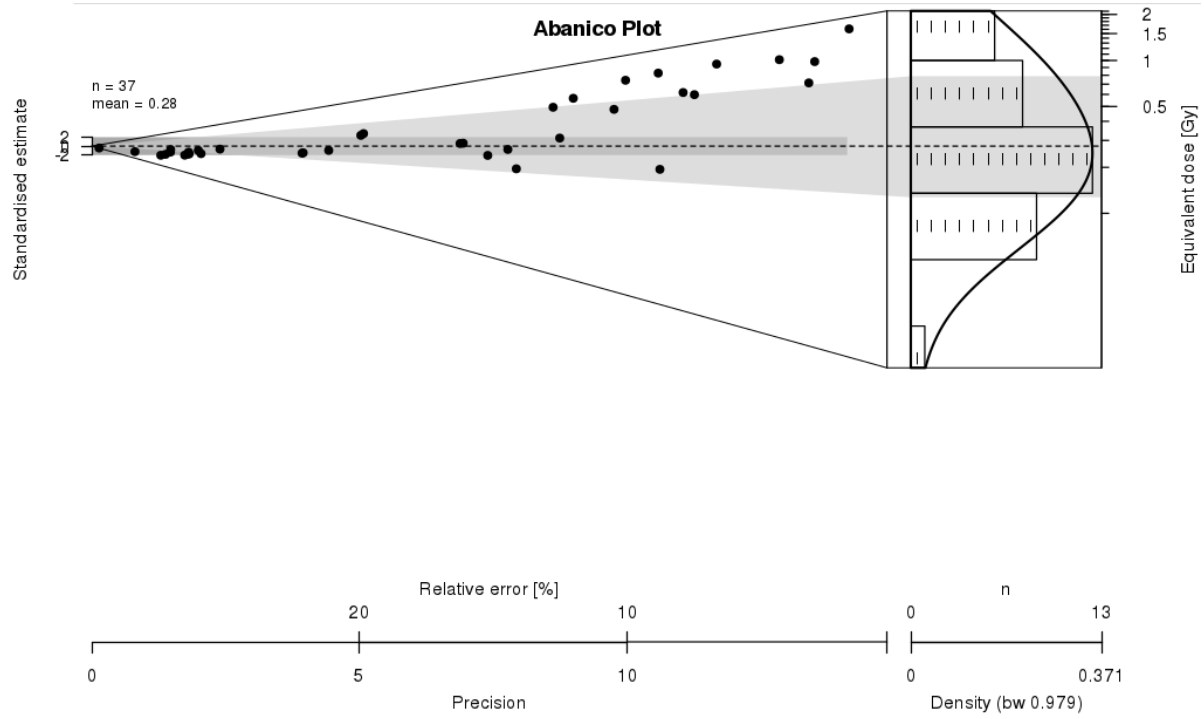

Shfd18132
S1-T

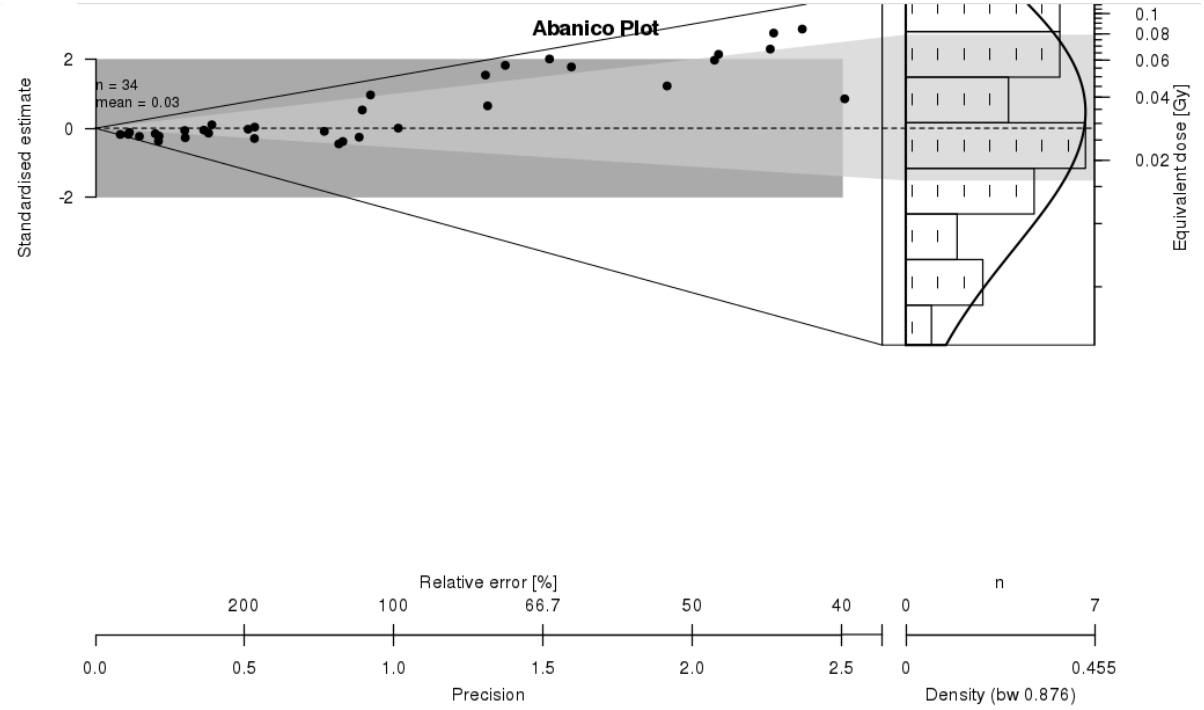

Shfd18133
S1-B

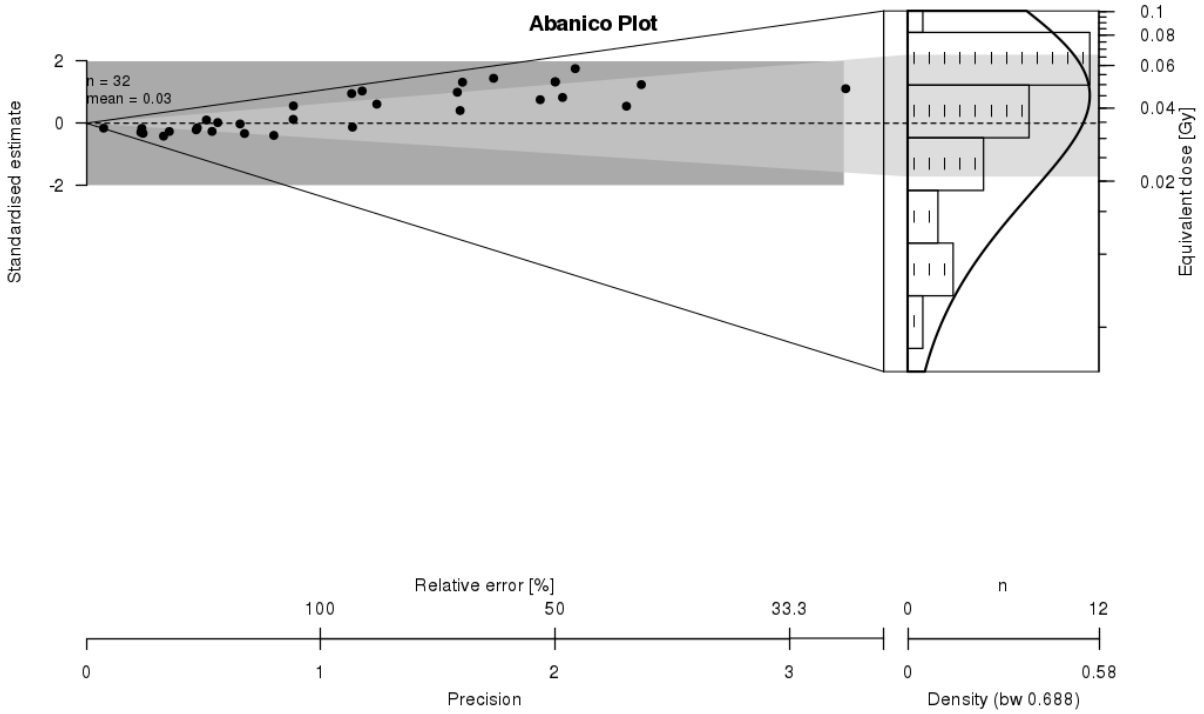

Shfd18134
S2-T

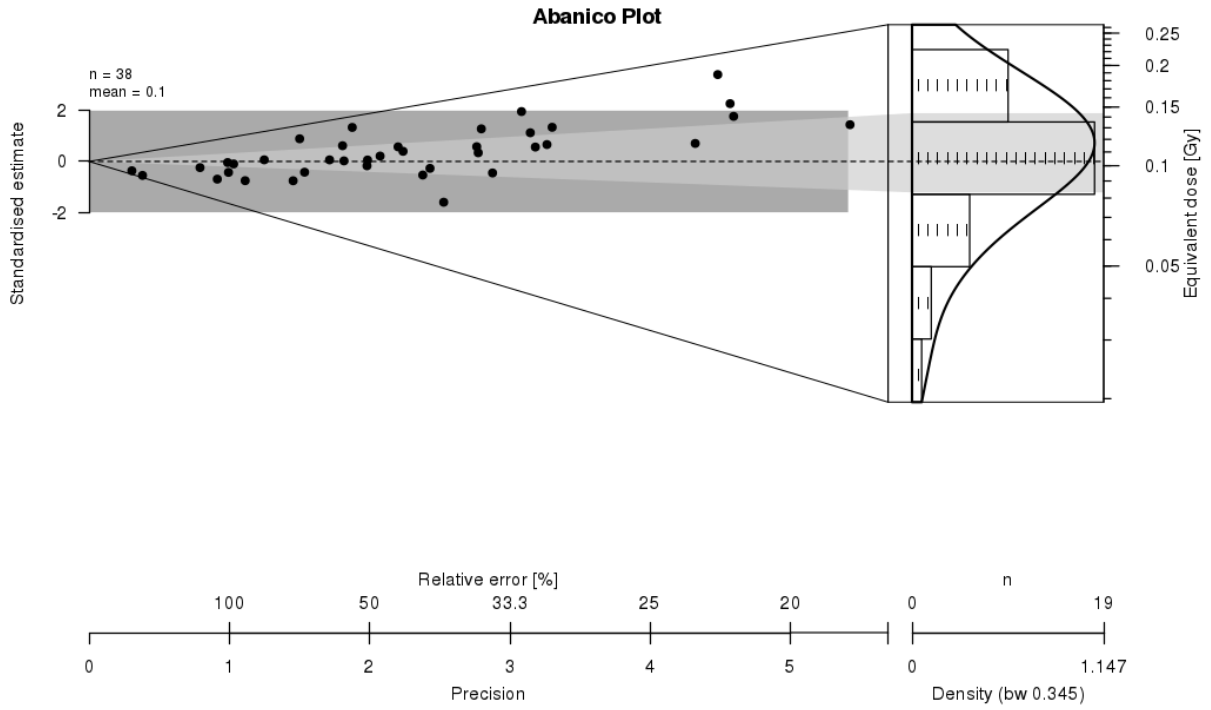

Shfd18135
S2-B

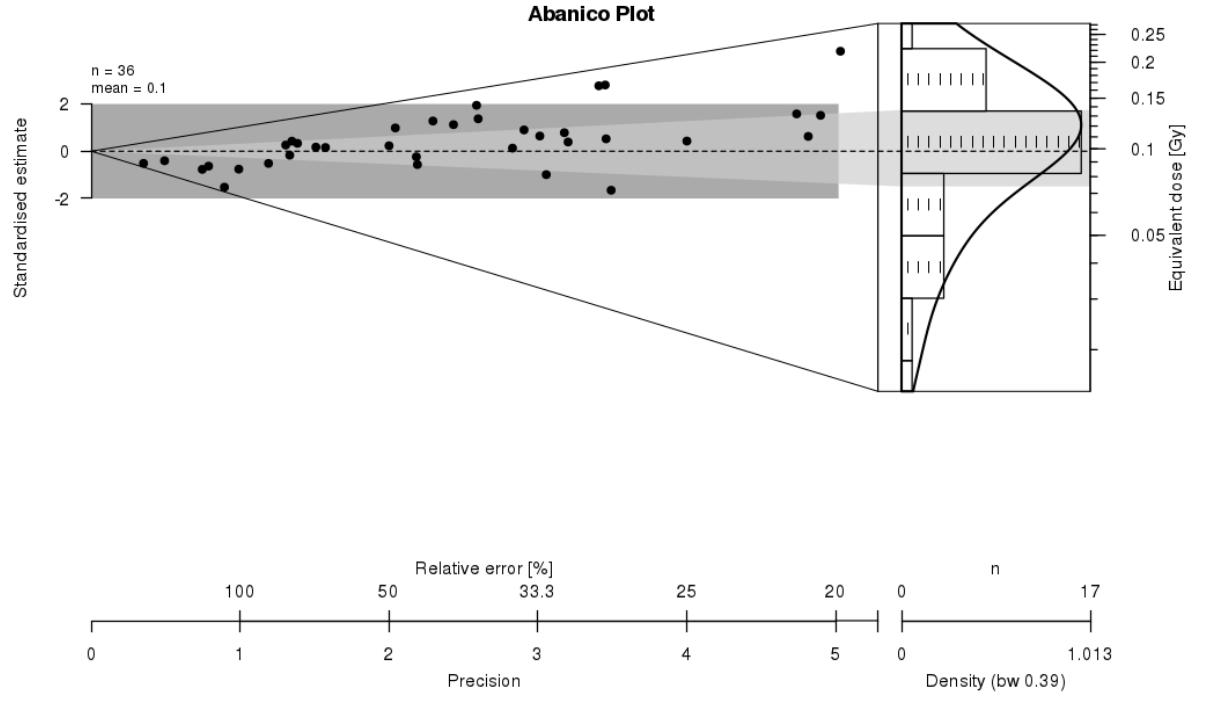

Shfd18136
F2-T

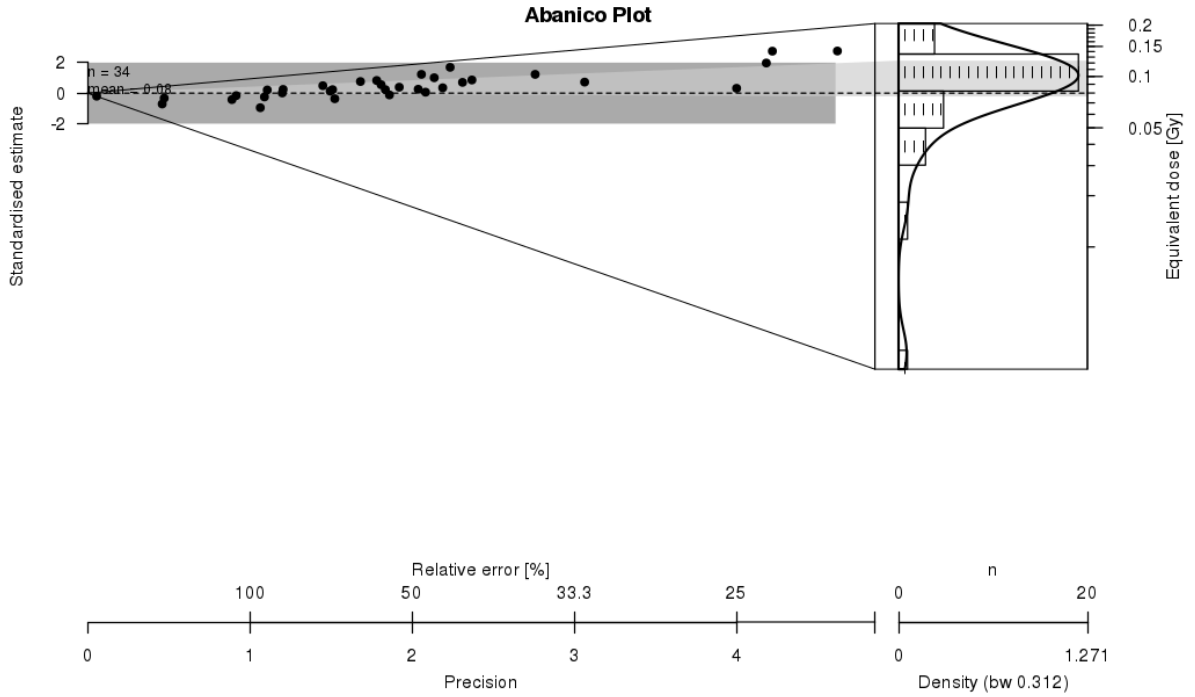

Shfd18137
F2-B

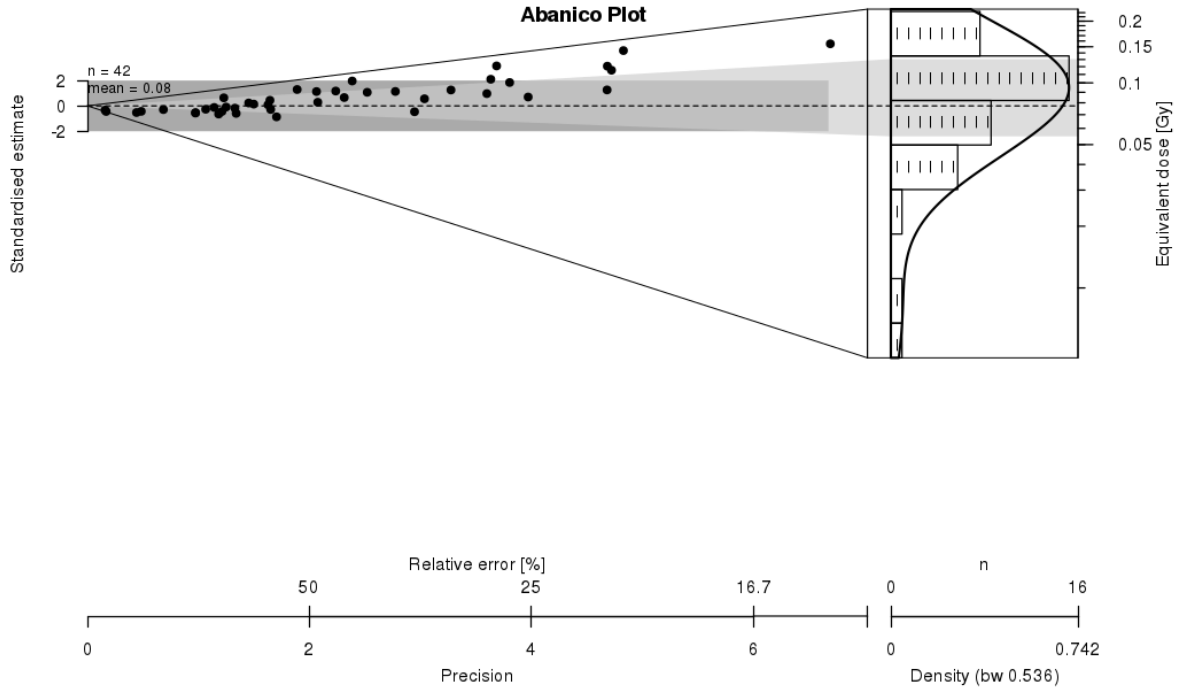

Table 5.6. POSL and PSA data from foredune sites. Yellow highlights indicate mean particle sizes or sorting > 5% above or below average for that dune.

Foredune 1

Sample ID	Depth (m)	Mean (M_z)	Sorting (σ_I)	Skew (SK_I)	Kurtosis (K_G)	Age (Cal Year)
F1-T	0.30	2.39	0.43	0.04	1.11	1919 ± 35
F1-50	0.50	2.35	0.44	0.05	1.09	
F1-70	0.70	2.38	0.44	0.05	1.12	
F1-90	0.90	2.41	0.46	0.00	1.17	
F1-110	1.10	2.43	0.44	0.02	1.14	
F1-130	1.30	2.40	0.48	0.00	1.18	
F1-150	1.50	2.31	0.47	0.05	1.09	
F1-170	1.70	2.34	0.43	0.05	1.09	
F1-190	1.90	2.27	0.45	0.07	1.10	
F1-210	2.10	2.32	0.44	0.05	1.09	
F1-230	2.30	2.34	0.44	0.05	1.10	
F1-250	2.50	2.22	0.47	0.08	1.12	
F1-270	2.70	2.33	0.44	0.04	1.10	
F1-290	2.90	2.33	0.43	0.04	1.10	
F1-310	3.10	2.41	0.43	0.04	1.12	
F1-330	3.30	2.41	0.42	0.05	1.11	
F1-350	3.50	2.39	0.44	0.06	1.11	
F1-370	3.70	2.25	0.48	0.06	1.09	
F1-390	3.90	2.32	0.43	0.05	1.09	
F1-410	4.10	2.30	0.44	0.06	1.08	
F1-430	4.30	2.42	0.42	0.05	1.11	
F1-450	4.50	2.38	0.43	0.04	1.10	
F1-470	4.70	2.32	0.43	0.05	1.08	
F1-490	4.90	2.40	0.43	0.05	1.11	
F1-510	5.10	2.29	0.45	0.07	1.09	
F1-530	5.30	2.19	0.47	0.06	1.07	

F1-550	5.50	2.19	0.47	0.06	1.07	
F1-570	5.70	2.38	0.42	0.04	1.11	
F1-590	5.90	2.34	0.44	0.05	1.09	
F1-B	6.10	2.43	0.41	0.04	1.10	1821 ± 53
Foredune 2						
Sample ID	Depth (m)	Mean (M_z)	Sorting (σ_I)	Skew (SK_I)	Kurtosis (K_G)	
F2-T	0.30	2.26	0.47	0.09	1.09	1962 ± 25
F2-50	0.50	2.24	0.46	0.08	1.09	
F2-70	0.70	2.41	0.43	0.05	1.10	
F2-90	0.90	2.30	0.44	0.06	1.09	
F2-110	1.10	2.37	0.43	0.04	1.11	
F2-130	1.30	2.39	0.44	0.06	1.10	
F2-150	1.50	2.46	0.43	0.03	1.11	
F2-170	1.70	2.30	0.43	0.05	1.08	
F2-190	1.90	2.28	0.43	0.05	1.09	
F2-210	2.10	2.36	0.43	0.05	1.09	
F2-230	2.30	2.34	0.43	0.04	1.09	
F2-250	2.50	2.33	0.44	0.04	1.09	
F2-270	2.70	2.02	0.59	0.12	1.01	
F2-290	2.90	2.39	0.44	0.03	1.12	
F2-310	3.10	2.44	0.43	0.03	1.12	
F2-330	3.30	2.27	0.45	0.05	1.10	
F2-350	3.50	2.36	0.43	0.03	1.09	
F2-370	3.70	2.37	0.43	0.03	1.10	
F2-390	3.90	2.30	0.45	0.04	1.09	
F2-410	4.10	2.35	0.43	0.03	1.09	
F2-430	4.30	2.39	0.43	0.04	1.11	
F2-450	4.50	2.35	0.43	0.04	1.10	
F2-470	4.70	2.34	0.43	0.05	1.10	

F2-490	4.90	2.39	0.43	0.04	1.11	
F2-510	5.10	2.34	0.41	0.05	1.09	
F2-B	5.30	2.32	0.45	0.06	1.09	1942 ± 26
Secondary 2						
Sample ID	Depth (m)	Mean (M_z)	Sorting (σ_I)	Skew (SK_I)	Kurtosis (K_G)	
S2-T	0.30	2.28	0.46	0.08	1.09	1927 ± 8
S2-50	0.50	2.34	0.45	0.04	1.10	
S2-80	0.80	2.35	0.43	0.05	1.10	
S2-110	1.10	2.39	0.42	0.04	1.11	
S2-130	1.30	2.40	0.43	0.05	1.11	
S2-150	1.50	2.41	0.42	0.04	1.11	
S2-170	1.70	2.34	0.45	0.05	1.09	
S2-190	1.90	2.32	0.44	0.04	1.09	
S2-210	2.10	2.36	0.43	0.05	1.09	
S2-230	2.30	2.37	0.43	0.05	1.12	
S2-270	2.70	2.43	0.45	0.04	1.14	
S2-290	2.90	2.35	0.43	0.05	1.08	
S2-310	3.10	2.40	0.42	0.04	1.11	
S2-330	3.30	2.34	0.44	0.04	1.10	
S2-350	3.50	2.35	0.43	0.03	1.10	
S2-370	3.70	2.26	0.48	0.08	1.08	
S2-390	3.90	2.33	0.46	0.06	1.08	
S2-410	4.10	2.40	0.43	0.04	1.11	
S2-430	4.30	2.42	0.43	0.04	1.11	
S2-450	4.50	2.27	0.45	0.06	1.08	
S2-490	4.90	2.02	0.49	0.04	1.05	
S2-B	5.10	2.34	0.45	0.03	1.10	1927 ± 9

Chapter 6.

Synthesis, limitations, and future directions.

Chapter 1 laid out three overarching challenges this thesis sought to explore.

1. Instrumental records of storm surges are too short term in scope. This results in high uncertainty in risk-based approaches to coastal flood risk. Approaches to tackling this using sedimentary archives have largely been constrained to back-barrier deposits, limiting the potential locations where such data can be derived.

2. Sea-level change presents an important background signal to changes in storm surges and coastal evolution. Resolution of unanswered questions in regional sea level histories is required to improve understanding of the relationship of past storms with sea level and changing climate and to determine the impact of these on coastal evolution.

3. The importance of coastal storms in dictating the evolution of coasts on timescales most relevant to coastal management (decades to centuries) is poorly understood due to a lack of high-resolution monitoring data on most shorelines.

6.1. The brevity of instrumental records

The first objective of this thesis was to explore methods by which the brevity of instrumental records of storms and extreme sea levels might be improved upon (1.2, 2.1). This was first tackled in Chapter 3 which explored how the sedimentary archives preserved in coastal dunes may be used to enhance storm records (2.2). This work built on from the findings of Bateman *et al*. (2015) of distinct hiatuses in the relative age profiles of coastal dunes in North Norfolk measured using portable OSL. Developing on this with additional POSL and

OSL sampling, Chapter 3 was successfully able to produce the first ever reconstruction of coastal storms and their morphological impacts in coastal dunes based on relative dating and particle size data.

This new method provides not only information of dunefield evolution from the dating of dunes but also on past coastal storms through identification of hiatuses in dune building observed in POSL profiles. Seven storm events were reconstructed from the Holkham dunes over the last 140 years. The longest tide gauges records for the western coasts of the North Sea extend, at most, to the 1960s (Wadey *et al.* 2015), with the longest of those being Moray Firth, over 635 km away from the study region. This places five of these reconstructed events outside of the range of instrumental datasets (three late 19th century, one in the early 20th century, and one in the 1930s). This highlights the large potential for this technique for tackling the challenge of short-term instrumental records.

As the findings of Cunningham *et al*. (2011) of a distinct shell layer in dunes have yet to be replicated elsewhere, this study sought to attempt to apply the methods in Chapter 3 to another region to verify its wider applicability. This was achieved in Chapter 5 in the examination of North Wales dunes where further storms were successfully reconstructed from a coastline of different orientation and ocean basin. Successful application in multiple locations suggest this method may be confidently added to the suite of already more widely applied techniques for the reconstruction of coastal storms using sedimentary archives (2.2) and that this work should be further explored in coastal dune systems worldwide.

Aside from the more readily apparent advantage of being applicable to an additional coastal morphology (and thereby increasing the range of coastlines to which storm reconstructions may be applied) this new approach offers some key advantages over many of the previous methods for storm reconstruction discussed in 2.2, particularly over the barrier-based methods discussed in 2.2.3. Studies that have utilised coastal barriers typically examine storms that occur over multiple centuries and, in some cases, thousands of years (Hayne and Chappell, 2001, Nott *et al*. 2009). However, the time between events recorded in such

datasets is usually hundreds of years. Barrier derived archives typically only record exceptionally extreme events that operate on timescales of multiple centuries. This is both a boon and hindrance with regard to understanding coastal storm recurrence. Whilst these extreme events are worthy of note due to their large-scale impacts, they are often reconstructed for events many centuries or thousands of years in the past. As a result, they can potentially be too far removed from contemporary climatic or sea level conditions to be relevant to a modern understanding of storm recurrence. Further, the large time between individual storms in these records means they are of little practical use from a risk perspective due to the lack of context from more modest events that occur in the same period. The dune archive presented in Chapter 3 was able to identify seven events in a 140-year timeframe, a temporal resolution superior to any of the barrier-based reconstructions reviewed in 2.2.2 or washover based reconstruction in 2.2.1. Whilst the dune archives have yet to be shown (in Chapter 3 or subsequently in Chapter 5) to reach the same temporal range as reconstructions from barriers; there remains potential that in progradational coastal dune systems relict foredune ridges may allow for expansion of these comparatively higher resolution dune archives further into the past (3.4).

Due to the novel nature of this method, it was considered appropriate to ensure these reconstructed storms could be verified in other ways. In Chapter 3 and 5 this was achieved by combining the dune storm record with historical accounts of storms and their impacts in the same region. Previously such records have seen limited application to coastal storm studies, except for Lamb (1977), Zong and Tooley (2003) and Brooks *et al*. (2016), and even more rarely in combination with luminescence dating in any morphological setting (Benito *et al*. 2011). This allowed for all dune reconstructed storms to be related to an event within historic records, lending credence to these reconstructions. A limitation of the historic archives used in both Chapters 3 and 5 is an over-reliance of the works of a few academics (e.g., Lamb 1977). Whilst other sources are utilised (newspaper archives from the Irish coast for example) this represents only a minor contribution to the historic datasets in Chapters 3

and 5. Future work should attempt to explore further municipal, state, port, and newspaper archives to further enhance regional storm records from documentary datasets (Garnier *et al*. 2018). In Chapter 3, records of past storms from so-called flood stones are also noted as a future venture quantifying the impacts of these historic storm events. This may be effectively implemented through citizen science approaches such as SurgeWatch (Haigh *et al*. 2015)

It is worth noting that the dune archives presented in Chapter 3, despite their relatively high-resolution view of the regional storm record, did not record all events that manifested in regional flooding in documentary datasets. The same finding was seen in the reconstructions in Chapter 5. There are two plausible explanations for this; these events did not reach a sufficient threshold to result to result in dune impacts, or past storm impacts are at are erased by later events. This is also a challenge for barrier-based reconstructions and is likely a large factor in the low temporal resolution of such records (Buynevich *et al*. 2006, Scheffers *et al*. 2011, Tamura, 2012). This remains an outstanding challenge for this methodology.

Some methodological refinements could be explored in future iterations of this POSL based approach. The approach presented here largely relies on grain size and sorting as metrics to identify a storm deposit. Further exploring other metrics such a D-50, skewness and kurtosis may reveal anomalous deposits where an age jump does not have a corresponding grain size change. In particular, further interrogation of subpopulations within grain size distributions may reveal clusters that are unique to storm deposits. Such approaches, relying on statistical techniques including parametric curve-fitting, end-member modelling and hierarchical cluster analysis, have been shown to useful in identifying seasonal variations in loess (Schulte and Lehmkuhl 2018, Varga *et al.* 2019) and may be transferrable to identifying more subtle sedimentary features within dune samples. Chapter 3 noted that application of GPR may be a worthwhile addition to this approach as a means to reveal erosive effects of multiple large storms. This was one of the motivating factors for its addition

in Chapter 5, though this challenge has yet to be fully resolved. Future work may better tackle this limitation through higher vertical spatial resolution in POSL sampling. As storm impacts can be spatially variable based on either coincidence with tidal levels or with varying wave direction, it may also be tackled by the expanding dune-based reconstructions to multiple dune systems in the same region, for example the work of Bullard *et al.* 2019 which examined the storm response and recovery of the east-facing dunes of the Lincolnshire coast. In Norfolk application of these methods to other dune systems to the east and west of the Chapter 3 study site at Holkham may allow for other events to be reconstructed that were erased at Holkham, but not erased in other regional dune sites. In North Wales this may be achieved by exploration of dune systems in Aberffraw and Caernarfon. This may build on from the work of Bailey *et al* (2001) and Bailey and Bristow (2004) which quantified rates of sand deposition and movement in the last millennium at Aberffraw and showed them to be of appropriate age.

The addition of GPR to this dune-based method in Chapter 5 did show a means by which some of its core limitations may be overcome. One challenge of potentially applying this dune reconstruction method to other regions is knowing where to sample. Not every dune will necessarily have been impacted by the same storm within a single ridge (shown in both Chapters 3 and 5). These are not challenges exclusive to studies of coastal dunes but also in desert dunes, Leighton *et al* (2013) found that visible stratigraphy is not sufficient for targeting of OSL samples, particularly in young dunes where hiatuses in dune development may be more subtle than can be determined visually. In the application of GPR to dunes at Traeth Penhros, it was possible to first identify possible erosional facies within the radargram and then target sampling based on this. In doing so, this also overcame one of the main limitations highlighted in Chapter 3; that initially there was no means by which dune reconstructions could be verified by tying them into internal morphology.

Application of GPR alongside OSL in this manner is not entirely novel (Clemenssen *et al*. 2007), though the combination with portable techniques in the study of storms here is.

Progress on this is still incomplete however, in Chapter 5 only one of the storms could be tied directly into an erosional feature in the radargram. The other, speculated to be more minor storms, could not be seen in GPR data. This may in future work be overcome by utilising multiple GPR antenna, with higher frequency antennae used to target more subtle reflections (Rees-Hughes *et al.* 2021, Robin, *et al*. 2021. Rodriguez-Santalla *et al.* 2021). This may fit well with growing applications of such antennae to coastal dunes now being applied in these other studies.

The most significant limitation of this dune-based approach is the lack of means by which storm magnitude (maximum ESL elevations and wave heights) can be determined. In the works presented in this thesis this is only determined by means of comparison with historic data, and even in these instances is not quantitative, but qualitative based on storm impacts. Future work could explore how storm magnitudes may be quantitively derived from such datasets. This may potentially be achieved by better constraining instantaneous dune response to events of known magnitude from coastal monitoring and using such knowledge to model storm characteristics based on the nature of preserved erosional dune facies detected by GPR (Dissanayake, *et al*. 2021, Santos, *et al.* 2019. Splinter *et al*. 2018).

This study has produced a powerful novel methodology for enhancing the record of coastal storms and their impacts utilising coastal dunes. By combination historic archives the storm chronologies of two storm prone regions have been extended by up to 140 years beyond instrumental datasets. Future work should explore how these methods of reconstruction can be further refined and its application and use should be extended in regions beyond the UK (as in work such as Clemmenssen *et al*. 2007) particularly to regions lacking such a strong history of instrumental measurements of storms.

6.2. Resolving challenges in RMSL

The second challenge this thesis sought to explore was to resolve outstanding questions in UK RMSL and identify the suitability of North Wales for storm reconstructions. This was

explored in Chapter 4 which attempted to resolve a long-standing question over the existence of a mid-Holocene highstand in the region. This was successfully achieved by developing a new foraminifera-based transfer function alongside a study of preserved foraminifera in a 3000-year-old salt-marsh in the Malltraeth estuary. RMSL reconstructions using salt-marshes is a long-standing methodology that has successfully applied in many regions (Barlow *et al*. 2013), however, records from salt-marshes of such length are rare. Some salt-marshes have been used to reconstruct relative sea-level change over such a timescale (Barlow *et al.* 2014, Gehrels, *et al.* 2006, Shaw *et al*. 2018), for instance Barnett *et al*. (2015) were able to reconstruct 3300 years of sea level from such a record in Norway using testate amoebae and foraminifera, none have done so such at such resolution as in this study. This was enabled in the region by a very slow rate of RMSL rise in late-Holocene, a rare phenomenon as it requires a sustained close match between rates of barystatic rise and isostatic fall. Basal SLIPs derived from a regional freshwater marsh by Richards (2019) lended credence to this record and ultimately left no room for a mid-Holocene highstand in North Wales.

Comparison with GIA modelled showed that there is poor agreement between GIA models and the now more complete sea-level record for North Wales (4.5). Richards (2019) explored this further by comparison of the record with a greater range of models with varying earth viscosities; they concluded that there is still no single model that can produce a good fit for Holocene empirical data even if different Earth viscosities are assumed. Further work requires experimentation with Earth parameters and regional GIA model assumptions to resolve these mismatches. This problem extends beyond North Wales, but also into South Wales. This is particularly true in Pembrokeshire where, after expanding the empirical RMSL with six SLIPs, Richards (2019) also found extremely poor agreement between various GIA approaches and empirical data with GIA models over predicting rates of Holocene sea-level rise. As in North Wales, the late-Holocene portion of the record for Pembrokeshire remains poorly constrained. As a result, it is recommended further work includes resolving the poor fit

for GIA models in south Wales through further improvements of the regional record of Pembrokeshire, including the late-Holocene.

In addition to resolving the existence of a highstand in North Wales the results of Chapter 4 also demonstrate the suitability of North Wales for studies of changing North Atlantic storminess. As discussed in 2.1, one of the primary difficulties in studying changing storminess is unpicking the relative role of RMSL from changing storm parameters driven by climate. Given the relatively minor rate of late-Holocene relative sea-level rise in North Wales, it is recommended that more work be undertaken to improve and expand the North Wales storm chronology explored in Chapter 5 in order to explore the role of changing North Atlantic storminess.

6.3. Decadal to centennial coastal change

The final challenge this work sought to explore was the poor understanding of decadal scale to centennial evolution of coastal systems in response to hydrodynamic forcing. 2.4 highlights that this challenge largely arises from a data availability problem, with understanding change on such timescales being contingent upon a large amount of morphological data. Few beaches globally possess such longitudinal data from monitoring (Brooks *et al*. 2016) and obtaining such data requires an abundance of both time and money to find frequent surveys. Chapter 5 explored a means by which this challenge might be overcome by a unique combination of historic maps, satellite derived shorelines, GPR and dune reconstructions against regional storm data derived from tide gauges.

On the centennial scale Chapter 5 successfully reconstructs 500 years of coastal evolution utilising historic maps in combination with OSL data and GPR of coastal dunes. This revealed substantial evolution of the beach-dune system at Traeth Penhros that, when compared against the storm chronology from documentary datasets, had been punctuated by large storms in the late 19th and early 20th centuries. Particularly noteworthy was the potential impacts of the 1938 storm (referred to in regional historic memory as “the great

storm of Aberystwyth"), which may have resulted in the near annihilation of the primary foredunes at Traeth Penhros. Forestry documentation during the early planting of Newborough forest records indicate that there was "no substantial littoral ridge" present to protect the new forest plantations (Holmes 1957). To remedy these sand fences were installed to encourage dune growth and the formation of a full ridge. An interesting implication of this is that these fences implemented in the late 1940s may have effectively inadvertently acted as a storm recovery scheme for the dunes at Traeth Penhros.

This work is unique in its combination of these tools to reconstructing the influence of changing drivers of change in coastal systems on such scale. A shortcoming of this analysis has been difficulty in expressing margins of error in reconstructed shoreline and dune positions, particularly regarding the planimetric accuracy of historic maps (Jongepier *et al.* 2014). Further work is needed to see how the mean positional error approaches proposed by Jongepier *et al*. (2014) may be used to provide error margins in this data. Given the scale of interpretations historic maps are used for in Chapter 5 (kilometres of change), it is unlikely that errors from the maps (typically, 25-100m for maps that predating the introduction of standardised cartographic techniques in the 19th century) would change these interpretations (Jongepier *et al.* 2014)

On decadal timescales temporal resolution of shoreline change was determined using satellite derived data. This was then combined with this work demonstrated statistically significant correlations between annual and 5-year averages shoreline positions with the largest tidal levels to occur in those years. These satellite derived shoreline datasets have seen increasing application in recent years (Adebisi *et al*. 2021, Cuttler, *et al* 2020, Splinter and Coco, 2021, Taveneau *et al*. 2021, Vos *et al.* 2019a, b, 2020) however this is the first to attempt to elucidate quantitative relationships with hydrodynamic drivers. Such approaches have been tried before with monitoring data (Pye and Blott 2008) but this is the first with satellite datasets. Whilst significant, none of the correlations shown in Chapter 5 are particularly strong (usually modest negative correlations). This is likely a result of

complexities that arise from the overlapping influence of multiple drivers including wave conditions across the year, and wave-tide-surge interactions (Hsiao *et al*. 2019, Kang and Kim 2015, Marsooli and Lin 2018, Poulose *et al.* 2018, Song *et al*. 2020). Further exploration of this should be a priority for future work. At Traeth Penrhos in particular, local bathymetric data in concert with hindcasted wave data, would greatly enhance both morphological and hydrodynamic context for this site. Utilising recent approaches for high-resolution storm surge hindcasting may also aid in isolating specific events as drivers of change (Fernández-Montblanc *et al.* 2020).

Whilst the existence of statistically significant correlations in these data is promising, it is far from conclusive in elucidating the role of storms in governing shoreline change. Further limiting is the distance between the reconstructed shorelines and the hydrodynamic datasets themselves (average of 44 km for the combined Barmouth-Holyhead dataset). Future work should further explore how satellite derived shorelines can be combined with hydrodynamic data on beaches of differing morphological types, orientations, and hydrodynamic settings. Ideally, such work should first be applied on beaches with a relative abundance of monitoring and hydrodynamic data to truth findings against on the ground observations.

Combined these works have presented techniques for the reconstruction of both storms and coastal morphological change. This was achieved by an interdisciplinary combination of techniques that have until now, largely remained isolated in application. These approaches offer fruitful avenues by which regional understanding of both coastal storms and morphological change in response to hydrodynamic drivers may be better understood in the future.

Chapter 7.

Conclusions

This work has developed and presented a novel methodology for enhancing the record of coastal storms and their impacts utilising coastal dunes. This was achieved through the first ever applications of a technique combining portable OSL with full OSL ages and particle size analysis (Chapter 3 and Chapter 5).

Combining the dune records with historic archives of storms illustrated the potential of utilising palaeo-environmental datasets with such archives to produce robust storm chronologies. From these datasets 200-year storm chronologies were produced for both the Norfolk coast and North Welsh coasts. The occurrence 10 coastal storms were reconstructed from dunes based on the co-occurrence of hiatuses in dune building concurrent with particle size and sorting variations. Seven were reconstructed on the coast of North Norfolk (Chapter 3, ranging from 1874 CE ± 20 years to 1995 CE ± 30) and three in North Wales (Chapter 5, 1850s-60s, the 1880s-90s and the late 1930s to early 1940s). Of these ten, eight were outside the range of regional instrumental datasets; effectively extending the record of large storms in these storm prone regions by 50-60 years. At both sites, dunes seem to be only recording the highest storm levels that were associated with significant flooding (based on comparison with historic records) or large-scale coastal change (based on maps or satellite data). As such, the approach seems to hold promise to obtain a better understanding of the frequency of large storms by extending the dune archive records further back to times when documentation of storm surges was sparse. Further work is needed to explore how these methods may be enhanced through use of more detailed sediment characterisation.

Through the development of a new foraminifera-based transfer function alongside a study of preserved foraminifera in a unique 3000-year-old salt-marsh this work was able to produce

one of the world's longest continuous sea-level records from a salt-marsh (Chapter 4). Using this record, in tandem with basal SLIPs derived from a regional freshwater marsh and 22 other SLIPs from literature we present a more complete view of North Welsh Holocene relative sea level than in any prior study. This record shows that RSL rose ~0.65 m in the last 3300 years and has now reached its highest level in the Holocene. Post-industrial acceleration of sea-level rise is evident in the Malltraeth data (Figure 4.8a) and begins in the early- to mid-20th century. The salt-marsh reconstruction matches with the lower limit of the tide-gauge data. Sea-level rise was linear between 12 and 7 ka BP at a rate of ~5.3 m ka−1. There is nothing in the data to suggest that sea level was at any point >0 m after 7 ka BP. Although there is some suggestion for RSL stability between 6 and 4 ka BP, or even potentially a small sea-level fall, the vertical uncertainty of the individual SLIPs prevents attaching any great significance to this. The new relative sea-level record presented here shows that at no point >7ka BP was sea level above 0m, rejecting the notion of a mid-Holocene highstand. Using this record, in tandem with basal SLIPs derived from a regional freshwater marsh, a long-standing question over the existence of a mid-Holocene sea level highstand in North Welsh was finally resolved. These findings have implications for approaches to GIA modelling in the UK and beyond. Further they demonstrate that storm chronologies for North Wales are highly suited to examining the role of changing storminess due to the relatively minor sea level signal in the late-Holocene.

By combining the techniques used throughout this study (dune reconstructions, historic maps, historic storm archives) with shoreline positions derived from satellite data it was possible to reconstruct the evolution of a North Wales beach dune system over 500 years at varying different resolutions. Reconstructed shorelines show that the system, has expanded ~650 m northwest in the last 500 years. This is hypothesised to have been accelerated associated with construction of a sea wall in the adjacent estuary in the 1890s. Sedimentological data from coastal dunes shows dune expansion was punctuated by storm erosion associated with storms in the 1850s-60s, the 1880s-90s and particularly 1938.

By comparing these reconstructed shorelines with the tidal characteristics of storms available from instrumental data it was possible to demonstrate a statistically significant correlations between local scale shoreline change with the very largest storm events to occur each year. Statistical analysis of annual average shoreline position against thresholds in tide gauge data showed that only the largest storm events (sea level > 3.00 m OD) exhibited a significant control on shoreline position across multiple years

The successful application to dunes in different regions suggests these techniques may be applicable to not only other coastal dunes in the UK but also globally. This approach is therefore a powerful addition to the suite of palaeo-environmental approaches to storm reconstruction alongside washover and barrier-based reconstructions. Further work is required to determine how such records may be used to quantitatively infer storm magnitudes.

In summary, the works presented in this thesis illustrate the potential of combining data from instrumental sources, historic sources, palaeo-environmental reconstructions, and remote sensing in the study of both coastal storms and their influence in coastal change on decadal and longer timescale.

Bibliography

Adebisi, N., Balogun, AL., Mahdianpar, M., Min, TH. Assessing the Impacts of Rising Sea Level on Coastal Morpho-Dynamics with Automated High-Frequency Shoreline Mapping Using Multi-Sensor Optical Satellites. *Remote Sensing*, 13(18)

Aigner, TA. 1985. Storm depositional systems: Dynamic stratigraphy in modern and ancient shallow-marine sequences: Berlin, Springer-Ver-lag.

Aitken, M. 1998. An Introduction to Optical Dating: The Dating of Quaternary Sediments by the use of Photon-stimulated Luminescence. Oxford: Oxford University Press.

Allenbach, K., Garonna, I., Herold, C., Monioudi, I., Giuliani, G., Lehmann, A., Velegrakis, AF. 2015. Black Sea beaches vulnerability to sea level rise. *Environmental Science and Policy*. 46, 95-109.

Andrews JE., Boomer I., Bailiff I., Balson P., Bristow C., Chroston PN., Funnell BM., Harwood GM., Jones R., Maher BA., Shimmield GB. 2000. Sedimentary evolution of the north Norfolk Barrier coastline in the context of Holocene sea level change. In *Holocene Land-Ocean Interaction and Environmental Change around the North Sea*, I Shennan, J Andrews (eds), Vol. 166. Geological Society, London, Special Publications: London; 219– 251.

Angnuureng, D.B., Almar, R., Senechal, N., Castelle, B., Addo, K.A., Marieu, V., Ranasinghe, R., 2017. Shoreline resilience to individual storms and storm clusters on a meso-macrotidal barred beach. *Geomorphology* 290, 265–276.

Appleby PG. 2001. Chronostratigraphic Techniques in Recent Sediments. In: Last WM and Smol JP (eds) Tracking environmental change using lake sediments. 2. Physical and geochemical methods. 171-203.

Argus, DF., Peltier, WR., Drummond, R., Moore, AW. 2014. The Antarctica component of postglacial rebound model ICE-6G_C (VM5a) based on GPS positioning, exposure age dating of ice thicknesses, and relative sea level histories. Geophysical Journal International. 198: 537-563

Bailey, SD., Bristow, CS. 2004. Migration of parabolic dunes at Aberffraw, Anglesey, north Wales. *Geomorphology*, 59(1-4).

Bailey, SD., Wintle, AG., Duller, GAT., Bristow, CS. 2001. Sand deposition during the last millennium at Aberffraw, Anglesey, North Wales as determined by OSL dating of quartz. Quaternary Science Reviews, 20, 701-704.

Bales, JD., Oblinger, CJ., Sallenger, AH. 2000. Two months of flooding in eastern North Carolina, September-October 1999; hydrologic water quality, and geological effects of hurricanes Dennis, Floyd, and Irene, IS Geological Survey Report WR1 00-4093.

Balk, D., Montgomery, MR., McGranahan G., Kim, D., Mara, V., Todd, M., Buttener, T., Dorelien, A. 2009. Mapping urban settlements and the risks of climate change in Africa, Asia and South America. In: Guzmán JM., Martine, G., McGranahan, G., Schensul D., Tacoli, C, editors. *Population Dynamics and Climate Change.* New York, London: United

Nations Population Fund (UNFPA), International Institute for Environment and Development (IIED); 2009. Pp. 80-103.

Ballarini, M., Wallinga, J., Murray, AS., van Heteren, S., Oost, AP., Bos, AJJ., van Eijk, CWE. 2003. Optical dating of young coastal dunes on a decadal time scale. *Quaternary Science Reviews*, 22, 1011-1017.

Banno, M., Kuriyama, Y. 2020. Supermoon Drive Beach Morphological Changes in the Swash Zone. *Geophysical Research Letters*. 47(22).

Baptista, P., Coelho, C., Pereira, C., Bernardes, C., Veloso-Gomes, F. 2014. Beach morphology and shoreline evolution: Monitoring and modelling medium-term responses (Portuguese NW coastal study site). *Coastal Engineering*, 84, 23-37.

Barlow NL., Long AJ., Saher MH., Gehrels WR., Garnett MH., Scaife RG. 2014. Salt-marsh reconstructions of relative sea-level change in the North Atlantic during the last 2000 years. Quaternary Science Reviews 99: 1-16.

Barlow NL., Shennan I., Long AJ., Gehrels WR., Saher MH., Woodroffe SA., Hillier C. 2013. Salt marshes as late Holocene tide gauges. *Global and Planetary Change* 106: 90-110.

Barlow, NLM., Long, AJ., Saher, MH., Gehrels, WR., Garnett, MH., Scaife, RG. 2014. Salt-marsh reconstructions of relative sea-level change in the North Atlantic during the last 2000 years. *Quaternary Science Reviews*, 99, 1-16.

Barnett, RL., Gehrels, WR., Charman, DJ., Saher, MH., Marshall, WA. 2015. Late Holocene sea-level change in Arctic Norway. *Quaternary Science Reviews*, 107, 214-230.

Best, SN., Van der Wegen, M., Dijkstra, J., Willemsen, PWJM., Borsje, BW., Roelvink, DJA. 2018. Do salt marshes survive sea level rise? Modelling wave action, morphodynamics and vegetation dynamics. *Environmental Modelling Software*, 109, 152-166.

Bateman MD., Catt JA. 1996. An absolute chronology for the raised beach and associated deposits at Sewerby, East Yorkshire, England. *Journal of Quaternary Science* 11: 389– 395.

Bateman MD., Stein S., Ashurst RA., Selby K. 2015. Instant luminescence chronologies? High resolution luminescence profiles using a portable luminescence reader. *Quaternary Geochronology* 30: 141– 146.

Bateman, MD. 2015. The application of luminescence dating in sea-level studies. In Handbook of Sea-Level Research, eds. I. Shennan, A. J. Long & B. P. Horton. London: John Wiley & Sons.

Bateman, MD., Boulter, CH., Carr, AS., Frederick, CD., Peter, D. Wilder, M. 2007. Detecting post-depositional sediment disturbance in sandy deposits using optical luminescence. *Quaternary Geochronology*, 2, 57-64.

Bateman, MD., Carr, AS., Murray-Wallace, CV., Roberts, DL., Holmes, PL. 2008. A dating intercomparison study on Late Stone Age coastal midden deposits, *South Africa. Geoarchaeology*, 23, 715-741.

Bateman, MD., Frederick, CD., Jaiswal, MK., Singhvi, AK. 2003. Investigations into the potential effects of pedoturbation on luminescence dating. *Quaternary Science Reviews*, 22, 1169-1176.

Bateman, MD., McHale, K., Bayntun, HJ., Williams N. 2020. Understanding Historical Coastal Spit Evolution: a Case Study from Spurn, East Yorkshire, UK. *Earth Surface Processes and Landforms*. 45, 3670-3686.

Bateman, MD., Rushby, G., Stein, S., Ashurst, RA., Stevenson, D., Jones, JM., Gehrels, WR. 2018. Can sand dunes be used to study historic storm events? *Earth Surface Processes and Landforms*. 43(4), 779-790.

Bateman, MD., Stein, S., Ashurst RA., Selby, K. 2015. Instant Luminescence Chronologies? High resolution luminescence profiles using a portable luminescence reader. *Quaternary Geochronology* 30, 141-146

Batstone, C., Lawless, M., Tawn, J., Horsburgh, K., Blackman, D., McMillan, A., Worth, D., Laeger, S., Hunt, T. 2013. A UK best-practice approach for extreme sea-level analysis along complex topographic coastlines. *Ocean Engineering*, 71, 28-39.

Baxter, PJ. 2005. The east coast Big Flood, 31 January–1 February 1953: a summary of the human disaster. *Philosophical Transactions of the Royal Society A - Mathematical, Physical and Engineering Sciences*, 363, 1293-1312.

BBC. 2009. Aberystwyth's great storm of 1938. BBC News. Available at: http://news.bbc.co.uk/local/midwales/hi/people_and_places/history/newsid_8305000/8305530.stm.

BBC. 2010. 'Looking back at the Towyn floods of February 1990'. BBC Northwest Wales. Available at: http://news.bbc.co.uk/local/northwestwales/hi/people_and_places/history/newsid_8516000/8516287.stm (Accessed: 11 May 2020)

BBC. 2014. '250 evacuated over Aberystwyth flood fear'. BBC News. Available at: http://www.bbc.co.uk/news/uk-wales-25626256 (Accessed: 11 May 2020)

Beck, J., 1953. The Church Brief for the Inundation of the Lancashire Coast in 1720. Available at: https://www.hslc.org.uk/wp-content/uploads/2017/06/105-6-Beck.pdf (Accessed: 11 May 2020).

Bedlington, D. 1994. *Holocene sea-level changes and crustal movement in North Wales and Wirral*, PhD thesis, University of Durham, Durham.

Benito G., Thorndycraft VR., Rico MT., Sánchez-Moya Y., Sopeña A., Botero BA., Machado MJ., Davis M., Pérez-González A. 2011. Hydrological response of a dryland ephemeral river to southern African climatic variability during the last millennium. *Quaternary Research* 75: 471– 482.

Beniston, M., Stephenson, DB., Christensen OB., Ferro, CAT., Frei, C., Goyette, S., Halsnaes, K., Holt, T., Jylha, K., Koffi, B., Palutikof, J., Scholl, R., Semmler, T., Woth, K. 2007. Future extreme events in European climate: an exploration of regional climate model projections. *Climatic Change*, 71, 71-95.

Bennett, O., Hartwell-Naguib, S. 2014. Flood defence spending in England. ed. H. o. C. Library. London: House of Commons Library.

Bennett, WG., Karunarathna, H., Reeve, DE., Mori, N. 2019. Computational modelling of morphodynamic response of a macro-tidal beach to future climate variabilities. *Marine Geology*, 415.

Blaauw, M. 2010. Methods and code for “classical” age-modelling of radiocarbon sequences. *Quaternary Geochronology*, 5, 512-518.

Blaauw M and Christen JA. 2011. Flexible paleoclimate age-depth models using an autoregressive gamma process. *Bayesian Analysis* 6: 4 57-474.

Bochev-van der Burgh, LM., Wijnbergm, KM., Hulscher, SJMH. 2011. Decadal-scale morphologic variability of managed coastal dunes. *Coastal Engineering* 58, 927-936.

BODC. 2021. UK Tide Gauge Network. Available at: https://www.bodc.ac.uk/data/hosted_data_systems/sea_level/uk_tide_gauge_network/ (Accessed 01/03/2019)

Boldt, KV., Lane, P., Woodruff, JD., Donnelly, JP. 2010 Calibrating a sedimentary record of overwash from southeastern New England using modelled historic hurricane surges. Marine *Geology*, 275, 127-139.

Bradley SL., Milne GA., Shennan I., Edwards R. 2011. An improved glacial isostatic adjustment model for the British Isles. *Journal of Quaternary Science* 26: 541-552.

Bradley SL., Milne GA., Teferle FN., Bingley RM., Orliac EJ. 2009. Glacial isostatic adjustment of the British Isles: new constraints from GPS measurements of crustal motion. *Geophysical Journal International* 178: 14–22.

Bradley., SL., Milne, GA., Horton, BP., Zong, Y. 2016. Modelling sea level data from China and Malay-Thailand to estimate Holocene ice-volume equivalent sea level change. *Quaternary Science Reviews*. 137: 54-68

Bradshaw, E., Woodworth, PL., Hibbert, A., Bradley, LJ. 2015. A Century of Sea Level Measurements at Newlyn, Southwest England. *Marine Geodesy*, 39(2), 1-26.

Brain MJ., Long AJ., Woodroffe SA., Petley DN. Milledge DG., Parnell AC. 2012. Modelling the effects of sediment compaction on salt marsh reconstructions of recent sea-level rise. *Earth and Planetary Science Letters.* 345-348: 180-193.

Bravo, J., Donnelly, JP., Downling, J., Webb, T. 1997. Lithologic and biostratigraphic evidence of the 1938 Hurricane even in New England. Journal of American Meteorological Society, 22nd Conference on Hurricanes and Tropical Meteorology Supplement, P, 395-396.

Bregy, JC., Wallace, DJ., Minzoni, RT., Cruz, VJ. 2018. 2500-year paleotempestological record of intense storms for the north Gulf of Mexico, United States. Marine Geology. 396, 26-42

Bristow, CS. 2003. The Impact of Forestry on Coastal Geomorphology at Newborough Warren/Ynys Llanddwyn NNR, SSSI, pSAC. CCW Contract Number FC 73-05-18.

Bristow CS., Chroston NP., Bailey SD. 2000. The structure and development of foredunes on a locally prograding coast: insights from ground-penetrating radar surveys, Norfolk, UK. *Sedimentology* 47: 923– 944.

Bristow, CD., Pucillo, K. 2006. Quantifying rates of coastal progradation from sediment volume using GPR and OSL: the Holocene fill of Guichen Bay, south-east South Australia. *Sedimentology*, 53(4), 769-788.

Bristow, CS., Chroston, PN., Bailey SD. 2001. The structure and development of foredunes on a locally prograding coast: insights from ground-penetrating radar surveys, Norfolk, UK. *Sedimentology*. 47(5), 923-944.

Bristow, CS., Duller G., Lancaster N. 2007. Age and dynamics of linear dunes in the Namib desert. *Geology*. 35, 555-558.

Britton, CE., 1937. 'A Meteorological Chronology To A.D. 1450'. Geophysical Memoirs, 70. London: H. M. Stationary Office. 177

Bromirski, PD., Flick, RE., Cayan, DR. 2003. Storminess Variability along the California Coast: 1858 – 2000. *Journal of Climate*, 16(6), 982 – 993.

Brooks AJ., Bradley SL., Edwards RJ., Milne GA., Horton B., Shennan I. 2008. Postglacial relative sea-level observations from Ireland and their role in glacial rebound modelling. *Journal of Quaternary Science* 23: 175-192.

Brooks SM., Spencer T., McIvor A., Möller I. 2016. Reconstructing and understanding the impacts of storms and surges, southern North Sea. *Earth Surface Processes and Landforms* 41: 855– 864.

Brooks, S. 2017. Coastal resilience and vulnerability: storm impacts, extreme weather and regional variability in the UK, winter 2013-14. *Geography*. 102, 60-70.

Brooks, SM., Spencer, T., McIvor, A., Möller, I. 2016. Reconstructing and understanding the impacts of storms and surges, southern North Sea. *Earth Surface Processes and Landforms* 41(6), 855-864.

Brown, CW. 1939. Hurricanes and shoreline changes in Rhode Island. *Geographic Review*, 29, 416-430.

Brown, JM., Souza, AJ., Wolf, J. 2010. Surge modelling in the eastern Irish Sea: present and future storm impact. *Ocean Dynamics*, 60(2), 227-236

Bruun P. 1962. Sea-level rise as a cause of shore erosion. *Journal of the Waterways and Harbors Division* 88: 117-132.

Bullard, JE., Ackerley, D., Millett, J., Chandler, JH., Montreuil, AL. 2019. Post-storm geomorphic recover and resilience of a prograding coastal dune system. *Environmental Research Communications*, 1(1), 011004.

Burvingt, O. 2018. *Storm Impact and Recovery Along the South West Coast of England*. University of Plymouth, School of Biological and Marine Sciences. PhD Thesis.

Burvingt, O., Masselink G., Russell, P., Scott, T. 2016. Classification of beach response to extreme storms. *Geomorphology* 295, 722-737.

Burvingt, O., Masselink, G., Russell, P., Scott, T. 2016. Beach response to consecutive extreme storms using LiDAR along the SW coast of England. *Journal of Coastal Research*, 1(75), 1052-1056.

Buyevnich, IV., Donnelly, JP. 2006. Geological signatures of barrier breaching and overwash, southern Massachusetts. *Journal of Coastal Research*, 112-116, 112-116.

Buynevich, IV., Fitzgerald, DM., Van Heteren, S. 2004. Sedimentary records of intense storms in Holocene barrier sequences, Maine, USA. *Marine Geology*, 210, 135-148.

Carruthers, EA., Lane, DP., Evans, RL., Donnelly, JP., Ashton, AD. 2013. Quantifying overwash flux in barrier systems: An example from Martha's Vineyard, Massachusetts, USA. *Marine Geology*, 343, 15-28.

Castelle, B., Bujan, S., Ferreira, S., Dodet, G. 2017. Foredune morphological changes and beach recovery from the extreme 2013/2014 winter at a high-energy sandy coast. *Marine Geology*, 385, 41-55.

Castelle, B., Marieu, V., Bujan, S., Splinter, KD., Robinet, A., Senechal, N., Ferreira, S. 2015. Impact of the winter 2013-2014 series of sever Western Europe storms on a double-barred sandy coast: Beach and dune erosion and megacusp embayments. *Geomorphology*, 238, 135-148.

Castelle, B., Masselink, G., Scott, T., Stokes, C., Konstantinou, A., Marieu, V., Bujan, S. 2021. Satellite-derive shoreline detection at a high-energy meso-macrotidal beach. *Geomorphology*, 383.

Choi, KH., Choi, JH., Kim, JW. 2014. Reconstruction of Holocene coastal progradation on the east coast of Korea based on OSL dating and GPR surveys of beach-foredune ridges. *The Holocene*, 24, 24-34.

Church JA., Clark PU., Cazenave A., Gregory JM., Jevrejeva S., Levermann A., Merrifield MA., Milne GA., Nerem RS., Nunn PD., Payne AJ., Pfeffer WT., Stammer D., Unnikrishnan AS. 2013. Sea level change. In *Climate Change 2013: The Physical Science Basis*, TF Stocker, D Qin., G-K Plattner., M Tignor., SK Allen, J Boschung., A Nauels., Y Xia., V Bex., PM Midgley (eds). The Fifth Assessment Report of the Intergovernmental Panel on Climate Change. Cambridge University Press: Cambridge, UK and New York, NY, USA.

Church, JA., Hunter, J., McLnnes, K., White NJ. 2004. Sea-level rise and the frequency of extreme events around Australia. Coast to Coast conference, Hobart, Australia. (http://www.cdesign.com.au/proceedings_c2c2004/pages/coastfinal00123.pdf)

Church, JA., White, NJ., Aarup, T., Wilson, WS., Woodworth, PL., Domingues, CM., Hunter, JR., Lambeck, K. 2008. Understanding global sea levels: past, present and future. *Sustainability Science*, 3, 9-22.

Chute, NE., 1946. Shoreline changes along the south shore of Cape Cod caused by the hurricane of September 1944, and the storms of November 30, 1944, and January 1, 1945. Massachusetts Department of Public Works Bulletin, 9.

Clark, CD. Ely, JC. Greenwood, SL. Hughes, ALC. Meehan, R. Barr LD., Bateman, MD. Bradwell, T. Doole, J. Evans, DJA. Jordan, CJ, Monteys, X. Pellicer, XM. Sheehy, M. 2018. BRITICE Glacial Map, version 2: a map and GIS database of glacial landforms of the last British–Irish Ice Sheet. Boreas. 47: 11-27

Clark, JA., Farrell, WE., Peltier, WR. 1978. Global Changes in postglacial sea level: A numerical calculations. *Quaternary Research*, 9, 265-287.

Clarke, DJ., Eliot, IG. 1988. Low-frequency changes of sediment volume on the beachface at Warilla Beach, New-South-Wales, 1975-1985. *Marine Geology*, 79 (3-4), 187-211.

Clemmensen LB, Murray A, Heinemeier J *et al*. 2009. The evolution of Holocene coastal dunefields, Jutland, Denmark: A record of climate change over the past 5000 years. *Geomorphology* 105: 303–313.

Clemmensen LB., Bjørnsen, M., Murray, A., Pedersen, K. 2007. Formation of aeolian dunes on Anholt, Denmark since AD 1560: A record of deforestation and increased storminess. *Sedimentary Geology*. 199, 171-187.

Clemmensen LB., Bendixen M., Hede MU., Kroon A., Nielsen L., Murray AS. 2014. Morphological records of storm floods exemplified by the impact of the 1872 Baltic storm on a sandy spit system in south-eastern Denmark. *Earth Surface Processes and Landforms* 39: 499– 508. https://doi.org/10.1002/esp.3466

Clout HD. 2007. Contemporary Rural Geographies: Land, Property, and Resources in Britain: Essays in Honour of Richard Munton. London: Routledge.

Collins A and Buchan C. 2004. Provenance and age constraints of the South Stack Group, Anglesey, UK: U–Pb SIMS detrital zircon data. *Journal of the Geological Society* 161: 743–746.

Cunningham AC., Bakker MAJ., van Heteren S., van der Valk B., van der Spek AJF., Schaart DR., Wallinga J. 2011. Extracting storm-surge data from coastal dunes for improved assessment of flood risk. *Geology* 39: 1063– 1066.

Cuttler, MVW., Vos, K., Branson, P., Hansen, JE., O'Leary, M., Browne, NK., Lowe, RJ. Interannual Response of Reef Islands to Climate-Driven Variations in Water Level and Wave Climate. *Remote Sensing*, 12(4089).

Davids, F., Duller, GAT., Roberts, HM. 2010. Testing the use of feldspars for optical dating of hurricane overwash deposits. *Quaternary Geochronology*, 5, 125-130.

Davis, RA., Andronaco, M., Gibeaut, JC. 1989. Formation and development of a tidal inlet from a washover fan west-central Florida coast, USA. *Sedimentary Geology*. 65(1-2), 87-94.

Dawson, RJ., Dickson, ME., Nicholls, RJ., Hall, JW., Walkden, MJA., Stansby, PK., Mokrech, M., Richards, J., Zhou, J., Milligan, J., Jordan, A., Pearson, S., Rees, J., Bates, PD., Koukoulas, S., Watkinson, AR. 2009. Integrated analysis of risks of coastal flooding and cliff erosion under scenarios of long term change. *Climatic Change*, 95(1-2), 249-288.

Dawson, RJ., Hall, JW., Bates, PD., Nicholls, RJ. 2005. Quantified Analysis of the Probability of Flooding in the Thames Estuary under Imaginable Worst-case Sea Level Rise Scenarios. *Water Resources Development*, 21, 577–591.

De Rijk S. 1995. Agglutinated Foraminifera as Indicators of Salt Marsh Development in Relation to Late Holocene Sea Level Rise (Great Marshes at Barnstable, Massachusetts), Utrecht: Febo.

Delgado-Fernández, I., Davidson-Arnott, RGD., Hesp, PA. 2019. Is “remobilization” nature restoration or nature destruction? A commentary. *Journal of Coastal Conservation* 23, 1093-1103.

Dezileau, L., Sabatier, P., Blanchemanche, P., Joly, B., Swingedouw, D., Cassou, C., Castaings, J., Martinez, P., Von Grafenstein, U. 2011. Intense storm activity during the Little Ice Age on the French Mediterranean coast.

Dissanayake, P., Brown, J. Sibbertsen, P., Winter, C. 2021. Using a two-step framework for the investigation of storm impacted beach/dune erosion. *Coastal Engineering*, 168.

Dissanayake, P., Brown, J., Karunarathna, H. 2015. Impact of storm chronology on the morphological changes of the Formby beach and dune system, UK. *Natural Hazards and Earth System Sciences* 15, 1533-1543.

Dodet, G., Castelle, B., Masselink, G., Scott, T., Davidson, M., Floc’h, F., Jackson, D., Suanez, S. 2019. Beach recovery from extreme storm activity during the 2013-14 winter along the Atlantic coast of Europe. *Earth Surface Processes and Landforms* 44, 393-401.

Donnelly, JP. 2005. Evidence of past intense tropical cyclones from back-barrier salt pond sediments: a case study from Isla de Culebrita, Puerto Rico, USA. *Journal of Coastal Research*. 201–210.

Donnelly, JP., Bryant, SS., Butler, J., Dowling, J., Fan, L., Hausmann, N., Newby, P., Shuman, B., Stern, J., Westover, K., Webb, T. 2001 700 yr sedimentary record of intense hurricane landfalls in southern New England. *Geological Society of America Bulletin*, 113, 714-727.

Donnelly, JP., Webb, T. 2004. Back-barrier sedimentary records of intense hurricane landfalls in the north-eastern United States. In: Liu, K. (Ed.), Murnane, R. Past, Present and Future, Columbia Press, New York, Hurricanes and Typhoons, pp. 58–96.

Dougherty, AJ. 2014. Extracting a record of Holocene storm erosion and deposition preserved in the morphostratigraphy of a prograded coastal barrier. *Continental Shelf Research*, 86, 116-131.

Dougherty, AJ., FitzGerald, DM., Buynevich, IV. 2004. Evidence for storm-dominated early progradation of Castle Neck Barrier, Massachusetts, USA. *Marine Geology*, 210, 123-134.

Duke, WL. 1985. Hummocky cross-stratification, tropical hurricanes, and intense winter storms: *Sedimentology*, 32, 167-194.

Duller, GAT. 2004. Luminescence dating of quaternary sediments: recent advances. *Journal of Quaternary Science*, 19, 183-192.

East Anglian Coastal Group. 2010. *North Norfolk Shoreline Management Plan Final Plan*. http://www.eacg.org.uk/docs/smp5/the%20smp%20main%20report.pdf. [last accessed 9/5/17]

Eden, P., 2008. Great British Weather Disasters. London: Continuum.

Edwards RJ. and Horton BP. 2000. Reconstructing relative sea-level change using UK salt-marsh foraminifera. *Marine Geology* 168.

Edwards RJ. Wright AJ, van de Plassche O. 2004. Surface distributions of salt-marsh foraminifera from Connecticut, USA: modern analogues for high-resolution sea level studies. *Marine Micropaleontology* 51: 1-21.

Emery, KO. 1961. A simple method of measuring beach profiles. *Limnology and Oceanography* 6, 90–93.

Emery, KO. 1969. A Coastal Pond Studied by Oceanographic Methods. American Elsevier Publication Company, New York.

Environment Agency. 2019. Coastal flood boundary conditions for the UK: update 2018. Technical summary report: SC060064/TR6. Available at: https://www.gov.uk/government/publications/coastal-flood-boundary-conditions-for-uk-mainland-and-islands-design-sea-levels [Accessed 05/08/2021]

Esteves, LS., Williams, JJ., Brown, JM. 2011. Looking for evidence of climate change impacts in the eastern Irish Sea. *Natural Hazards and Earth System Sciences* 11, 1641-1656.

Esteves, LS., Williams, JJ., Nock, A., Lymbery, G. 2008. Quantifying Shoreline Changes along the Sefton Coast (UK) and the Implications for Research-Informed Coastal Management. *Journal of Coastal Research*, 56.

Farrell, WE., Clark, JA. 1976. Postglacial sea-level. *Geophysical Journal of the Royal Astronomical Society*. 46, 647-667

Fernández-Montblanc, T., Vousdoukas, MI., Mentaschi, L., Ciavola, P. 2020. A Pan-European high resolution storm surge hindcast. *Environment International*, 135.

Feser, F., Barcikowaska, M., Krueger, O., Schenk, F., Weisse, R., Xia, L. 2015. Storminess over the North Atlantic and northwester Europe – A Review. *Quarterly Journal of the Royal Meteorological Society*. 141(697), 350-382.

Flor-Blanco, G., Carrió, JA, Jackson, DWT., Flor, G., Flores-Soriano, C. 2021 Coastal erosion in NW Spain: Recent patterns under extreme storm wave events. *Geomorphology*. 387, 107767

Forbes, DL., Parkes GS., Manson, GK., Ketch, LA. 2004. Storms and shoreline retreat in the southern Gulf of St. Lawrence. *Marine Geology* 210, 169-204.

Forsyth AJ., Nott J., Bateman MD. 2010. Beach ridge plain evidence of a variable late-Holocene tropical cyclone climate, North Queensland, Australia. *Palaeogeography, Palaeoclimatology, Palaeoecology* 297: 707– 716.

Foster I., Mighall T., Proffitt H., Walling DE., Owens, PN. 2006. Post-depositional 137Cs Mobility in the Sediments of Three Shallow Coastal Lagoons, SW England. Journal of *Paleolimnology* 35: 881-895.

Fortunato, AB., Meredith, EP., Rodrigues, M., Freire, P., Feldmann, H. 2019. Near-future changes in storm surges along the Atlantic Iberian coast. *Natural Hazards*, 98(3), 1003-1020.

Fox-Kemper, B., Hewitt, HT., Xiao, C., Aðalgeirsdóttir, G., Drijfhout, SS., Edwards. TL., Golledge, NR., Hemer, M., Kopp, RE., Krinner, G., Mix, A., Notz, D., Nowicki, S., Nurhati, IS., Ruiz, L., Sallée, JB., Slangen, ABA., Yu, Y. 2021. Ocean Cryosphere and Sea Level Change. In Masson-Delmotte, V., Zhai, P., Pirani, A., Connors, SL., Péan, C., Berger, S., Caud, N., Chen, T., Goldfarb, L., Gomis, MI., Huang, M., Leitzell, K., Lonnoy, E., Matthews, JBR., Maycock, TK., Waterfield, T., Yelekci, O., Yu, R., Zhou, B (eds). *Climate Change 2021: The Physical Science Basis. Contribution of Working Group I to the Sixth Assessment Report of the Intergovernmental Panel on Climate Change.* Cambridge University Press, Cambridge, United Kingdom and New York, NY, USA, pp. 1211-1362, doi:10.1017/9781009157896.011.

French, JR., Burningham, H. 2013. Coasts and climate: Insights from geomorphology. *Progress in Physical Geography*. 37(4), 550-561.

Galbraith, RF., Green, PF. 1990. Estimating the component ages in a finite mixture. *Nuclear Tracks and Radiation Measurements*. 17, 197–206.

Galbraith, RF., Laslett, GM. 1993. Statistical models for mixed fission track ages. *Nuclear Tracks and Radiation Measurements*. 21, 459-470.

Gale SJ and Hoare PG. 1991. *Chemical Composition and Analysis. Quaternary Sediments*. Chichester and New York: Wiley, 262-265.

Galloway JA. 2013. Coastal flooding and socioeconomic change in eastern England in the later Middle Ages. *Environment and History* 19: 173– 207.

Garnier, E., Ciavola, P., Spencer, T., Ferreira, O., Armaroli, C., McIvor, A. 2018. Historical analysis of storm events: case studies in France, England, Portugal and Italy. *Coastal Engineering*, 134.

Gaslikova, L., Grabemann, I., Groll, N. 2013. Changes in North Sea storm surge conditions for four transient future climate realizations. *Natural Hazards*, 66(3), 1501-1518.

Gehrels WR. 1994. Determining Relative Sea-Level Change from Salt-marsh Foraminifera and Plant Zones on the Coast of Maine, U.S.A. *Journal of Coastal Research* 10: 990-1009.

Gehrels WR. 2000. Using foraminiferal transfer functions to produce high-resolution sea-level records from salt-marsh deposits, Maine, USA. *The Holocene* 10: 367-376.

Gehrels WR. 2010. Late Holocene land- and sea-level changes in the British Isles: Implications for future sea-level predictions. *Quaternary Science Reviews,* 29(13): 1648-1660

Gehrels, WR. 2010. Sea-level changes since the Last Glacial Maximum: an appraisal of the IPCC Fourth Assessment Report. *Journal of Quaternary Science*, 25(1), 26-38.

Gehrels WR and Anderson WP. 2014. Reconstructing Holocene sea-level change from coastal freshwater peat: A combined empirical and model-based approach. *Marine Geology* 353: 140-152.

Gehrels, WR., Dawson, DA., Shaw, J., Marshall, WA. 2011. Using Holocene relative sea-level data to inform future sea-level predictions: An example from southwest England. 78(3-4): 116-126

Gehrels, WR., Long, AJ. 2008. Sea level is not level: The case for a new approach to predicting UK sea-level rise. *Geography Compass*, 93, 11-16.

Gehrels, WR., Szkornik, K., Bartholdy, J., Kirby, JR., Bradley, SL., Marshall, WA., Heinemeier, J., Pedersen JBT. 2006. Late Holocene sea-level changes and isostasy in western Denmark. *Quaternary Research*. 66(2), 288-302.

Gerritsen H. 2005. What happened in 1953? The Big Flood in the Netherlands in retrospect. *Philosophical Transactions of the Royal Society London* 363A: 1271– 1291.

Giannini, PCF., Sawakuchi, AO., Martinho, CT., Tatumi, SH. 2007. Eolian depositional episodes controlled by Late Quaternary relative sea level changes on the Imbituba–Laguna coast (southern Brazil). *Marine Geology*, 237, 143-168.

Gómez -Pujol, L., Orfila, A., Alvarez-Ellacuria, A., Tintore, J. Controls on sediment dynamics and medium-term morphological change in a barred microtidal beach (Cala Millor, Mallorca, Western Mediterranean). *Geomorphology*. 132(3-4), 87-98.

Gorelick, N., Hancher, M., Dixon, M., Ilyushchenko, S., Thau, D., Moore, R. 2017. Google Earth engine: planetary-scale geospatial analysis for everyone. *Remote Sensing of the Environment*, 202, 18-27.

Greenly. 1919, Geology of Anglesey, Geological Survey Memoir.

Grinsted, A., Moore, JC., Jevrejeva, S. 2004. Application of the cross wavelet transform and wavelet coherence to geophysical time series. *Nonlinear Processes in Geophysics*. 11:561-566.

Guillemoteau, J., Bano, M., Dujardin, JR. 2012. Influence of grain size, shape and compaction on georadar waves: examples of aeolian dunes. *Geophysics Journal International*. 190, 1455-1463.

Haigh, ID. 2009. *Extreme Sea Levels in the English Channel 1900 to 2006*. University of Southampton, School of Civil Engineering, and the Environment. PhD Thesis.

Haigh, I., Nicholls, R., Wells, N. 2009. Mean sea level trends around the English Channel over the 20th century and their wider context. *Continental Shelf Research*, 29(17), 2083-2098.

Haigh, ID., Wadey, MP., Gallop, SL., Loehr, H., Nicholls, RJ., Horsburgh, K., Brown, JM., Bradshaw, E. A user-friendly database of coastal flooding in the United Kingdom from 1915-2014. *Scientific Data*. 2, 150021.

Harland MG., Harland HJ. 1980. *The Flooding of Eastern England*. Minimax Books: Norwich.

Harwood, P. 2012. Atlantic storm 2005. *eSurge*. Available at: http://www.storm-surge.info/atlantic-storm-2005 (Accessed: 1 October 2015).

Haslett, SK. 2009. *Coastal Systems*. 2nd Edition, New York, Routledge.

Hassani H., Covey-Crump SJ. Rutter EH. 2004. On the structural age of the Rhoscolyn antiform. *Geological Journal* 39: 141–156.

Hayes, MO. 1967. Hurricanes as geological agents: case studies of Hurricanes Carla, 1961, and Cindy 1963. Austin, University of Texas Bureau of Economic Geology, Report of Investigation, 61, 54.

Hayne, M., Chappell, J. 2001. Cyclone frequency during the last 5000 years from Curocoa Island, Queensland. *Palaeogeography, Palaeoclimatology, Palaeoecology*. 168, 201-219.

Hearty, PJ, Hollin, JT., Neumann, AC., O'Leary, MJ., McCulloch, M. 2007. Global sea-level fluctuations during the Last Interglaciation (MIS 5e). *Quaternary Science Reviews*, 26, 2090-2112.

Hesp, P. 2002. Foredunes and blowouts: initiation, geomorphology and dynamics. *Geomorphology*, 48, 245-268.

Hesp, P. Morphology, dynamics and internal stratification of some established foredune in Southeast Australia. *Sedimentary Geology*. 55, 17-41.

Heyworth A., Kidson C. 1982. Sea-level changes in southwest England and Wales. *Proceedings of the Geologists' Association* 93: 91-111.

Hickey, KR., 1997. *Documentary records of coastal storms in Scotland, 1500-1991 A.D.* Coventry University. Available at: https://curve.coventry.ac.uk/open/file/aa6dfd04-d53f-4741-1bb7-bdf99fb153be/1/hick1comb.pdf.

Hijima, MP., Engelhart, SE., Törnqvist, TE., Horton, BP., Hu, P., Hill, DF. 2015. A protocol for a geological sea-level database, in Shennan, I., Long, AJ., Horton, BP. (eds), *Handbook of Sea-Level Research,* 1st Edition, American Geophysical Union.

Hiskey C. 2003. *The Drainage of Holkham Marshes*. Unpublished report for Holkham Estate Archives.

Holford, I. 1976. *British Weather Disasters*. Newton Abbot: David and Charles.

Holmes, GD. 1957. Newborough Forest, Anglesey. *Journal of the Forestry Commission*. 26, 90-92

Horak JM., Evans JA. 2011. Early Neoproterozoic limestones from the Gwna Group, Anglesey. *Geological Magazine* 148(1): 78-88

Horn, DP. 2015. *Chapter 6 – Storm Surge Warning, Mitigation and Adaptation*. In: Coastal and Marine Hazards, Risks and Disasters: Hazards and Disaster Series. 153-180.

Horton BP., Edwards RJ. Lloyd JM. 1999. UK intertidal foraminiferal distributions: implications for sea-level studies. *Marine Micropaleontology* 36: 205-223.

Howard, T., Palmer MD., Bricheno, LM. 2019. Contributions to 21st century projections of extreme sea-level change around the UK. *Environmental Research Communications*, 1(9), 095002.

HR Wallingford, 2008. *Conwy Tidal Flood Risk Assessment, Stage 1 — Final Report*. Report EX 4667 (release 3.0), Wallingford

Hsiao, SC., Chen, H., Chen, WB., Change, CH., Lin, LE. 2019. Quantifying the contribution of nonlinear interactions to storm tide simulations during a super typhoon event. *Ocean engineering*, 194.

Huntingford, C., Marsh, T., Scaife, AA., Kendon, EJ., Hannaford, J. Kay, AL., Lockwood, M., Prudhomme, C., Reynard, NS., Parry, S., Lowe, JA., Screen, JA., Ward, HC., Roberts, M., Stott, PA., Bell, VA., Bailey, M., Jenkins, A., Legg, T., Otto, FEL., Massey, N., Schaller, N., Slingo, J., Allen, MR. 2014 Potential influences on the United Kingdom's floods of winter 2013/14. *Nature Climate Change*, 4, 769-777.

Hurrell, JW. 1995. Decadal Trends in the North Atlantic Oscillation: Regional Temperatures and Precipitation. *Science*, 269, 676-679

Jacobs, Z. 2008. Luminescence chronologies for coastal and marine sediments. *BOREAS*, 37, 508-535.

Jensen, HAP. 1953 Tidal Inundations, Past and Present. *Weather*, 8, 85-89 and 108-119.

Jiang, AW., Ranasinghe, R., Cowell, P. 2013. Contemporary hydrodynamics and morphological change of a microtidal estuary: a numerical modelling study. *Ocean Dyanmics*, 63(1), 21-41.

Jones, M., Laurence M., Sowerby, A., Rhind, PM. 2010. Factors affecting vegetation establishment and development in a sand dune chronosequence in Newborough Warren, North Wales. *Journal of Coastal Conservation*, 14(2). 127-137.

Jones, PD, Jonsson, T., Wheeler, D. 1997. Extension to North Atlantic oscillation using early instrumental pressure observation from Gibraltar and south-west Iceland. *International Journal of Climatology*. 17, 1433-1450.

Jongepier, I., Soens, T., Temmerman, S., Missiaen, T. 2014. Assessing the Planimetric Accuracy of Historical Maps (Sixteenth to Ninetieth Centuries): New Methods and Potential for Coastal Landscape Reconstruction. *The Cartographic Journal,* 53(2).

Juggins S. 2003. User Guide C2, Software for Ecological and Palaeoecological Data Analysis and Visualisation, User Guide Version 1.3, Newcastle: Department of Geography.

Karim, MF., Mimura, N. 2008. Impacts of climate change and sea-level rise on cyclonic storm surge floods in Bangladesh. *Global Environmental Change - Human and Policy Dimensions*. 18, 3.

Kang, KR., Kim, S., 2015. Wave-tide interactions during a strong storm event in Kyunggi Bay, Korea. *Ocean Engineering*, 108.

Karunarathna, H., Pender, D., Ranasinghe, R., Short, A.D., Reeve, D.E., 2014. The effects of storm clustering on beach profile variability. *Marine Geology*. 348, 103-112.

Kelley, JT., Gehrels, WR., Bellknap, DF. 1995. The geological development of tidal marshes at Wells, Maine, USA. *Journal of Coastal Research*, 11, 136-153.

Kemp AC., Horton BP., Vane CH., Bernhardt CE., Corbett DR., Engelhart SE., Anisfeld SC., Parnell AC., Cahill N. 2013. Sea-level change during the last 2500 years in New Jersey, USA. *Quaternary Science Reviews* 81: 90-104

Kington JA. 2010. *Climate and Weather*. Collins: London.

Kirby, JA., Masselink, G, Essex, S., Poate, T., Scott, T. 2021. Coastal adaptation to climate change through zonation: A review of coastal change management areas (CCMAs) in England. *Ocean and Coastal Management*, 215, 105950.

Kirwan, ML., Temmerman, S., Skeehan, EE., Gutenspergen, GR., Fagherazzi, S. 2016. Overestimation of marsh vulnerability to sea level rise. *Nature Climate Change,* 6(3), 253-260.

Kim, S., Oh, J., Suh, KD., Mase, H. 2017. Estimation of Climate Change Impact on Storm Surges: Application to Korean Peninsula. *Coastal Engineering Journal*, 59(2).

Kombiadou, K., Costa, S., Carrasco, AR., Plomaritis, TA., Ferreira, O., Matias, A. 2019. Bridging the gap between resilience and geomorphology of complex coastal systems. *Earth-Science Reviews*, 198.

Kominz, MA., Browning, JV., Miller, KG., Sugarman, PJ., Misintseva, S., Scotese, CR. 2008. Late Cretaceous to Miocene sea-level estimates from the New Jersey and Delaware coastal plain coreholes: An error analysis. *Geology*, 26, 311-314.

Kopp RE., Kemp AC., Bittermann K., Horton BP., Donnelly JP., Gehrels WR., Hay CC., Mitrovica JX., Morrow ED., Rahmstorf S. 2016. Temperature-driven global sea-level variability in the Common Era. *Proceedings of the National Academy of Sciences* 113: E1434.

Kraft, JC., Chrzastowski, MJ. 1985. Coastal stratigraphic sequences. *Coastal Sedimentary Environments*. P625-663.

Kuchar, J., Milne, G., Hubbard, A., Patton, H., Bradley, S., Shennan, I., Edwards, R. 2012. Evaluation of a numerical model of the British-Irish ice sheet using relative sea-level data: Implications for the interpretation of trimline observations. *Journal of Quaternary Science*, 27(6), 597-605.

Lamb HH. 1977. *Climate Past Present and Future. Volume 2., Climatic History and the Future*. Methuen and Co: London.

Lamb, HH. 1991. *Historic Storms of the North Sea, British Isles and Northwest Europe*. Cambridge University Press.

Lambeck K. 1996. Glaciation and sea-level change for Ireland and the Irish Sea since Late Devensian/Midlandian time. *Journal of the Geological Society* 153: 853.

Lancaster N. 2013. *Geomorphology of Desert Dunes*. Routledge: Oxford.

Larson, M., Kraus, NC. 1994. Temporal and spatial scales of beach profile change, Duck, North Carolina. *Marine Geology*, 117(1-4), 75-94.

Le Mauff, B., Juigner, M., Ba, A., Robin, M., Launeau, P., Fattal, P. 2018. Coastal monitoring solution of the geomorphological response of beach-dune systems using multi-temporal LiDAR datasets (Vendée coast, France). *Geomorphology* 304, 121-140.

Leighton, CL., Bailey, RM., Thomas, DSG. 2013. The utility of desert sand dunes as Quaternary chronostratigraphic archives: evidence from the northeast Rub' al Khali. *Quaternary Science Reviews*, 78. 303-318.

Lewis M., Schumann G., Bates P., Horsburgh K. 2013. Understanding the variability of an extreme storm tide along a coastline. *Estuarine, Coastal and Shelf Science* 123: 19– 25.

Lian, OB., Roberts, RG. 2006. Dating the Quaternary: progress in luminescence dating of sediments. *Quaternary Science Reviews*, 25, 2449-2468.

Lisle RJ. 1988. Anomalous vergence patterns on the Rhoscolyn anticline, Anglesey: Implications for structural analysis of refolded regions. *Geological Journal* 23: 211–220.

Liu, KB., Fearn, ML. 1993. Lake-sediment record of late Holocene hurricane activities from coastal Alabama. *Geology*, 21(9), 793-796.

Liu, Q., Trinder, J., Turner, IL. 2017. Automatic super-resolution shoreline change monitoring using Landsat archival data: a case study at Narrabeen-Collaroy Beach, Australia. *Journal of Applied Remote Sensing*, 11, 016036.

Lloyd JM., Zong Y., Fish P., Innes., JB. 2013. Holocene and Late glacial relative sea-level change in north-west England: implications for glacial isostatic adjustment models. *Journal of Quaternary Science* 28: 59-70.

Lowe, JA., Gregory, JM. 2005 The effects of climate change on storm surges around the United Kingdom. *Philosophical Transactions of the Royal Society London*, 363, 1313–1328.

Lowe, JA., Woodworth, PL., Knutston, T., McDonald, RE., McInnes, KL., Woth, K., von Storch, H. Wolf, J., Swail, V., Bernier, NB., Gulev, S., Horsburgh, KJ., Unnikrishnan, AS., Hunter, JR., Weisse, R. 2011. Past and Future Changes in Extreme Sea Levels and Waves. In Understanding Sea-Level Rise and Variability, eds. J. A. Church, P. L. Woodworth, T. Aarup & W. S. Wilson. London: Blackwell Publishing Ltd.

Lyard, FH., Allain, DJ., Cancet, M., Carrere, L., Picot, N. 2021. FES2014 global ocean tide atlas: design and performance. *Ocean Science*., 17, 615-649.

Maan, ME. 2002. Little Ice Age. In Encyclopaedia of global environmental change. Volume 1, The Earth system: Physical and chemical dimensions of global environmental change, eds. M. C. MacCracken & J. A. Perrey, 504-509. Chichester: Wiley & Sons.

Madsen, AT., Duller, GAT., Donneley, JP., Roberts, HM., Wintle, AG. 2009a. A chronology of hurricane landfalls at Little Sippewissett Marsh, Massechusetts, USA, using optical dating. *Geomorphology*, 109, 36-45.

Madsen, AT., Murray, AS. 2009b. Optically stimulated luminescence dating of young sediments: A review. *Geomorphology*, 109, 3-16.

Madsen, AT., Murray, AS., Andersen, TJ., Pejrup, M., Breuning-Madsen, H. 2005. Optically stimulated luminescence dating of young estuarine sediments: a comparison with 210Pb and 137Cs dating. *Marine Geology*, 214, 251-268.

Madsen, AT., Murray, AS., Jain, M., Andersen, TJ., Pejrup, M. 2011. A new method for measuring bioturbation rates in sandy tidal flat sediments based on luminescence dating. *Estuarine, Coastal and Shelf Science*, 92, 464-471.

Marcos, M., Tsimplis, MN., Shaw, AGP. 2009. Sea level extremes in southern Europe. *Journal of Geophysical Research: Oceans*, 144(C1).

Marshall WA., Gehrels WR., Garnett MH., Freeman SPHT., Maden C., Xu S. 2007. The use of‘ bomb spike’ calibration and high-precision AMS 14C analyses to date salt-marsh sediments deposited during the past three centuries. *Quaternary Research* 68: 325-337.

Marsooli, R., Lin, N. 2018. Numerical Modelling of Historical Storm Tides and Waves and Their Interactions Along the US East and Gulf Coasts. *Journal of Geophysical Research, Oceans.* 123(5).

Marusek, JA. 2011. A Chronological Listing of Early Weather Events. SPPI Reprint Series. Available at: http://www.breadandbutterscience.com/Weather.pdf (Accessed: 11 May 2020).

Masselink, G., Castelle, B., Scott, T., Dodet, G., Suanez, S., Jackson, D., Floc’h, F. 2016. Extreme wave activity during 2013/2014 winter and morphological impacts along the Atlantic coast of Europe. *Geophysical Research Letters* 43, 2135-2143.

Masselink, G., Hughes, MG., Knight. J. 2011. *Introduction to Coastal Processes & Geomorphology*. London: Hodder Education.

Masselink, G., Lazarus, ED. 2019. Defining Coastal Resilience. *Water*, 11, 2587.

Masselink, G., Scott, T., Davidson, M., Russell, P., Conley, D., 2015. The extreme 2013/2014 winter storms: hydrodynamic forcing and coastal response along the southwest coast of England. *Earth Surface Processes and Landforms* 41, 378-391.

Masselink, G., Scott, T., Poate, T., Russell, P., Davidson, M., Conley, D. 2015. The extreme 2013/2014 winter storms: hydrodynamic forcing and coastal response along the southwest coast of England. *Earth Surface Processes and Landforms*, 41(3), 378-391.

Matthews, T., Murphy, C., Wilby, RL., Harrigan, S. 2014. Stormiest winter on record for Ireland and UK. *Nature Climate Change*, 4, 738-740.

Mauz, B. & Bungenstock, F. 2007. How to reconstruct trends of late Holocene relative sea level: A new approach using tidal flat clastic sediments and optical dating. *Marine Geology*, 237, 225-237.

Mclean, RF., Thom, BG. 1975. Beach changes at Moruya, 1974-74. Second Australian Conference on Coastal and Ocean Engineering, 1975: The Engineer, the Coast and Ocean.

McGranahan G., Balk, D., Anderson, B. 2007. The rising tide: assessing the risks of climate change and human settlements in low elevation coastal zones. *Environment and Urbanization*. 19: 17-37.

McMillan, A., Batstone, C., Worth, D., Tawn, J., Horsburgh, KJ., Lawless, M. 2011. *Coastal flood boundary conditions for UK mainland and islands*. Project: SC060064/TR2: Design sea levels. ed. E. Agency. Bristol, UK.

Menéndez, M., Woodworth, PL. 2010. Changes in extreme high water levels based on a quasi-global tide-gauge data set. *Journal of Geophysical Research: Oceans*, 115, C10011.

Met Office, 1986. Monthly Weather Report of the Meteorological Office. Monthly Weather Report, 103(11)

Met Office, 2010. March 2010. Climate Summaries. Available at: http://www.metoffice.gov.uk/climate/uk/summaries/2010/march (Accessed: 11 May 2020)

MET Office. 2014. Winter storms, December 2013 to January 2014. [Online]. Available at: [Accessed January 20th, 2015]

Met Office. 2016. January 2016. Climate Summaries. Available at: https://www.metoffice.gov.uk/climate/uk/summaries (Accessed: 11 May 2020).

Met Office. 2017. September 2017. Climate Summaries. Available at: https://www.metoffice.gov.uk/climate/uk/summaries (Accessed: 11 May 2020).

Met Office. 2018. January 2018. Climate Summaries. Available at: https://www.metoffice.gov.uk/climate/uk/summaries (Accessed: 11 May 2020).

Míguez, BM., Testut, L., Wöppelmann, G. 2012. Performance of modern tide gauges: towards mm-level accuracy. *Advances in spanish physical oceanography*, 76S1, 221-228.

Miller, KG., Kominz, MA., Browning, JV., Wright, JD., Mountain, GS., Katz, ME., Sugarman, PJ., Christie-Blick, CBSN., Pekar, SF. 2005. The Phanerozoic Record of Global Sea-Level Change. *Science*, 310, 1293-1298.

Miller, KG., Mountain, GS., Wright, JD., Browning, JV. 2011. A 180-million-year record of sea level and ice volume variations from continental margin and deep-sea isotopic records. *Oceanography*, 24, 40-53.

Milne GA., Shennan I., Youngs BAR., Waugh AI., Teferle FN., Bingley RM., Bassett SE., Cuthbert-Brown C., Bradley SL. 2006. Modelling the glacial isostatic adjustment of the UK region. *Philosophical Transactions of the Royal Society A: Mathematical, Physical and Engineering Sciences* 364: 931-948.

Mitrovica, JX., Tamisiea, ME., Davis, JL., Milne, GA. 2001. Recent mass balance of polar ice sheets inferred from patterns of global sea-level change. *Nature*, 409, 1026-1029

Moller, I., Kudella, M., Rupprect F., Spencer, T., Paul, M., van Wesenbeeck, BK., Wolters, G., Jensen, K., Bouma, TJ., Miranda-Lange, M., Schimmels, S. 2014. Wave attenuation over coastal salt marshes under storm surge conditions. *Natura Geoscience*, 7(10), 727-731.

Monecke, K., Finger, W., Klarer, D., Kongko, W., McAdoo, BG., Moore, AL., Sunrajat, SU. 2008, A 1,000-year sediment record of tsunami recurrence in northern Sumatra. *Nature*. 455, 1232-1234.

Monegaglia, F., Zolezzi, G., Güneralp, I, Henshaw, AJ. Tubino, M. 2018. Automated extraction of meandering river morphodynamics from multitemporal remotely sensed data. *Environmental Modelling Software*, 105, 171-186.

Montreuil A-L., Bullard JE. 2012. A 150-year record of coastline dynamics within a sediment cell: Eastern England. *Geomorphology* 179: 168– 185.

Mori, N., Shimura, T., Yoshida, K., Mizuta, R., Okada, Y., Fujita, M., Khunjanazarov T., Nakakita, E. 2019. Future changes in extreme storm surges based on mega-ensemble projection using 60-km resolution atmospheric global circulation model. *Coastal Engineering Journal*, 61(3), 295-307.

Morton, R. A., Sallenger, JAH. 2003. Morphological Impacts of Extreme Storms on Sandy Beaches and Barriers. *Journal of Coastal Research*, 19, 560-573.

Morton, RA. 1976. Effects of Hurricane Eloise on beach and coastal structures, Florida Panhandle, *Geology*, 4, 277-280.

Morton, RA., Paine JG., Gibeaut, JC. 1994. Stages and durations of post-storm beach recovery, southeastern Texas Coast. *Journal of Coastal Research*, 10, 884-908.

Morton, RA. 2002. Factors controlling storm impacts on coastal barriers and beaches – A preliminary basis for near real-time forecasting. *Journal of Coastal Research*, 18(3), 486-501.

Morton, RA., Paine, JG. 1985. *Beach and vegetation-line changes at Galveston Island, Texas: erosion, deposition, and recovery from Hurricane Alicia, Austin*, University of Texas Bureau of Economic Geology, Geological Circular, 85-5.

Moskalewicz, D., Szczuciński, W., Mroczek, P., Vaikutienė, G. 2020. Sedimentary record of historical extreme storm surges on the Gulf of Gdańsk coast, Baltic Sea. *Marine Geology*. 420.

Mũnoz-Salinas E., Castillo M., Arce JL. 2017. OSL signal resetting in young deposits determined with a pulsed photon-stimulated luminescence (PPSL) unit. *Boreas* 46: 325–337.

Murray, AS., Wintle, AG. 2000. Luminescence dating of quartz using an improved single-aliquot regenerative-dose protocol. *Radiation Measurements*, 32, 57-73.

Murray AS., Wintle AG. 2003. The single aliquot regenerative dose protocol: potential for improvements in reliability. *Radiation Measurements* 37: 377-381.

Murray-Wallace, CV. 2002. Pleistocene coastal stratigraphy, sea-level highstands and neotectonism of the southern Australian passive continental margin—a review. *Journal of Quaternary Science*, 17, 469-489.

National Library of Wales. 2020. Plans of harbours, bars, bays and roads in St. George's Channel lately survey'd under the direction of the Lords of the Admiralty, and now publish'd by their permission, with an appendix concerning the improvements that might be made in the several harbours & for better securing the navigation in those parts together with a short account of the trade and manufactures on that coast. Available at: http://hdl.handle.net/10107/1445668 [Accessed 10 July 2020]

National Oceanic and Atmospheric Administration (NOAA). 2007. Technical Memorandum NWS TPC 5, http://www.nhc.noaa.gov/pdf/sshws_statement.pdf.

Neal, A. 2004. Ground-penetrating radar and its use in sedimentology: principles, problems and progress. *Earth Science Reviews*, 66: 261-330.

Needham, HF., Keim BD., Sathiaraj, D. 2015. A review of tropical cyclone-generate storm surges: Global data sources, observations and impacts. *Review of Geophysics*, 53(2), 545-591.

Neumann, B., Vafeidis, AT., Zimmermann, J., Nicholls, RJ. 2015. Future Coastal Population Growth and Exposure to Sea-Level Rise and Coastal Flooding – A Global Assessment. *PLoS ONE*, 10(3).

Nielsen, A., Murray, AS., Pejrup, M., Elberling, B. 2006. Optically stimulated luminescence dating of a Holocene beach ridge plain in Northern Jutland, Denmark. *Quaternary Geochronology*, 1, 305-312.

Nobes, DC., Jol, HM., Duffy, B. 2016. Geophysical imaging of disrupted coastal dune stratigraphy and possible mechanisms, Haast, South Westland, New Zealand. New Zealand *Journal of Geology and Geophysics*. 59:3, 426-435

Nott, J. 2011. A 6000-year tropical cyclone record from Western Australia. *Quaternary Science Reviews*, 30, 713-722.

Nott, J., Smithers, K., Walsh, K., Rhodes, EE. 2009. Sand beach ridges record 6000-year history of extreme tropical cyclone activity in northeastern Australia. *Quaternary Science Reviews*. 28, 1511-1520.

NPPF, 2019. February 2019 Ministry of Housing, Communities and Local Government National Planning Policy Framework.

Oliver, TSN., Tamura, T., Short, AD., Woodroffe, CD. 2018. Rapid shoreline progradation followed by vertical foredune building at Pedro Beach, southeastern Australia. *Earth Surface Processes and Landforms.* 44(2), 655-666.

OPW. 2021. Flood Maps, Past Flood Events. OPW. Available at: https://www.floodinfo.ie/map/floodmaps/ (Accessed 01/08/2021)

Oronsaye WI. 1990. Wind action and sand movement near Holkham Bay, North Norfolk Coast, England. *Environmental Geology and Water Sciences* 15: 77– 82.

Orson, RA., Warren, RS., Niering, WA. Interpreting sea level rise and rates of vertical marsh accretion in a southern New England tidal salt marsh. *Estuarine, Coastal and Shelf Science*, 47, 419-429.

Ortega-Sanchez, M., Fachin, S., Sancho, F., Losada, MA. 2008. Relation between beachface morphology and wave climate at Trafalgar beach (Cadiz, Spain). *Geomorphology*. 99(1-4), 171-185.

Oumeraci, H., Kortenhaus, A., Burzel, A., Naulin, M., Dassanayake, DR., Jensen, J., Wahl, T., Mudersbach, C., Gönnert, G., Gerkensmeier, B., Fröhle, P., Ujeyl, G. 2015. XtremRisK – Integrated Flood Risk Analysis for Extreme Storm Surges at Open Coasts and in Estuaries: Methodology, Key Results and Lessons Learned. *Coastal engineering journal*, 57(1).

Packham JR and Liddle MJ. 1970. The Cefni Salt Marsh Anglesey and its recent development. *Field Studies* 3: 331-356.

Patterson RT., Roland Gehrels W., Belknap DF., Dalby AP. 2004. The distribution of salt marsh foraminifera at Little Dipper Harbour New Brunswick, Canada: implications for development of widely applicable transfer functions in sea-level research. *Quaternary International* 120: 185-194.

Peltier WR. 1994. Ice Age Paleotopography. *Science* 265: 195.

Peltier WR. 2002. Global glacial isostatic adjustment: palaeogeodetic and space-geodetic tests of the ICE-4G (VM2) model. *Journal of Quaternary Science* 17: 491-510.

Peltier WR. 2004. GLOBAL GLACIAL ISOSTASY AND THE SURFACE OF THE ICE-AGE EARTH: The ICE-5G (VM2) Model and GRACE. *Annual Review of Earth and Planetary Sciences* 32: 111-149.

Peltier, WR., Shennan, I., Drummond, R., Horton, B. 2002. On the Postglacial Isostatic adjustment of the British Isles and the Shallow Viscoelastic Structure of the Earth. *Geophysics Journal International*, 148, 443-475.

Poulose, J., Rao, AD., Bhaskaran, PK. Role of continental shelf of non-linear interaction of storm surges, tides and wind waves: An idealized study representing the west coast of India. *Estuarine, coastal and shelf science*, 207.

Prescott, JR., Hutton, JT. 1994. Cosmic ray contributions to dose rates for luminescence and ESR dating: Large depths and long-term time variations. *Radiation Measurements*, 23, 497-500.

Prince HE. 1988. Late-glacial and Post-glacial sea-level movements in North Wales with particular reference to the techniques for the analysis and interpretation of unconsolidated estuarine sediments.: University of Wales, Aberystwyth.

Proctor, R., Flather, RA. 1989. 'Storm surge prediction in the Bristol Channel – the floods of 13 December 1981'. *Continental Shelf Research*, 9(10), pp.889–918

Pugh, DT., Maul, GA. 1999. Coastal sea level prediction for climate change. In: Coastal Ocean Prediction, Coastal and Estuarine Studies, Volume 56. Editors: Mooers, CNK., Washington, DC., *American Geophysical Union*, 377-404.

Pugh, DT., Woodworth, PL. 2014. *Sea-Level Science.* Cambridge University Press.

Puijenbroek MEB., Limpens J., deGroot AV., Riksen MJPM., Gleichman M., Slim PA., van Dobben HF., Berendse F. 2017. Embryo dune development drivers: beach morphology, growing season precipitation and storms. *Earth Surface Processes and Landforms* 42: 1733– 1744.

Pye K., Blott, S. 2007. Holderness Erosion and Evolution of the Spurn Peninsula. Unpublished report. http://www2.hull.ac.uk/science/PDF/ECSA%20Ken%20Pye.pdf [last accessed 9/5/17]

Pye K., Saye SE., Blott SJ. 2007. Sand dune processes and management for flood and coastal defence. Parts 1–5. Joint DEFRA/EA Flood and Coastal Erosion Risk Management R and D Programme, R and D Technical Report FD1302/TR. DEFRA/EA, London, 5 volumes.

Pye, K., Blott, S. 2016. Assessment of beach and dune erosion and accretion using LiDAR: Impact of the stormy 2013-14 winter and longer-term trends on the Sefton Coast, UK. *Geomorphology* 266, 146-167.

Pye, K., Blott, SJ. 2008. Decadal-scale variation in dune erosion and accretion rates: An investigation of the significant of changing storm tide frequency and magnitude on the Sefton coast, UK. *Geomorphology* 102, 652-666.

Pye, K., Blott, SJ. 2016. Assessment of beach and dune erosion and accretion using LiDAR: impact of the stormy 2013-14 winter and longer-term trends on the Sefton Coast, UK. *Geomorphology*, 266, 146-167.

Pye, K., Blott, SJ., Howe, MA. 2014. Coastal dune stabilization and requirements for rejuvenation. *Journal of Coastal Conservation* 18(1), 27-54

Pye, K., Saye, SE., Blott, SJ. 2007. Sand Dune Processes and Management for Flood and Coastal Defence. Part 2: Sand Dune Processes and Morphology. ed. F. a. R. A. Department for Environment, 22. London.

Ranwell, 1958. Movement of Vegetated Sand Dunes at Newborough Warren, Anglesey. *Journal of Ecology*. 46(1), 83-100.

Ranwell, 1960. Newborough Warren, Anglesey III. Changes in vegetation on parts of the dune system after the loss of rabbits by myxomatosis. *Journal of Ecology*. 48(2), 385-395.

Rees-Hughes, L., Barlow, NLM., Booth., AD., West, LJ., Tuckwell G., Grossey, T. 2021. Unveiling buried aeolian landscapes: reconstructing a late Holocene dune environment using 3D ground-penetrating radar. *Journal of Quaternary Science*. 36(3), 337-390

Reimer, PJ., Baille, MGL., Bard, E., Bayliss, A., Beck, JW., Blackwell, PG., Ramsey, CB., Buck, CE., Burr, GS., Edwards, RL., Friedrich, M., Guilderson, TP., Hajdas, I., Heaton, TJ., Hogg, AG., Hughen, KA., Kaiser, KF., Kromer, B., McCormac, FG., Manning, SW., Reimer, RW., Richards, DA., Southon, JR., Talamo, S., Turney, CSM., van der Plicht, J., Weyhenmeye, CE. 2009. IntCal09 and Marine09 radiocarbon age calibration curves, 0– 50,000 years cal BP. Radiocarbon, 51, 1111-1150.

Reimer, PJ., Brown, TA., Reimer, RW. 2004. Discussion: Reporting and Calibration of Post-Bomb 14C Data. *Radiocarbon*, 46(1): 1299-1304

Rhind PM., Blackstock TH., Hardy HS., Jones, RE. Sandison, W. 2001. *The evolution of Newborough Warren dune system with particular reference to the past four decades*, Liverpool: Liverpool Univ Press.

Rhodes, EG., Polach, HA., Thom, BG., Wilson, SR. 1980. Age structure of Holocene coastal sediments, Gulf of Carpentaria, Australia. *Radiocarbon*, 22, 718-727

Ritphring, S., Somphong, C., Udo, K., Kazama, S. 2018. Projections of Future Beach Loss due to Sea Level Rise for Sandy Beaches along Thailand's Coastlines. *Journal of Coastal Research*. 85, 541-545.

Ritphring, S., Somphong, C., Udo, K., Kazama, S. 2018. Projections of Future Beach Loss due to Sea Level Rise for Sandy Beaches along Thailand's Coastlines. *Journal of Coastal Research*. 85, 541-545.

Roberts MJ., Scourse JD., Bennell JD., Huws, DG. Jago CF. Long BT. 2011. Late Devensian and Holocene relative sea-level change in North Wales, UK. *Journal of Quaternary Science* 26: 141-155.

Roberts RG., Galbraith RF., Yoshida H., Laslett GM., Olley GM. 2000. Distinguishing dose populations in sediment mixtures: a test of single-grain optical dating procedures using mixtures of laboratory-dosed quartz. *Radiation Measurements* 32: 459-465.

Roberts, DL., Bateman, MD., Murray-Wallace, CV., Carr, AS., Holmes, PJ. 2008. Last Interglacial fossil elephant trackways dated by OSL/AAR in coastal aeolianites, Still Bay, South Africa. Palaeogeography, Palaeoclimatology, Palaeoecology, 257, 261-279.

Roberts, HM., Plater AJ. 2007. Reconstruction of Holocene foreland progradation using optically stimulated luminescence (OSL) dating: an example from Dungeness, UK. *The Holocene*, 17, 495-505.

Roberts, M., Scourse, J., Bennell, J., Huws, D., Jago, C., Long, B. 2011. Late Devensian and Holocene relative sea-level change in North Wales, UK. *Journal of Quaternary Science*, 26(2), 141-155.

Robin, N., Billy, J., Castelle, B., Hesp, P., Lerma, AN., Laporte-Fauret, Q., Marieu, V., Rosebery D., Bujan, S., Destribats, B., Michalet, R. 2021. 150 years of foredun initiation and evolution driven by human and natural processes. *Geomorphology*. 374.

Robinson, M., Bristow, C., McKinley, J., Ruffell, A. 2013. 1.5.5 Ground Penetrating Radar. In: *Geomorphological Techniques, Part 1, Sec. 5.5. British Society for Geomorphology*

Rodríguez-Santalla, I., Gomez-Ortiz, D., Martín-Crespo, T., Sánchez-García, MJ., Montoya-Montes, Martín-Velázquez, S., Barrio, F., Serra, J., Ramírez-Cuesta, JM., Gracia, FJ. 2021. Study and Evolution of the Dune Field of La Banya Spit in Ebro Delta (Spain) Using LiDAR Data and GPR. *Remote Sensing*. 13(4), 802.

Roe HM., Doherty CT., Patterson RT., Swindles, GT. 2009. Contemporary distributions of saltmarsh diatoms in the Seymour– Belize Inlet Complex, British Columbia, Canada: implications for studies of sea-level change. *Marine Micropaleontology* 70: 134-150.

Roman, CT., Peck, JA., Allen, JR., King, JW., Appleby, PG. 1997. Accretion of a New England (USA) salt marsh in response to inlet migration, storms and sea-level rise. *Estuarine Coastal Shelf Science*, 45, 717-727.

Ruocco, A. Nicholls, RJ., Haigh, ID., Wadey, M. 2011. 'Reconstructing Coastal Flood Occurrence Combining Sea Level and Media Sources: A case study of the Solent UK since 1935'. *Natural Hazards*, 59(3): 1773-1796.

Rushby, GT., Richards, GT., Gehrels, WR., Anderson, WP., Bateman, MD., Blake, WH. 2019. Testing the mid-Holocene relative sea-level highstand hypothesis in North Wales, UK. *The Holocene* 29(9), 1491-1502.

Sanderson DW, Murphy S. 2010. Using simple portable OSL measurements and laboratory characterisation to help understand complex and heterogeneous sediment sequences for luminescence dating. *Quaternary Geochronology* 5: 299– 305.

Santos, VM., Wahl, T., Long, JW., Passeri, DL., Plant, NG. 2019. Combining Numerical and Statistical Models to Predict Storm-Induced Dune Erosion. *Journal of Geophysical Research – Earth Surface*, 124(7), 1817-1834.

Scheffers, A., Engel, M., Scheffers, S., Squire P., Kelletat, D. 2011. Beach ridge systems – archives for Holocene coastal events? *Progress in Physical Geography* 36: 5-37.

Schuerch, M., Spencer, T., Temmerman, S. Kirwan, ML., Wolff, C., Lincke, D., McOwen, CJ., Pickering, MD., Reef, R., Vafeidis, AT., Hinkel, J., Nicholls, RJ., Brown, S. Future response of global coastal wetlands to sea-level rise. *Nature*, 561 (7722).

Schulte, P., Lekmkuhl, F. 2018. The difference of two laser diffraction patterns as an indicator for post-depositional grain size reduction in loess-palesol sequences. *Palaeogeography, Palaeoclimatology, Palaeoecology,* 509, 126-136

Scott DBM, F S. 1980. *Quantitative studies of marsh foraminiferal distributions in Nova Scotia : implications for sea level studies*, Washington, D.C. : Cushman Foundation for Foraminiferal Research.

Scott DS and Medioli FS. 1978. Vertical zonations of marsh foraminifera as accurate indicators of former sea-levels. *Nature* 272: 528-531.

Scott, T., Masselink G., O'Hare, T., Saulter, A., Poate, T., Russell, P., Davidson, M., Conley, D. 2016. The extreme 2013/2014 winter storms: Beach recovery along the southwest coast of England. *Marine Geology* 382, 224-241.

Scott, T., Masselink G., O'Hare, T., Saulter, A., Poate, T., Russell, P., Davidson, M., Conley, D. 2016. The extreme 2013/2014 winter storms: Beach recovery along the southwest coast of England. *Marine Geology* 382, 224-241.

Scott, T., Masselink, G., O'Hare, T., Saulter, A., Poate, T., Russell, P., Davidson, M., Conley, D. 2016. The extreme 2013/2014 winter storms: Beach recovery along the southwest coast of England. *Marine Geology*, 382, 224-241

Seftoncoast. 2002. 'Coastlines- winter 2002 – Tidal flooding'. Available at: http://www.seftoncoast.org.uk/articles/02winter_tidalflooding.html (Accessed: 24 August 2014).

Sensors and Software, 2021. Common Mid-Point survey using the DVL-500P. Available at: https://www.sensoft.ca/blog/cmp-survey-using-the-dvl-500p/

Shaw, TA., Plater, AJ., Kirby, JR., Roy, K., Holgate, S., Tutman, P., Cahill, N., Horton, BP. 2018. Tectonic influences on late Holocene relative sea levels from the central-eastern Adriatic coast of Croatia. *Quaternary Science Reviews,* 200, 262-275.

Shennan I, Milne G, Bradley S, 2012. Late Holocene vertical land motion and relative sea-level changes: lessons from the British Isles. *Journal of Quaternary Science* 27(1): 64-70

Shennan I, Horton BP. 2002. Holocene land- and sea-level changes in Great Britain. *Journal of Quaternary Science* 17: 511– 526.

Shennan I., Bradley S., Milne G., Brooks., A. Bassett., S. Hamilton., S. 2006. Relative sea-level changes, glacial isostatic modelling, and ice-sheet reconstructions from the British Isles since the Last Glacial Maximum. *Journal of Quaternary Science* 21: 585-599.

Shennan I., Bradley SL, Edwards R. 2018. Relative sea-level changes and crustal movements in Britain and Ireland since the Last Glacial Maximum. *Quaternary Science Reviews* 188: 143-159.

Shinn, EA., Steinen, RP., Dill, RF., Major, R. 1993. Lime-mud layers in high-energy tidal channels: A record of hurricane deposition. *Geology*, 21, 603-606.

Sibley A, Cox D, Titley H. 2015. Coastal flooding in England and Wales from Atlantic and North Sea storms during the 2013/2014 winter. *Weather* 70: 62– 70.

Simon KM, Riva REM, Kleinherenbrink M, Frederikse, T. 2018. The glacial isostatic adjustment signal at present day in northern Europe and the British Isles estimated from geodetic observations and geophysical models. *Solid Earth* 9: 777-795.

Small, D. Clark, CD. Chiverrell, RC. Smedley, RK. Bateman, MD. Duller, GAT. Ely, JC. Fabel, D. Medialdea, A. Moreton, SG. 2017. Devising quality assurance procedures for assessment of legacy geochronological data relating to deglaciation of the last British-Irish Ice Sheet. *Earth-Science Reviews*. 164: 232-250

Somphong, C., Udo, K., Ritphring, S., Shirakawa, H. Beach Nourishment as an Adaptation to Future Sandy Beach Loss Owing to Sea-Level Rise in Thailand. *Journal of Marine Science and Engineering*. 8(9).

Song, H., Kuang, C., Gue, J., Zou, Q., Liang, H., Sun, X., Ma, Z. 2020. Nonlinear tide-surge-wave interaction at a shallow coast with large scale sequential harbor constructions. *Estuarine, coastal and shelf science,* 233.

Spencer, T., Brooks, SM., Evans, BR., Tempest, JA., Möller, I. 2016. Southern North Sea storm surge event of 5 December 2013: water levels, waves, and coastal impacts. *Earth Science Reviews*, 146, 120-145.

Splinter, KD., Carley, JT., Golshani, A., Tomlinson, R. 2014. A relationship to describe the cumulative impact of storm clusters on beach erosion. *Coastal Engineering* 83, 49-55.

Splinter, KD., Coco, G. 2021. Challenges and Opportunities in Coastal Shoreline Prediction. *Frontiers in Marine Science*, 8.

Splinter, KD., Kearney, ET., Turner, IL. 2018. Drivers of alongshore variable dune erosion during a storm event: Observations and modelling. *Coastal Engineering*, 131, 31-41.

Steers JA, Stoddart DR, Bayliss-Smith TP, Spencer T, Durbidge PM. 1979. The storm surge of 11 January 1978 on the east coast of England. *The Geographical Journal* 145: 192– 205.

Stephens, SA., Bell, RG., Haigh, ID. 2020. Spatial and temporal analysis of extreme storm-tide and skew-surge events around the coastline of New Zealand. *Natural Hazards Earth System Science*, 20, 783-796.

Stockamp J., Bishop P., Li Z., Petire EJ., Hansom J., Rennie A. 2016. State-of-the-art in studies of glacial isostatic adjustment for the British Isles: a literature review. *Earth and Environmental Science Transactions of the Royal Society of Edinburgh* 106: 145-170

Stone, AEC., Bateman, MD., Thomas, DSG. 2015. Rapid age assessment in the Namib Sand Sea using a portable luminescence reader. *Quaternary Geochronology*, 30B, 134-140.

Stuiver M., Reimer PJ, Reimer RW. 2018. CALIB 7.1 [WWW program] at http://calib.org.

Sutton-Grier, AE., Wowk, K., Bamford, H. 2015. Future of our coasts: The potential for natural and hybrid infrastructure to enhance the resilience of our coastal communities, economies and ecosystems. *Environmental Science and Policy,* 51, 137-148.

Switzer, AD., Bristow, CS., Jones, BG. 2006. Investigation of large-scale washover of a small barrier system on the southeast Australian coast using ground penetrating radar. *Sedimentary Geology*, 183(1-2), 145-156.

Szkornik, K., Gehrels, WR., Murray, AS. 2008. Aeolian sand movement and relative sea-level rise in Ho Bugt, western Denmark, during the `Little Ice Age'. *The Holocene*, 18, 951-965.

Talke, SA., Jay, DA. 2013. Nineteenth Century North American and Pacific Tidal Data: Lost or Just Forgotten? *Journal of Coastal Research*, 29(6a), 118-127.

Tamura, T. 2012. Beach ridges and prograded beach deposits as palaeoenvironment records. *Earth-Science Reviews*, 144(3-4), 279-297.

Tamura, T., Bateman, MD., Kodama, Y., Saitoh, Y., Watanabe, K., Yamaguchi, N., Matsumoto, D. 2011 a. Building of shore-oblique transverse dune ridges revealed by ground-penetrating radar and optical dating over the last 500 years on the Tottori coast, Japan Sea. *Geomorphology*. 132(3-4), 153-166

Tamura, T., Kodama, Y., Bateman, MD., Saitoh, Y., Watanabe, K., Matsumoto, D., Yamaguchi, N. 2011. Coastal barrier dune construction during sea-level highstands in MIS 3 and 5a on Tottori coast-line, Japan. *Palaeogeography, Palaeoclimatology, Palaeoecology*, 308, 492-501.

Tamura, T., Oliver, TSN., Cunningham , AC., Woodroffe, CD. 2019. Recurrence of Extreme Coastal Erosion in SE Australia Beyond Historical Timescales Inferred from Beach Ridge Morphostratigraphy. *Geophysical Research Letters*, 46(9), 4705-4714.

Tamura, T., Ta, TKO, Saito, Y., Bateman, MD., Murray-Wallace, CV., Nguyen, TML., Sato, T., Nguyen, VL. 2020. Seasonal control on coastal dune morphostratigraphy under a monsoon climate, Mui Ne dunefield, SE Vietnam. *Geomorphology*. 370.

Taveneau, A., Almar, R., Bergsma, EWJ., Sy, BA., Ndour, A., Sadio, M., Garlan, T. 2021. Observing and Predicting Coastal Erosion at the Langue de Barbarie Sand Spit around Sant Louis (Senegal, West Africa) through Satellite-Derived Digital Elevation Model and Shoreline. *Remote Sensing*, 13(13).

Temmerman, S., Meire, P., Bouma, TJ., Herman, PM., Ysebaert, T., De vriend, HJ. Ecosystem-based coastal defence in the face of global change. *Nature*, 204.

The Floods of 1720. (no date). Lytham St. Annes, Lancashire, England. Amounderness.co.uk. Available at: https://amounderness.co.uk/1720_floods.html (Accessed: 11 May 2020).

Thorne, C. 2014. Geographies of UK flooding in 2013/4. *The Geographical Journal*, 180, 297-309.

Troels-Smith J. 1955. Characterisation of unconsolidated sediments. *Danmarks Geologiske Undersøgelse* 4: 1–73.

Uehara K., Scourse JD., Horsburgh KJ., Lambeck., K. Purcell., AP. 2006. Tidal evolution of the northwest European shelf seas from the Last Glacial Maximum to the present. *Journal of Geophysical Research: Oceans* 111.

Van Dam, RL., Schlager, W. 2002. Identifying causes of ground-penetrating radar reflections using time-domain reflectometry and sedimentological analyses. *Sedimentology*. 47, 435-449.

Van den Brink, HW., Können, GP., Opsteegh, JD. 2005. Uncertainties in extreme surge level estimates from observational records. *Royal Society of London Philosophical Transactions*, 363, 1377-1386.

Varga, G., Újvári, G., Kovács, J. 2019. Interpretation of sedimentary (sub)populations extracted from grain size distributions of Central European loess-palesol series. *Quaternary International*, 502(A), 60-70.

Vitousek, S., Barnard, PL., Limer, P. 2017. Can beaches survive climate change? *Journal of Geophysical Research – Earth Surface*. 122(4), 1060-1067.

Vos, K., Harley, MD., Splinter KD., Walker, A., Turner IL. 2020. Beach Slopes From Satellite-Derived Shorelines. *Geophysical research letters*, 47(14).

Vos, K., Splinter KD., Harley, MD., Simmons, JA., Turner, IL. 2019a. CoastSat: a Google Earth Engine-enable Python toolkit to extract shorelines from publicly available satellite imagery. *Environmental Modelling and Software*. 122, 104-528.

Vos, K., Harley, MD., Splinter, KD., Simmons, JA., Turned, IL. 2019b. Sub-annual to multi-decadal shoreline variability from publicly available satellite imagery. *Coastal Engineering*. 150, 160-174

Vousdoukas MI, Voukouvalas E, Annunziato A, Giardino A, Feyen L. 2016. Projections of extreme storm surge levels along Europe. *Climate Dynamics* 47: 3171– 3190.

Wadey, M.P. 2013. Understanding Defence Failures and Coastal Flood Events: a Case Study Approach. University of Southampton

Wadey, MP., Haigh, ID., Brown, JM. 2014. A century of sea level data and the UK's 2013/14 storm surges: an assessment of extremes and clustering using Newlyn tide gauge record. *Ocean Science Discussions*, 11.

Wadey, MP., Haigh, ID., Nicholls, RJ., Brown, JM., Horsburgh, K., Carroll, B., Gallop, SL., Mason, T., Bradshaw, E. 2015. ‘A comparison of the 31 January–1 February 1953 and 5–6 December 2013 coastal flood events around the UK’. *Frontiers in Marine Science*, 2.

Wahl T. 2017. Sea-level rise and storm surges, relationship status: complicated! *Environmental Research Letters*, 12(11), 111001.

Wahl, T., Haigh, ID., Nicholls, RJ., Arns, A., Dangendorf, S., Hinkel, J., Slangen, ABA. 2017. Understanding extreme sea levels for broad-scale coastal impact and adaptation analysis. *Nature Communications*, 8, 16075.

Walker, J., Gaffney, V., Fitch, S., Muru, M., Fraser, A., Bates, M., Bates, R. 2020. A great wave: the Storegga tsunami and the end of Doggerland? *Antiquity*, 94(378).

Wallinga, J., Murray, AS., Duller, GAT., Törnqvist, TE. 2001. Testing optically stimulated luminescence dating of sand-sized quartz and feldspar from fluvial deposits. *Earth and Planetary Science Letters*, 193, 617-630.

Wanner H, Brönnimann S, Casty C, Gyalistras D, Luterbacher J, Schmutz C, Stephenson DB, Xoplaki E. 2001. North Atlantic oscillation—Concepts and studies. *Surv. Geophys.* 22: 321–381.

Watcham., EP., Shennan, I., Barlow, NLM. 2013. Scale considerations in using diatoms as indicators of sea-level change: lessons from Alaska. *Journal of Quaternary Science*. 28(2): 165-179.

Williams, LL., Lück-Vogel, M. 2020. Comparative assessment of the GIS based bathtub model and enhanced bathtub model for coastal inundation. *Journal of Coastal Conservation*, 24(23).

Wintle, AG. 2008. Luminescence dating: where it has been and where it is going. *Boreas,* 37, 471-482.

Wintle, AG., Murray, AS. 2006. A review of quartz optically stimulated luminescence characteristics and their relevance in single-aliquot regeneration dating protocols. *Radiation Measurement*s, 41, 369-391.

Wolf J, Flather RA. 2005. Modelling waves and surges during the 1953 storm. *Philosophical Transactions of the Royal Society of London Series A* 363: 1359– 1375.

Woodroffe, CD. 2007. The natural resilience of coastal systems: primary concepts. In: McFadden, L., Penning-Rowsell, E., Nicholls, RJ. (Eds.), 2007. Managing Coastal Vulnerability. Elsevier, Amsterdam, pp. 45-60.

Woodruff, JD., Donnelly, JP., Okusu, A. 2009. Exploring typhoon variability over the mid to late Holocene: evidence of extreme coastal flooding from Kamikoshiki, Japan. *Quaternary Science Reviews*. 28, 1774–1785.

Woodworth PL. 2022. Advances in the observation and understanding of changes in sea level and tides. *Annals of the New York Academy of Sciences*.

Woodworth, PL., Blackman, DL. 2002. Changes in extreme high waters at Liverpool since 1768. *International Journal of Climatology*. 22(6), 697 – 714

Woodworth, PL., Rickards, LJ., Pérez B. 2009. A survey of European sea level infrastructure. *Nat. Hazards Earth Syst. Sci*., 9, 927-934.

Woth, K., Weisse, R., von Storch, H. 2006. Climate change and North Sea storm surge extremes: an ensemble study of storm surge extremes expected in a changed climate projected by four different regional climate models. *Ocean Dynamics*, 56(1), 3-15.

Wright, LD., Swaye, FJ., Coleman, JM. 1970. Effects of Hurricane Camille on the landscape of the Brenton-Chandeleur island chain and the eastern portion of the lower Mississippi delta. Baton Rouge: Louisiana State University Coastal Studies Institute, Technical Report 76, 34

Wright, LD., Thom, BG. 1977. Coastal depositional landforms: a morphodynamic approach. *Progress in Physical Geography: Earth and Environment,* 1(3), 412-459.

Yasuda, T., Nakajo S., Kim, S., Mase, H., Mori, N., Horsburgh, K. Evaluation of future storm surge risk in East Asia based on state-of-the-art climate change projection. *Coastal Engineering*, 83, 76-71.

Zappa GZ, Shaffrey LC, Hodges KI, Sansom PG, Stephenson DB. 2013. A multimodel assessment of future projections of North Atlantic extratropical cyclones in the CMIP5 climate models. *Journal of Climate* 26: 5846– 5862.

Zhang, K., Douglas, BC., Leatherman, SP. 2000. Twentieth-century storm activity along the US east coast. *Journal of Climate*, 13, 1748-1761.

Zielger, JM., Hayes, CR., Tuttle, SD. 1959. Beach changes during storms on outer cape-cod Massachusetts. *Journal of Geology*, 67(3).

Zong Y, Tooley MJ. 2003. A historical record of coastal floods in Britain: frequencies and associated storm tracks. *Natural Hazards* 29: 13– 36.